

MFN 10-319

Enclosure 1

ESBWR Licensing Topical Report

NEDO-33373-A

**Dynamic, Load-Drop and Thermal-Hydraulic Analyses
for ESBWR Fuel Racks**

Revision 5

October 2010



HITACHI

GE Hitachi Nuclear Energy

NEDO-33373-A

Revision 5

Class I

eDRF Section 0000-0122-8900, Rev. 1

October 2010

Licensing Topical Report

**DYNAMIC, LOAD-DROP AND THERMAL-
HYDRAULIC ANALYSES FOR ESBWR FUEL
RACKS**

Important Notice Regarding the Contents of this Report

Please Read Carefully

The information contained in this document is furnished as reference to the NRC Staff for the purpose of obtaining NRC approval of the ESBWR Certification and implementation. The only undertakings of GE Hitachi Nuclear Energy (GEH) with respect to information in this document are contained in contracts between GEH and participating utilities, and nothing contained in this document shall be construed as changing those contracts. The use of this information by anyone other than for which it is intended is not authorized; and with respect to any unauthorized use, GEH makes no representation or warranty, and assumes no liability as to the completeness, accuracy, or usefulness of the information contained in this document.

Summary of Changes

NEDO-33373-A Revision 5

Location	Comment
All	“-A” is added to the document number for this revision denoting NRC acceptance of this revision for ESBWR design certification.
Appendix G, Section 2.3	Provided additional discussion to elaborate on conclusions regarding the peak cladding temperature. These changes were provided via Letter MFN 10-326, Richard E. Kingston to U.S. Nuclear Regulatory Commission, “Transmittal of Markup for Licensing Topical Report NEDO-33373, Revision 5, ‘Dynamic, Load-Drop and Thermal-Hydraulic Analyses for ESBWR Fuel Racks’,” dated October 15, 2010.
Attachment 1	Added the NRC letter describing the acceptance of this revision of this Licensing Topical Report. The NRC letter as well as Enclosure 1 of the letter, which contains the Final Safety Evaluation for this Licensing Topical Report, has been added to the end of this document.

Contents

1.	Dynamic Load Analysis for Spent Fuel Racks in the Spent Fuel Pool	17
1.1	Introduction.....	17
1.1.1	Purpose.....	17
1.1.2	Scope.....	17
1.2	Input Data.....	20
1.3	Summary of Results.....	22
1.4	Analysis Summary	24
1.4.1	Spent Fuel High Density Storage Rack Description.....	24
1.4.1.1	Rack Layout at Spent Fuel Pool.....	25
1.4.2	Analysis Methodology Description	25
1.4.3	Materials	26
1.4.4	Design Code.....	27
1.4.5	Analysis Loads.....	28
1.4.5.1	Dead Weight + Buoyancy (D).....	28
1.4.5.2	Fuel Handling Loads (P_f).....	28
1.4.5.3	Differential Temperature Induced Loads (T_o , T_a)	29
1.4.5.4	Safe Shutdown Earthquake (SSE).....	29
1.4.5.5	Safety Relief Valve Discharge (SRVD).....	30
1.4.5.6	Loss of Coolant Accident (LOCA).....	30
1.4.5.7	Lifting FSR During Installation (L_R).....	30
1.4.6	Load Combinations.....	30
1.4.7	Stress Limits.....	31
1.5	Detailed Model: Response spectrum analysis.....	32
1.5.1	Assumptions.....	33
1.5.2	FSR Detail Model	33
1.5.2.1	Structural Considerations on the Borated Plates	35
1.5.3	Response Spectra Analysis Methodology Description.....	36
1.5.4	Results of the Response Spectra Analysis	37
1.5.4.1	Model Results.....	37
1.5.4.2	Deformation Results.....	39
1.5.4.3	Plate Stress Results.....	39
1.5.4.4	Global Bending Moments and Reactions on the FSR.....	45
1.5.5	(Deleted)	45
1.6	Simplified and global Models, transient DYNAMIC Analysis.....	45
1.6.1	Assumptions.....	46
1.6.2	Fluid-Structure Interaction, Water Model.....	46
1.6.3	Single FSR Simplified Model.....	48
1.6.4	20-FSR Global Model.....	49
1.6.5	Transient Dynamic Analysis Methodology Description.....	51
1.6.5.1	Scenario-Cases in Study.....	53
1.6.6	Results of the Transient Analysis	53
1.6.7	Pool Floor Liner Reactions	57
1.6.8	(Deleted)	58

1.7	Local Stress Analysis.....	58
1.8	Total Stress Results.....	61
1.9	Stresses in the Linking Devices.....	64
1.9.1	Lower Links (Bearing Pads).....	64
1.9.2	Upper Links (Assembly Crossarms).....	64
1.10	Conclusions.....	65
1.11	References.....	66
Appendix A - Figures.....		67
Appendix B - Output Analysis File.....		146
Appendix B1 - Analysis Of Compressive Stresses.....		273
2.	Dynamic Load Analysis for Spent Fuel Racks in the Buffer Pool.....	280
2.1	Introduction.....	280
2.1.1	Purpose.....	280
2.1.2	Scope.....	280
2.2	Input Data.....	281
2.3	Summary of Results.....	282
2.4	Analysis Summary.....	282
2.4.1	Spent Fuel Storage Rack Description.....	283
2.4.2	Materials.....	283
2.4.3	Design Code.....	284
2.4.4	Assumptions.....	284
2.4.5	FSR Analysis Model.....	285
2.4.5.1	Structural Considerations on the Borated Plates.....	287
2.4.6	Analysis Loads.....	288
2.4.6.1	Dead Weight + Buoyancy (D).....	288
2.4.6.2	Fuel Handling Loads (P_f).....	289
2.4.6.3	Differential Temperature Induced Loads (T_o, T_a).....	289
2.4.6.4	Safe Shutdown Earthquake (SSE).....	290
2.4.6.5	Safety Relief Valve Discharge (SRVD).....	290
2.4.6.6	Loss of Coolant Accident (LOCA).....	290
2.4.6.7	Lifting FSR During Installation (L_R).....	290
2.4.7	Load Combinations.....	290
2.4.8	Analysis Methodology Description.....	290
2.4.9	Stress Limits.....	291
2.5	Results of the Analysis.....	292
2.5.1	Displacement Results.....	294
2.5.2	Plate Stress Results.....	294
2.5.2.1	10 mm Thick Enveloping Plate.....	294
2.5.2.2	47 mm Thick Upper Level Plates.....	297
2.5.2.3	20 mm Thick Base Plate Stiffener Plates.....	297
2.5.2.4	20 mm Thick Base Plate and 60 mm Thick Bolted Support Plates.....	298
2.5.3	Bolt Stress Results.....	299
2.5.4	Fuel Impact Forces Analysis.....	300
2.6	Conclusions.....	301
2.7	References.....	302
Appendix C - Figures.....		303

Appendix D - Analysis Of Compressive Stresses.....	337
3. Dynamic Load Analysis for New Fuel Racks in the Buffer Pool.....	343
3.1 Introduction.....	343
3.1.1 Purpose.....	343
3.1.2 Scope.....	343
3.2 Input Data.....	344
3.3 Summary of Results.....	345
3.4 Analysis Summary.....	345
3.4.1 New Fuel Storage Rack Description.....	346
3.4.2 Materials.....	346
3.4.3 Design Code.....	347
3.4.4 Assumptions.....	347
3.4.5 FSR Analysis Model.....	348
3.4.6 Analysis Loads.....	350
3.4.6.1 Dead Weight + Buoyancy (D).....	350
3.4.6.2 Fuel Handling Loads (P_f).....	351
3.4.6.3 Differential Temperature Induced Loads (T_o , T_a).....	351
3.4.6.4 Safe Shutdown Earthquake (SSE).....	351
3.4.6.5 Safety Relief Valve Discharge (SRVD).....	352
3.4.6.6 Loss of Coolant Accident (LOCA).....	352
3.4.6.7 Lifting FSR During Installation (L_R).....	352
3.4.7 Load Combinations.....	352
3.4.8 Analysis Methodology Description.....	352
3.4.9 Stress Limits.....	353
3.5 Results of the Analysis.....	354
3.5.1 Displacements Results.....	356
3.5.2 Plate Stress results.....	356
3.5.2.1 8 mm Thick Channel Plate.....	356
3.5.2.2 12 mm Thick Door Plates.....	357
3.5.2.3 10 mm and (10+8) mm Assembly Grid Plates.....	358
3.5.2.4 Axis and Hinge Plates.....	359
3.5.2.5 15 mm Thick Support-Base Stiffener Plates.....	360
3.5.2.6 15 mm Thick Folded Base Plate and (15+15) mm Thick Bolted Support Plates.....	361
3.5.3 Bolt Stress Results.....	361
3.5.4 Fuel Impact Forces Analysis.....	363
3.6 Conclusions.....	365
3.7 References.....	365
Appendix E - Figures.....	367
Appendix F - (Deleted).....	398
4. Load-Drop (Impact) Analysis.....	399
4.1 Introduction.....	399
4.1.1 Object.....	399
4.1.2 Scope.....	399
4.1.3 Layout of Report.....	400
4.2 Description of the Problem.....	400

4.2.1	The Fuel Element and Handling Tool.....	400
4.2.2	Spent Fuel Racks.....	401
4.2.2.1	Description	401
4.2.2.2	Postulated Accidents	402
4.2.3	Fresh Fuel Racks.....	402
4.2.3.1	Description	402
4.2.3.2	Postulated Accidents	403
4.3	Spent Fuel Racks: Impacts on the Base Plate	409
4.3.1	Introduction.....	409
4.3.2	Impact Above a Leg.....	409
4.3.3	Impact Between Legs.....	410
4.4	Spent Fuel Racks: Impacts at the Top of the Cells	425
4.4.1	Introduction.....	425
4.4.2	Impacts on Cell Walls.....	425
4.4.2.1	Walls Slotted Below	426
4.4.2.2	Walls Slotted Above.....	426
4.4.3	Impacts on Cell Contacts	427
4.5	Fresh Fuel Racks.....	449
4.5.1	Impact on the Base Plate.....	449
4.5.2	Impact on the Wall.....	449
4.6	Conclusions.....	459
4.7	References.....	460
5.	Thermal-Hydraulic Analysis (17.3 MW Case).....	461
5.1	Introduction.....	461
5.1.1	Inputs / Assumptions	461
5.1.2	Acceptance Criteria.....	462
5.2	Calculation Methodology.....	462
5.2.1	General Description	462
5.2.1.1	Pool Inlet Temperature Determination.....	462
5.2.1.2	Calculation of the Velocities and Temperatures within the Spent Fuel Pool (SFP).....	462
5.2.2	Pool Inlet Temperature Determination	463
5.2.2.1	Normal Conditions Case.....	463
5.2.2.2	Abnormal Conditions Case.....	463
5.2.3	Calculation of the Velocities and Temperatures within the Spent Fuel Pool (SFP)	464
5.2.3.1	Loss Coefficient Calculation	465
5.2.3.2	Heat Generation Calculation in Each Rack Under the Normal Conditions Case	467
5.2.3.3	Heat Generation Calculation in Each Rack Under the Abnormal Conditions Case	467
5.2.4	Summary Tables	469
5.2.5	CFD Model Sensitivity	470
5.3	Results.....	472
5.3.1	Temperature Distribution Under Normal Conditions Case	472
5.3.2	Temperature Distribution Under Abnormal Conditions Case	474

5.3.3	Velocity Distribution Under Normal Conditions Case.....	476
5.3.4	Velocity Distribution Under Abnormal Conditions Case.....	479
5.3.5	Maximum Cladding Temperature.....	483
5.3.6	Maximum Fluid Temperature Under 80% Blockage of Rack Outlet.....	487
5.3.6.1	Under Normal Conditions Case.....	487
5.3.6.2	Under Abnormal Conditions Case.....	488
5.4	Reactor Buffer pool.....	490
5.5	Conclusions.....	491
5.6	References.....	492
Appendix G – Discussion of Abnormal Condition heat load at 19.0 mw		493
Appendix H – analysis at a heat load of 29 mw		497
5.1	Introduction.....	497
5.1.1	Inputs/Assumptions	497
5.2	Calculation Methodology.....	498
5.2.1	General Description	498
5.2.1.1	Pool Inlet Temperature Determination.....	498
5.2.1.2	Calculation of the Velocities and Temperatures within the Spent Fuel Pool (SFP).....	498
5.2.2	Pool Inlet Temperature Determination	498
5.2.2.1	Normal Conditions Case.....	499
5.2.2.2	Abnormal Conditions Case.....	499
5.2.3	Calculation of the Velocities and Temperatures within the Spent Fuel Pool (SFP)	499
5.2.3.1	Loss Coefficient Calculation	500
5.2.3.2	Heat Generation Calculation in Each Rack Under the Normal Conditions Case	502
5.2.3.3	Heat Generation Calculation in Each Rack Under the Abnormal Conditions Case	503
5.2.4	Summary Tables	503
5.2.5	CFD Model Sensitivity	504
5.3	Results.....	506
5.3.1	Temperature Distribution Under Normal Conditions Case	506
5.3.2	Temperature Distribution Under Abnormal Conditions Case	508
5.3.3	Velocity Distribution Under Normal Conditions Case.....	510
5.3.4	Velocity Distribution Under Abnormal Conditions Case.....	513
5.3.5	Maximum Cladding Temperature.....	516
5.3.6	Maximum Fluid Temperature Under 80% Blockage of Rack Outlet.....	520
5.3.6.1	Under Normal Conditions Case.....	520
5.3.6.2	Under Abnormal Conditions Case.....	521
5.4	Reactor Buffer pool.....	522
5.5	Summary of results	523
5.6	References.....	524

List of Tables

Table 1-1 List of Document Input Data (ID).....	20
Table 1-2 Maximum Displacements and Forces Summary.....	22
Table 1-3 FSR Main Stresses Summary.....	23
Table 1-3a Pool Floor Liner Maximum Reactions.....	23
Table 1-4 Material Properties at 250°F (121.1°C).....	27
Table 1-5 Load Combinations.....	31
Table 1-6 Mass Breakdown.....	35
Table 1-7 Main Eigenfrequencies.....	38
Table 1-8 Combined Effective Masses.....	39
Table 1-9 10 mm Thick Enveloping Plate Maximum Stress Results.....	40
Table 1-10 10 mm Thick Enveloping Plate Welds Maximum Stress Results.....	41
Table 1-11 7 mm Thick Upper Level Plates Maximum Stress Results.....	42
Table 1-12 20 mm Thick Base Plate Stiffener Plates Maximum Stress Results.....	43
Table 1-13 20 mm thick Base Plate and Cylindrical Feet Plate Maximum Stress Results (S.I.)	44
Table 1-14 Global Bending Moments and Foot Reactions.....	45
Table 1-15 Comparison of Models.....	49
Table 1-16 Maximum Displacements and Forces.....	54
Table 1-17 Summary of Enveloping Maximum Displacements and Forces.....	57
Table 1-17a. Pool Floor Liner Maximum Reactions.....	58
Table 1-18 Local Stresses in FSR from Impact Loads.....	60
Table 1-19 FSR Total Stress Results.....	63
Table 2-1 List of Document Input Data (ID).....	281
Table 2-2 SFR Main Analysis Results.....	282
Table 2-3 Material Properties at 250°F (121.1°C).....	283
Table 2-4 Mass Breakdown.....	287
Table 2-5 Load Combinations.....	290
Table 2-6 Main Eigenfrequencies.....	293
Table 2-7 Combined Effective Masses.....	293
Table 2-8 10mm Thickness Enveloping Plate Stress Results.....	294
Table 2-9 10mm Thickness Enveloping Plate Welds Stress Results.....	296
Table 2-10 7 mm Thickness Upper Level Plates Stress Results.....	297
Table 2-11 20mm Thickness Base Plate Stiffener Plates Stress Results.....	298
Table 2-12 20 mm Thickness Base Plate and 60 mm Thickness Bolted Support Plates Stress Results.....	299
Table 2-13 Bolt Stress Results.....	299
Table 3-1 List of Document Input Data (ID).....	344
Table 3-2 FSR Main Analysis Results.....	345
Table 3-3 Material Properties at 250°F (121.1°C).....	347
Table 3-4 Mass Breakdown.....	350
Table 3-5 Load Combinations.....	352
Table 3-6 Main Eigenfrequencies.....	355
Table 3-7a Combined Effective Masses.....	355

Table 3-7b Acceleration for Missing Masses	356
Table 3-8 8mm Thick Channel Plate Stress Results	357
Table 3-9 Channel to Support-Base Weld Stress Results	357
Table 3-10 12 mm Thick Door Plates Stress Results	358
Table 3-11 10 mm and (10+8) mm Thickness Assembly Grid Stress Results	359
Table 3-12 Axis and Hinge Stress Results.....	360
Table 3-13 15mm Thick Stiffener Plates Stress Results.....	360
Table 3-14 15 mm Thick Folded Base Plate and (15+15) mm Thick Bolted Support Plates Stress Results	361
Table 3-15 Bolt Stress Results.....	362
Table 5-1 Approximate Range of Values hm Ordinarily Encountered	486
Table H5-1 Approximate Range of Values hm Ordinarily Encountered	519

List of Figures

Figure 1-1. Layout of Fuel Support Racks and Base Plates 19

Figure A-1a. SSE Horizontal X Floor Response Spectra 68

Figure A-1b. SSE Horizontal Y Floor Response Spectra 69

Figure A-2. SSE Vertical Z Floor Response Spectra..... 70

Figure A-3. SSE Horizontal X Acceleration Time History 71

Figure A-4. SSE Horizontal Y Acceleration Time History 72

Figure A-5. SSE Vertical Z Acceleration Time History 73

Figure A-6. SRVD Horizontal Enveloping Floor Response Spectra..... 74

Figure A-7. SRVD Vertical Floor Response Spectra 75

Figure A-8. LOCA Horizontal Enveloping Floor Response Spectra 76

Figure A-9. LOCA Vertical Floor Response Spectra 77

Figure A-10. FSR FEM..... 78

Figure A-11. FSR FEM..... 79

Figure A-12. FSR FEM 10mm Thick SS Plates 80

Figure A-13. FSR FEM 7mm Thick SS Plates 81

Figure A-14a. FSR FEM 3.4mm Thick BSS Plates..... 82

Figure A-14b. Couples in Slotted Areas 83

Figure A-15. FSR FEM 20mm Thick SS Base Plate..... 84

Figure A-16. FSR FEM 20mm Thick SS Base Plate Stiffeners and Feet..... 85

Figure A-17. FSR FEM Foot-Nut & Screw-Detail (1/4 removed)..... 86

Figure A-18. FSR Fuel Handling Loads 87

Figure A-19. FSR Deformed Shape Eigenmode 1..... 88

Figure A-20. FSR Deformed Shape Eigenmode 2..... 89

Figure A-21. FSR Deformed Shape Eigenmode 3..... 90

Figure A-22. FSR Deformed Shape Eigenmode 4..... 91

Figure A-23. FSR Deformed Shape Eigenmode 12..... 92

Figure A-24. FSR Deformed Shape Eigenmode 15..... 93

Figure A-25. FSR Deformed Shape Eigenmode 17..... 94

Figure A-26. FSR Deformed Shape Eigenmode 36..... 95

Figure A-27. FSR Horizontal X-Displacement (m). Level D..... 96

Figure A-28. FSR Horizontal Y-Displacement (m). Level D..... 97

Figure A-29. FSR Vertical Z-Displacement (m). Level D 98

Figure A-30. FSR 10 mm Enveloping Plates. Level D Vertical Stress (N/m²) 99

Figure A-31. FSR 7 mm Upper Level Plates. Level A Vertical Stress (N/m²)..... 100

Figure A-32. FSR 7 mm Upper Level Plates. Level D Horizontal Stress (N/m²) 101

Figure A-33. FSR Base Plate Stiffener Plates. Level D Vertical Stress (N/m²) 102

Figure A-34. FSR Base Plate. Level D Stress (N/m²)..... 103

Figure A-35. Base Plate. Lifting Load stresses (N/m²)..... 104

Figure A-36. Spent Fuel Pool+20FSR Model for Hydrodynamic Mass Calculations 105

Figure A-37. FSR Cell+Fuel Model for Hydrodynamic Mass Calculations 106

Figure A-38. Hydrodynamic Mass (kg/m) Full Matrix for X (N-S) Direction 107

Figure A-39. Hydrodynamic Mass (kg/m) Full Matrix for Y (E-W) Direction 108

Figure A-40. (Deleted)..... 109

Figure A-41. (Deleted).....	109
Figure A-42. Hydrodynamic Mass (kg/m) Coupling Matrix. Fuel Assembly-FSR Cell	109
Figure A-43. FSR Simplified Model	110
Figure A-44. Global Model. One N-S Row 2-D View	111
Figure A-45. (Deleted).....	112
Figure A-46. ANSYS Global Model (without hydrodynamic couplings) ANSYS Global Model (without hydrodynamic couplings)	113
Figure A-47. ANSYS Global Model E-.....	114
Figure A-48. Displacement (m) Time-History. X(N-S) Direction.	115
Figure A-49. Displacement (m) Time-History. Y(E-W) Direction.	116
Figure A-50. Displacement (m) Time-History. Z (Vertical) Direction	117
Figure A-51. Relative Horizontal Displacement (m) FSR Foot-Pool Floor. N-S Direction. Case C-3	118
Figure A-52. Relative Horizontal E-W Displacement (m) FSR Foot-Pool Floor. Case C-6.....	119
Figure A-53. Relative Vertical Displacement (m) FSR Foot-Pool Floor Case C-5	120
Figure A-54. Horizontal Force (N) FSR Foot-Pool Floor. Case C-4.....	121
Figure A-55. Vertical Force (N) FSR Foot-Pool Floor. Case C-4.....	122
Figure A-56. Relative Horizontal N-S Displacement (m) FSR Top-Pool Wall. Case C-3	123
Figure A-57. Relative Horizontal E-W Displacement (m) FSR Top-Pool Wall. Case C-6	124
Figure A-58. Horizontal Force (N) between two FSR at the Bottom Link Device. Case C-4 ..	125
Figure A-59. Horizontal Force (N) between two FSR at the Upper Link Device. Case C-4	126
Figure A-60. Relative Horizontal Displacement (m) Top Fuel- FSR Top Cells. Case C-4	127
Figure A-60a. Relative Vertical Displacement (m) Bottom Fuel- FSR Base Plate. Case C-4 ..	128
Figure A-60b. Horizontal Force (N) Top Fuel-FSR Top Cells. Case C-1.....	129
Figure A-61. Horizontal Force (N) Bottom Fuel-FSR Base Plate. Case C-4.....	130
Figure A-62. Vertical Force (N) Fuel-FSR Base Plate. Case C-4	131
Figure A-63. N-S Bending Moment (N·m) on the FSR Base Plate. Case C-4	132
Figure A-64. E-W Bending Moment (N·m) on the FSR Base Plate. Case C-4	133
Figure A-65. Case I-1. Top Cell Plates in Compression. Impact Pressure Loads (N/m ²)	134
Figure A-66. Case I-2. Top Cell Plates in Tension. Impact Pressure Loads (N/m ²).....	135
Figure A-67. Case I-3. Base Plate in Compression. Impact Pressure Loads (N/m ²)	136
Figure A-68. Case I-4. Base Plate in Tension. Impact Pressure Loads (N/m ²)	137
Figure A-69. Case I-1. 10 mm Thick Enveloping Plates. Impact Stresses (N/m ²)	138
Figure A-70. Case I-1. 7 mm Thick Upper Level Plates. Impact Stresses (N/m ²)	139
Figure A-71: Case I-2. 10 mm Thick Enveloping Plates. Impact Stresses (N/m ²).....	140
Figure A-72: Case I-2. 7 mm Thick Upper Level Plates. Impact Stresses (N/m ²)	141
Figure A-73: Case I-3. Base Plate. Impact Stresses (N/m ²).....	142
Figure A-74: Case I-3. Base Plate Stiffeners. Impact Stresses (N/m ²)	143
Figure A-75: Case I-4. Base Plate. Impact Stresses (N/m ²).....	144
Figure A-76: Case I-4. Base Plate Stiffeners. Impact Stresses (N/m ²)	145
Figure C-1. FSR FEM.....	303
Figure C-2. FSR FEM 10 mm Thickness SS Plates	304
Figure C-3. FSR FEM 7 mm Thickness SS Plates	305
Figure C-4a. FSR FEM 3.4 mm Thickness BSS Plates.....	306
Figure C-4b. Couples in Slotted Areas	307

Figure C-5. FSR FEM 20 mm Thickness SS Base Plate	308
Figure C-6. FSR FEM 20 mm Thickness SS Base Plate Stiffeners.....	309
Figure C-7. FSR FEM 60 mm Thickness SS Bolted Support Plates	310
Figure C-8. FSR FEM Bolted Support Plate Detail (With High Stiffness Bars).....	311
Figure C-9. SSE Horizontal Floor Response Spectra	312
Figure C-10. SSE Vertical Floor Response Spectra	313
Figure C-11. SRVD Horizontal Floor Response Spectra	314
Figure C-12. SRVD Vertical Floor Response Spectra.....	315
Figure C-13. LOCA Horizontal Floor Response Spectra	316
Figure C-14. LOCA Vertical Floor Response Spectra	317
Figure C-15. FSR Fuel Handling Loads	318
Figure C-16. FSR Deformed Shape Eigenmode 1	319
Figure C-17. FSR Deformed Shape Eigenmode 2.....	320
Figure C-18. FSR Deformed Shape Eigenmode 3.....	321
Figure C-19. FSR Deformed Shape Eigenmode 4.....	322
Figure C-20. FSR Deformed Shape Eigenmode 13.....	323
Figure C-21. FSR Deformed Shape Eigenmode 15.....	324
Figure C-22. FSR Deformed Shape Eigenmode 16.....	325
Figure C-23. FSR Deformed Shape Eigenmode 36.....	326
Figure C-24. FSR Horizontal Displacement X (m)	327
Figure C-25. FSR Horizontal Displacement Y (m)	328
Figure C-26. FSR 10 mm Enveloping Plates. Level D Vertical Stress (N/m ²).....	329
Figure C-27. FSR 7 mm Upper Level Plates. Level A Vertical Stress (N/m ²).....	330
Figure C-28. FSR 7 mm Upper Level Plates. Level D Horizontal Stress (N/m ²).....	331
Figure C-29. FSR Base Plate Stiffener Plates. Level D Vertical Stress (N/m ²)	332
Figure C-30. FSR Base Plate. Level D Stress (N/m ²).....	333
Figure C-31. FSR Bolted Support Plate. Level D Stress (N/m ²)	334
Figure C-32. Base Plate. Lifting Load Stresses (N/m ²)	335
Figure C-33. Fuel Impact Forces. Base Plate Stresses (N/m ²).....	336
Figure E-1. FSR FEM.....	367
Figure E-2. FSR FEM.....	368
Figure E-3. FSR FEM 8 mm Thick Channel Plates.....	369
Figure E-4. FSR FEM (10+8) mm Thick (Grid+Channel) Plates in Red, and 10 mm Thick Grid Plates in Purple.....	370
Figure E-5. FSR FEM 12 mm Thick Door Plates, 7.5 mm Thick Door Axis Plate and 10 mm Thick Hinge Plates	371
Figure E-6. FSR FEM 15 mm Thick Support-Base Plate and Stiffener Plates, and (15+15) mm Reinforced Bolted Plate in Lblue	372
Figure E-7a. SSE Horizontal X Enveloping Floor Response Spectra	373
Figure E-7b. SSE Horizontal Y Enveloping Floor Response Spectra	374
Figure E-8. SSE Vertical Enveloping Floor Response Spectra	375
Figure E-9. SRVD Horizontal Enveloping Floor Response Spectra	376
Figure E-10. SRVD Vertical Enveloping Floor Response Spectra	377
Figure E-11. LOCA Horizontal Enveloping Floor Response Spectra.....	378
Figure E-12. LOCA Horizontal Enveloping Floor Response Spectra.....	379

Figure E-13. FSR Fuel Handling Loads	380
Figure E-14. FSR Deformed Shape Eigenmode 1	381
Figure E-15. FSR Deformed Shape Eigenmode 2	382
Figure E-16. FSR Deformed Shape Eigenmode 3	383
Figure E-17. FSR Deformed Shape Eigenmode 4	384
Figure E-18. FSR Deformed Shape Eigenmode 5	385
Figure E-19. FSR Deformed Shape Eigenmode 31	386
Figure E-20. FSR Deformed Shape Eigenmode 61	387
Figure E-21. FSR Deformed Shape Eigenmode 63	388
Figure E-22. FSR Deformed Shape Eigenmode 69	389
Figure E-23. FSR Deformed Shape Eigenmode 71	390
Figure E-24. FSR Horizontal Displacement X (m)	391
Figure E-25. FSR 8 mm Channel Plates. Level A Vertical Stress (N/m ²)	392
Figure E-26. FSR 8 mm Channel Plates. Level D Vertical Stress (N/m ²)	393
Figure E-27. FSR 12 mm Door Plates. Level D Horizontal Stress (N/m ²)	394
Figure E-28. FSR Assembly Grid Plate. Level D Horizontal Stress (N/m ²)	395
Figure E-29. Lifting Load Stresses (N/m ²)	396
Figure E-30. Fuel Impact Forces. Base Plate Stresses (N/m ²)	397
Figure 4-1. Elevation View of the Spent Fuel Rack	404
Figure 4-2. Base Plate of the Spent Fuel Rack	405
Figure 4-3. Stress-Strain Curve for Structural Steel	406
Figure 4-4. Elevation View of the Fresh Fuel Rack	407
Figure 4-5. Base Plate of the Fresh Fuel Rack	408
Figure 4-6. Spent Fuel, Above Leg. View of the Mesh	411
Figure 4-7. Spent Fuel, Above Leg with Tool. Impact Forces	412
Figure 4-8. Spent Fuel, Above Leg, with Tool. Plastic Deformations	413
Figure 4-9. Spent Fuel, Above Leg, with Tool. Fuel Velocities	414
Figure 4-10. Spent Fuel, Above Leg, without Tool. Impact Forces	415
Figure 4-11. Spent Fuel, Above Leg, without Tool. Plastic Deformations	416
Figure 4-12. Spent Fuel, Above Leg, without Tool. Fuel Velocities	417
Figure 4-13. Spent Fuel, Between Legs. View of the Mesh	418
Figure 4-14. Spent Fuel, Between Legs, with Tool. Impact Forces	419
Figure 4-15. Spent Fuel, Between Legs, with Tool. Plastic Deformations	420
Figure 4-16. Spent Fuel, Between Legs, with Tool. Fuel Velocities	421
Figure 4-17. Spent Fuel, Between Legs, without Tool. Impact Forces	422
Figure 4-18. Spent Fuel, Between Legs, without Tool. Plastic Deformations	423
Figure 4-19. Spent Fuel, Between Legs, without Tool. Fuel Velocities	424
Figure 4-20. Spent Fuel, Slots Below. View of the Mesh	428
Figure 4-21. Spent Fuel, Slots Below, with Tool. Impact Forces	429
Figure 4-22. Spent Fuel, Slots Below, with Tool. Fuel Displacements	430
Figure 4-23. Spent Fuel, Slots Below, with Tool. Plastic Deformations	431
Figure 4-24. Spent Fuel, Slots Below, without Tool. Impact Forces	432
Figure 4-25. Spent Fuel, Slots Below, without Tool. Fuel Displacements	433
Figure 4-26. Spent Fuel, Slots Below, without Tool. Plastic Deformations	434
Figure 4-27. Spent Fuel, Slots Above. View of the Mesh	435

Figure 4-28. Spent Fuel, Slots Above, with Tool. Impact Forces.....	436
Figure 4-29. Spent Fuel, Slots Above, with Tool. Fuel Displacements.....	437
Figure 4-30. Spent Fuel, Slots Above, with Tool. Plastic Deformations.....	438
Figure 4-31. Spent Fuel Slots Above, without Tool. Impact Forces.....	439
Figure 4-32. Spent Fuel, Slots Above, without Tool. Fuel Displacements.....	440
Figure 4-33. Spent Fuel, Slots Above, without Tool. Plastic Deformations.....	441
Figure 4-34. Spent Fuel, Intersection. View of the Mesh.....	442
Figure 4-35. Spent Fuel, Intersection. Impact Force.....	443
Figure 4-36. Spent Fuel, Intersection, with Tool. Fuel Displacements.....	444
Figure 4-37. Spent Fuel, Intersection, with Tool. Plastic Deformations.....	445
Figure 4-38. Spent Fuel, Intersection, without Tool. Impact Forces.....	446
Figure 4-39. Spent Fuel, Intersection, without Tool. Fuel Displacements.....	447
Figure 4-40. Spent Fuel, Intersection, without Tool. Plastic Deformations.....	448
Figure 4-41. Fresh Fuel, Bottom Plate. View of the Mesh.....	451
Figure 4-42. Fresh Fuel, Bottom Plate, with Tool. Impact Forces.....	452
Figure 4-43. Fresh Fuel, Bottom Plate, with Tool. Plastic Deformations.....	453
Figure 4-44. Fresh Fuel, Bottom Plate, without Tool. Impact Forces.....	454
Figure 4-45. Fresh Fuel Bottom Plate, without Tool. Plastic Deformations.....	455
Figure 4-46. Fresh Fuel, Wall. View of the Mesh.....	456
Figure 4-47. Fresh Fuel, Wall with Tool. Plastic Deformations.....	457
Figure 4-48. Fresh Fuel, Wall, without Tool. Plastic Deformations.....	458
Figure 5-1. SFP Model.....	464
Figure 5-2. Loss coefficient in Racks.....	466
Figure 5-3. Temperature Distribution under the Normal Conditions Case (x,y).....	472
Figure 5-4. Temperature Distribution under the Normal Conditions Case (y,z).....	473
Figure 5-5. Temperature Distribution under the Abnormal Conditions Case (x,y).....	474
Figure 5-6. Temperature Distribution under the Abnormal Conditions Case (y,z).....	475
Figure 5-7. Velocity under the Normal Conditions Case (y,z).....	476
Figure 5-8. Velocity under the Normal Conditions Case (y,z).....	477
Figure 5-9. Streamlines from Inlets to Outlets under the Normal Conditions Case.....	478
Figure 5-10. Velocity under the Abnormal Conditions Case (y,z).....	479
Figure 5-11. Velocity under the Abnormal Conditions Case (y,z).....	480
Figure 5-12. Streamlines from Inlets and to Outlets under the Abnormal Conditions Case.....	481
Figure 5-12a. Stream Lines From Inlet #1 Through Rack #5.....	482
Figure 5-13. Rod Heat Balance.....	484
Figure H5-1. SFP Model.....	500
Figure H5-2. Loss coefficient in Racks.....	501
Figure H5-3. Temperature Distribution under the Normal Conditions Case (x,y).....	506
Figure H5-4. Temperature Distribution under the Normal Conditions Case (y,z).....	507
Figure H5-5. Temperature Distribution under the Abnormal Conditions Case (x,y).....	508
Figure H5-6. Temperature Distribution under the Abnormal Conditions Case (y,z).....	509
Figure H5-7. Velocity under the Normal Conditions Case (x,y).....	510
Figure H5-8. Velocity under the Normal Conditions Case (y,z).....	511
Figure H5-9. Streamlines from Inlets and to Outlets under the Normal Conditions Case.....	512
Figure H5-10. Velocity under the Abnormal Conditions Case (x,y).....	513

Figure H5-11. Velocity under the Abnormal Conditions Case (y,z) 514
Figure H5-12. Streamlines from Inlets and to Outlets under the Abnormal Conditions Case.. 515
Figure H5-13. Rod Heat Balance 517

1. DYNAMIC LOAD ANALYSIS FOR SPENT FUEL RACKS IN THE SPENT FUEL POOL

1.1 INTRODUCTION

1.1.1 Purpose

The purpose of this document is to analyze the dynamic behavior and to present the structural analysis of Spent Fuel High Density Fuel Storage Racks (FSR) for the Spent Fuel Pool located in the Fuel Building (FB) of the ESBWR.

The layout of the FSR and the associated base plates is shown in Figure 1-1. The FSR are structures fabricated from stainless steel and borated stainless steel plates forming cells to house the spent fuel assemblies. The FSR are freestanding racks on the floor of the Spent Fuel Pool at EL -10000. The analysis evaluates the ten-year fuel storage configuration. Twenty (20) FSR will be located in the Spent Fuel Pool, providing a total of 3504 storage spaces. Two sizes of FSR are analyzed: 15x12 cell and 14x12 cell.

The configuration being analyzed consists of the 20 FSR joined to each adjacent FSR with link devices which couple the horizontal displacements. Two levels of links are analyzed between racks. At the lower level, the feet of adjacent FSR are coupled in the both horizontal directions with a bearing pad resting on the pool floor liner. At the upper level, the corners of four adjacent FSR are coupled in both horizontal directions with an assembly crossarm. For the external FSR, only two FSR are coupled in both the upper and lower levels.

The first part of this report develops a detailed analysis of one FSR by considering the most conservative analysis loads and boundary conditions. A detailed stress state of the different parts of the FSR is then obtained.

The second part of this report covers the evaluation of the dynamic behavior of the FSR as a freestanding structure, which is influenced by the surrounding FSR. Also analyzed are the link conditions between FSR and the hydrodynamic effects of the submergence in the pool water. The maximum displacements of the FSR and impact load reactions considering the freestanding boundary conditions are then obtained.

A design requirement of the analysis is to ensure that no interaction occurs between the FSR and pool walls (ID 4).

1.1.2 Scope

The scope of this document covers the design principles, load analysis, and justification of the configuration of the FSR assembly.

The analysis includes the results of the relative displacements between the FSR feet and the pool floor liner (sliding and uplifting), the maximum reactions between the FSR feet and the pool floor (through the lower bearing pad), and the maximum transmission forces between two FSRs at both the upper and lower links. In addition, the maximum lateral forces between fuel

assemblies and the top of FSR cell, and the maximum vertical forces between fuel assemblies and the FSR base plate, are also obtained.

The analysis includes the results of the maximum stresses on the different parts of the FSR structure and the different welds. These maximum stresses are compared with the maximum allowable stresses. In addition, the maximum stresses in the plates of the link devices is calculated.

The structural evaluation of the spent fuel assemblies enclosed in the FSR is not within the scope of this document, but their geometric and dynamic properties have been taken into account in the FSR analysis.

The structural evaluation of the pool liner is not within the scope of this report. The maximum loads on the liner are provided for pool liner evaluation.

The structural evaluation of the FSR against accidental equipment drop and fatigue analysis is not within the scope of this document.

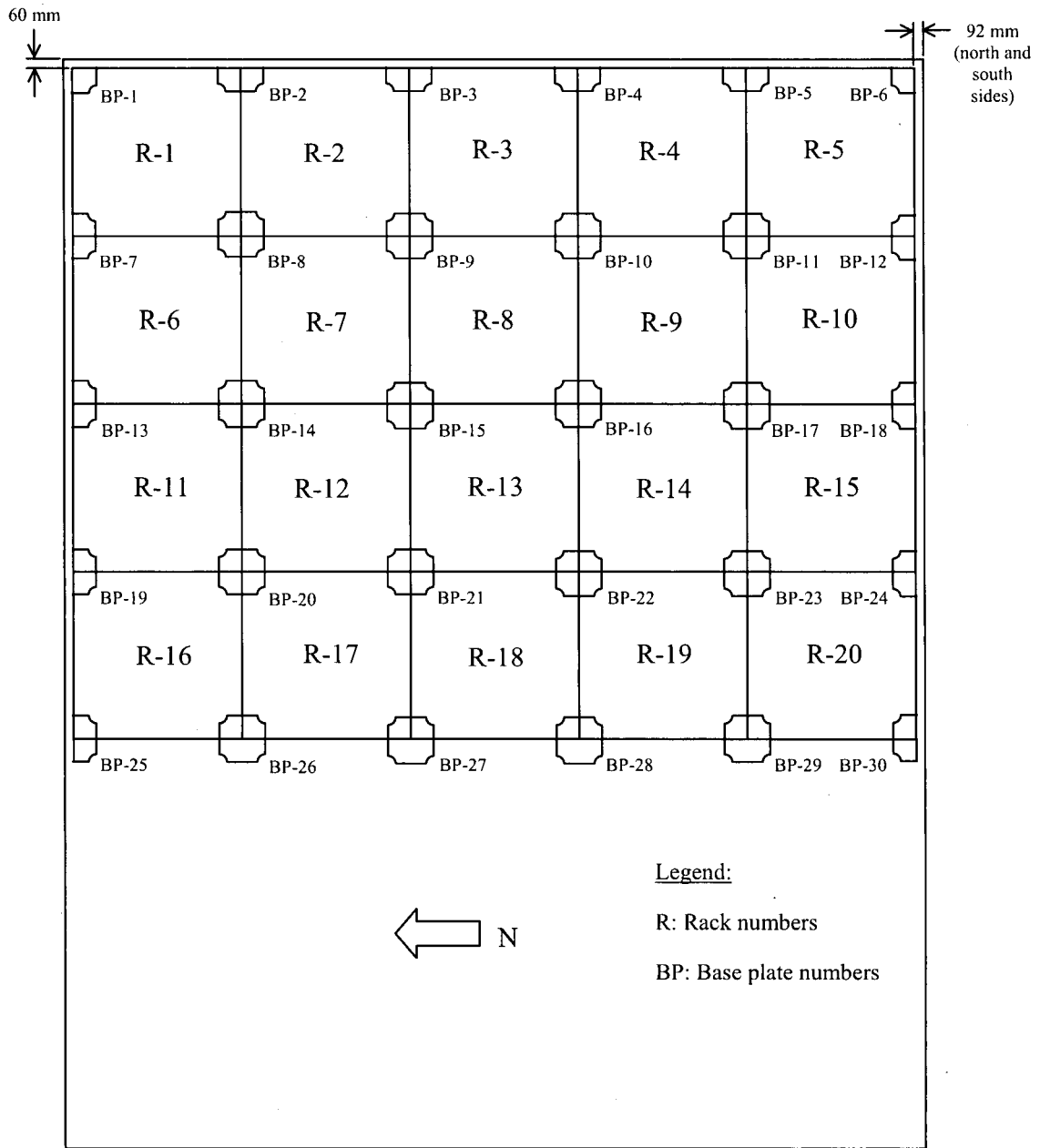


Figure 1-1. Layout of Fuel Support Racks and Base Plates

1.2 INPUT DATA

Table 1-1
List of Document Input Data (ID)

No.	Source Document			Requirement/Data	Status
	No.	Issue	Title		
1	5926.D200	03	Rack Assembly Drawing (Type-15x12)	Geometry.	V
2	5926.D210	03	Rack Base Plate (Type-15x12)	Geometry, Materials	V
3	5926.D220	00	Rack Cutting Drawing Sheet (Type-15x12)	Geometry, Materials	V
4	26A7032	4	Fuel Storage Rack Design Specification	Design Codes. Design Requirements. Fuel assembly weight. Fuel handling loads. Applicable Response Spectra and damping. Loading Combinations. Spent Fuel Pool Water Temperatures. Fuel assembly properties: weight, axial area and moment of inertia.	V
5	26A6552	4	Fuel Storage Equipment Requirement Specification	Stress free temperature	V
6	5926.D100	05	Rack Layout at Spent Fuel Building	Rack layout. Distance between racks and distance to the walls Pool dimensions.	V
7	105E3908	03	General Arrangement. ESBWR Nuclear Island	Plant axes	V
8	55926ATN02	01	ESBWR Fuel Building Pool Bottom Synthesized SSE accelerations time histories	SSE Acceleration time histories	V
9	5926.D600	00	Rack Assembly Drawing (Type-14x12)	Geometry	V
10	5926.D610	00	Rack Base Plate (Type-14x12)	Geometry, Materials	V

Table 1-1
List of Document Input Data (ID)

No.	Source Document			Requirement/Data	Status
	No.	Issue	Title		
11	5926.D620	00	Rack Cutting Drawing Sheet (Type-14x12)	Geometry, Materials	V
12	5926.D120	02	Bearing Pads Layout	Geometry, Materials	V
13	5926.D700	00	Assembly Crossarm	Geometry, Materials	V
14	30-July-2008	-	Email from GEH to ENSA; ESBWR fuel assemblies frequency and accidental impact matters	Fuel assembly axial frequency	V

1.3 SUMMARY OF RESULTS

Table 1-2 summarizes the enveloping maximum displacements and forces for the FSR, obtained from the dynamic analysis.

**Table 1-2
Maximum Displacements and Forces Summary**

Displacement/Force	Horizontal	Vertical
Relative displacement between FSR foot and pool floor (mm)	39.5 (N-S direction) 36.1 (E-W direction)	26.0
Force by FSR foot between bearing pad and pool floor (kN)	Shear 1344	Compression 1843
Relative horizontal displacement between FSR top and pool wall (mm)	39.5 (N-S direction) 48.9 (E-W direction)	-
Force between two FSRs at the lower link device (kN)	1306	-
Force between two FSRs at the upper link device (kN)	1227	-
Relative displacement between fuel and FSR (mm)	10 (at top)	3.7
Force between fuel (all assemblies) and FSR (kN)	1017 (at top) 814 (at bottom)	1708
Global bending moment on the FSR base plate (kN·m)	1645 (E-W axis) 2176 (N-S axis)	-

Table 1-3 summarizes the critical stress results obtained from the analysis of the FSR and the comparison with the allowable values in accordance with the design code (Reference 3).

Table 1-3
FSR Main Stresses Summary

Steel Plates	Stress (MPa)	Stress Limit (MPa)	Ratio
10 mm thick Enveloping Plate	226	292.8	0.77
10 mm thick Enveloping Plate Welds	163	198.6	0.82
7 mm thick Upper Level Plates	227	292.8	0.78
7 mm thick Upper Level Plate Welds	91	198.6	0.46
Fuel Support Base Plate	274	292.8	0.94
20 mm thick Base Plate Stiffener Plates	208	292.8	0.71
20 mm thick Base Plate Stiffener Plate Welds	136	198.6	0.68
Foot Cylindrical Nut	253	292.8	0.86
Foot Cylindrical Nut Welds	141	198.6	0.71
Nut Thread	107	198.6	0.54
Lower Links (Bearing Pad)	363	419.9	0.86
Upper links (Assembly Crossarm)	927	1049.7	0.88

Table 1-3a summarizes the enveloping maximum reactions by bearing pad in the pool floor liner.

Table 1-3a
Pool Floor Liner Maximum Reactions

Shear (kN)	Compression (kN)
1398	1843

1.4 ANALYSIS SUMMARY

Section 1.4.1 presents a brief description of the FSR.

Section 1.4.2 presents a brief description of the FSR analysis methodology.

Section 1.4.3 presents the properties of the FSR materials.

Section 1.4.4 indicates the applicable design code to analysis of the FSR.

Section 1.4.5 describes the different load cases which apply to the FSR analysis.

Section 1.4.6 presents the load combinations applied for the FSR analysis.

Section 1.4.7 gives the allowable stress limits used in the FSR analysis.

Section 1.5 presents the response spectrum analyses of the FSR detailed model.

Section 1.6 presents the transient dynamic analysis of the 20-FSRs global simplified model.

Section 1.7 presents the local stress analysis of the FSR.

Section 1.8 presents the total stress results in the FSR.

Section 1.9 presents the stresses in the link devices.

1.4.1 Spent Fuel High Density Storage Rack Description

The FSRs support and protect the stored fuel assemblies. The FSRs are structures made of stainless steel and borated stainless steel plates, forming 15x12 (or 14x12) cells to house the spent fuel assemblies. The FSR are located in the Spent Fuel Pool within the Fuel Building and are freestanding on the pool floor at EL -10000.

A detailed description of the FSRs is shown in the assembly and detail drawings of the FSR (IDs 1, 2 and 3 for the 15x12 array, and IDs 9, 10 and 11 for the 14x12 array).

The main dimensions of the FSR are 2542x2038 mm for the 15x12 array, 2374x2038 for the 14x12 array, and 3846 mm in height for both sizes. Different plate thicknesses are used in the FSR: 10 mm for enveloping stainless steel (SS) plates, 3.4 mm for the internal borated stainless steel (BSS) plates, 7 mm for SS plates of the top level of cells, and 20 mm for the support base SS plate and the reinforcing stiffener plates.

The enveloping plates and the top level plates are welded together. The internal BSS plates are not welded, but are slotted to allow assembly between perpendicular plates that form the cells. The assembly is welded around the perimeter of the base plate, which is stiffened underneath with reinforcing plates in both orthogonal directions. The FSR is supported on its four bottom-corner feet, each of which is made of a 150 mm diameter and 230 mm high cylinder (nut) housing a M110 screw inside. The screw acts to level the FSR and regulate its height.

The FSR have 15 mm thick spacer plates welded to the corners of the 10 mm enveloping plate at the upper elevation. The FSR have 9 mm spacer plates welded to the border of the base plate at

the lower elevation. The thickness of the spacer plates could be adapted to adjust to construction tolerances, and the lower spacer plates are eliminated in the sides close to the wall.

Each FSR is able to store 180 (15x12) or 168 (14x12) spent fuel assemblies.

1.4.1.1 Rack Layout at Spent Fuel Pool

Drawing ID 6 depicts the FSR layout in the spent fuel pool to accommodate ten years of spent fuel plus a full-core offload. It shows twenty (20) FSRs (twelve of the 15x12 size, and eight of the 14x12 size), arranged in four (4) rows running N-S and five (5) rows running E-W. This layout provides storage capacity for 3504 fuel assemblies.

The layout distance between the FSR 10 mm thick enveloping plates is 33 mm in both directions, N-S and E-W. The layout distance between the FSR lower spacer plates is 3 mm in both directions. The layout distance between the FSR upper spacer plates is 3 mm in both directions.

At the north and south walls, the minimum gap distance between a FSR base plate and the pool wall liner is 101 mm. At the east wall, the minimum gap distance between a FSR base plate and the pool wall liner is 69 mm. At the north and south walls, the minimum layout distance between a FSR upper spacer plate and the pool wall liner is 92 mm. At the east wall, the minimum layout distance between a FSR upper spacer plate and the pool wall liner is 60 mm.

The distance between FSR and the west wall is considerably higher (greater than six meters).

Drawing ID 12 depicts the lower links (bearing pads) layout. The typical lower link device is a 40 mm thick bearing plate with eight triangular vertical plates linking the foot of four adjacent FSRs. Close to the pool wall, the device is reduced to link only two FSRs. In the four corner racks a single bearing pad to only support the corner foot is installed.

Drawing ID 13 depicts the upper links (assembly crossarm). The typical upper link device is a 15 mm thick plate crossarm connecting the spacer plates welded to the upper corners of four adjacent FSRs. Close to the pool wall, the device becomes a "T" to connect only two adjacent FSRs. In the four upper corner without adjacent rack there is no upper link device.

All the plates forming the link devices are made of stainless steel.

1.4.2 Analysis Methodology Description

In the layout presented in ID 6, each FSR rests on the bearing pads, which rest on the pool floor. Each FSR will be linked to the adjacent FSRs, but not to the pool walls.

The FSRs may be full, partially filled, or empty of fuel assemblies, but they are always submerged in the pool water.

In the event of dynamic excitations caused by an earthquake (SSE), the FSRs may be displaced due to a low friction value between the bearing pads and the pool floor. In contrast, high friction values may cause one of the feet to lift off the bearing pads and the subsequent impact effect when the FSR settles back into place.

These structures are simply supported under their own weight, unrestricted except for friction (freestanding), and involve the phenomenon of the fluid-structure interaction. Studying their behavior requires complex analytical techniques with non-linear contact elements, and small integration time steps to achieve the convergence of the solution. This (along with the many possibilities for filling the FSRs with the fuel assemblies, uncertainty of the applied friction factors, and various parameters of convergence involved in the process) makes it necessary to adopt simplifying hypotheses so that these calculations can be performed efficiently.

The analysis procedure is divided into two stages:

- In the first stage, a detailed study of the characteristics (masses and frequencies) of the FSR is performed. A detailed model of the FSR is developed and a response spectrum analysis is performed by considering the conservative load state given by combining the response spectra from the different dynamic events (SSE, LOCA, SRVD). This linear analysis of the detailed model of the FSR is performed considering the four FSR feet with displacements restrained. Stresses are calculated for the various parts of the FSR.
- In the second stage, a simplified model of the FSR (15x12) is created utilizing beams and lumped masses, adjusting their dynamic properties to the ones obtained with the detailed model. Proportionality relations are used to obtain the dynamic properties of 14x12 FSR simplified model. A global model of the 20 FSRs is then created, representing the position of the FSRs in the pool. Once all possible contacts, link conditions and hydrodynamic couplings have been simulated, a transient dynamic analysis is performed for the acceleration time-histories obtained from the SSE response spectra. This non-linear analysis of the 20 FSR global model is performed considering the freestanding boundary conditions. Relative displacements, reactions, and transmission forces are calculated.

The global bending moments acting in the FSR are calculated for the above calculation stages. The maximum global stresses in the FSR are then obtained by multiplying the stresses in the detailed model by the ratio coefficient of the moments between both calculation stages. The local stresses caused by impact loads are added to the global stress to calculate the total stresses in the FSR.

1.4.3 Materials

The FSR plates are manufactured using SA-240 Type 304L stainless steel and ASTM A 887 Type 304B7 borated stainless steel. The FSR feet material is SA-479 Type 304L for nuts and SA-564 Type 630 for screws. The material of the upper link devices (assembly crossarms) is SA-693 Type 630 H1075. The lower link devices (bearing plates) material is SA-240 Type 304L.

The mechanical properties of type 304L stainless steel are greater than those of type 304, so the mechanical properties of the latter are used. The mechanical test requirements of ASTM A 887 Type 304B7 are similar to those for SA-240 Type 304, therefore the mechanical properties of type 304 are used.

Table 1-4 shows the material properties in accordance with Section II, Part D of the ASME Code (Reference 2). Material properties at 250°F are assumed based on ID 4.

Table 1-4
Material Properties at 250°F (121.1°C)

Material	E	ρ	α	S_y	S_u	S
	(MPa)	(kg/m ³)	(1/°C)	(MPa)	(MPa)	(MPa)
SA-240 Type 304L ⁽¹⁾	1.9·10 ⁵	7850	16.4·10 ⁻⁶	162.7	472.9	134.1
ASTM A 887 Type 304B7 ⁽¹⁾	1.9·10 ⁵	7850	16.4·10 ⁻⁶	162.7	472.9	134.1
SA-479 Type 304L ⁽¹⁾	1.9·10 ⁵	7850	16.4·10 ⁻⁶	162.7	472.9	134.1
SA-564 Type 630 H1075	1.91·10 ⁵	7850	11.3·10 ⁻⁶	779.1	999.7	285.4
SA-693 Type 630 H1075	1.91·10 ⁵	7850	11.3·10 ⁻⁶	779.1	999.7	285.4

⁽¹⁾ Properties shown are those corresponding to type 304 stainless steel

ρ = Density (Reference 1)

E = Modulus of elasticity (Reference 2, Table TM-1)

α = Coefficient of thermal expansion (Reference 2, Table TE-1)

S_y = Yield strength (Reference 2, Table Y-1)

S_u = Ultimate strength (Reference 2, Table U)

S = Maximum allowable Stress (Reference 2, Table 1A)

1.4.4 Design Code

Stresses in the structural components of the FSR shall not exceed the allowable stress limits given in the ASME B&PV Code, Section III, Division I, Subsection NF (Reference 3), according to ID 4.

1.4.5 Analysis Loads

The following loads are considered in the analysis of the FSR:

D	Dead Weight + Buoyancy
P _f	Upward force by postulated stuck fuel assembly
T _o	Differential temperature induced loads (normal or upset conditions)
T _a	Differential temperature induced loads (abnormal design condition)
SSE	Safe Shutdown Earthquake
SRVD	Safety Relief Valve Discharge
LOCA	Loss of Coolant Accident
L _R	Lifting FSR during installation

1.4.5.1 Dead Weight + Buoyancy (D)

In addition to the dead weight of the FSR and fuel assemblies, it is also necessary to consider buoyancy, that is, the thrust that the water applies on the FSR and the immersed fuel. This effect is taken into account in the analysis by reducing the gravity acceleration by a reducing factor obtained as follows (calculation based on 15x12 size):

FSR steel mass: $M_s = 2554 + 1069 + 1885 + 4836 = 10344 \text{ kg}$ (see Table 1-6)

Steel volume: $V_s = M_s / \rho = 10344 / 7850 = 1.3 \text{ m}^3$

Fuel assemblies, mass: $M_f = 245 * 180 = 44100 \text{ kg}$ (ID 4)

Fuel assemblies, volume: $V_f = 0.03 * 180 = 5.4 \text{ m}^3$ (ID 4)

Total mass: $M_T = 10344 + 44100 = 54444 \text{ kg}$

Total volume: $V_T = 1.3 + 5.4 = 6.7 \text{ m}^3$

This means a total of 6700 kg of water mass moved. Thus, the reducing factor is:

$$F = (54444 - 6700) / 54444 = 0.876$$

And the reduced gravity acceleration is obtained from

$$g' = 0.876 \cdot g = 8.6 \text{ m/s}^2$$

1.4.5.2 Fuel Handling Loads (P_f)

The FSR will be designed to withstand a pull-up force of 17.79 kN, which is necessary in the event of a fuel assembly or grapple device hanging up during removal and a horizontal force of 4.45 kN being applied at the top of the FSR (ID 4).

1.4.5.3 Differential Temperature Induced Loads (T_o , T_a)

The maximum Spent Fuel Pool water temperatures are 48.9°C (120°F) in normal conditions and 60°C (140°F) in abnormal conditions (ID 4).

The stress-free temperature is assumed to be 15.5 °C (ID.5).

The maximum FSR width is $L=2560$ mm in the N-S direction and $L=2056$ mm in the E-W direction (ID 1).

The maximum FSR thermal expansion, conservatively assuming a maximum temperature of 121.1°C (250°F)(ID 4), is:

$$\text{N-S direction: } \alpha \cdot L \cdot \Delta T = 16.4 \text{ E-6} \cdot 2560 \cdot (121.1 - 15.5) = 4.4 \text{ mm}$$

$$\text{E-W direction: } \alpha \cdot L \cdot \Delta T = 16.4 \text{ E-6} \cdot 2056 \cdot (121.1 - 15.5) = 3.6 \text{ mm}$$

The FSRs are submerged in water and can expand in the vertical and horizontal directions without restrictions. The minimum distance between bottom FSR spacer plates is 3 mm < 4.43 mm; this means one FSR could contact the FSR adjacent in the event that the water temperature will reach 121.1 °C. Since there is enough distance to the pool walls, each FSR can expand, pushing each other. In this case the contact forces between FSRs are considerably lower than the impact forces during seismic. Therefore no thermal induced stresses are calculated in the present analysis. The temperature gradient in the vertical direction is considered negligible for structural analysis.

Maximum displacement due to the seismic event is 39.5 mm at the north and south walls and 48.9 mm at the east wall (Table 1-2). If the maximum pool temperature were to occur simultaneously with a seismic event, the resulting total displacement is calculated as:

$$\text{North-south walls: } 39.5 \text{ mm} + 2.5(4.4) - 2(3) = 44.5 \text{ mm} < 92 \text{ mm}$$

$$\text{East wall: } 48.9 \text{ mm} + 2(3.6) - 1.5(3) = 51.6 \text{ mm} < 60 \text{ mm}$$

As these displacements are less than the minimum horizontal distance to the pool walls, the FSRs will not impact the walls.

1.4.5.4 Safe Shutdown Earthquake (SSE)

The FSR will be designed to withstand the SSE loads. Applicable response spectra are specified in ID 4 Appendix A30. A structural damping value of 4% for SSE conditions is used (Reference 16).

For the linear analysis of the detailed model, the SSE response spectra are input directly. Figures A-1a, A-1b and A-2 show the spectra applied in the three directions.

For the non-linear analysis of the global model, the earthquake spectra are converted into three floor acceleration time histories (one for each direction)(ID 8). The acceleration versus time in the X, Y, and Z directions for SSE is shown in Figures A-3, A-4 and A-5. The total duration of the transient is 16 sec.

1.4.5.5 Safety Relief Valve Discharge (SRVD)

The FSR will be designed to withstand the SRVD loads specified in ID 4 Appendix A30. A structural damping value of 4% for SRVD conditions is used (Reference 16).

For the linear analysis of the detail model, the SRVD response spectra are input directly. Of the two applicable response spectra in the horizontal directions, X (N-S) and Y (E-W), the enveloping one (the X-direction) is chosen and conservatively applied in both horizontal directions. Figures A-6 and A-7 in show the spectra applied in both horizontal and vertical directions.

For the reasons explained in section 1.6.1, acceleration time histories for SRVD are not obtained.

1.4.5.6 Loss of Coolant Accident (LOCA)

The FSR will be designed to withstand the LOCA loads specified in ID 4 Appendix A30. A structural damping value of 4% for LOCA conditions is used (Reference 16).

For the linear analysis of the detail model, the LOCA response spectra are input directly. Of the two applicable response spectra in the horizontal directions, X (N-S) and Y (E-W), the enveloping one (the X-direction) is chosen and conservatively applied in both horizontal directions. Figures A-8 and A-9 in show the spectra applied in both horizontal and vertical directions.

For the reasons explained in Section 1.6.1, acceleration time histories for LOCA are not obtained.

1.4.5.7 Lifting FSR During Installation (L_R)

The FSR is verified to withstand the lifting load during installation. The FSR is supported in the four base plates holes indicated in ID 1 and ID 2.

1.4.6 Load Combinations

The load combinations shall be per Appendix D of SRP 3.8.4 (Reference 8), according to ID 4. Table 1-5 shows the envelope load combinations that will be used for the design of the FSR, based on the aforementioned load combinations. Conservatively, SRVD and LOCA have also been computed in the linear analysis of the detailed model.

**Table 1-5
Load Combinations**

Level A: $D + P_f$
Level D: $D + SSE + SRVD + LOCA + T_a$ (response spectrum analysis, see Section 1.5.3)
Level D: $D + SSE + T_a$ (transient dynamic analysis, see Section 1.6.5)

$D + P_f$ is a Level B load combination, but it is conservatively assumed as a Level A load combination.

1.4.7 Stress Limits

The stress limits are taken from ASME B&PV Code, Section III, Division I, Subsection NF (Reference 3) and Appendix F (Reference 4) corresponding to the Design by Analysis for Class 3 Plate and Shell Type Supports.

Definitions of terms are provided below as per References 3 and 4:

P_m – membrane stress (MPa)

P_b – bending stress (MPa)

τ – shear stress (MPa)

S – allowable stress (MPa)

S_u – tensile strength (MPa)

S_y – yield strength (MPa)

Base metal Type 304L (with mechanical characteristics of Type 304)

Level A Conditions (NF-3251.1 and Table NF-3552(b)-1)

$$P_m \leq S = 134.1 \text{ MPa}$$

$$P_m + P_b \leq 1.5 \cdot S = 201.1 \text{ MPa}$$

$$\tau \leq 0.6 \cdot S = 80.4 \text{ MPa}$$

Level D Conditions (Appendix F, F-1332)

$$P_m \leq \text{Minimum of } 1.2 S_y \text{ or } 0.7 S_u = 195.2 \text{ MPa}$$

$$P_m + P_b \leq 1.5 \cdot (P_m \text{ limit}) = 292.8 \text{ MPa}$$

$$\tau \leq 0.42 \cdot S_u = 198.6 \text{ MPa}$$

For compressive stresses, see Appendix B1.

Welds

Level A Conditions (NF-3324.5 and Table NF-3324.5(a)-1)

Fillet welds:

$$\text{Shear Stress on effective throat} \leq 0.3 \cdot S_u^{(1)} = 165.4 \text{ MPa}$$

$$\text{Shear Stress on base metal} \leq 0.4 \cdot S_y = 65.1 \text{ MPa}$$

Tension or compression parallel to axis of weld \leq Same as base metal

⁽¹⁾ Base metal tensile strength range between 489.5 MPa and 551.5 MPa (71 and 80 ksi), minimum weld metal tensile strength, 551.5 MPa (80 ksi).

Level D Conditions (Appendix F, F-1332)

$$\text{Shear Stress} \leq 0.42 S_u = 198.6 \text{ MPa}$$

Tension or compression parallel to axis of weld \leq Same as base metal

Links metal Type 630 H1075

Level D Conditions (Appendix F, F-1332)

$$P_m \leq \text{Minimum of } 1.2 S_y \text{ or } 0.7 S_u = 699.8 \text{ MPa}$$

$$P_m + P_b \leq 1.5 \cdot (P_m \text{ limit}) = 1049.7 \text{ MPa}$$

$$\tau \leq 0.42 \cdot S_u = 419.9 \text{ MPa}$$

1.5 DETAILED MODEL: RESPONSE SPECTRUM ANALYSIS

A detailed finite element model (FEM) for the 15x12 FSR is developed and analyzed with the response spectrum analysis method.

1.5.1 Assumptions

The calculation procedure used for the present stress report has been performed based on the following assumptions of FSR behavior:

- It is assumed that the material of the structure (stainless steel) has a linear elastic behavior within the field of the small displacement/deformations.
- FSRs with a 100% fuel load are assumed. Since the fuel assemblies have a large mass but do not provide any stiffness to the assembly, it is reasonable to expect that this case will present the maximum deformations and stresses.
- For the fuel assembly the dry weight is assumed to be 540 lbs (245 kg) and the net immersed weight to be 474 lbs (215 kg) (ID 4).
- The fuel assembly shall be conservatively considered rigid enough that it is only supported in the horizontal direction on the top part of the cells, in addition to the support base plate.
- The water mass acting in the vertical direction is not considered because the water could flow inside each one of the cells in the vertical direction.
- The inner BSS plates are considered non-structural components, but they are included in the analysis model so that a representative dynamic behavior can be obtained (e.g., by avoiding local modes in the 10 mm envelope plates). Section 1.5.2.1 shows how including the inner BSS plates in the model has little impact on the value of the first two global bending eigenfrequencies of the FSR.
- The hydrodynamic coupling between adjacent FSRs and between FSRs and the walls, through the water around them is conservatively disregarded in order to simplify the calculations. Another conservative assumption will take into account the added mass included in the models, without considering neighboring FSRs or walls.

1.5.2 FSR Detail Model

A detailed FEM for the analysis of the FSR is built with ANSYS 10.0 (Reference 7). A description of the FEM (see Figures A-10 and A-11) follows:

- The external boundary plates of the FSR (see Figure A-12) are modeled with a 10 mm thick stainless steel plate (Reference 7, SHELL 63 ANSYS elements). These boundary plates are welded in all of their plate connections and are considered a continuous plate without cuts in the model.
- The upper level FSR cells (6A and 6L, see ID 3) (see Figure A-13) are modeled with 7 mm stainless steel plates (Reference 7, SHELL 63 ANSYS elements). These plate cells are welded to each other and are considered connected plates with common nodes in the model.
- The borated stainless steel plates (see Figure A-14) are modeled with 3.4 mm plates (Reference 7, SHELL 63 ANSYS elements). These plates have slots that are used to connect two perpendicular plates. The plate slots are modeled considering the cut in the plate with different nodes overlapped. The connections between perpendicular slotted plates are represented by coupled unions in the corresponding horizontal direction between nodes of the two connected plates (see Figure A-14a).

- The base support of the FSR is modeled with stainless steel plates (Reference 7, SHELL 63 ANSYS elements). This support includes the 20 mm thick fuel support plate with 92 mm diameter holes for each one of the fuel storage cells (see Figure A-15), the vertical 20 mm thick stiffeners welded under the plate in the two horizontal directions (see Figure A-16), and the four FSR feet (nut & screw) (see Figures A-16 and A-17). For the modal analysis with the detailed model, the three displacements are restricted in the node located on the screw axes at the floor level for each of the four FSR foot screws.
- 50% of the fuel mass ($245 \times 180 \times 0.5 = 22050$ kg) acting in each of the two horizontal directions is distributed in the nodes of the model located in the FSR upper end, and the other 50% (22050 kg) is distributed in the nodes of the model located in the base support plate. 100% of the mass (44100 kg) will apply vertically in the nodes of the model located in the base support plate. These fuel assembly masses are included as lumped masses (Reference 7, MASS 21 ANSYS elements) in the model.
- The internal water mass acting in the two horizontal directions is distributed in the inner nodes of the model. The node mass distribution is proportional to the volume associated with each inner node. The internal water mass is obtained from the total FSR internal volume where the fuel volume and metal volume is subtracted. Metal mass is ANSYS calculated. Each fuel assembly has a volume of 0.03 m^3 . The internal water masses are included as lumped masses (Reference 7, MASS 21 ANSYS elements) in the model.
- The external water added mass has been obtained from Reference 6, where the added mass of a rigid rectangular block is calculated using the equation $m_w = k \cdot \rho \cdot \text{Volume}$, where (ρ) is the water density and (k) is a factor with an approximate value of ($k=0.5$) considering the rectangular dimensions of the FSR. The added mass of the FSR is approximately 9280 kg. This added mass corresponds to the following assumptions: (a) infinitely stiff prism, (b) moving as a stiff solid body (c) in an infinite mass of water. The external water added masses are included in the model multiplying the internal water masses by a factor.
- The mass of the SS plates is accounted for by means of its density. The BSS plates are modeled without mass density in order to avoid local frequencies of the borated plates produced by the vibration of their free ends between two slots. There are a high number of these local frequencies with values around 55-60 Hz. These frequencies are not significant because they do not move any significant amount of mass and could be filtered in the spectral analysis. For this same reason, the horizontal water masses are not introduced in perpendicular direction to the borated plates and are applied only in horizontal longitudinal direction. The borated stainless steel plate masses in horizontal directions are included in the model multiplying the internal water masses by a factor. The borated stainless steel plate masses in vertical directions are included as additional lumped masses (Reference 7, MASS 21 ANSYS elements) in the model .
- The coordinate system adopted in the FEM is the right-hand Cartesian coordinate system. The X-direction represents the N-S direction, the Y-direction represents the E-W direction, and the Z-direction is vertical (ID 7).
- The units used in the FSR FEM are kilograms for mass, meters for length, and seconds for time.

The FSR mass considered in the analysis model is presented in Table 1-6:

Table 1-6
Mass Breakdown

Component	Horizontal Mass (kg)	Vertical Mass (kg)
10 mm thickness enveloping SS Plates	2554	2554
7 mm thickness upper level SS Plates	1069	1069
Support Plates (Base, Stiffeners and Nuts & Screws)	1885	1885
BSS Plates	4836	4836
Fuel Assemblies (180 elements)	44100	44100
Internal Water	12047	-
External Added Water	9280	-
Total Mass	75771	54444

1.5.2.1 Structural Considerations on the Borated Plates

To obtain the most realistic FSR eigenfrequencies, it is necessary to include the inner BSS plates in the model. The purpose is to avoid the local eigenfrequencies of the outer plates of the FSRs.

To show that the inner BSS plates do not contribute any additional stiffness to the dynamic behavior of the main two horizontal bending frequencies of the FSRs, the results of the two main horizontal frequencies have been analyzed for the detail model anchored in the base plate and compared with the frequencies obtained by formula for a cantilever beam.

The characteristics of the analyzed beam are:

- Total length of the beam $\Rightarrow L = 3.587$ m.
- Inertia of the beam is given by the 10 mm boundary plate of the FSR. The sections of the rectangular boundary plates have a geometry of 2520x2016x10mm, with inertia values of $\Rightarrow I_x = 6.48E-2$ m⁴, $I_y = 9.07E-2$ m⁴.
- Horizontal water mass \Rightarrow Inner water mass of 12047 kg plus external added water mass of 9280 kg, uniformly distributed along the beam length.
- Dead weight of the FSR $\Rightarrow 2554 + 1069 + 4836 = 8459$ kg uniformly distributed along the beam length.
- The water mass and dead weight of the FSR are applied as a single load $\Rightarrow w = 8303$ kg/m.
- Fuel mass $\Rightarrow \frac{1}{2}$ fuel mass ($W = 22050$ Kg) located at the free end of the beam.

- The two main bending frequencies of the beam, computed from (Reference 9),

$$f_{x,y} = \frac{1.732}{2\pi} \times \left(\frac{E \times I_{y,x}}{W \times L^3 + 0.236 \times w \times L^4} \right)^{1/2}$$

are calculated to be 26.4 Hz and 31.2 Hz

Analyzing the FSR with the finite element model, the following first frequencies are obtained:

- Upper FSR breathing mode \Rightarrow 21.93 Hz
- First bending mode \Rightarrow 22.01 Hz
- Second bending mode \Rightarrow 23.67 Hz
- Local mode of the upper part of the FSR \Rightarrow 32.59 Hz

Comparing calculated results with the detail model analysis results, the main bending frequencies of the FSR are seen to be higher in the analysis by formula than in the detail analysis \Rightarrow (26.4 Hz > 22.01 Hz) and (31.2 Hz > 23.67 Hz). Therefore, it is reasonable to consider that the inner borated plates do not contribute any additional substantial stiffness to the main frequencies of the FSRs. Even so, the results from the detail model include some local frequencies of the FSRs that could have an impact on the final results and should therefore be taken into account.

In conclusion, the inner borated stainless steel plates must be considered as non-structural components, even though the finite element model includes them, so that more accurate results can be obtained.

1.5.3 Response Spectra Analysis Methodology Description

Static and dynamic loads are considered in the analysis. The response spectra analysis method is used to analyze the dynamic behavior of the detailed model.

The static load case (D) is resolved by structural static analysis by applying the reduced gravity acceleration g' (see Section 1.4.6.1).

The fuel handling load case (P_f) is analyzed by applying the forces prescribed in section 1.4.6.2 in a central node of the 7 mm thick upper level plates (see Figure A-18).

The lifting load during installation load case (L_R) is analyzed by applying the gravity acceleration g , and supporting the FSR in the appropriate four base plate holes.

The dynamic load cases are resolved by response spectrum analysis. Prior to the response spectrum analysis, a modal analysis is performed to determine the natural frequencies and mode shapes of the FSR. The subspace method is used for mode extraction in modal analysis. One hundred (100) eigenfrequencies are requested in the modal analysis.

Once the eigenfrequencies of the model have been determined with the modal analysis, a response spectra analysis for each dynamic event (SSE, SRVD and LOCA) is performed for each of the three directions, X, Y, and Z.

The input response spectra are represented by twenty (20) or fewer points (ANSYS limitation), beginning at a frequency lower than the lowest obtained in the FSR modal analysis.

Once the response spectrum analysis has been performed for each direction, the modal responses are combined according to the grouping method established in Regulatory Guide 1.92 (Reference 5).

More than 90% of the mass is considered in each direction for the modal combination (see Table 1-8). Therefore, no consideration has been taken to compute the missing mass associated with the eigenmodes not intervening in the modal combination (see the note in Section 1.10).

Since the load combination includes multiple dynamic loads, these loads are combined by the SRSS method.

1.5.4 Results of the Response Spectra Analysis

The ANSYS output for response spectrum analyses is included in Appendix B.

1.5.4.1 Model Results

Table 1-7 represents the main eigenfrequencies that have the highest effective mass as obtained from the modal analysis. Additionally, two lower frequency modes (modes 3 and 4) are included as examples of typical “breathing” mode shapes that do not contribute to the solution response. These eigenfrequencies represent the dominant frequencies for the structural analysis. The complete data set for all eigenmodes is shown in Appendix B.

Figures A-19 through A-26 in Appendix A show the deformed shapes of these eigenmodes.

Table 1-7
Main Eigenfrequencies

Mode	Frequency (Hz)	Effective Mass (kg)	Description	Figure in Appendix A
1	13.78	46688	Y Bending	A19
2	16.69	48144	X Bending	A20
3	17.53	-	Breathing	A21
4	30.17	-	Breathing	A22
12	44.08	45684	Base Plate Bending	A23
15	53.20	24015	2nd Y Bending	A24
17	54.15	18621	2nd X Bending	A25
36	97.41	6121	2nd Base Plate Bending	A26

Table 1-8 indicates the amount of mass considered in the modal combination and the corresponding percentage with respect to the total mass.

Table 1-8
Combined Effective Masses

Event	X direction		Y direction		Z direction	
	Mass (kg)	(%)	Mass (kg)	(%)	Mass (kg)	(%)
SSE	74837 (98.7%)		73356 (96.8%)		53388 (98.0%)	
LOCA	74838 (98.7%)		74174 (97.9%)		53413 (98.1%)	
SRVD	73818 (97.4%)		73047 (96.4%)		53429 (98.1%)	

1.5.4.2 Deformation Results

The maximum deformation obtained at the top of the FSR for the most unfavorable load combination (level D) is 2.0 mm for horizontal X-direction, 3.2 mm for horizontal Y-direction, and 0.9 mm for the vertical Z-direction (see Figures A-27, A-28 and A-29, respectively).

1.5.4.3 Plate Stress Results

The stress results obtained for the different load combinations are checked in the most critical sections of the different plates of the FSR.

1.5.4.3.1 10 mm Thick Enveloping Plate

The maximum stresses obtained for the 10 mm thick enveloping plate compared with the corresponding allowable stresses are presented in Table 1-9, where:

S_Z ≡ Vertical direction (Z) membrane stress

S_H ≡ Horizontal direction (X or Y) membrane stress

S_{HZ} ≡ Shear stresses on the plane of the plate

Bending stresses across the plate thickness are negligible and are classified as secondary stresses; however, other directions of the plate contain primary bending stresses that are included in the stress analysis results.

Table 1-9
10 mm Thick Enveloping Plate Maximum Stress Results

Service Level	Calculated Stress (MPa)	Allowable Stress (MPa)
Level A Conditions	$S_z = 16.9$	201.1
	$^{(1)}S_H = 2.9 \times 2 = 5.8$	201.1
	$S_{HZ} = 4.9$	80.4
Level D Conditions	$S_z = 157$ (Figure A-30)	292.8
	$^{(1)}S_H = 31 \times 2 = 62$	292.8
	$S_{HZ} = 39$	198.6

Notes:

- ⁽¹⁾ The horizontal stresses (general membrane) are multiplied by a factor of (2) in order to take into account that the 10 mm plates are not continuous in the vertical direction because they are slotted to support the borated plates.

The maximum stresses obtained for the horizontal welds compared with the corresponding allowable stresses are presented in Table 1-10.

Table 1-10
10 mm Thick Enveloping Plate Welds Maximum Stress Results

Weld Location	Calculated Stress (MPa)	Allowable Stress (MPa)
Horizontal lower 6 mm fillet ⁽¹⁾ welds (160-168). Near the corners (3 cells)	$(93) \times (10/6) \times (168/160) = 163$	198.6
Horizontal lower 6 mm fillet ⁽¹⁾ welds (100-168). Mid-plate	$(41) \times (10/6) \times (168/100) = 115$	198.6
Horizontal 6 mm butt ⁽²⁾ welds (150-168). Near the corners (3 cells). Level Z=356mm	$(56) \times (10/6) \times (168/150) = 104$	195.2
Horizontal 6 mm butt ⁽²⁾ welds (100-168). Mid-plate. Level Z=356mm	$(30) \times (10/6) \times (168/100) = 85$	195.2
Horizontal 6 mm butt ⁽²⁾ welds (150-168). Near the corners (1 cells). Level Z=712mm	$(47) \times (10/6) \times (168/150) = 88$	195.2
Horizontal 6 mm butt ⁽²⁾ welds (100-168). Mid-plate. Level Z=712mm	$(39) \times (10/6) \times (168/100) = 109$	195.2
Horizontal 6 mm butt ⁽²⁾ welds (100-168). Level Z=1068mm	$(37) \times (10/6) \times (168/100) = 104$	195.2
Horizontal 6 mm butt ⁽²⁾ welds (100-168). Level Z=1424mm	$(29) \times (10/6) \times (168/100) = 80$	195.2
Horizontal 3 mm butt ⁽²⁾ welds (100-168). Level Z=1780mm	$(22) \times (10/3) \times (168/100) = 123$	195.2
Horizontal 3 mm butt ⁽²⁾ welds (100-168). Level ⁽³⁾ Z=2136mm	$(16) \times (10/3) \times (168/100) = 91$	195.2

Notes:

- (1) The stress used to check the fillet welds is the maximum shear stress on the weld localization, given by $(S_z^2 + S_{HZ}^2)^{1/2}$
- (2) The stress used to check the butt welds is the maximum stress in the vertical direction on the weld localization (S_z)
- (3) Butt welds located at levels with ($Z > 2136$) have lower stresses than those at ($Z = 2136$) level, and the same 3 mm butt welds (100-168) will apply.

Sufficient stress margin is obtained for welds of the 10 mm thick plates, even with the conservative assumptions in the analysis. This margin is judged to be useful to absorb any small differences between the FEM and the actual structure. It should be taken into account that the integrity of the upper part of the FSRs is provided by the welds of the 10 mm plates (the plates themselves have low stresses).

1.5.4.3.2 7 mm Thick Upper Level Plates

The maximum stresses obtained for the 7 mm thick upper level plates compared with the corresponding allowable stresses are presented in table 1-11, where:

S_Z ≡ Vertical direction (Z) membrane stress

S_H ≡ Horizontal direction (X or Y) membrane stress

S_{HZ} ≡ Shear stresses on the plane of the plate

Bending stresses across the plate thickness are negligible and are classified as secondary stresses; however, other directions of the plate contain primary bending stresses that are included in the stress analysis results.

Table 1-11
7 mm Thick Upper Level Plates Maximum Stress Results

Service Level	Calculated Stress (MPa)	Allowable Stress (MPa)
Level A Conditions	$S_Z = 7.9$ (Figure A-31)	201.1
	$S_H = 3.6$	201.1
	$S_{HZ} = 1.1$	80.4
Level D Conditions	$S_Z = 17$	292.8
	$S_H = 42$ (Figure A-32)	292.8
	$S_{HZ} = 6.0$	198.6

The 7 mm thick plates are welded with a 3 mm fillet weld 30 mm in length, in each corner connection between perpendicular plates.

The maximum stress on these welds due to the pull-up force of 17.79 kN (section 1.4.6.2) is obtained assuming that this force is transmitted through the four fillet welds of one cell. That is, $S_{max} = 17790 / (4 \times 30 \times 3) = 49.4 \text{ MPa} < 65.1 \text{ MPa}$.

The maximum vertical force in a corner between perpendicular plates for level D conditions is 9292 N. Therefore, the maximum stress on the fillet weld is:

$$S_{\max} = 6223 \times 1.4142 / (30 \times 3) = 97.8 \text{ MPa} < 198.6 \text{ MPa.}$$

1.5.4.3.3 20 mm Thick Base Plate Stiffener Plates

The maximum stresses obtained for the 20 mm thick base plate stiffener plates and welds compared with the corresponding allowable stresses are presented in Table 1-12, where:

S_Z ≡ Vertical direction (Z) membrane stress

S_H ≡ Horizontal direction (X or Y) membrane stress

S_{HZ} ≡ Shear stresses on the plane of the plate

Bending stresses across the plate thickness are negligible and are classified as secondary stresses; however, other directions of the plate contain primary bending stresses that are included in the stress analysis results.

Table 1-12
20 mm Thick Base Plate Stiffener Plates Maximum Stress Results

Service Level and Weld Location	Calculated Stress (MPa)	Allowable Stress (MPa)
Level A Conditions	$S_Z = 13.9$	201.1
	$S_H = 15.5$	201.1
	$S_{HZ} = 5.6$	80.4
Level D Conditions	⁽¹⁾ $S_Z = 69$ (Figure A-33)	292.8
	$S_H = 46$	292.8
	$S_{HZ} = 48$	198.6
Welds ⁽²⁾ to base support plate. Near the corners (3 cells) 2x6 mm fillet weld (160–168)	$S_{\max} = 57 \times (20/12) \times (168/160) = 100$	198.6
Welds ⁽²⁾ to base support plate. Mid-plate, 2x6 mm fillet welds (100–336) 'maximum'	$S_{\max} = 15.1 \times (20/12) \times (336/100) = 85$	198.6

Notes:

- (1) Stress value linearized in section shown in Figure A-33
- (2) The stress used to check the fillet weld is the linearized shear stress on the weld localization, given by $(S_Z^2 + S_{HZ}^2)^{1/2}$

1.5.4.3.4 20 mm Thick Base Plate and Foot Cylindrical Nut

The maximum stress intensities obtained for the 20 mm thick base plate and in the foot cylindrical nut compared with the corresponding allowable stresses are indicated in Table 1-13.

Table 1-13

20 mm thick Base Plate and Cylindrical Feet Plate Maximum Stress Results (S.I.)

Service Level and Location	Calculated Stress (S.I.) (MPa)	Allowable Stress (MPa)
Level A Conditions. Base plate	22	201.1
Level D Conditions. Base plate	⁽¹⁾ 151 (Figure A-34)	292.8
Lifting Load. Base Plate	76 (Figure A-35)	201.1
Level A Conditions. Foot Cylindrical Nut	⁽²⁾ 18	201.1
Level D Conditions. Foot Cylindrical Nut	⁽³⁾ 147	292.8
Vertical 15 mm fillet welds between Foot Cylindrical Nut and 20 mm thick Stiffeners.	⁽⁴⁾ 141	198.6
Nut Thread	⁽⁵⁾ 62	198.6

Notes:

- (1) Stress value linearized in section shown in Figure A-34
- (2) Stress calculated as the vertical mass of the FSR (54444 kg, Table 1-6), divided by four times the nut section area ($\pi \cdot (150^2 - 115^2) / 4 = 7284.5 \text{ mm}^2$)
- (3) Stress calculated as the maximum vertical reaction load in the FSR foot ($R_Z = 1071 \text{ kN}$, Table 1-14), divided by the nut section area (7284.5 mm^2)

- (4) Stress calculated by $S_{max} = F_w / A_w = 433778 / (205 \times 15)$, where the value of the shear force in the weld is given by $F_w = (F_H^2 + F_Z^2)^{1/2}$
- (5) Stress calculated by $S_{max} = R_z / A_T = 1071000 / (100 \cdot \pi \cdot 110 / 2)$, where $R_z = 1071$ kN is the maximum vertical reaction load in the FSR foot (Table 1-14)

Stresses in the screw are enveloped for stresses in the cylindrical nut since the resistant section of the screw is higher and the strength properties of the screw material are better than the strength properties of the nut.

1.5.4.4 Global Bending Moments and Reactions on the FSR

Table 1-14 shows the reaction forces on each one of the four feet and the global bending moments acting at the level of the FSR support base plate.

Table 1-14
Global Bending Moments and Foot Reactions

Maximum Moments on the Base Plate (kN·m)	Maximum Force Reaction on a FSR Foot (kN)	
Horizontal Moment $\Rightarrow M_x = 2505$	Horizontal Force $\Rightarrow R_x = 364$	SRSS(R_x, R_y)= $R_H = 471$
Horizontal Moment $\Rightarrow M_y = 2354$	Horizontal Force $\Rightarrow R_y = 298$	
Vertical Moment $\Rightarrow M_z = 0$	Vertical Force $\Rightarrow R_z = 1071$	

1.5.5 (Deleted)

1.6 SIMPLIFIED AND GLOBAL MODELS, TRANSIENT DYNAMIC ANALYSIS

Simplified finite element models for each FSR are developed to build a 20 FSR global model used to analyze the dynamic behavior of the FSR assembly. The full transient dynamic analysis method is used. With these simplified models, the effect of the water can be taken into account less conservatively than in Section 1.5.

1.6.1 Assumptions

As discussed in Section 1.4.2 above, this type of analysis makes it necessary to make simplifications that facilitate the feasibility of the analyses. In the present stress report, the following assumptions are used:

- Of the countless numbers of possible fuel assembly fill levels, only two are contemplated: 100% (henceforth “full” FSR) and 0% (“empty” FSR).
- Regarding friction between the bearing pads and the pool floor, based on Reference 10, a mean value of 0.5 has been considered for the friction coefficient with a lower limit of 0.2 and an upper limit of 0.8.
- Since the bearing pads are linked extensions of the FSR feet in the horizontal directions, they are modeled as linked feet utilizing the corresponding contact area with the pool liner.
- Based on (Reference 12) and (Reference 13) only the SSE effects will be evaluated. There is no licensing basis for combining LOCA and SSE loads.
- It is assumed that the maximum temperature in accident case (250°F) is not simultaneous with the SSE load.

1.6.2 Fluid-Structure Interaction, Water Model

The transient dynamic analysis takes into account the effect of the water surrounding the outer walls of the FSR as well as the effect of the water surrounding the fuel assemblies within the cells. The dynamic coupling through the water is specifically determined by calculating the hydrodynamic masses. These masses are calculated by applying the thermal analogy (Reference 11). In the horizontal direction, the hydrodynamic mass couplings that exist between adjacent FSRs, between FSR and pool walls, and between the fuel assembly and the cell are calculated.

The hydrodynamic coupling effects in the vertical direction are negligible because the water could flow inside each cell in the vertical direction. Each cell is open at the top and bottom; therefore, there is a path for water between the nose of the fuel assembly and hole in the support base plate.

The following is assumed for the calculations:

- a. The movements are assumed to be small compared to the thickness of the wall of water.
- b. The fluid is assumed to be incompressible and nonviscous flow.
- c. The range of speeds in the fluid is less than 10% of the speed of sound in said fluid.
- d. Fluid damping is neglected.

The fluid in these conditions is considered to meet the potential theory, and is analogous with a stationary state of heat transmission where the hydrodynamic pressure is equal to the temperature range.

Disregarding local effects at the ends, a 2-D analysis can be performed considering the 2-D behavior at a generic elevation above the pool floor. The cross sections of the structural elements (racks) coupled by the fluid are considered non-deformable, i.e., they behave like rigid elements and impose their acceleration on the fluid as a boundary condition.

A 2-D pool water model of finite elements has been developed representing the pool water with the gaps that represent the FSR enclosures (Figure A-36). The water model was performed with ANSYS (Reference 7) and consists of 2-D thermal solid PLANE55 elements. This water model was used to calculate a steady heat state for the horizontal movements in the N-S direction. A unit acceleration is applied to one of the FSRs (heat flow in the thermal model of the analogy) and zero to the rest. The analysis is repeated 20 times, once per FSR, and an extra case is added with unit acceleration on the wall and zero in the 20 FSRs. This process is repeated for the E-W direction.

A similar cell water model was developed to study the interaction between the fuel assembly and the FSR cell, although it is much simpler since it only represents the water contained between each fuel assembly and its corresponding FSR cell (Figure A-37). In this case, only two heat cases are executed: one with unit acceleration in the fuel assembly and zero in the cell, and the other with unit acceleration in the cell and zero in the fuel assembly. In this case, the resultant coupled masses are valid for both N-S and E-W directions, given the double symmetry of the model.

The pressure forces are obtained from the temperature range, and are applied to the dynamic global model as hydrodynamic masses.

Figure A-38 presents the matrix of hydrodynamic masses per unit of length in the N-S direction for the set of FSRs. Figure A-39 presents the matrix of hydrodynamic masses per unit of length in the E-W direction for the set of FSRs. In these matrices, each column and row corresponds to each of the 20 FSRs, and the 21st row and column is for the pool walls.

Figure A-42 presents the matrix of hydrodynamic masses per unit of length in either horizontal direction for the fuel assembly-FSR cell coupling.

These hydrodynamic masses, once multiplied by their corresponding vertical length, represent the coupled hydrodynamic mass terms either between adjacent FSRs, between the FSR and the pool walls, or between the fuel assembly and the cell.

The diagonal terms of these matrices represent the added masses to be added to the dynamic global model and the off-diagonal terms are the inertial coupling terms.

Furthermore, to account for the outer FSR walls not being infinite and the water being able to flow through both the lower and upper parts, the coupled hydrodynamic mass terms are multiplied by a correction factor. The method for obtaining this correction factor is based on the reference "Analysis of the Fundamental Vibration Frequency of a Radial Vane Internal Steam Generator Structure" by E. Kiss (Reference 11).

For the FSR:

The equivalent radii are obtained:

$$A_{rack} = 2530 \cdot 2026 \text{ mm}^2 \qquad a = \sqrt{\frac{A_{rack}}{\pi}} = 1277 \text{ mm}$$

$$A_{water} = (2530 + 33) \cdot (2026 + 33) \text{ mm}^2 \qquad b = \sqrt{\frac{A_{water}}{\pi}} = 1296 \text{ mm}$$

$$a/b = 0.985$$

$$L = 3846 \text{ mm} \qquad L/a = 3.01$$

The correction factor for the FSR, obtained from Reference 11, is:

$$K_L = 0.67$$

For the fuel assembly:

$$A_{fuel} = 140^2 \text{ mm}^2 \qquad a = \sqrt{\frac{A_{fuel}}{\pi}} = 79 \text{ mm}$$

$$A_{water} = 161^2 \text{ mm}^2 \qquad b = \sqrt{\frac{A_{water}}{\pi}} = 90.8 \text{ mm}$$

$$a/b = 0.87$$

$$L = 3587 \text{ mm} \qquad L/a = 45.4$$

The correction factor obtained from Reference 11 for the fuel assembly is:

$$K_L = 0.99$$

1.6.3 Single FSR Simplified Model

Based on the detailed model developed in Section 1.5.2, a simplified finite element model for the FSR is built with ANSYS 10.0 (Reference 7), adjusting its dynamic properties to those of the detailed model. Proportionality relations are used to obtain the dynamic properties of the 14x12 FSR.

The simplified model is composed of 2-D elastic beam BEAM3 elements, and concentrated mass MASS21 elements.

A vertical line of beam elements represents the enveloping plate of the FSR cells. Two couples of horizontal lines X-shaped of high-stiffness beam elements are used: one is located at the

bottom level of the vertical beam to transmit the load to the four feet, which are also modeled by beam elements; the other couple is located at the top level of the vertical beam to represent the four upper corners of the FSR.

Mass elements reproducing the mass of borated stainless steel plates, the mass of the 180 fuel assemblies, and the mass of internal water and external water are concentrated on the connection nodes of the beam elements simulating the FSR cells.

The area properties and inertias of the beam have been adequately adjusted so that the model will have the same eigenfrequencies as the detail model in Section 1.5.2. In particular, high-precision adjustments were made for the first bending eigenfrequencies in each horizontal direction and the first vertical eigenfrequency, which together represent the low-frequency eigenmodes that excite the most mass.

Table 1-15 shows the values for mass and frequencies in the simplified model and in the detail model. Correct adjustment of all values is affirmed.

**Table 1-15
Comparison of Models**

Concept	Detail Model	Simplified Model
Horizontal Mass (kg)	75771	75771
Vertical Mass (kg)	54444	54444
1st Bending Frequency (Hz). E-W Direction	13.78	13.78
1st Bending Frequency (Hz). N-S Direction	16.69	16.69
1st Axial Frequency (Hz). Vertical Direction	44.09	44.08

The mass, area and inertia ratios between the 15x12 size and 14x12 size FSRs are used to calculate the dynamic properties of FSR 14x12.

1.6.4 20-FSR Global Model

Based on the simplified models of the single FSRs, a 3-D global model of the 20 FSR representing the position of each FSR in the pool is built. The global model consists of 3-D elastic beam BEAM4 elements, 3-D point-to-point contact CONTACT52 elements and mass matrix MATRIX27 elements. Its particulars are described in the paragraphs below.

The sketch in Figure A-43 represents the single FSR simplified model used to build the 20-FSR global model.

The sketch in Figure A-44 represents a simplified view of one of the N-S direction rows of the global model.

The concentrated masses corresponding to the external water mass are eliminated from the global model, since the coupled hydrodynamic masses are now entered through MATRIX27 elements. All terms of the coupling matrices between every two adjacent FSRs or between an FSR and the wall are applied by node pairs, once factored for the corresponding length and the correction factor $K_L=0.67$ calculated in section 1.6.2.

The concentrated masses of the fuel assemblies are eliminated since a new vertical line of beam elements is added (superimposed over the existing one), thereby representing the whole set of 180 (or 168) fuel assemblies. The structural characteristics of these beams are adjusted based on their first axial frequency, their axial area, and their moment of inertia (ID 4 and ID 14).

The terms of the matrix of fuel assembly-FSR cell coupling are entered through MATRIX27 elements applied by node pairs, once factored for the corresponding length and the correction factor $K_L=0.99$ calculated in section 1.6.2

The fuel beam is coupled in the horizontal directions with the FSR beam at the bottom node. One vertical contact element is located at this same location to evaluate whether the fuel uplifts then impacts with a vertical load when it falls and strikes the base plate.

Between the FSR beam top node and fuel beam top node, four (4) horizontal contact elements (one for each N, S, E and W direction of displacement) are located to evaluate any potential lateral impacts that may be produced against the FSR cells. The stiffness of these contacts has been estimated by a local analysis made with the detailed model, applying local loads at the top cell level.

Inserted between adjacent FSRs are horizontal coupling conditions to represent the linking devices. At the bottom level, the feet of four adjacent FSR have coupling conditions in both horizontal directions. For the external FSR only two FSR are coupled. At the upper level, the corner nodes of each adjacent FSR are coupled in both horizontal directions (N-S or E-W). For the external FSR, only two FSR are coupled. Transmission forces in the coupled nodes are calculated to provide input for the design of the linking devices as well as to calculate local stresses in the FSR plates. The 3-D analysis considers the forces and rack movements in all planes, not simply the X, Y, and Z directions. Therefore, phenomena such as pivoting, tilting or toppling, and sliding of racks are analyzed.

For FSRs adjacent to wall, contact elements simulating the gap existing at these points are added between the corresponding corner and the pool wall to determine whether the FSR interacts with the wall.

Each FSR bearing plate also has a contact element to simulate the FSR sliding and uplifting with respect to the pool floor. A high stiffness value is entered, and the friction coefficient is implemented as applicable in each case.

Figures A-46 and A-47 present the ANSYS global model for the 20 FSR. In Figure A-46 the hydrodynamic couplings have been removed for clarity.

1.6.5 Transient Dynamic Analysis Methodology Description

The dynamic behavior of the FSRs as freestanding structures is analyzed by means of the full transient dynamic method with the ANSYS program using the 20-FSR global model described in the previous section.

Based on the acceleration time-histories corresponding to the SSE (ID 8), double integration is used to generate the displacement histories to be applied at the nodes of the global model that represent the pool. Figures A-3, A-4, A-5 present the acceleration time-histories applicable in each direction (N-S, E-W, and vertical). Figures A-48, A-49, and A-50 show the equivalent displacement time-histories for each direction as well.

Because of the highly non-linear behavior of the system, a very small time interval between load steps must be used to make the calculation process converge correctly. Intervals of 0.005 s were used, which means 3200 load steps for a 16-s transient.

The dead weight and the buoyancy effect are considered during the process by application of a constant vertical downward acceleration value of 8.6 g (reduced gravity acceleration, see Section 1.4.5.1).

The method used to implement damping in a full transient dynamic analysis was Rayleigh's proportional damping, which is expressed as follows:

$$[C] = \alpha[M] + \beta[K]$$

where α and β are the damping constants to be calculated, and $[C]$, $[M]$, and $[K]$ are the matrices of damping, mass, and stiffness of the system, respectively. The values of α and β are not known directly, but are calculated from modal damping ratios, ξ_i . ξ_i is the ratio of actual damping to critical damping for a particular mode of vibration, i . If ω_i is the natural circular frequency of mode i , α and β satisfy the relation:

$$\xi_i = \alpha/2\omega_i + \beta\omega_i/2$$

To specify both α and β for a given damping ratio ξ , it is commonly assumed that the sum of the α and β terms is nearly constant over a range of frequencies. Therefore, given ξ and a frequency range f_i to f_j , two simultaneous equations can be solved for α and β , where the solutions are:

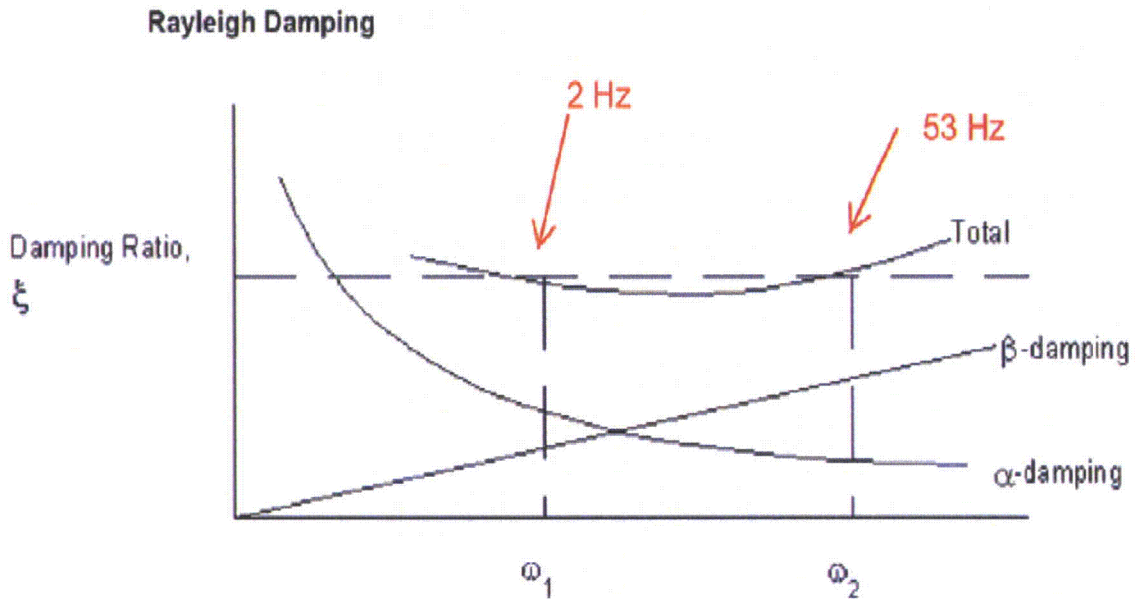
$$\alpha = 4 \cdot \pi \cdot \xi \cdot f_i \cdot f_j / (f_i + f_j)$$

$$\beta = \xi / (\pi \cdot (f_i + f_j))$$

The range of frequencies is selected based on the most important frequencies obtained from the modal analysis of the detailed model. Important frequencies are considered to be those which excite the largest effective mass. Applying $\xi = 0.04$ (4%) for the SSE, and considering a range of frequencies from 2 Hz up to 53 Hz (see Section 1.5.4), the following results are obtained:

$$\alpha = 0.96876 ; \beta = 0.2315 \cdot 10^{-3}$$

The range of 2 Hz to 53 Hz is considered bounding for the dominant mode shapes. The lower boundary of 2 Hz is significantly lower than the first eigenfrequency (13.78 Hz) and no significant excitation of effective mass occurs beyond 54.15 Hz. For eigenfrequencies between 2 Hz and 53 Hz, the effective damping ratio is less than 4%, and provides conservative results (see curve below). See Appendix B for the Participation Factor Calculation tables.



This value is applied in all the scenario-cases studied (see Section 1.6.5.1).

1.6.5.1 Scenario-Cases in Study

Based on assumptions given in 1.6.1 and Reference 14, the following scenario-cases are analyzed:

- Case C-1: All FSRs with friction coefficient of $\mu=0.5$ except R-16⁽¹⁾ with $\mu=0.2$ and R-20 with $\mu=0.8$. All FSRs full.
- Case C-2: All FSRs with friction coefficient of $\mu=0.5$ except R-16⁽¹⁾ with $\mu=0.2$ and R-20⁽²⁾ with $\mu=0.8$. All FSRs full, except R-01, R-08, R-16, and R-20 empty.
- Case C-3: All FSRs with friction coefficient of $\mu=0.2$. All FSRs full.
- Case C-4: All FSRs with friction coefficient of $\mu=0.8$. All FSRs full.
- Case C-5: All FSRs with friction coefficient of $\mu=0.5$. All FSRs empty.
- Case C-6: All FSRs with friction coefficient of $\mu=0.2$. All FSRs empty.

Notes:

- (1) R-16 with $\mu=0.2$ means that bearing pads BP-19, BP-20, BP-25 and BP-26 have $\mu=0.2$, that is to say: the four feet of R-16, the two West-feet of R-11, the two North-feet of R-17 and the North-West-foot of R-12 have $\mu=0.2$ in the 20-FSR global model.
- (2) R-20 with $\mu=0.8$ means that bearing pads BP-23, BP-24, BP-29 and BP-30 have $\mu=0.8$, that is to say: the four feet of R-20, the two West-feet of R-15, the two South-feet of R-19 and the South -West-foot of R-14 have $\mu=0.8$ in the 20-FSR global model.

The displacement time-histories for each direction are applied simultaneously at the nodes of the global model that represent the pool floor and walls for each of the six scenario-cases.

Once the responses are obtained for the scenario-cases analyzed, the most critical results of the 3200 loads step analysed for each case are extracted.

1.6.6 Results of the Transient Analysis

Table 1-16 shows the maximum displacement and force results for each of the six scenario-cases analysed.

Table 1-16
Maximum Displacements and Forces

Concept	Case C-1	Case C-2	Case C-3	Case C-4	Case C-5	Case C-6
Relative horizontal displacement (N-S) between FSR foot and pool floor (mm)	28.4	19.2	39.5 (A51)	3.1	5.4	10.9
Relative horizontal displacement (E-W) between FSR foot and pool floor (mm)	17.6	5.3	19.6	4.6	25.5	36.1 (A52)
Relative vertical displacement between FSR foot and pool floor (mm)	2.8	2.9	0.6	13.4	26.0 (A53)	25.5
Horizontal force by FSR foot between bearing pad and pool floor (kN)	727	708	88	1344 (A54)	264	106
Vertical force by FSR foot between bearing pad and pool floor (kN)	1020	958	440	1843 (A55)	529	557
Relative horizontal displacement (N-S) between FSR top and pool wall (mm)	28.6	19.5	39.5 (A56)	16.1	6.1	16.4
Relative horizontal displacement (E-W) between FSR top and pool wall (mm)	18.6	7.2	19.8	18.0	32.9	48.9 (A57)
Horizontal force between two FSRs at the lower link device (kN)	691	908	342	1306 (A58)	551	491
Horizontal force between two FSRs at the upper link device (kN)	557	1168	303	1227 (A59)	1173	922

Table 1-16
Maximum Displacements and Forces

Concept	Case C-1	Case C-2	Case C-3	Case C-4	Case C-5	Case C-6
Relative horizontal displacement (N-S&E-W) between top fuel and FSR top cells (mm)	10	10	10	10 (A60)	-	-
Relative vertical displacement between bottom fuel and FSR base plate (mm)	1.0	1.5	1.1	3.7 (A60a)	-	-
Horizontal force between fuel (all assemblies) and FSR top cells (kN)	1017 (A60b)	996	957	962	-	-
Horizontal force between fuel (all assemblies) and FSR base plate (kN)	813	833	711	814 (A61)	-	-
Vertical force between fuel (all assemblies) and FSR base plate (kN)	1220	1334	1147	1708 (A62)	-	-
Bending moment (N-S) on the FSR base plate (kN·m)	1017	1063	557	1645 (A63)	864	933
Bending moment (E-W) on the FSR base plate (kN·m)	1366	1480	722	2176 (A64)	842	961

Note: (n) means “see Figure n”

The horizontal forces between two FSRs at the upper or the lower link devices must be assumed as a tensile force through the linking plates when a FSR pulls the adjacent FSR. The horizontal forces between two FSRs at the upper or the lower link devices must be assumed as a compression force between the spacer plates of both FSRs when a FSR pushes the adjacent FSR.

Table 1-16 defines the maximum relative displacement between FSR and north-side walls as 39.5 mm. Given that the minimum gap between the FSR and north-south walls is 92 mm, it is ensured that no rack-to-pool wall interaction occurs at the north-south walls and therefore satisfies that design requirement. The maximum relative displacement between FSR and the east wall is 48.9 mm. Given that the minimum gap between the FSR and the east wall is 60 mm, it is ensured that no rack-to-pool wall interaction occurs at the east wall and therefore satisfies that design requirement.

Table 1-17 summarizes the maximum displacements and force results enveloping the six scenario-cases. The table also indicates the case from which the bounding value is obtained.

Generally, the most critical case regarding reaction loads in the pool floor liner, fuel impact loads and forces in the link devices, seems to be C-4, when the racks are fully loaded and the higher friction coefficient governs.

Table 1-17
Summary of Enveloping Maximum Displacements and Forces

Displacement/Force	Horizontal	Vertical
Relative displacement between FSR foot and pool floor (mm)	UB _X =39.5 (N-S) [C-3] UB _Y =36.1 (E-W) [C-6]	UB _Z =26 [C-5]
Force between bearing pad and pool floor (kN)	Shear RB _H =1344 [C-4]	Compression RB _Z =1843 [C-4]
Relative horizontal displacement between FSR top cell and pool wall (mm)	UT _X =39.5 (N-S) [C-3] UT _Y =48.9 (E-W) [C-6]	-
Force between two FSRs at the lower link device (kN)	LB _H =1306 [C-4]	-
Force between two FSRs at the upper link device (kN)	LT _H =1227 [C-4]	-
Relative displacement between fuel and FSR (mm)	UF _H =10 (N-S & E-W) [C-1,2,3,4]	UF _Z =3.7 [C-4]
Force between fuel (all assemblies) and FSR (kN)	at top FT _H =1017 [C-1] at bottom FB _H =814 [C-4]	FB _Z =1708 [C-4]
Bending moment on the FSR base plate (kN•m)	M _X =1645 [C-4] M _Y =2176 [C-4]	-

Note: [C-n] means “from scenario-case C-n”

1.6.7 Pool Floor Liner Reactions

Table 1-17a shows the maximum bounding reactions in the pool floor liner for each scenario-case. In addition, the bearing pad where the maximum value occurs is also indicated. The reactions are calculated for each bearing pad taking into account that the impacts from the FSRs sharing the bearing pad take place simultaneously.

Table 1-17a.
Pool Floor Liner Maximum Reactions

Case	Shear (kN)	Compression (kN)
C-1	956 (BP-23)	1349 (BP-22)
C-2	866 (BP-23)	1571 (BP-21)
C-3	250 (BP-21)	1250 (BP-21)
C-4	1398 (BP-15)	1843 (BP-3)
C-5	264 (BP-11)	529 (BP-11)
C-6	107 (BP-21)	557 (BP-15)

1.6.8 (Deleted)

1.7 LOCAL STRESS ANALYSIS

In this section the local stresses on the FSR structure produced by the impact forces during the SSE transient analysis are analyzed. Local stress is defined as the maximum concentrated stress obtained for the member being analyzed.

The stresses from impact forces are analyzed using the detail FSR model defined in Section 1.5. Four enveloping impact load cases are analyzed as follows:

- Case I-1: FSR top cells in compression. The FSR top cells are pushed by the four adjacent FSRs + the maximum impact forces between fuel assemblies and FSR top cells.
 - Maximum impact forces on the FSR top spacer plates. The force considered is the maximum force from Table 1-17 ($LT_H=1227$ kN). This value is applied eight times with a pressure load on the eight compression areas where the top spacer plates are located (see Figure A-65).

- Maximum impact forces between fuel assemblies and FSR top cells. The force considered is the maximum force from Table 1-17 ($FT_H=1017$ kN). It is conservatively assumed that this maximum impact occurs simultaneously in both horizontal directions. Therefore the force is applied in both horizontal directions with a pressure load on the last upper cell elements (7 mm thick cell plates and 10 mm thick enveloping plates, see Figure A-65).
- Case I-2: FSR top cells in tension. The FSR top cells are pulled by the four adjacent FSRs + the maximum impact forces between fuel assemblies and FSR top cells.
 - Maximum impact forces on the FSR top spacer plates. The force considered is the maximum force from Table 1-17 ($LT_H=1227$ kN). The force is transmitted between two FSRs through the assembly crossarm to the lateral spacer plate welded to the FSR. Therefore the force is applied eight times with a shear load distributed in the nodes corresponding to the perimeter weld of the spacer plate (see Figure A-66).
 - Maximum impact forces between fuel assemblies and FSR top cells. The force considered is the maximum force from Table 1-17 ($FT_H=1017$ kN). It is conservatively assumed that this maximum impact occurs simultaneously in both horizontal directions. This force is applied in both horizontal directions with a pressure load on the last upper cell elements (7 mm thick cell plates and 10 mm thick enveloping plates, see Figure A-66).
- Case I-3: FSR base plate in compression. The FSR base plate is pushed by the four adjacent FSRs + the maximum impact forces between fuel assemblies and FSR base plate.
 - Maximum impact forces on the FSR bottom spacer plates. The force considered is the maximum force from Table 1-17 ($LB_H=1306$ kN). Since this value is obtained in a corner of the FSR, it is assumed that twice this value will be distributed on the bottom spacer plate. This value is applied four times with nodal loads distributed on each border of the base plate (see Figure A-67).
 - Maximum impact forces between fuel assemblies and FSR base plate. The forces considered are the maximum forces from Table 1-17 ($FB_H=814$ kN, $FB_Z=1708$ kN). It is conservatively assumed that the maximum horizontal impact occurs simultaneously in both horizontal directions. These forces are applied in the three directions by means of nodal forces on the circular holes of the fuel support base plate (see Figure A-67).
- Case I-4: FSR base plate in tension. The FSR base plate stiffeners are pulled by the vertical plates of the lower link + the maximum impact forces between fuel assemblies and FSR base plate.
 - Maximum impact forces on the FSR base plate stiffeners. The force considered is the maximum force from Table 1-17 ($LB_H=1306$ kN). The force is transmitted between two FSRs through the bearing pad and vertical plates to the corresponding base plate stiffener. Therefore the force is applied eight times with

nodal loads distributed in the nodes of the stiffener where the impact occurs (see Figure A-68).

- Maximum impact forces between fuel assemblies and FSR base plate. The forces considered are the maximum forces from Table 1-17 ($FB_H=814$ kN, $FB_Z=1708$ kN). It is conservatively assumed that the maximum horizontal impact occurs simultaneously in both horizontal directions. These forces are applied in the three directions by means of nodal forces on the circular holes of the fuel support base plate. In Figure A-68, the base plate is removed for clarity. Impact forces from fuel assemblies are the same than in the Case I-3 (see Figure A-67) .

In addition, since the local stresses are analyzed with the detailed model of the FSR 15x12, all the impact force values are factorized by the ratio 15/14, in order to envelope that some maximum impact could occur in some of the 14x12 array FSR.

The maximum stresses calculated for each of the load cases I-1, I-2, I-3 and I-4 are shown in Table 1-18 and Figures A-69 to A-76. Local stress is the maximum concentrated stress obtained.

Table 1-18
Local Stresses in FSR from Impact Loads

Load Case and Location	Calculated Stress (MPa)	Allowable Stress (MPa)
Case I-1. 10 mm thick enveloping plates	80 (Figure A-69)	292.8
Case I-1. 7 mm thick upper level plates	188 (Figure A-70)	292.8
Case I-2. 10 mm thick enveloping plates	226 (Figure A-71)	292.8
Case I-2. 7 mm thick upper level plates	86 (Figure A-72)	292.8
Case I-3. Base Plate	⁽¹⁾ 135 (Figure A-73)	292.8
Case I-3. Base Plate Stiffeners	207 (Figure A-74)	292.8
Case I-4. Base Plate	124 (Figure A-75)	292.8
Case I-4. Base Plate Stiffeners	⁽²⁾ 144 (Figure A-76)	292.8

Notes:

(1) Stress value linearized in section shown in Figure A-73

(2) Stress value linearized in section shown in Figure A-76

1.8 TOTAL STRESS RESULTS

The structural integrity of the cell assembly (from the 20 mm thick base plate to the FSR top) during the dynamic events is assured by the integrity of the 10 mm thick enveloping plate and the 7 mm thick upper level plates.

The structural integrity of the lower part of the FSR (from the floor level to the base plate) during the dynamic events is assured by the integrity of the base plate, the 20 mm thick transversal stiffeners and the cylindrical nuts of the FSR feet.

The maximum global stresses in the plates and the welds of the FSR are given mainly by the maximum global bending moments acting at the level of the base plate.

The two maximum global bending moments (M_X , M_Y) on the base plate have been calculated from the response spectrum analysis for the fixed FSR and from the transient dynamic analysis for the freestanding FSR. The ratio coefficient f_M of the global bending moments from both analyses is obtained and used to calculate the maximum stresses on the FSR considering the freestanding boundary conditions, as follows:

$$f_M = \max((M_{X_{table1-17}}/M_{X_{table1-14}}), (M_{Y_{table1-17}}/M_{Y_{table1-14}})) = \max(1645/2505 ; 2176/2354)=0.925$$

$$\text{Stress}(\text{freestanding FSR}) = f_M \cdot \text{Stress}(\text{fixed FSR})$$

Table 1-19 summarizes the maximum total stresses for the freestanding FSR considering the seismic event SSE. The stresses are calculated multiplying the maximum global stresses from the response spectrum analysis by the factor $f_M=0.925$. In addition to these stresses, the local stresses from the local impacts are indicated or added as appropriate.

The maximum global stress in the 10 mm thick enveloping plates and welds calculated in Section 1.5.4.3.1 is located at the lower level of plates (Figure A-30). The maximum local stress from the impact loads calculated in Section 1.7 is located at the upper level of 10 mm thick enveloping plates (Figure A-71). Global and local stresses are not added for that reason.

The maximum global stress in the 7 mm thick upper level plates calculated in Section 1.5.4.3.2 (Figure A-32) and the maximum local stress from the impact loads calculated in Section 1.7 (Figure A-70) could be simultaneous. Global and local stresses are added for that reason.

The maximum global stress in the 20 mm thick base plate calculated in Section 1.5.4.3.4 (Figure A-34) and the maximum local stress from the impact loads calculated in Section 1.7 (Figure A-73) are very concentrated stresses that could be simultaneous although do not occur in the same point. Global and local stresses are conservatively added.

The maximum global stress in the 20 mm thick base plate stiffeners calculated in Section 1.5.4.3.3 is located at the corner areas, close to the foot (Figure A-33). The maximum local stress from the impact loads calculated in Section 1.7 is located at the bottom part of the central stiffeners (Figure A-74), but also high stress level occurs close to the foot (Figure A-76). Global and local stresses are added for that reason.

The maximum global stress in the base plate stiffener welds calculated in Section 1.5.4.3.3 Table 1-12 and the maximum local stress from the impact loads indicated in Table 1-19 are conservatively added, even though the global and local stresses do not occur at the same point.

The maximum stresses on the cylindrical nuts of the FSR feet are given mainly by the maximum vertical reactions in each one of the four feet of the FSR. The horizontal forces coming from the lower links are mainly transmitted through the base plate stiffeners up to the base plate. Therefore the total stress in the nut is directly the maximum compression force divided by the cross section area. For the same reason the total stress in the 15 mm fillet welds between the nut and the stiffener plates is conservatively taken as it results from the response spectrum analysis. The total shear stress in the nut thread directly represents the maximum compression force divided by the thread section area.

Stresses in the screw are enveloped by stresses in the cylindrical nut since the resistant section of the screw is higher than the resistant section of the nut, and the strength properties of the screw material are greater than the strength properties of the nut.

Table 1-19
FSR Total Stress Results

Location	Stress (MPa)	Stress Limit (MPa)
10 mm thick Enveloping Plate (lower level)	$157_{(Table\ 1-9)} \cdot f_M = 145$	292.8
10 mm thick Enveloping Plate (upper level)	$226_{(Table\ 1-18)}$	292.8
10 mm thick Enveloping Plate Welds	$163_{(Table\ 1-10)} \cdot f_M = 151$	198.6
7 mm thick Upper Level Plates	$42_{(Table\ 1-11)} \cdot f_M + 188_{(Table\ 1-18)} = 227$	292.8
7 mm thick Upper Level Plate Welds	$97.8_{(Section\ 1.5.4.3.2)} \cdot f_M = 91$	198.6
Fuel Support Base Plate	$151_{(Table\ 1-13)} \cdot f_M + 135_{(Table\ 1-18)} = 274$	292.8
20 mm thick Base Plate Stiffener Plates (central area)	$207_{(Table\ 1-18)}$	292.8
20 mm thick Base Plate Stiffener Plates (corner area)	$69_{(Table\ 1-12)} \cdot f_M + 144_{(Table\ 1-18)} = 208$	292.8
20 mm thick Base Plate Stiffener Plate Welds (out of corner area)	$85_{(Table\ 1-12)} \cdot f_M + ^{(1)}34 = 113$	198.6
20 mm thick Base Plate Stiffener Plate Welds (corner area)	$100_{(Table\ 1-12)} \cdot f_M + ^{(2)}43 = 136$	198.6
Foot Cylindrical Nut	$^{(3)}253$	292.8
Foot Cylindrical Nut Welds	$141_{(Table\ 1-13)}$	198.6
Nut Thread	$^{(4)}107$	198.6

Notes:

- (1) The stress value used to check the fillet weld is the linearized shear stress on the weld localization, given by $(S_Z^2 + S_{HZ}^2)^{1/2}$, for the Case I-3.
- (2) The stress value used to check the fillet weld is the linearized shear stress on the weld localization, given by $(S_Z^2 + S_{HZ}^2)^{1/2}$, for the Case I-4.
- (3) Stress calculated as the maximum vertical compression load in the FSR foot ($RB_Z = 1843$ kN, Table 1-17), divided by the nut section area (7284.5 mm²)
- (4) Stress calculated by $S_{max} = RB_Z / A_T = 1843000 / (100 \cdot \pi \cdot 110 / 2)$, where $RB_Z = 1843$ kN is the maximum vertical compression load in the FSR foot (Table 1-17).

1.9 STRESSES IN THE LINKING DEVICES

1.9.1 Lower Links (Bearing Pads)

The FSR foot compresses the 40 mm thick bearing plate with a maximum load of 1843 kN (Table 1-17).

The local shear stress concentrated in the bearing plate under the foot screw is calculated as follows:

$$1843000/(\pi \cdot 100 \cdot 40) = 147 \text{ MPa} < 198.6 \text{ MPa}$$

The compression area of the bearing plate is large enough to resist even four times the maximum compression load:

$$4 \cdot 1843000 / (660^2 - 2 \cdot 140^2) = 19 \text{ MPa} < 195.2 \text{ MPa}$$

The maximum transmission force between two FSRs at the lower link device is 1306 kN (Table 1-17). The shear stress in the triangular vertical plates of the bearing pad is calculated as follows:

$$1306000 / (30 \cdot 120) = 363 \text{ MPa} < 419.9 \text{ MPa}$$

In addition, consideration has been taken of the bending moment caused by the distribution of the load along the triangular plate height. The bending stress is calculated as follows:

$$1306000 \cdot (120/2) / (30 \cdot 180^2/6) = 484 \text{ MPa} < 1049.7 \text{ MPa}$$

The above calculations bound the internal and external bearing pads.

1.9.2 Upper Links (Assembly Crossarms)

The maximum transmission force between two FSRs at the upper link device is 1227 kN (Table 1-17).

The critical section in the spacer plates welded to the upper corners of the FSR is the weld section. The shear stress in the weld is calculated as follows:

$$1227000 / (8 \cdot 2 \cdot (500 + 275)) = 99 \text{ MPa} < 198.6 \text{ MPa}$$

The compression stress between the assembly crossarm and the spacer plates in the external FSRs is calculated as follows:

$$1227000 / (15 \cdot 151) = 542 \text{ MPa} < 699.8 \text{ MPa}$$

The shear stress in the assembly crossarm of the external FSRs is calculated as follows:

$$1227000 / (15 \cdot 250) = 327 \text{ MPa} < 419.9 \text{ MPa}$$

The bending stress in the assembly crossarm of the external FSRs is calculated as follows:

$$1227000 \cdot 170 / (15 \cdot 300^2/6) = 927 \text{ MPa} < 1049.7 \text{ MPa}$$

The above calculations for the assembly crossarm of the external FSRs are also valid for the internal crossarms as they have twice the thickness and twice the load value applies.

1.10 CONCLUSIONS

The analyses performed for the FSR assembly with the link conditions between racks demonstrate the integrity of the fuel storage racks when subjected to the dynamic loads. The analyses demonstrate that the FSR design satisfies the structural requirements of Reference 3 for all loading conditions specified. Pivoting or toppling of racks is minimized since the individual racks are coupled to form an assembly. Sliding of the rack assembly is limited such that interactions with the pool walls are prevented.

Table 1-3 summarizes the results obtained from the analysis of the FSR assembly.

Note to Section 1.5.3:

The response of the racks is mainly due to the first frequencies under the SSE loads. For the racks in the spent fuel pool, the minimum mass percentage combined in the SSE modal response is 96.8%, indicating 3.2% of missing mass. The most critical stress ratio is 0.94.

The global response of the rack from the response spectrum analysis developed can be expressed as:

$$R = (\sum R_{ij}^2)^{1/2} ; i = \text{SSE, LOCA, SRVD}; j = x, y, z$$

where R_{ij} is linearly dependant of $(\sum (M_k \cdot a_k)^2)^{1/2}$ and M_k and a_k are, respectively, the effective mass and acceleration for the mode k . Including the missing mass for each event and each direction means to add the term $M_{\text{miss}} \cdot a_{\text{ZPA}}$ in that SRSS. Since the ZPA acceleration is always lower than any of the modal accelerations, it can be conservatively assumed that the global response will be increased by $100/96.8=1.033$. Therefore, the most critical stress ratio becomes $0.94 \cdot 1.033=0.97$ (considering a conservative maximum stress ratio of 0.94 for spectrum analysis).

The free standing case was analyzed with all the mass and no additional calculations are required.

These increasing factors, in fact, will be much smaller because the ZPA acceleration and the missing mass are smaller than, for instance, the spectral acceleration and effective mass of the two main eigenmodes corresponding to the two first global bending eigenfrequencies. From the ANSYS output it is shown, as an example, that the acceleration in the X direction for the main frequency (16.69 Hz) is 16.638 m/s^2 (and the ZPA is 12.38 m/s^2) and the effective mass is 48143.7 kg (and the missing mass is $0.032 \cdot 75771=2425 \text{ kg}$).

Thus, it is concluded that the missing masses are small and do not affect the final results.

1.11 REFERENCES

1. ASME Boiler & Pressure Vessel Code, Section II Materials, Part A Ferrous Material Specifications, 2001 Edition with Add. 2003
2. ASME Boiler & Pressure Vessel Code, Section II Materials, Part D Properties (Customary), 2001 Edition with Add. 2003
3. ASME Boiler & Pressure Vessel Code, Section III Rules for Construction of Nuclear Facility Components, Division 1, Subsection NF, Supports, 2001 Edition with Add. 2003
4. ASME Boiler & Pressure Vessel Code, Section III Rules for Construction of Nuclear Facility Components, Division 1, Appendices, 2001 Edition with Add. 2003
5. Regulatory Guide 1.92, Revision 1, Combining Modal Responses and Spatial Components in Seismic Response Analysis
6. Sarpkaya: Mechanics of Wave Forces on Off-Shore Structures
7. ANSYS 10.0 Documentation (User Manual, Theoretical Manual)
8. NUREG-0800 Standard Review Plan 3.8.4 Other Seismic Category I Structures
9. ROARK'S Formulas for Stress & Strain
10. Rabinowicz, E., "Friction Coefficients of Water Lubricated Stainless Steels for a Spent Fuel Rack Facility," MIT, a report for Boston Edison Company, 1976
11. I.-W Yu, "Determination of Hydrodynamic Mass Using a General Purpose Finite Element Structural Code". Distributed by Pressure Vessels & Piping Division of American Society Mechanical Engineers, April 1980.
12. ESBWR LOCA and SSE combination: E-mail from David Davenport (GEH) to Luis Costas (ENSA) 06/13/2007
13. Standard Review Plan Section 3.8.4 Appendix D. Technical Position on Spent Fuel Racks
14. 5926ATN03 Rev.0 Load Cases for Fuel building Rack Free Standing Analysis
15. NUREG/CR-5912 (BNL-NUREG-52335) Review of the Technical Basis and Verification of Current Analysis Methods Used to Predict Seismic Response of Spent Fuel Storage Racks. October 1992
16. Regulatory Guide 1.61, Rev.1. Damping Values for Seismic Design of Nuclear Power Plants

APPENDIX A - FIGURES

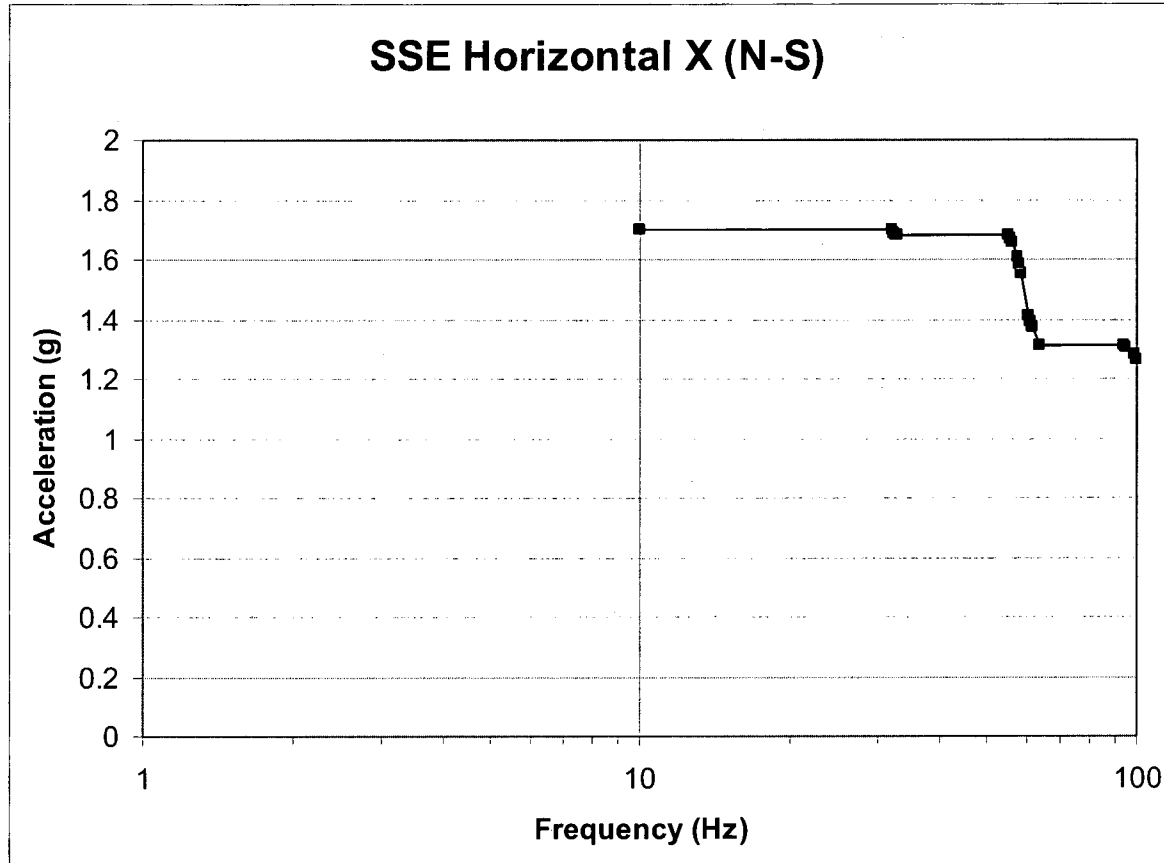


Figure A-1a. SSE Horizontal X Floor Response Spectra

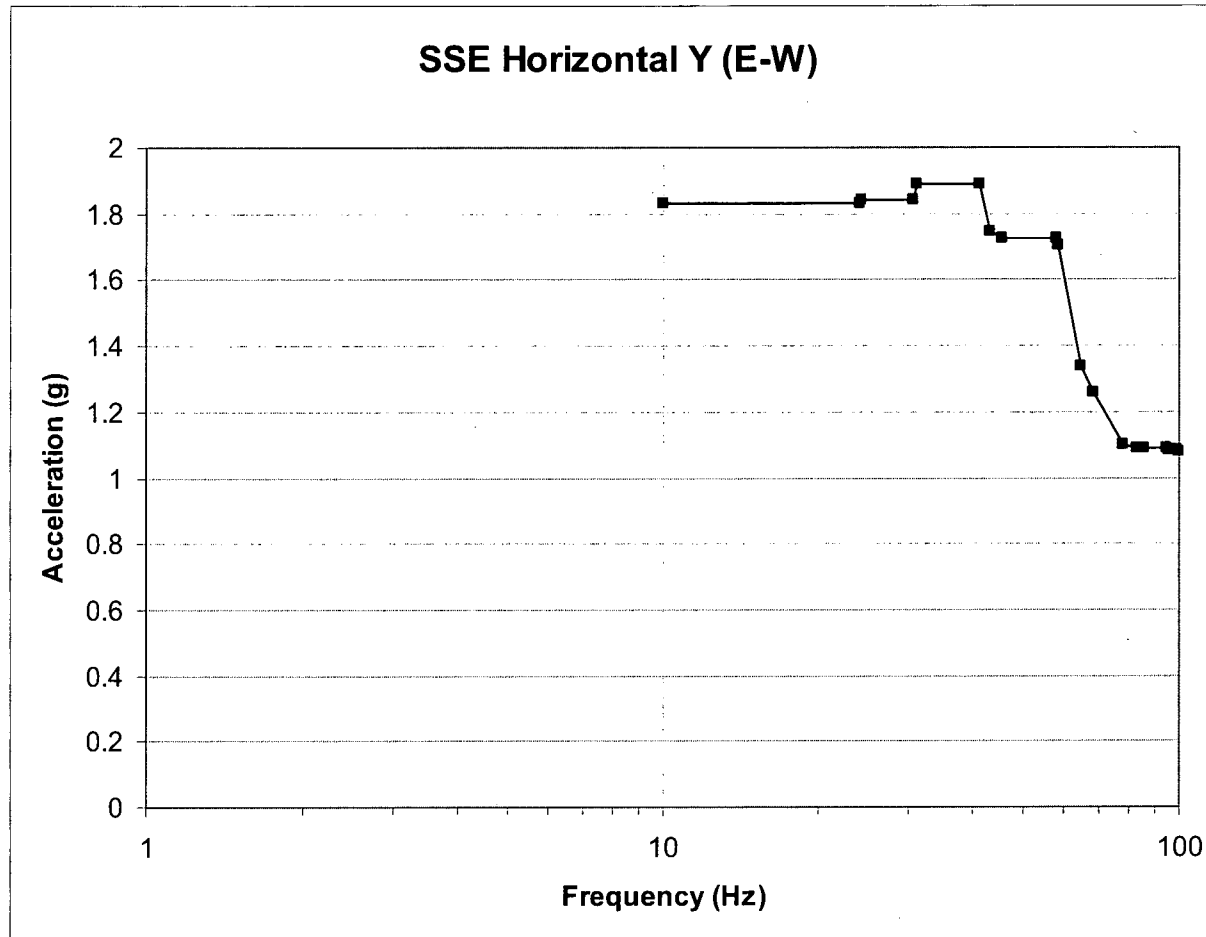


Figure A-1b. SSE Horizontal Y Floor Response Spectra

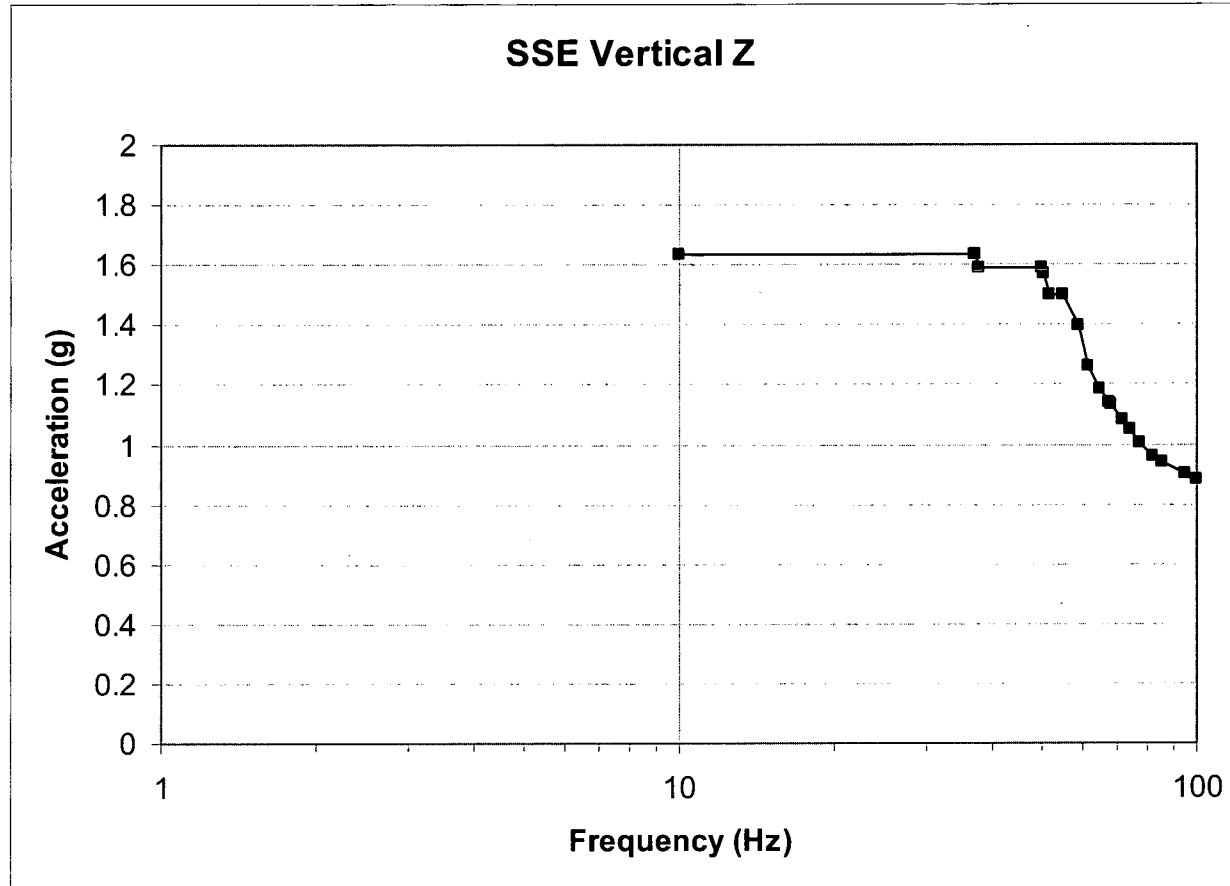


Figure A-2. SSE Vertical Z Floor Response Spectra

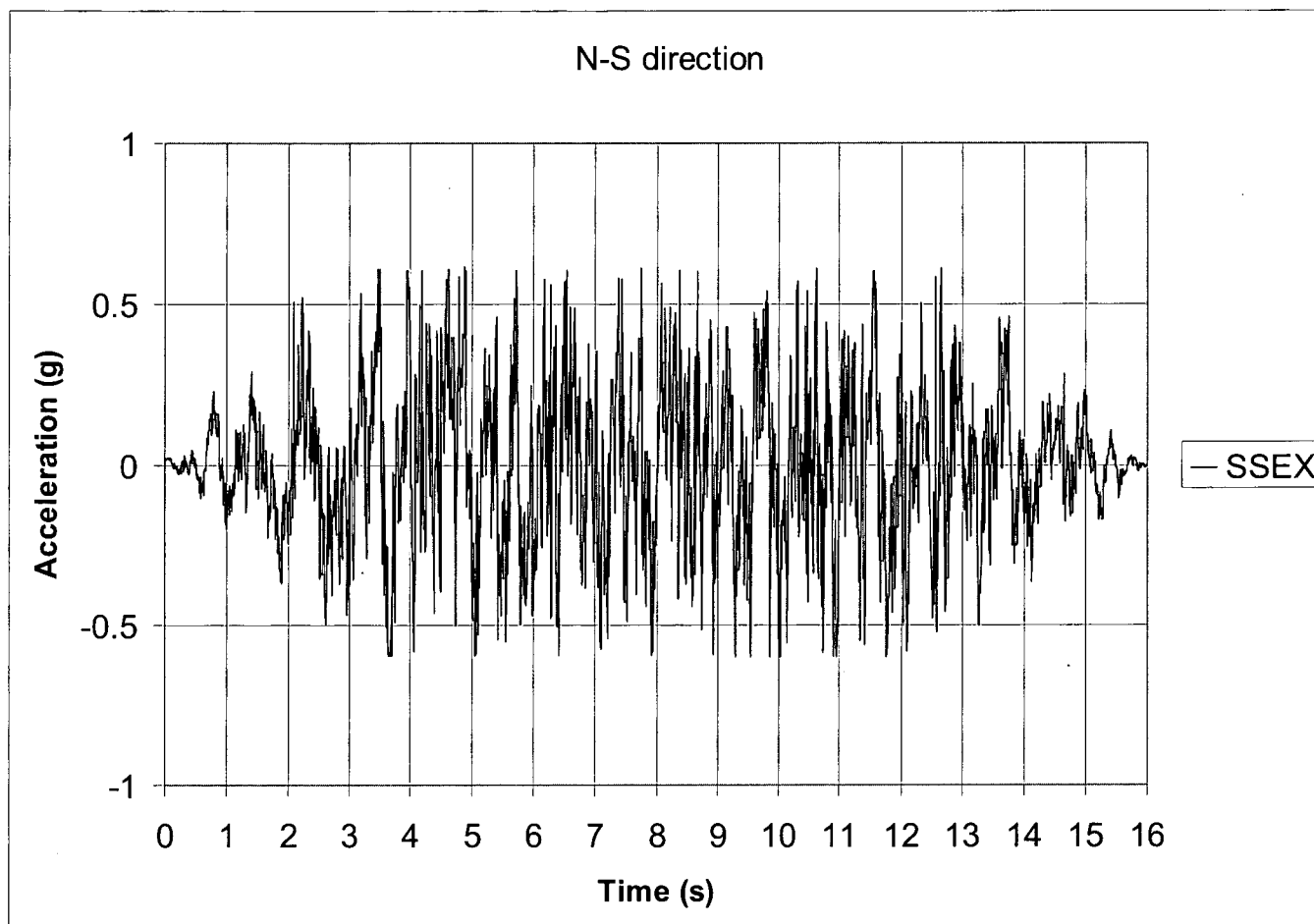


Figure A-3. SSE Horizontal X Acceleration Time History

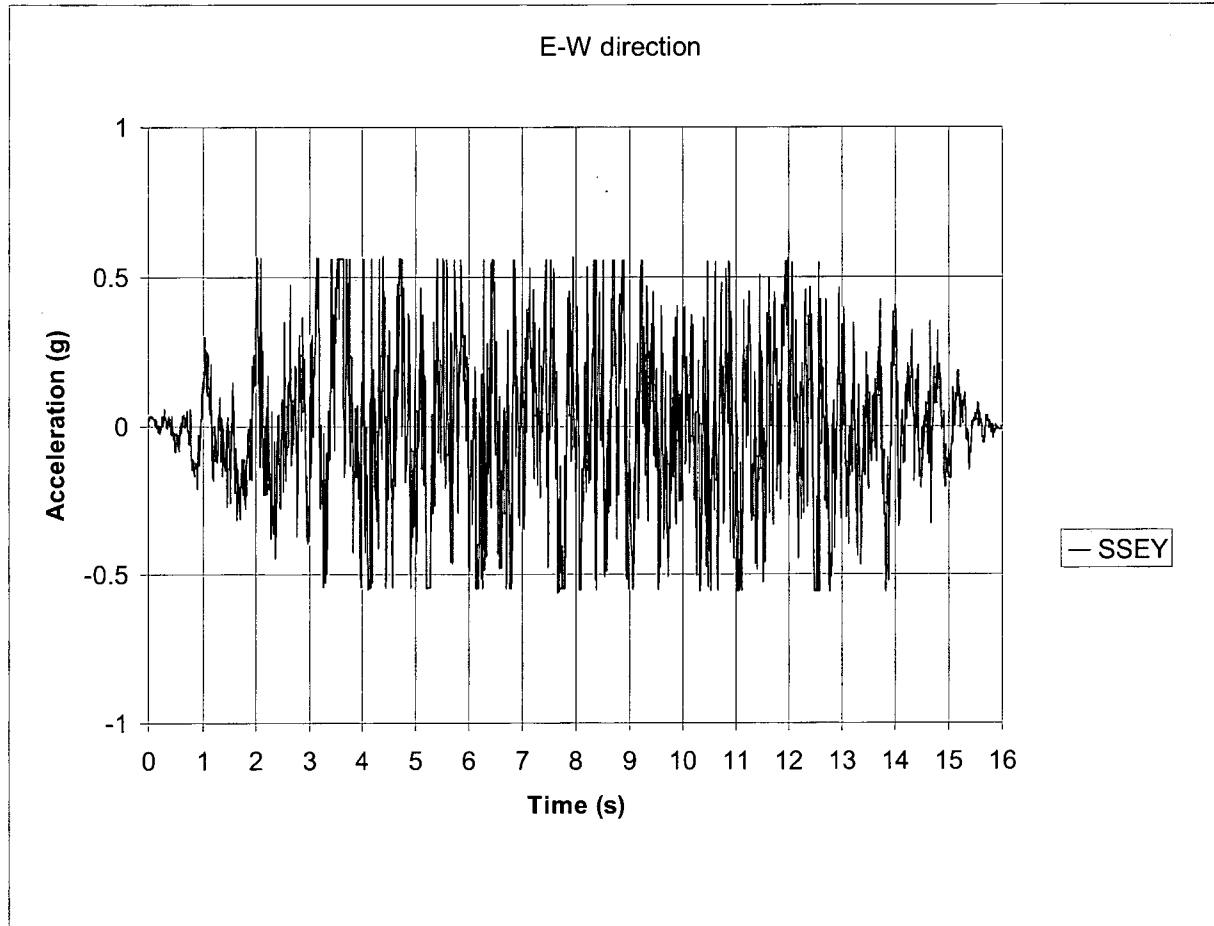


Figure A-4. SSE Horizontal Y Acceleration Time History

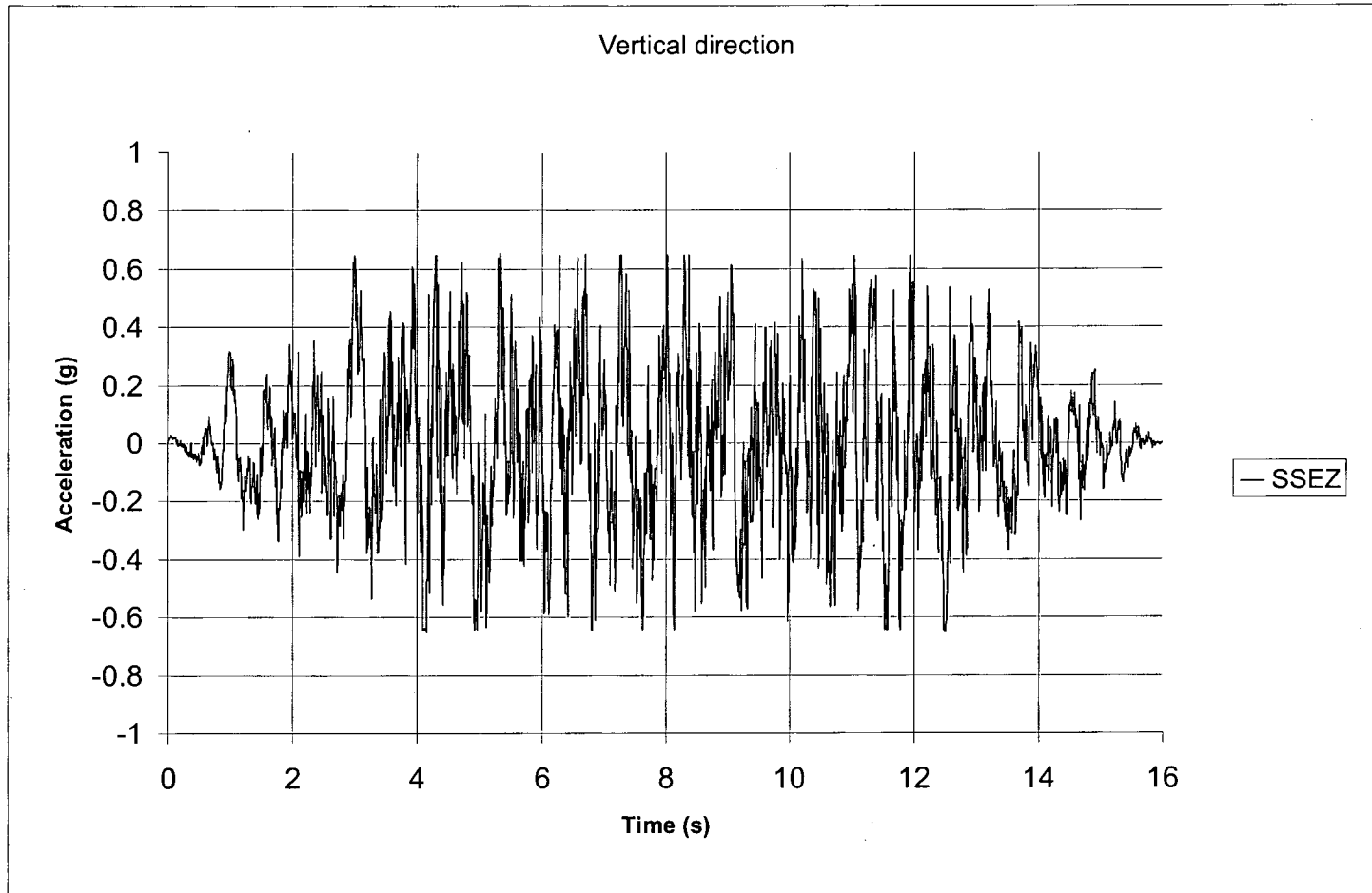


Figure A-5. SSE Vertical Z Acceleration Time History

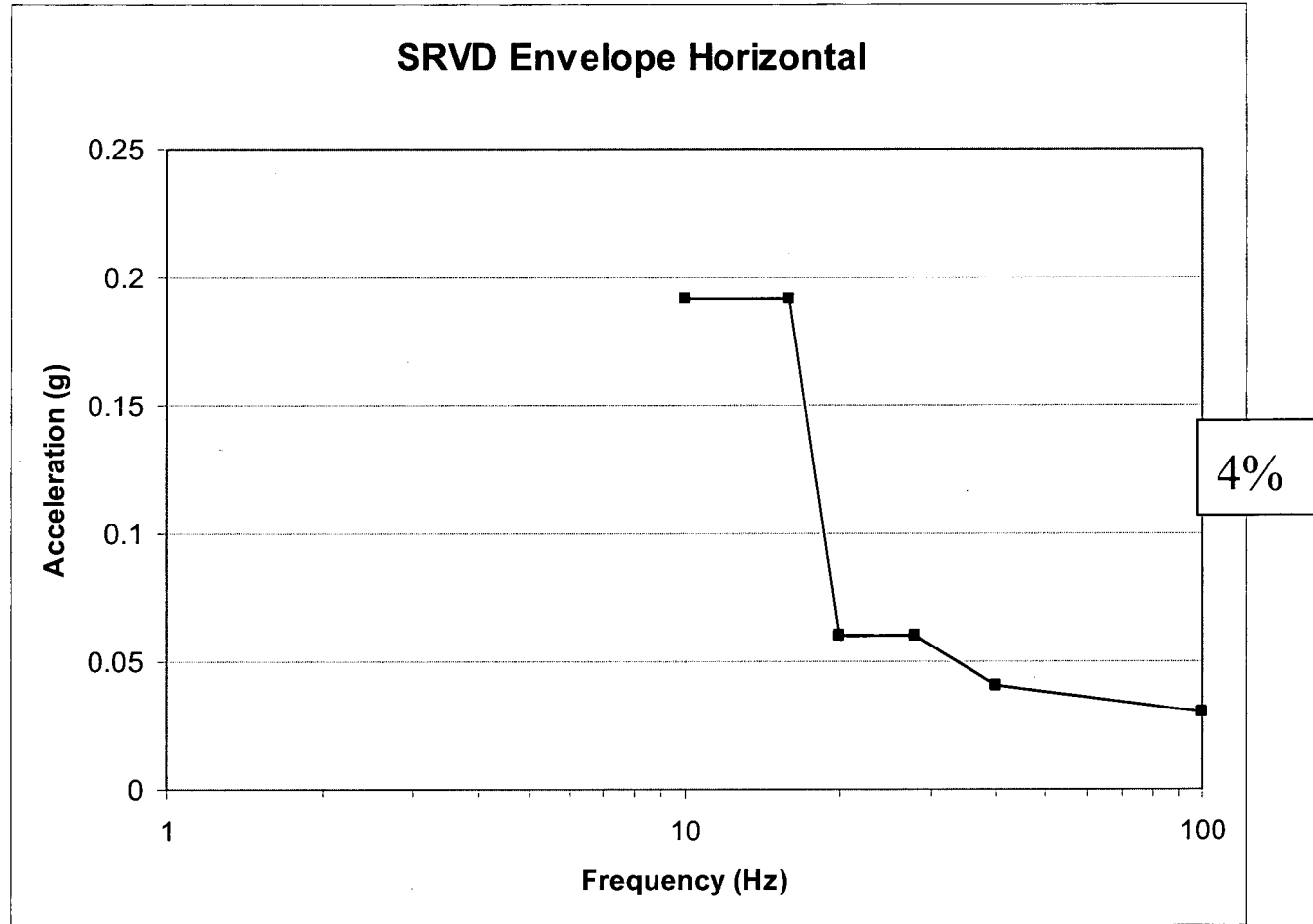


Figure A-6. SRVD Horizontal Enveloping Floor Response Spectra

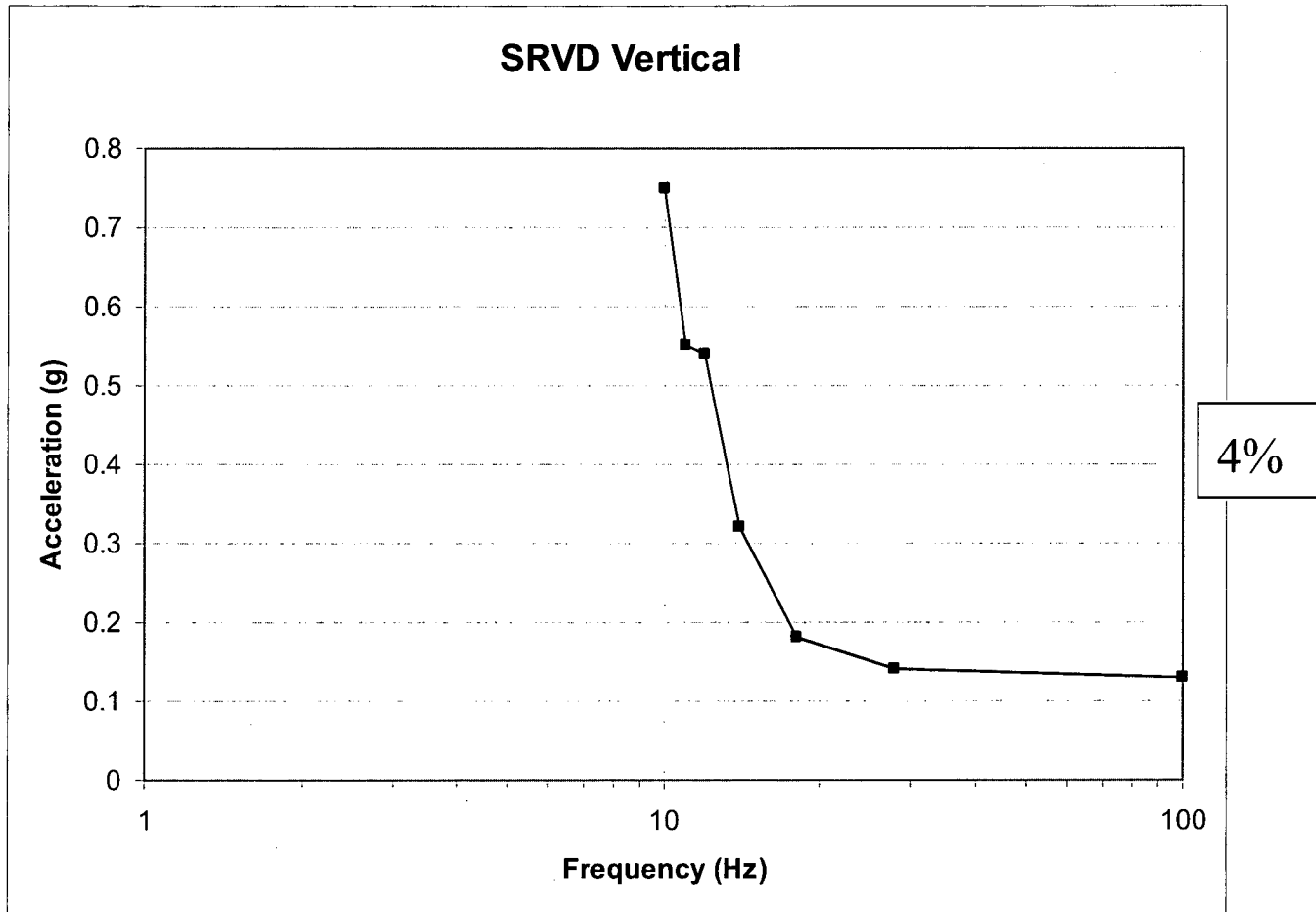


Figure A-7. SRVD Vertical Floor Response Spectra

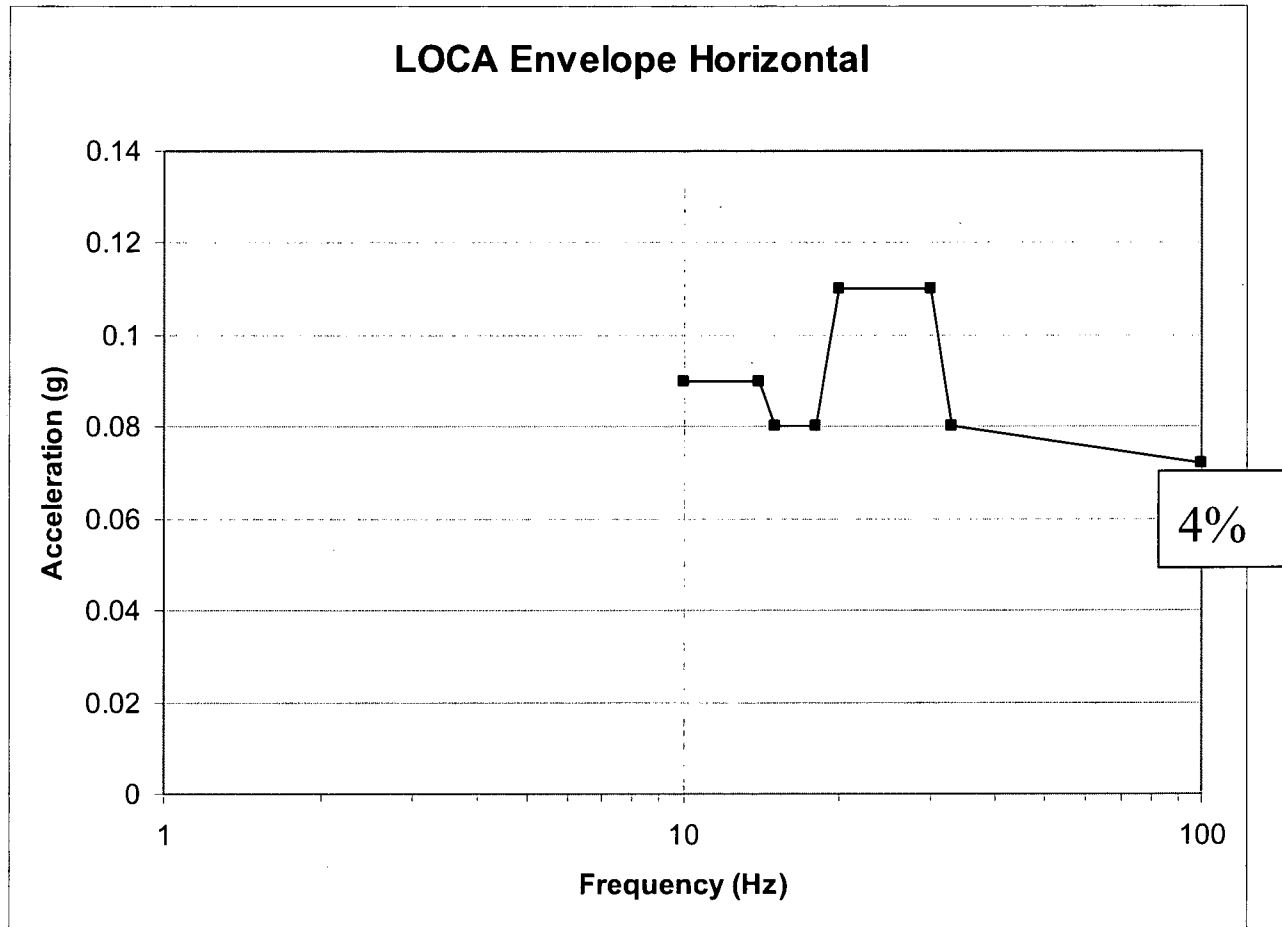


Figure A-8. LOCA Horizontal Enveloping Floor Response Spectra

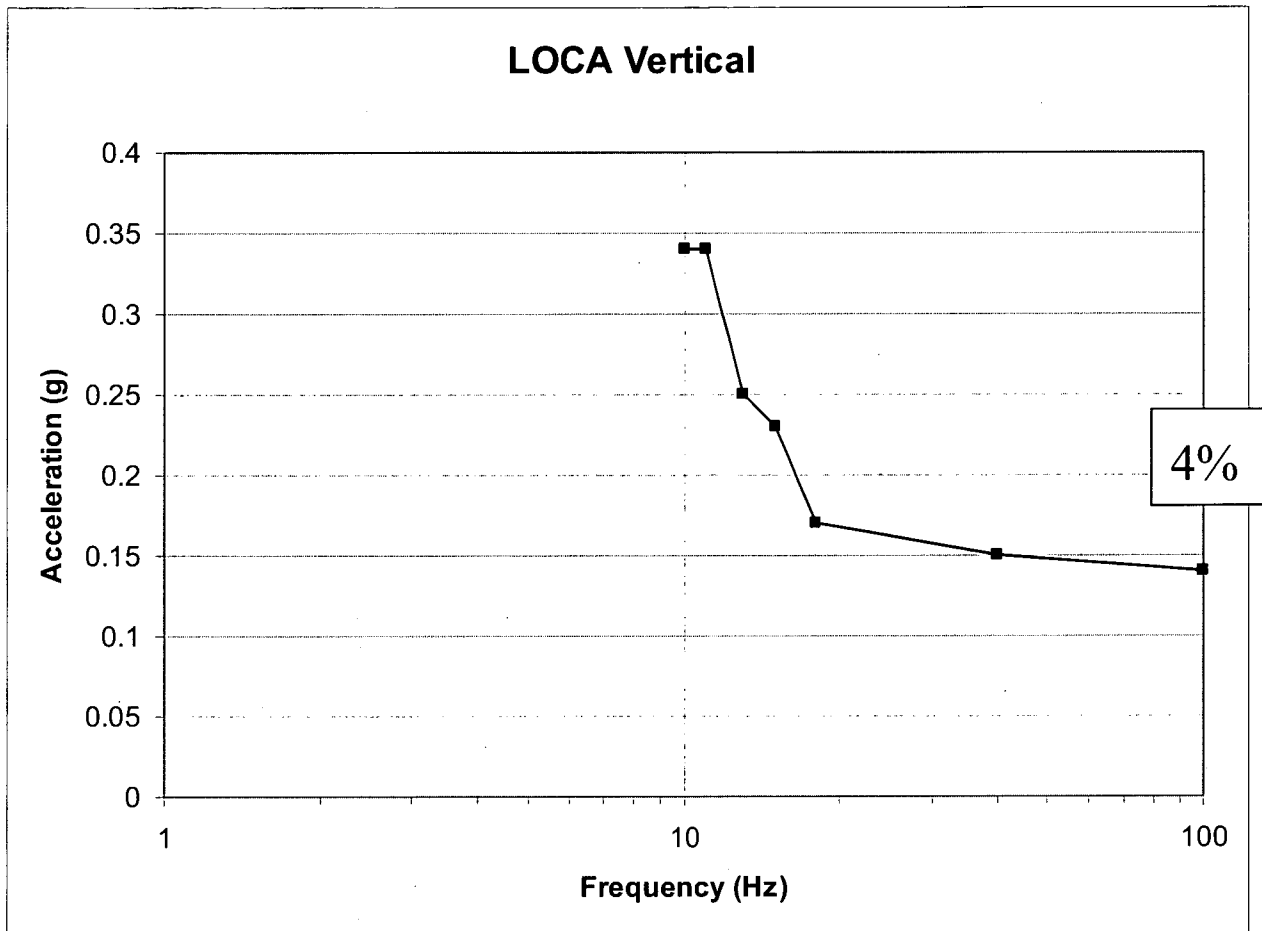


Figure A-9. LOCA Vertical Floor Response Spectra

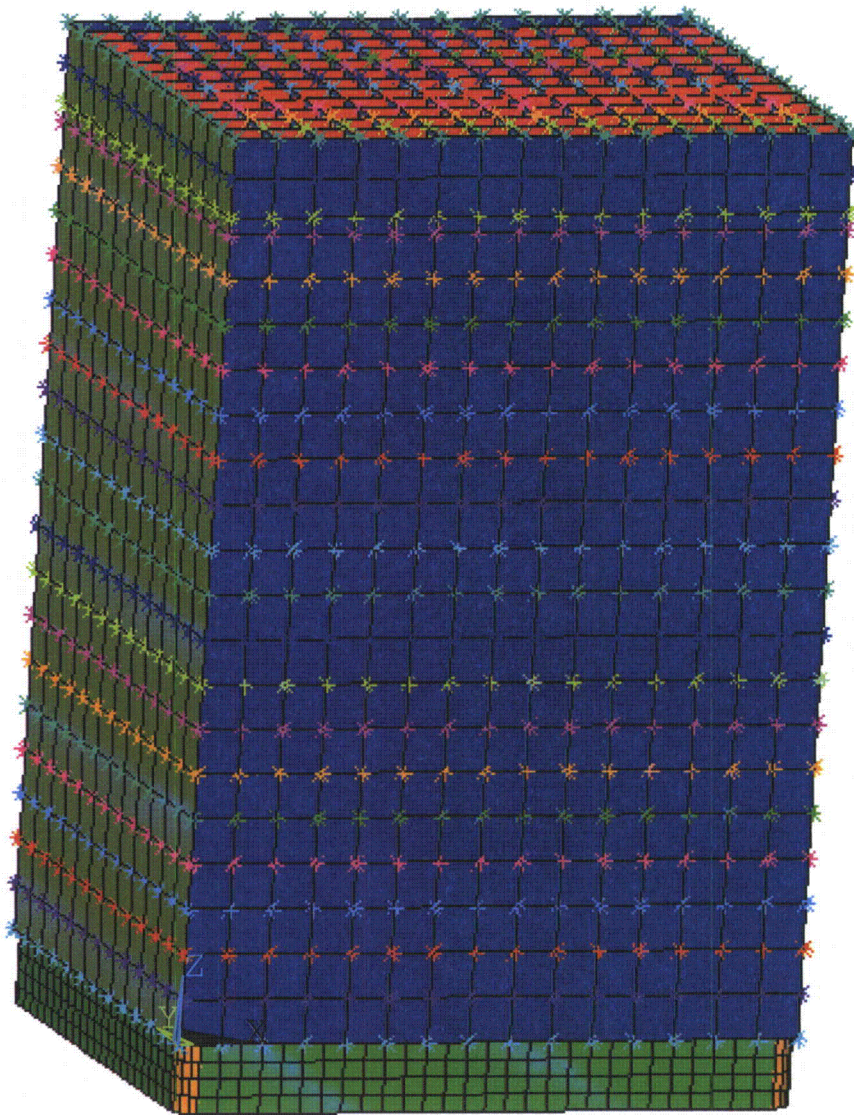


Figure A-10. FSR FEM

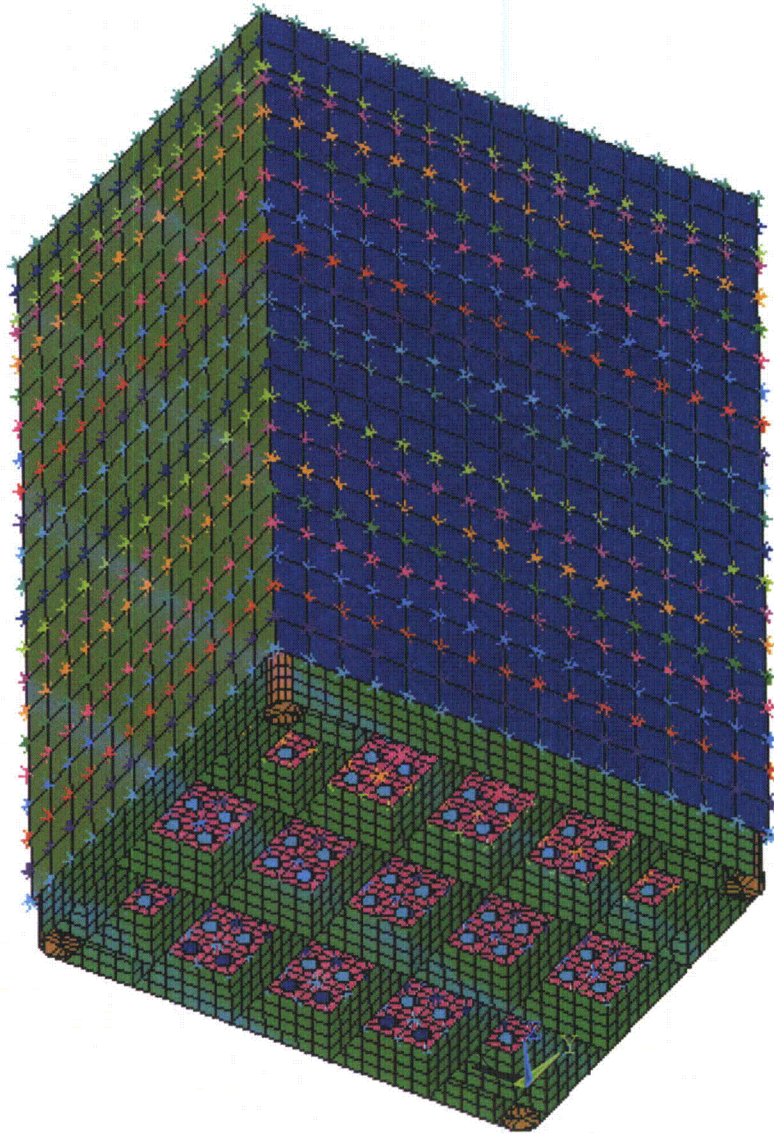


Figure A-11. FSR FEM

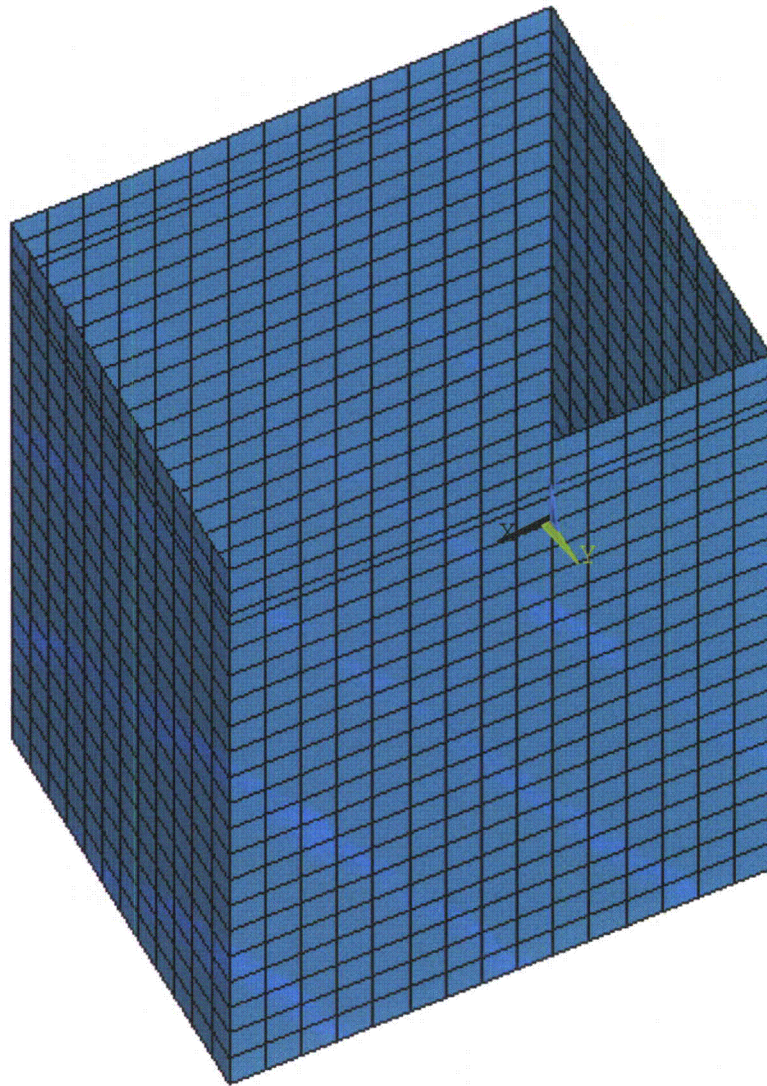


Figure A-12. FSR FEM 10mm Thick SS Plates

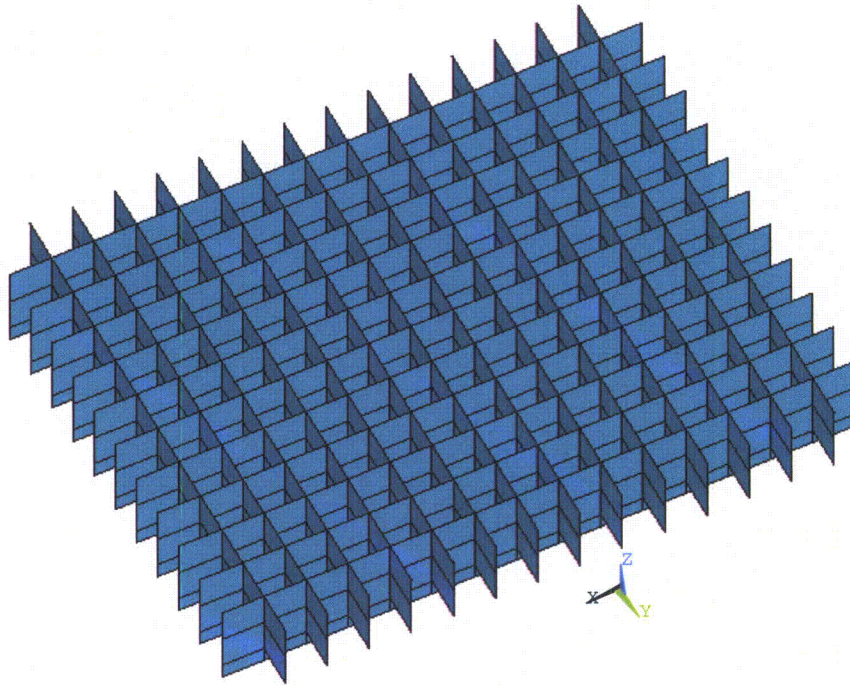


Figure A-13. FSR FEM 7mm Thick SS Plates

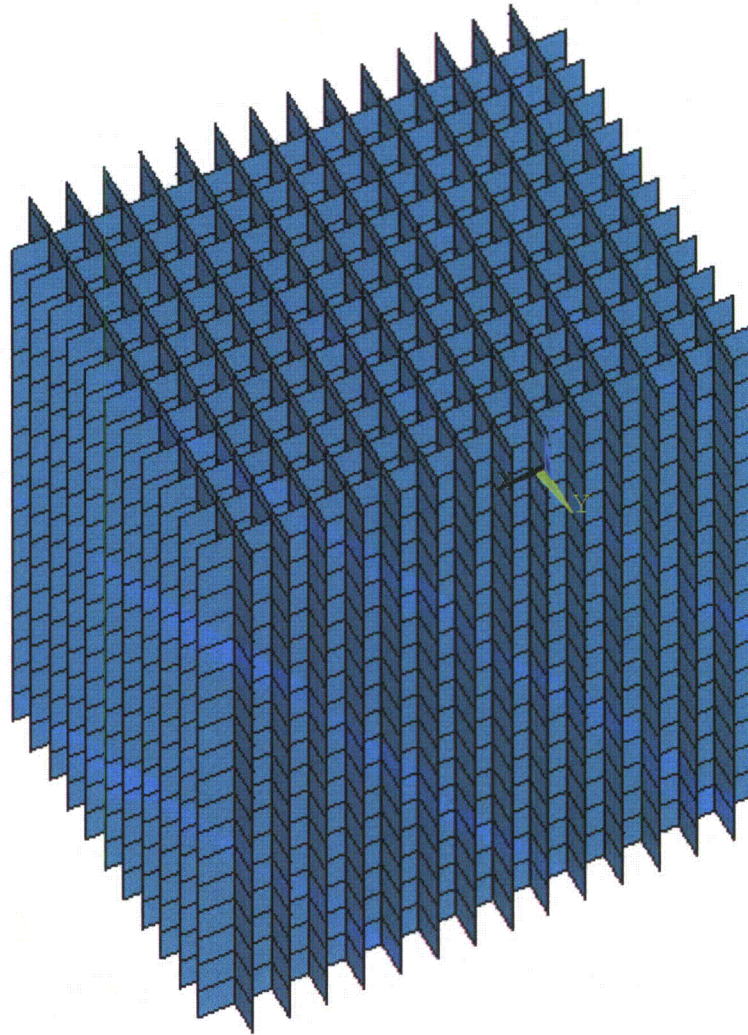
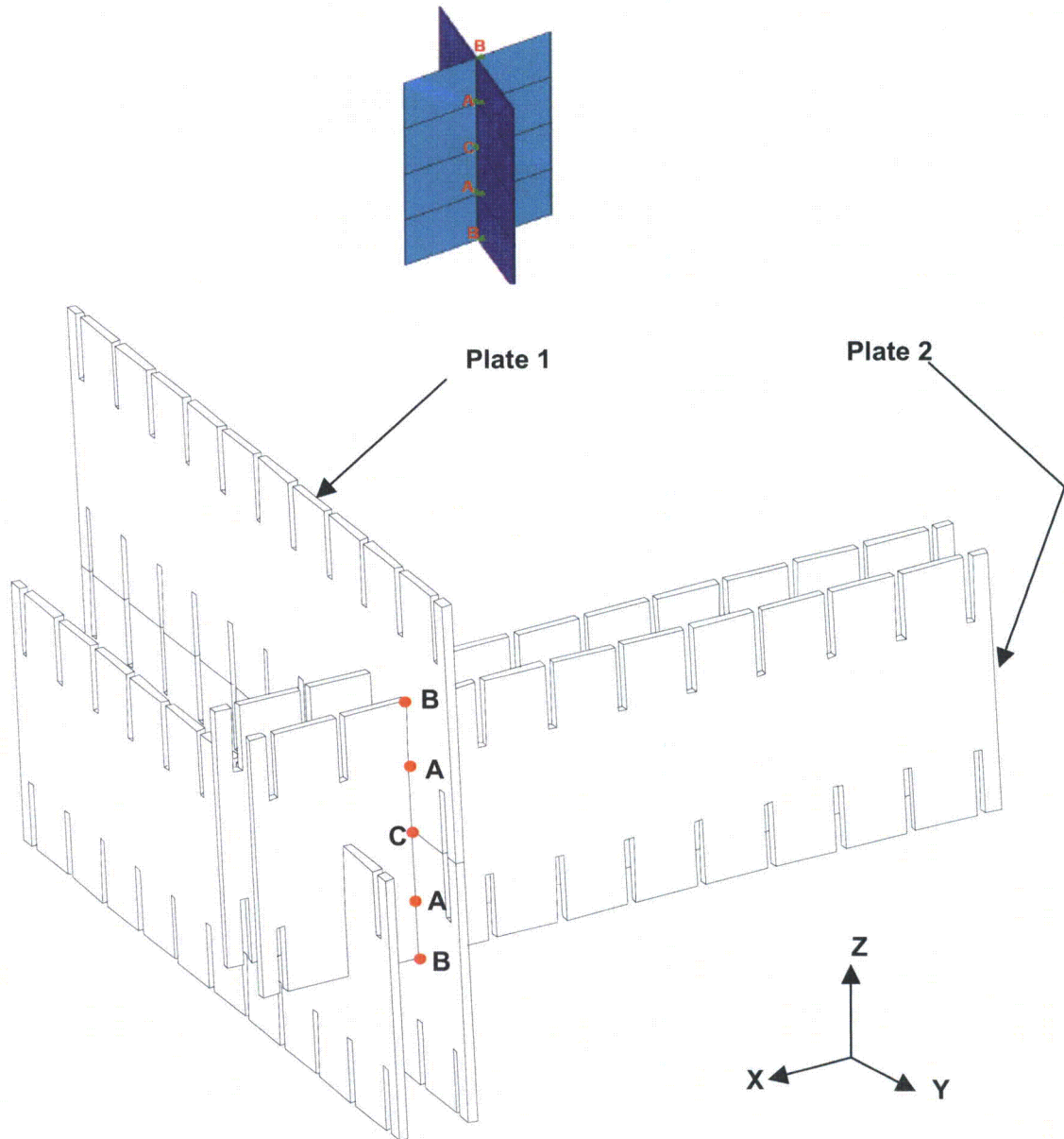


Figure A-14a. FSR FEM 3.4mm Thick BSS Plates



There are two (2) nodes on each intersection point: one node for Plate 1 and one node for

In Points A : $U_{1x} = U_{2x}$; $U_{1y} = U_{2y}$; $U_{1z} \neq U_{2z}$

In Points B : $U_{1x} = U_{2x}$; $U_{1y} \neq U_{2y}$; $U_{1z} \neq U_{2z}$

In Points C : $U_{1x} \neq U_{2x}$; $U_{1y} = U_{2y}$; $U_{1z} \neq U_{2z}$

Figure A-14b. Couples in Slotted Areas

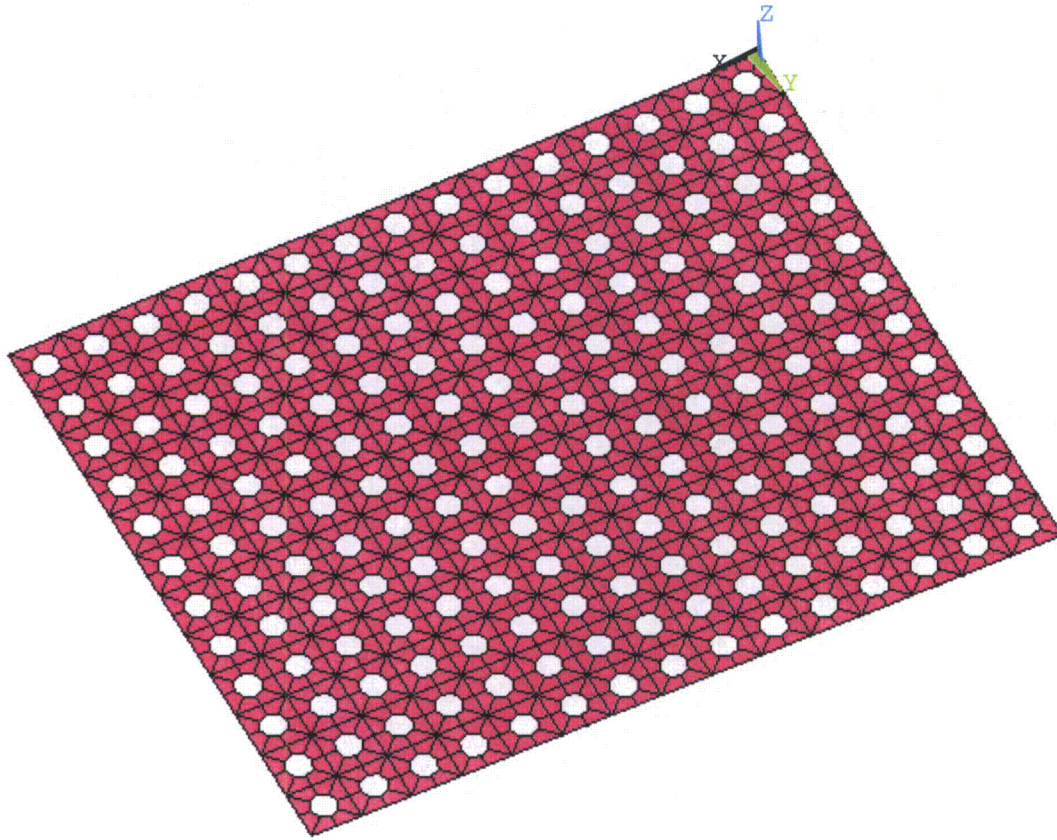


Figure A-15. FSR FEM 20mm Thick SS Base Plate

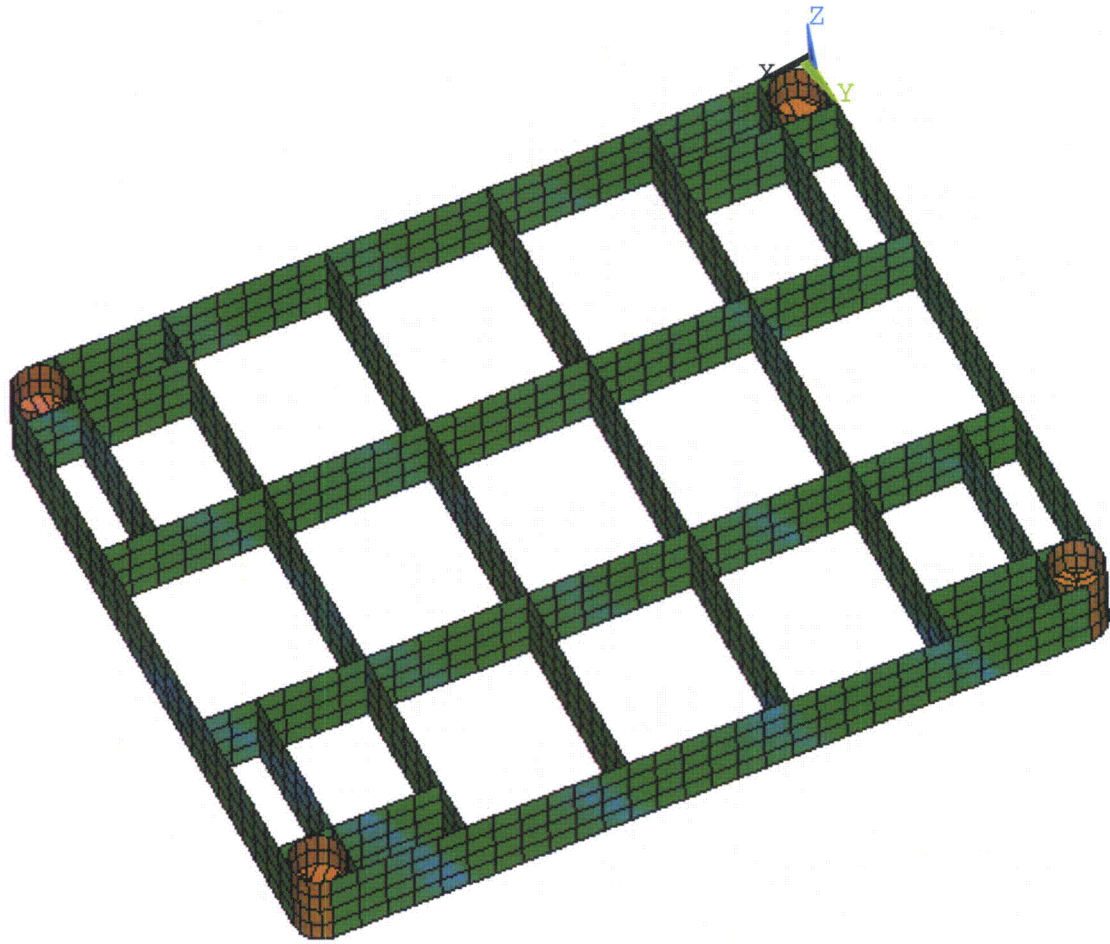


Figure A-16. FSR FEM 20mm Thick SS Base Plate Stiffeners and Feet

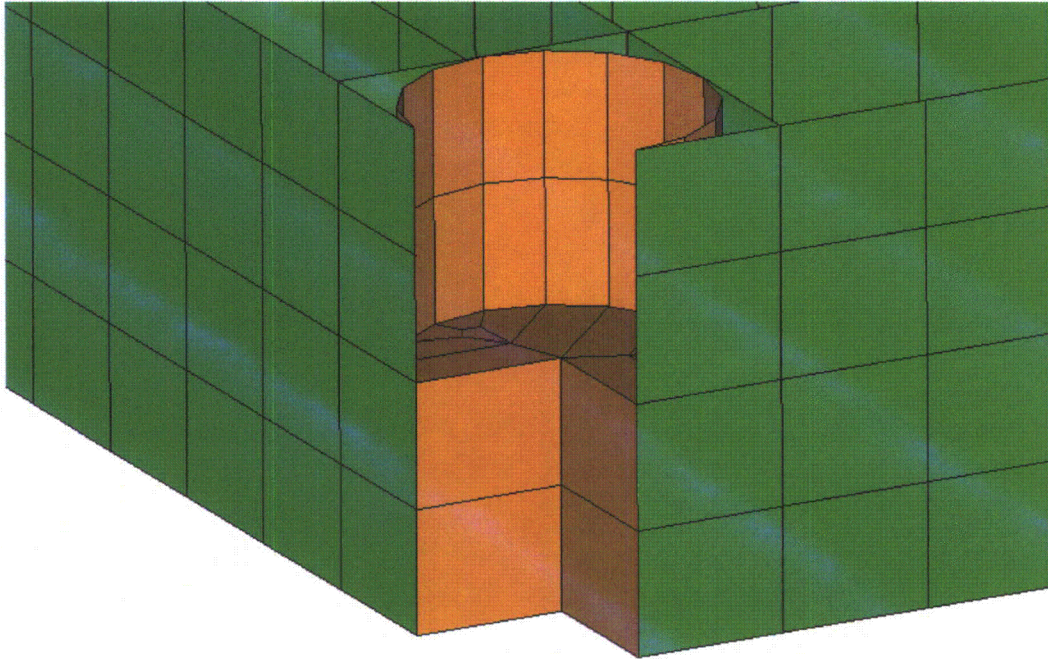


Figure A-17. FSR FEM Foot-Nut & Screw-Detail (1/4 removed)

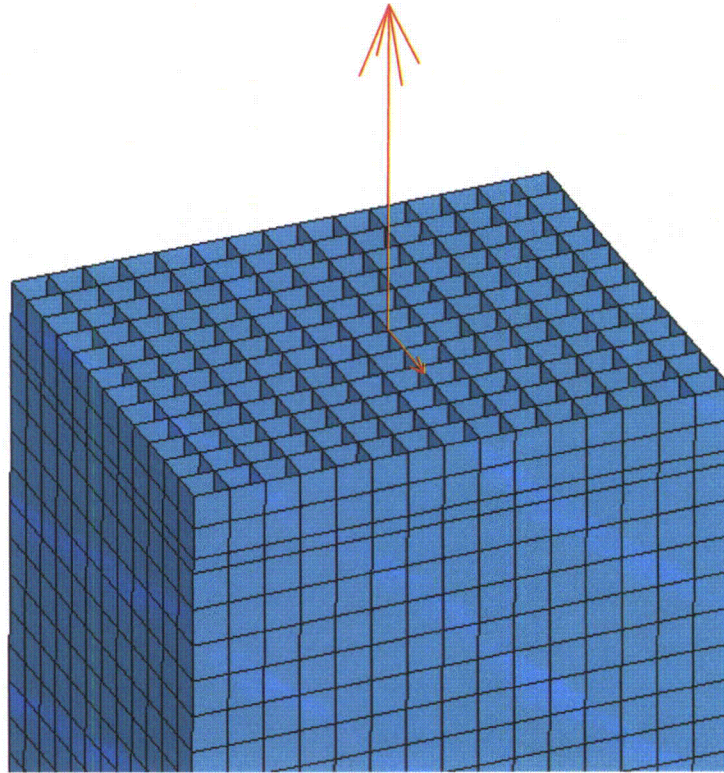


Figure A-18. FSR Fuel Handling Loads

DISPLACEMENT
STEP=1
SUB =1
FREQ=13.787
RSYS=0
DMX =.006148

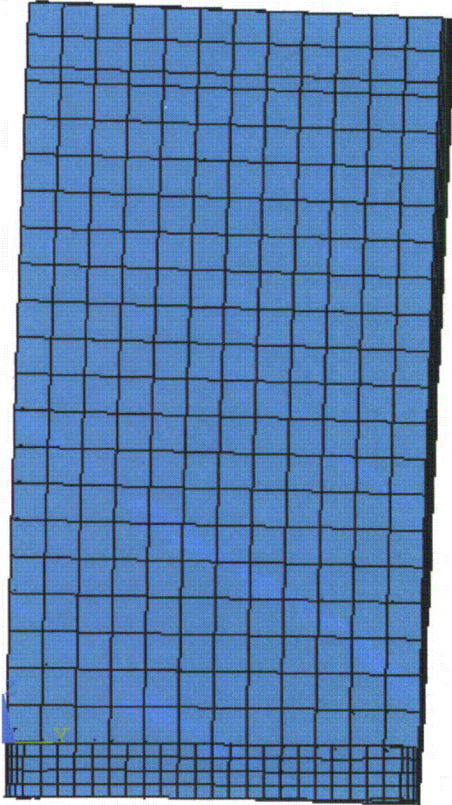


Figure A-19. FSR Deformed Shape Eigenmode 1

DISPLACEMENT

STEP=1

SUB =2

FREQ=16.694

RSYS=0

DMX =.006156

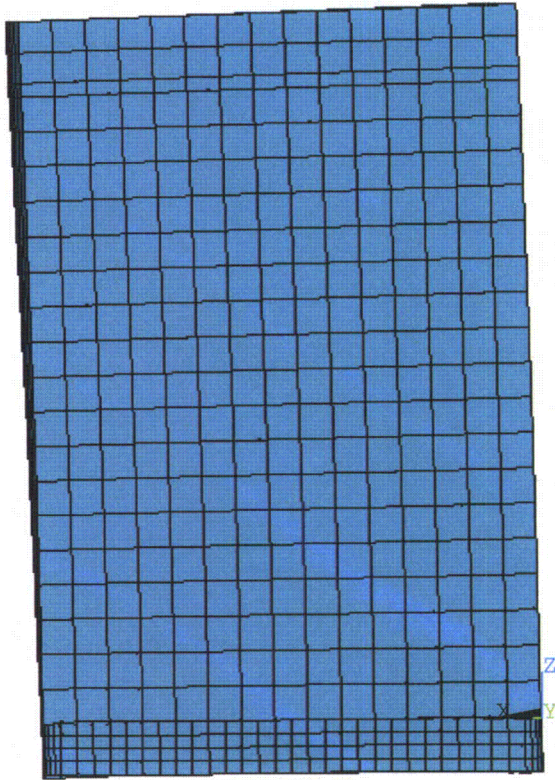


Figure A-20. FSR Deformed Shape Eigenmode 2

DISPLACEMENT
STEP=1
SUB =3
FREQ=17.527
RSYS=0
DMX =.008152

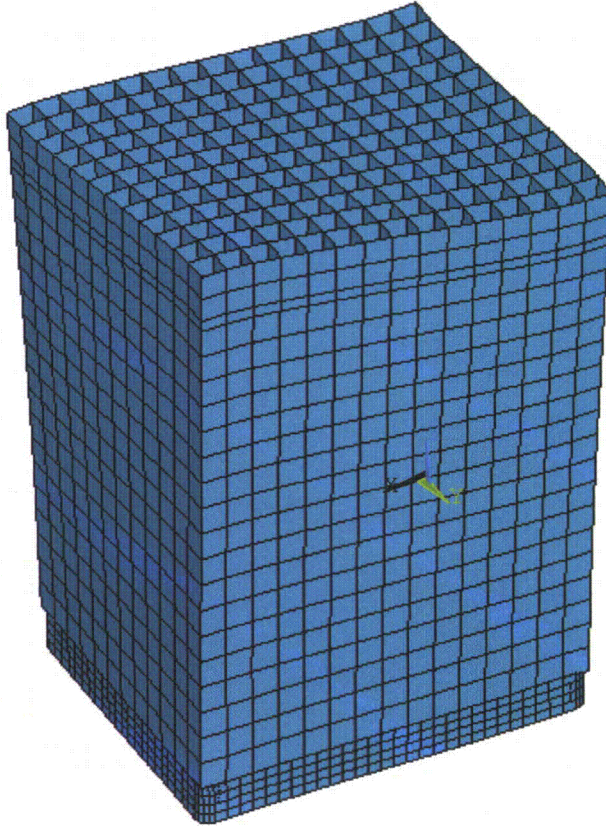


Figure A-21. FSR Deformed Shape Eigenmode 3

DISPLACEMENT
STEP=1
SUB =4
FREQ=30.166
RSYS=0
DMX =.007289

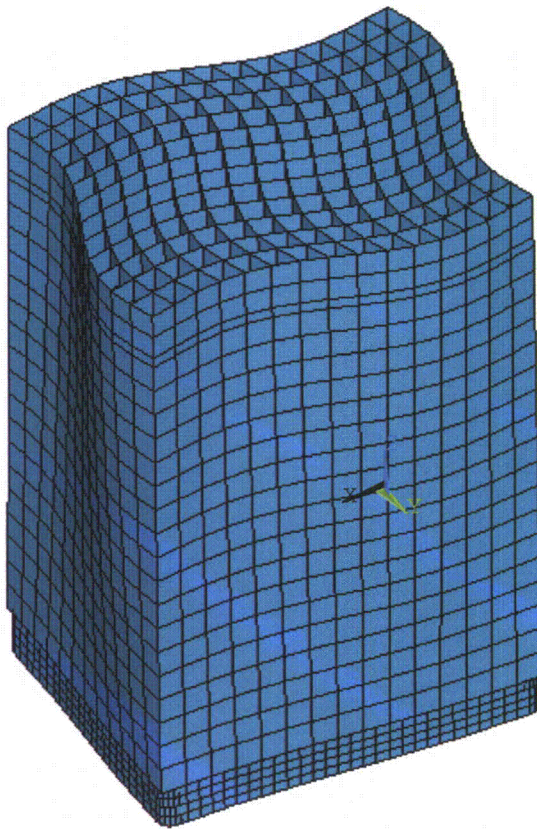


Figure A-22. FSR Deformed Shape Eigenmode 4

DISPLACEMENT

STEP=1

SUB =12

FREQ=44.083

RSYS=0

DMX =.00714

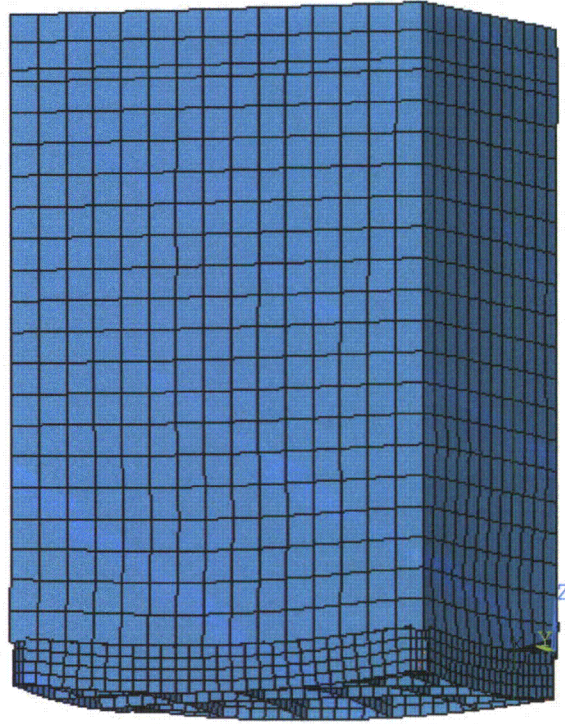


Figure A-23. FSR Deformed Shape Eigenmode 12

DISPLACEMENT

STEP=1

SUB =15

FREQ=53.2

RSYS=0

DMX =.006462

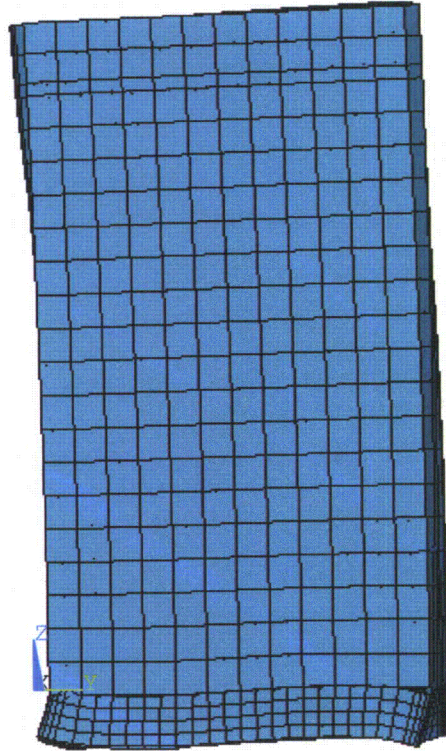


Figure A-24. FSR Deformed Shape Eigenmode 15

DISPLACEMENT

STEP=1

SUB =17

FREQ=54.147

RSYS=0

DMX =.006072

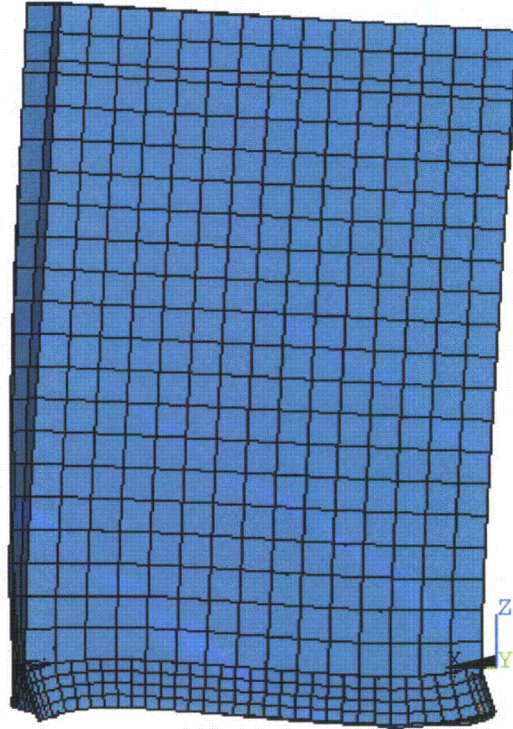


Figure A-25. FSR Deformed Shape Eigenmode 17

DISPLACEMENT

STEP=1

SUB =36

FREQ=97.41

RSYS=0

DMX =.009388

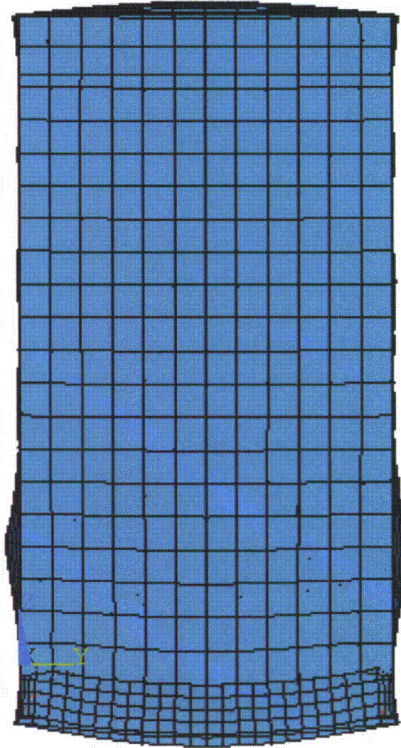


Figure A-26. FSR Deformed Shape Eigenmode 36

UX (AVG)
RSYS=0
DMX = .003749
SMX = .002

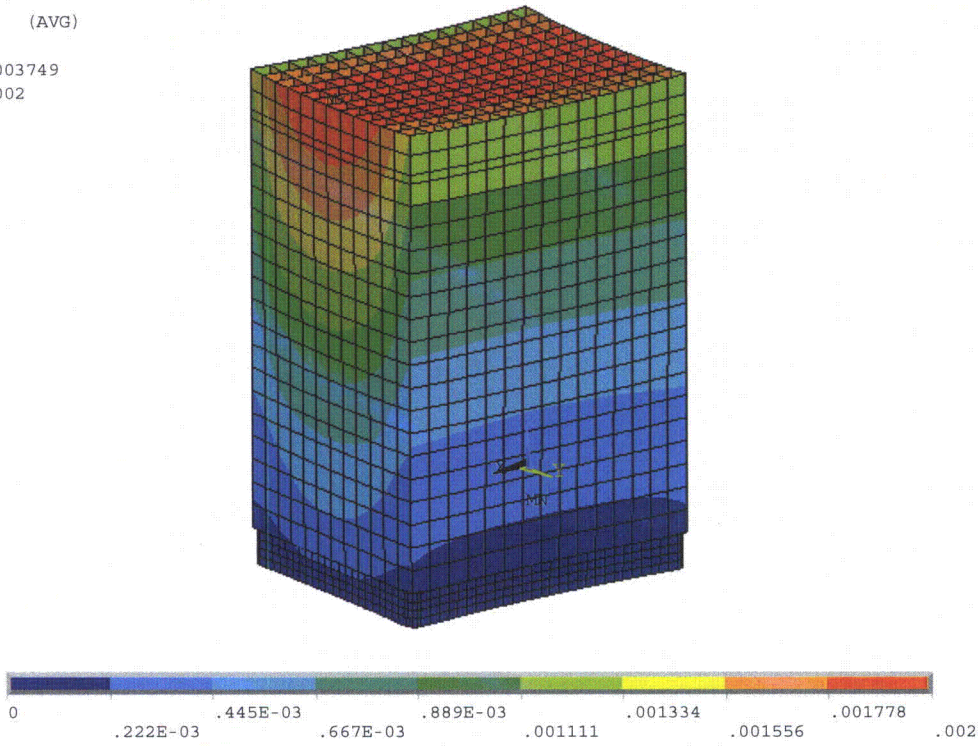


Figure A-27. FSR Horizontal X-Displacement (m). Level D

UY (AVG)
RSYS=0
DMX =.003749
SMX =.003174

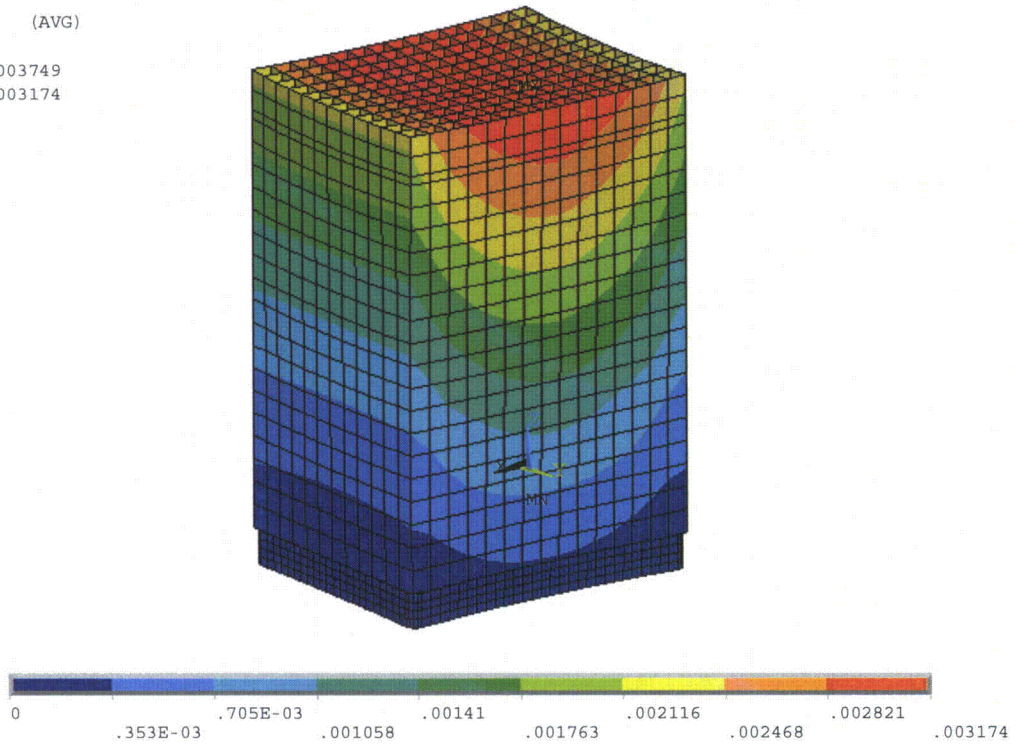


Figure A-28. FSR Horizontal Y-Displacement (m). Level D

UZ (AVG)
RSYS=0
DMX = .003749
SMX = .886E-03

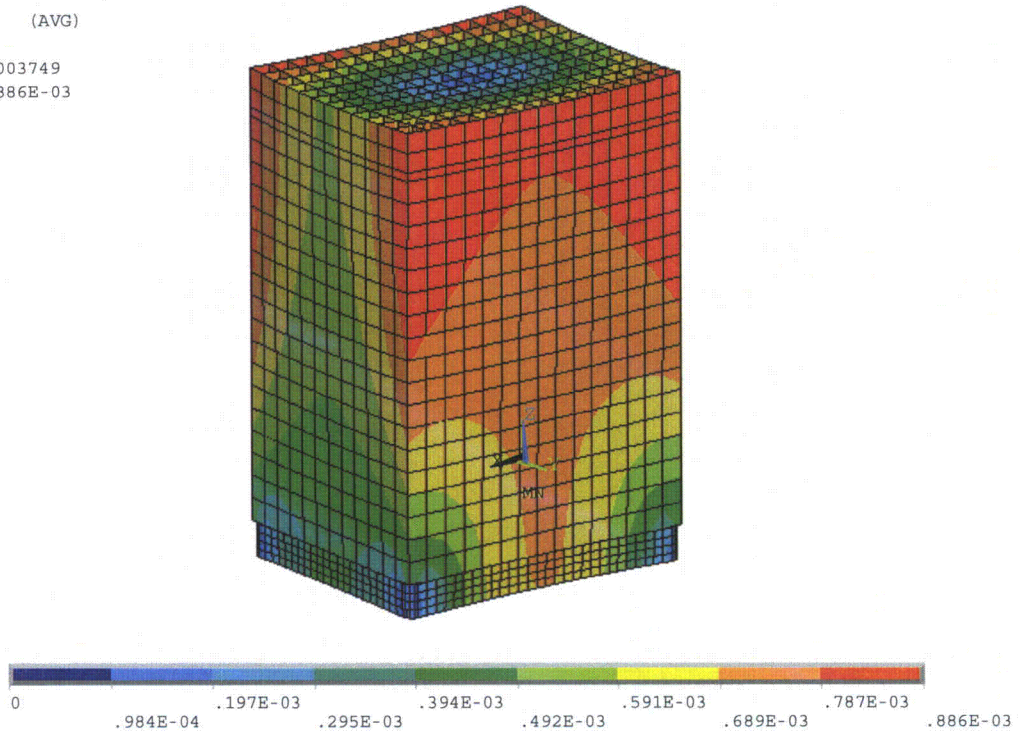


Figure A-29. FSR Vertical Z-Displacement (m). Level D

SZ (AVG)
MIDDLE
RSYS=0
DMX = .003528
SMN = .228E+07
SMX = .157E+09

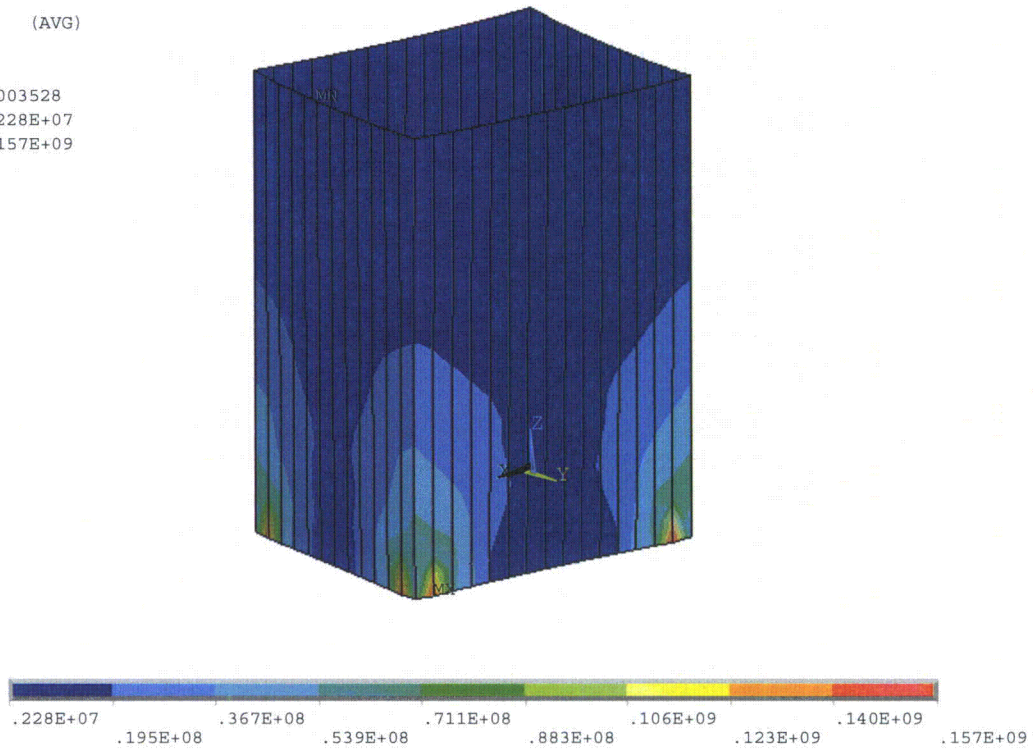


Figure A-30. FSR 10 mm Enveloping Plates. Level D Vertical Stress (N/m²)

SZ (AVG)
MIDDLE
RSYS=0
DMX = .850E-04
SMN = -873168
SMX = .787E+07

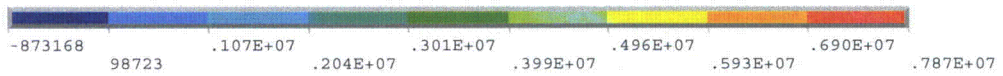
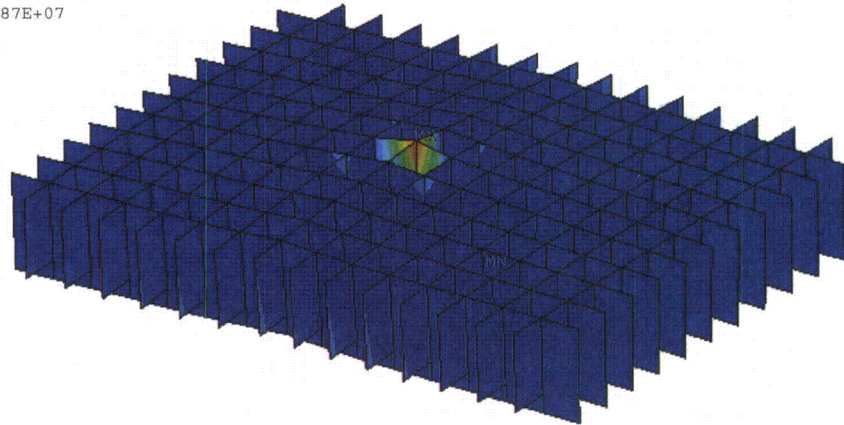


Figure A-31. FSR 7 mm Upper Level Plates. Level A Vertical Stress (N/m2)

SY (AVG)
MIDDLE
RSYS=0
DMX = .003749
SMN = 0
SMX = .423E+08

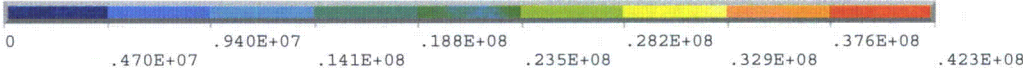
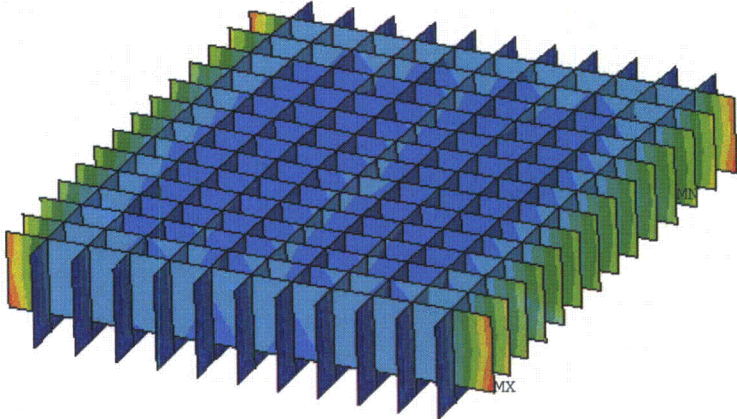


Figure A-32. FSR 7 mm Upper Level Plates. Level D Horizontal Stress (N/m²)

SZ (AVG)
MIDDLE
RSYS=0
DMX = .793E-03
SMN = 210956
SMX = .123E+09

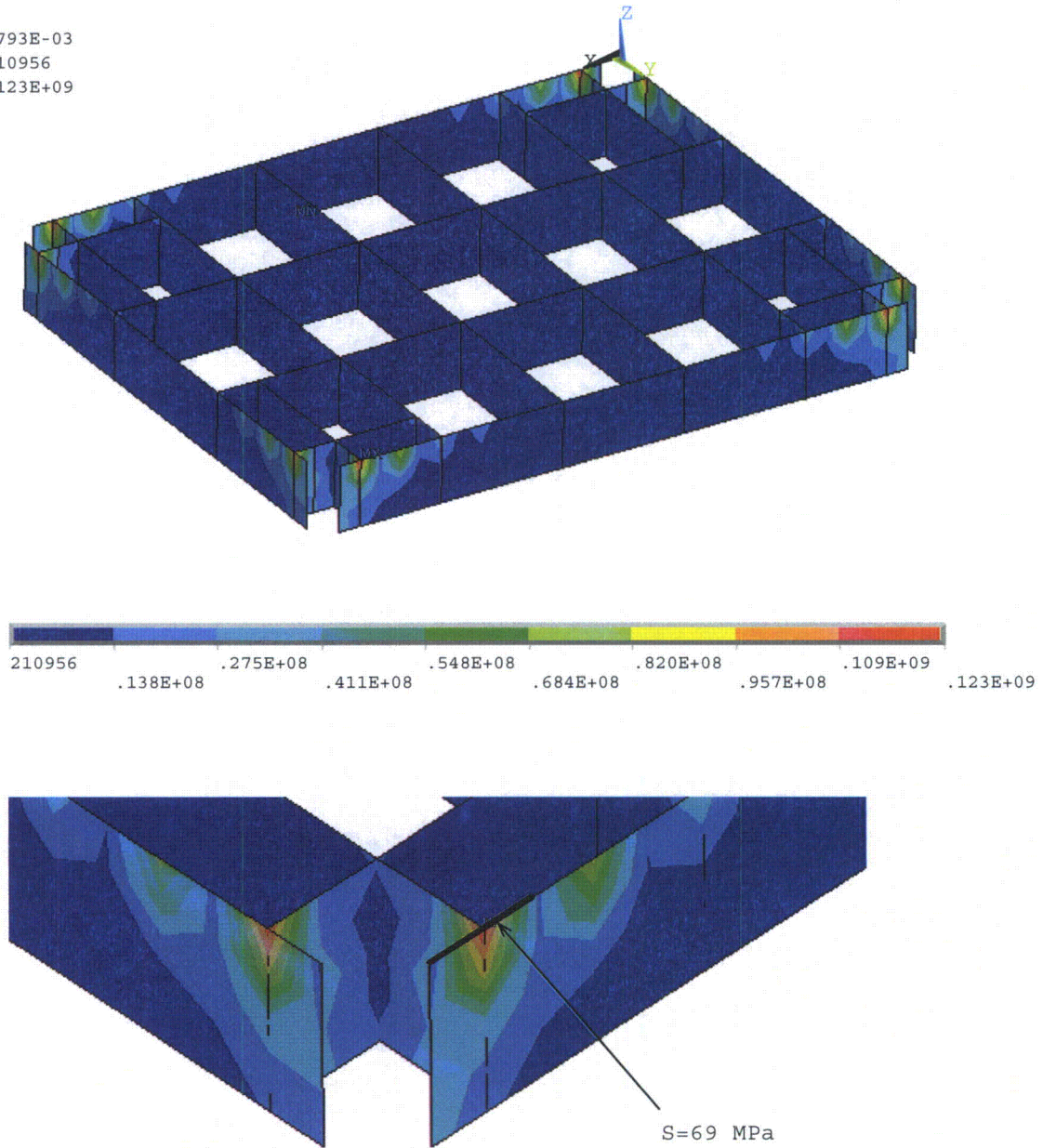
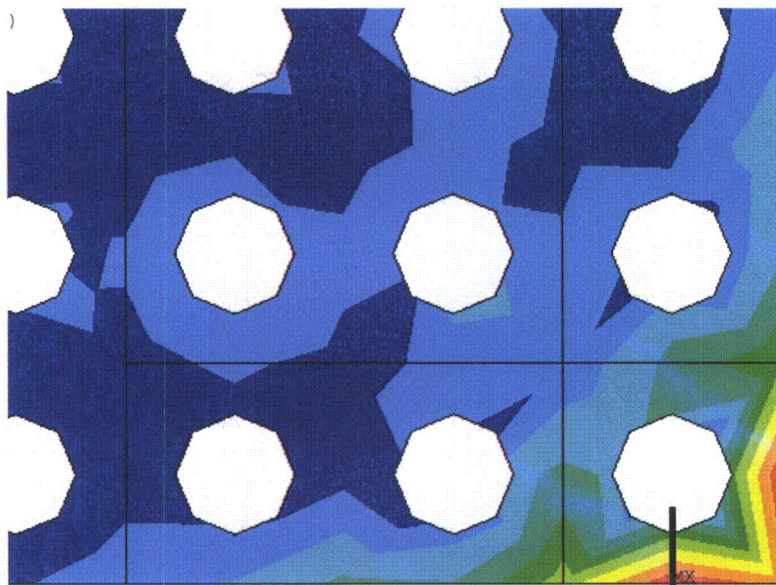
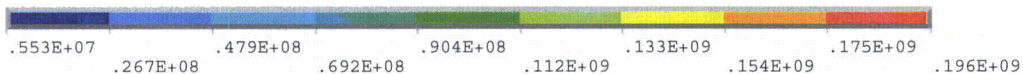
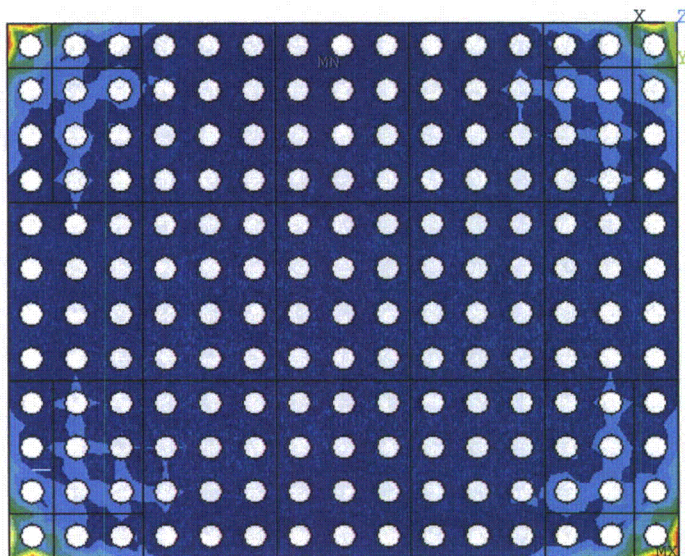


Figure A-33. FSR Base Plate Stiffener Plates. Level D Vertical Stress (N/m²)

SINT (AVG)
MIDDLE
DMX = .793E-03
SMN = .553E+07
SMX = .196E+09



S=151 MPa

Figure A-34. FSR Base Plate. Level D Stress (N/m²)

SINT (AVG)
TOP
DMX = .124E-03
SMN = 219851
SMX = .758E+08

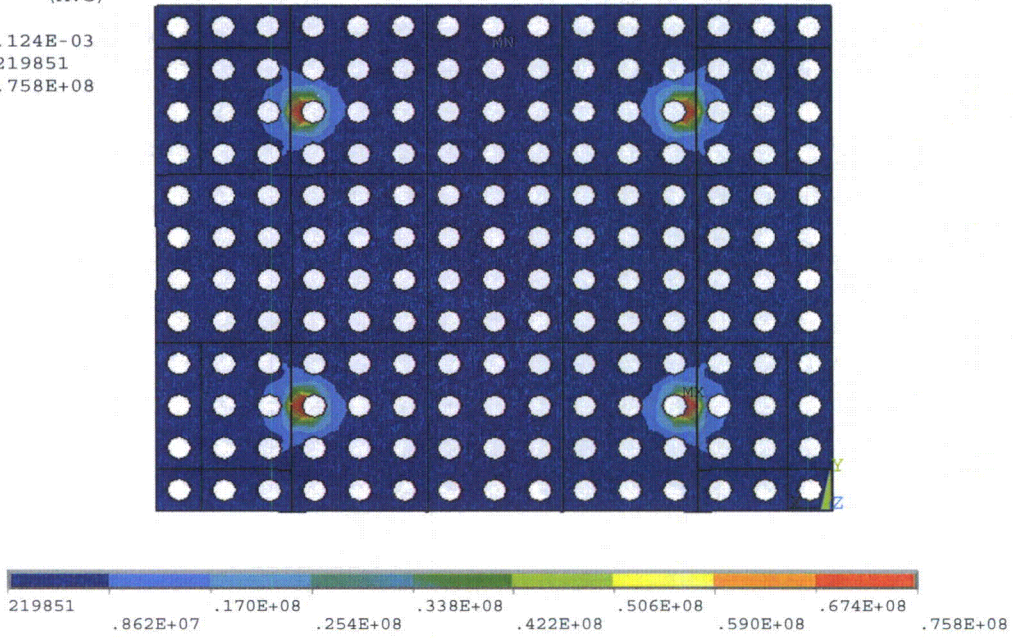


Figure A-35. Base Plate. Lifting Load stresses (N/m2)

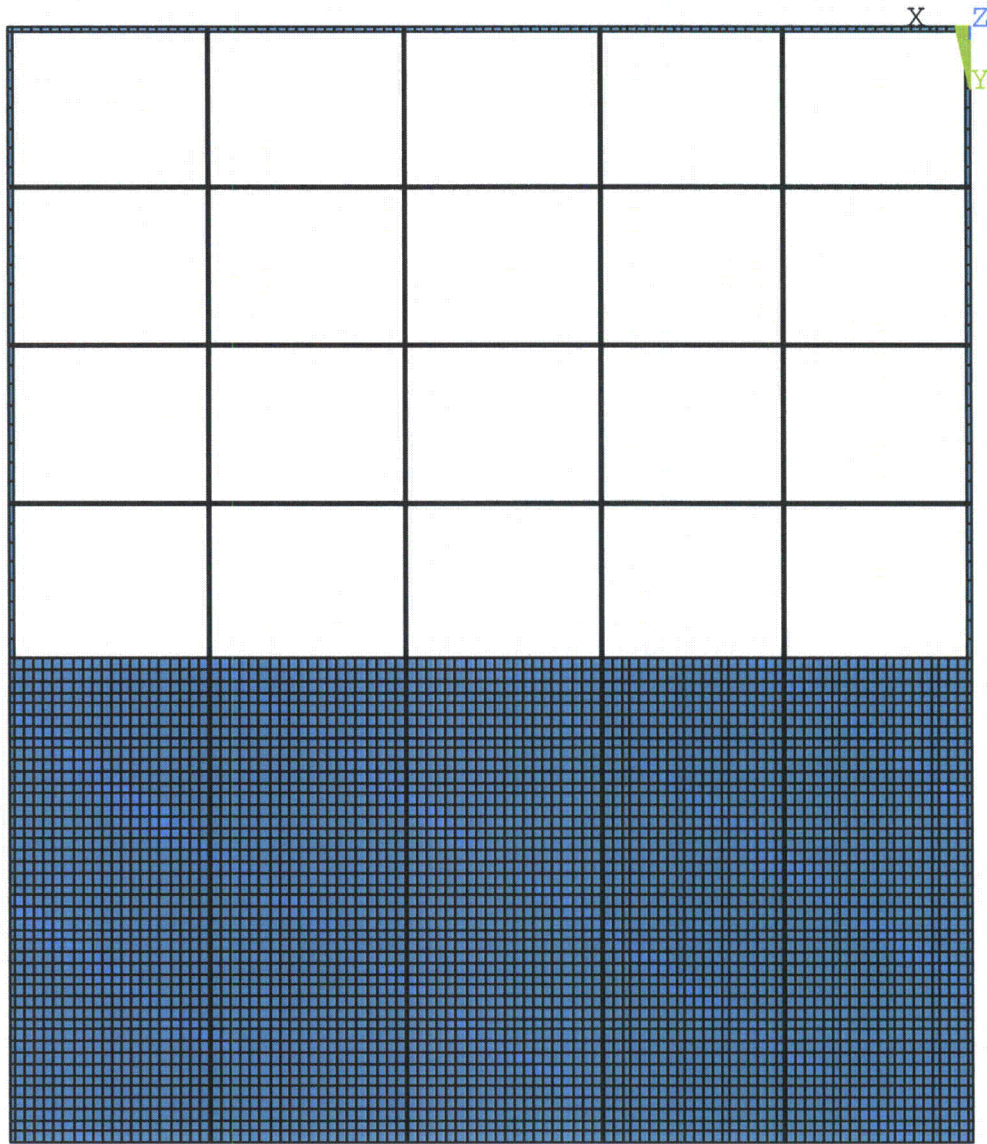


Figure A-36. Spent Fuel Pool+20FSR Model for Hydrodynamic Mass Calculations

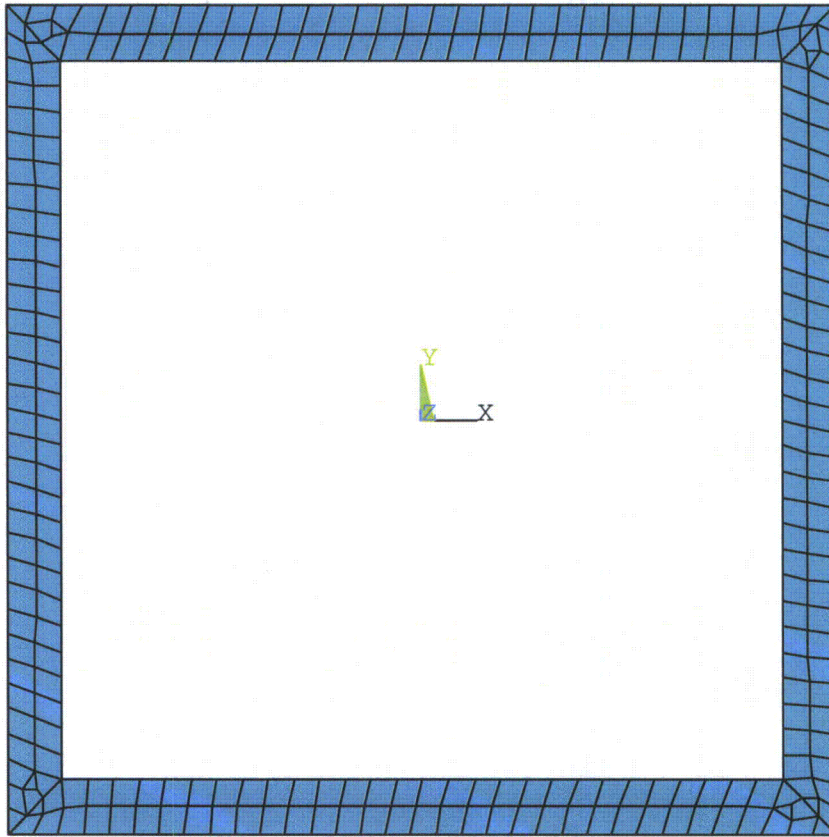


Figure A-37. FSR Cell+Fuel Model for Hydrodynamic Mass Calculations

NEDO-33373-A, Revision 5

129958	-26299	-5166	-2703	-1183	57089	-2296	-2261	-1539	-757	17322	3965	343	-423	-313	4212	1749	437	-7	-34	-176877
-26299	124971	-29542	-6310	-2682	-2288	55015	-4055	-3037	-1535	3991	17662	3605	-39	-422	1856	4543	1789	349	45	-142403
-5166	-29542	128837	-30218	-5399	-2256	-4054	57720	-4376	-2423	370	3610	19005	3617	273	536	1798	4984	1837	513	-144791
-2703	-6310	-30218	130185	-27304	-1536	-3037	-4378	58547	-2701	-407	-39	3612	19308	4122	57	350	1830	5038	1975	-151516
-1183	-2682	-5399	-27304	135750	-757	-1538	-2430	-2709	60945	-313	-438	245	4093	19047	-32	-14	413	1857	4714	-187390
57089	-2288	-2256	-1536	-757	115231	-28571	-4796	-2117	-857	50865	-5370	-3156	-1563	-638	11458	899	-588	-472	-191	-185170
-2296	55015	-4054	-3037	-1538	-28571	110517	-31228	-5584	-2091	-5345	47872	-7299	-3775	-1533	1044	10736	349	-822	-411	-132734
-2261	-4055	57720	-4378	-2430	-4796	-31228	113457	-31839	-4938	-3133	-7295	49827	-7704	-3261	-477	358	11337	274	-539	-129764
-1539	-3037	-4376	58547	-2709	-2117	-5584	-31839	114492	-29549	-1550	-3775	-7709	50595	-5974	-409	-820	267	11585	956	-140581
-757	-1535	-2423	-2701	60945	-857	-2091	-4938	-29549	119670	-638	-1545	-3286	-6002	53939	-189	-469	-649	801	12428	-195280
17322	3991	370	-407	-313	50865	-5345	-3133	-1550	-638	109344	-31588	-5701	-2153	-745	37708	-7721	-2916	-1042	-324	-160812
3965	17662	3610	-39	-438	-5370	47872	-7295	-3775	-1545	-31588	103608	-34472	-6358	-2110	-7544	34472	-9171	-3208	-973	-102089
343	3605	19005	3612	245	-3156	-7299	49827	-7709	-3286	-5701	-34472	105795	-35174	-5806	-2815	-9165	35518	-9527	-2860	-96107
-423	-39	3617	19308	4093	-1563	-3775	-7704	50595	-6002	-2153	-6358	-35174	106788	-32787	-993	-3206	-9532	36005	-8167	-107653
-313	-422	273	4122	19047	-638	-1533	-3261	-5974	53939	-745	-2110	-5806	-32787	113028	-323	-1019	-2958	-8352	39517	-168810
4212	1856	536	57	-32	11458	1044	-477	-409	-189	37708	-7544	-2815	-993	-323	67944	-25659	-2272	-655	-179	-88053
1749	4543	1798	350	-14	899	10736	358	-820	-469	-7721	34472	-9165	-3206	-1019	-25659	64059	-26809	-2458	-637	-45772
437	1789	4984	1830	413	-588	349	11337	267	-649	-2916	-9171	35518	-9532	-2958	-2272	-26809	64790	-27090	-2273	-42580
-7	349	1837	5038	1857	-472	-822	274	11585	801	-1042	-3208	-9527	36005	-8352	-655	-2458	-27090	65106	-26174	-48170
-34	45	513	1975	4714	-191	-411	-539	956	12428	-324	-973	-2860	-8167	39517	-179	-637	-2273	-26174	69195	-91707
-176877	142403	144791	151516	-187390	-185170	-132734	-129764	140581	-195280	-160812	102089	-96107	107653	-168810	-88053	-45772	-42580	-48170	-91707	2721548

Figure A-38. Hydrodynamic Mass (kg/m) Full Matrix for X (N-S) Direction

NEDO-33373-A, Revision 5

170713	68085	20254	6585	2935	-36578	-1186	7146	5209	3593	-5676	-1509	2721	3546	3348	-4181	-1511	1343	2742	3118	-255482
68085	156481	68373	18270	6364	-1181	-38927	-3393	6173	5110	-1505	-4801	-1904	2466	3529	-1498	-2601	-1142	1449	2769	-286904
20254	68373	182458	73174	20819	7149	-3392	-47866	-3692	7528	2722	-1903	-5855	-2064	2960	1356	-1137	-2952	-1223	1539	-323371
6585	18270	73174	184414	77931	5210	6173	-3692	-46931	-1409	3545	2466	-2066	-5608	-1714	2747	1449	-1228	-3044	-1690	-319708
2935	6364	20819	77931	201074	3593	5109	7524	-1414	-44023	3348	3531	2958	-1720	-6553	3116	2761	1523	-1706	-4883	-287413
-36578	-1181	7149	5210	3593	164794	66672	23060	10179	6316	-40721	-2676	8495	7935	6675	-9926	-3056	4064	6322	6521	-237633
-1186	-38927	-3392	6173	5109	66672	151363	66535	20804	9941	-2670	-41525	-4531	7617	7849	-3017	-7407	-3045	3936	6344	-251429
7146	-3393	-47866	-3692	7524	23060	66535	176235	71177	23862	8495	-4529	-50819	-4915	9051	4097	-3032	-8805	-3280	4521	-276497
5209	6173	-3692	-46931	-1414	10179	20804	71177	178452	76319	7931	7617	-4917	-49970	-3090	6335	3935	-3292	-8659	-3421	-273873
3593	5110	7528	-1409	-44023	6316	9941	23862	76319	194254	6675	7854	9051	-3096	-48856	6516	6325	4484	-3466	-11520	-260582
-5676	-1505	2722	3545	3348	-40721	-2670	8495	7931	6675	160753	65187	24344	12848	9354	-46530	-4275	11178	11536	10136	-241460
-1509	-4801	-1903	2466	3531	-2676	-41525	-4529	7617	7854	65187	148864	65442	22212	12630	-4179	-46266	-6409	10118	11481	-248389
2721	-1904	-5855	-2066	2958	8495	-4531	-50819	-4917	9051	24344	65442	173412	70002	25321	11251	-6387	-56600	-6934	12058	-270169
3546	2466	-2064	-5608	-1720	7935	7617	-4915	-49970	-3096	12848	22212	70002	175528	74643	11570	10115	-6952	-55518	-4806	-268961
3348	3529	2960	-1714	-6553	6675	7849	9051	-3090	-48856	9354	12630	25321	74643	189535	10130	11437	11977	-4917	-55580	-262856
-4181	-1498	1356	2747	3116	-9926	-3017	4097	6335	6516	-46530	-4179	11251	11570	10130	126625	64672	31921	18453	13327	-247572
-1511	-2601	-1137	1449	2761	-3056	-7407	-3032	3935	6325	-4275	-46266	-6387	10115	11437	64672	112281	62669	28767	18136	-251662
1343	-1142	-2952	-1228	1523	4064	-3045	-8805	-3292	4484	11178	-6409	-56600	-6952	11977	31921	62669	128153	66982	33324	-272321
2742	1449	-1223	-3044	-1706	6322	3936	-3280	-8659	-3466	11536	10118	-6934	-55518	-4917	18453	28767	66982	131300	74038	-272022
3118	2769	1539	-1690	-4883	6521	6344	4521	-3421	-11520	10136	11481	12058	-4806	-55580	13327	18136	33324	74038	148375	-268912
-255482	-286904	-323371	-319708	-287413	-237633	-251429	-276497	-273873	-260582	-241460	-248389	-270169	-268961	-262856	-247572	-251662	-272321	-272022	-268912	5560505

Figure A-39. Hydrodynamic Mass (kg/m) Full Matrix for Y (E-W) Direction

Figure A-40. (Deleted)

Figure A-41. (Deleted)

184	-204
-204	230

Figure A-42. Hydrodynamic Mass (kg/m) Coupling Matrix. Fuel Assembly-FSR Cell

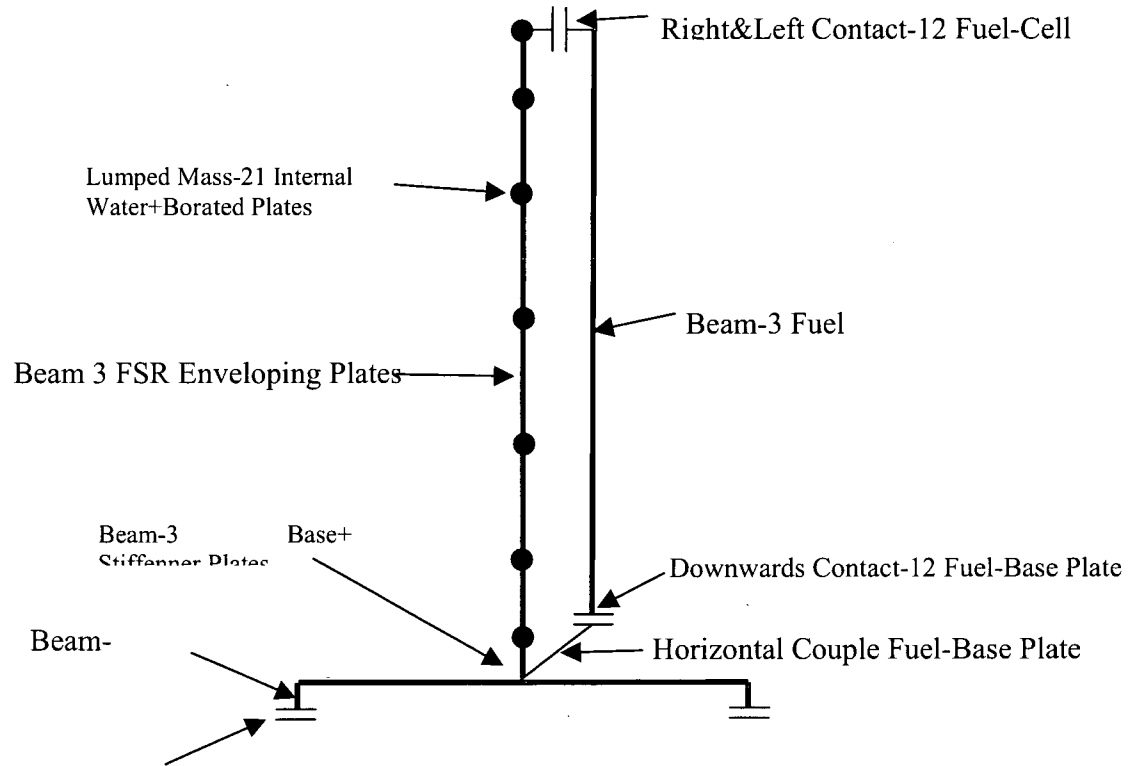


Figure A-43. FSR Simplified Model

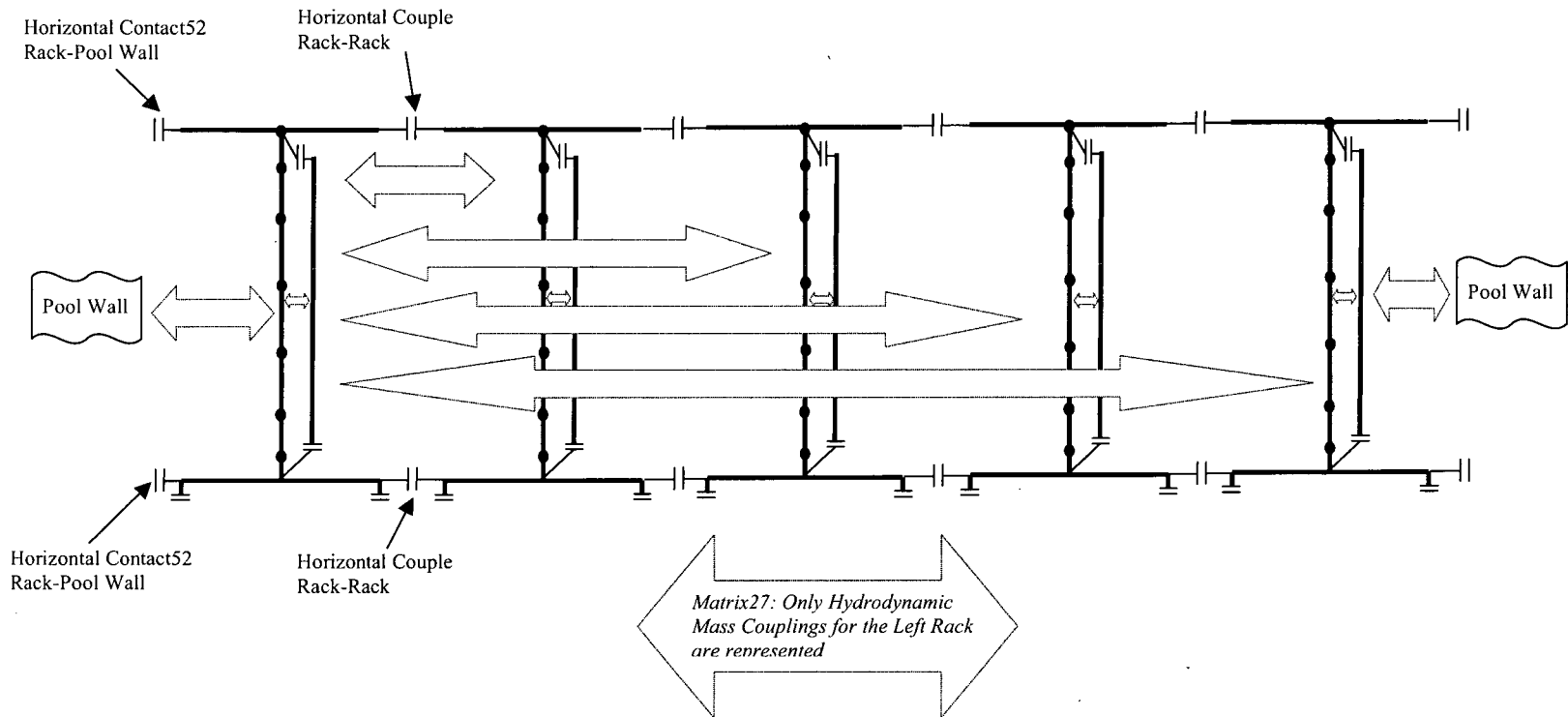


Figure A-44. Global Model. One N-S Row 2-D View

Figure A-45. (Deleted)

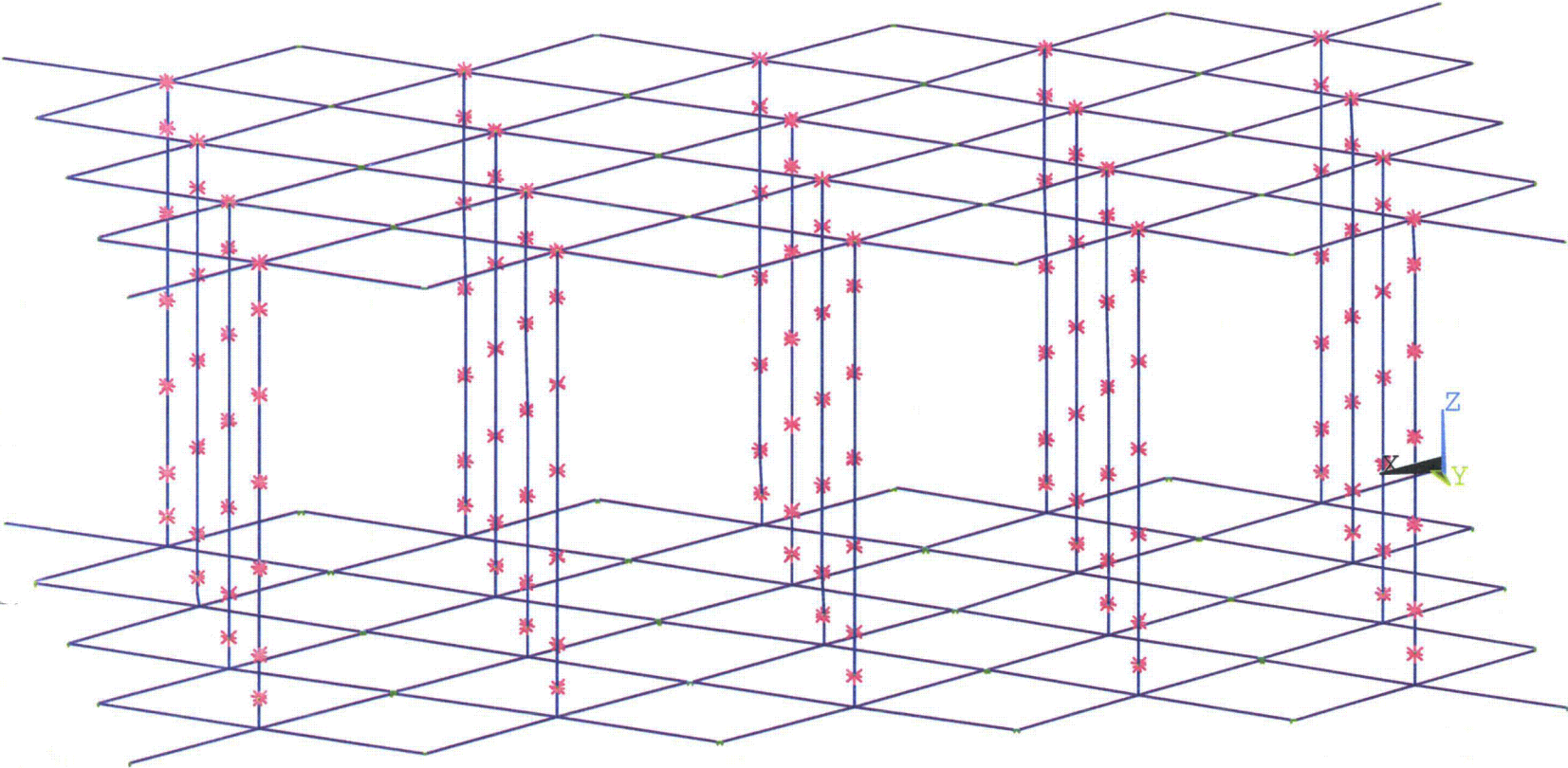


Figure A-46. ANSYS Global Model (without hydrodynamic couplings) ANSYS Global Model (without hydrodynamic couplings)

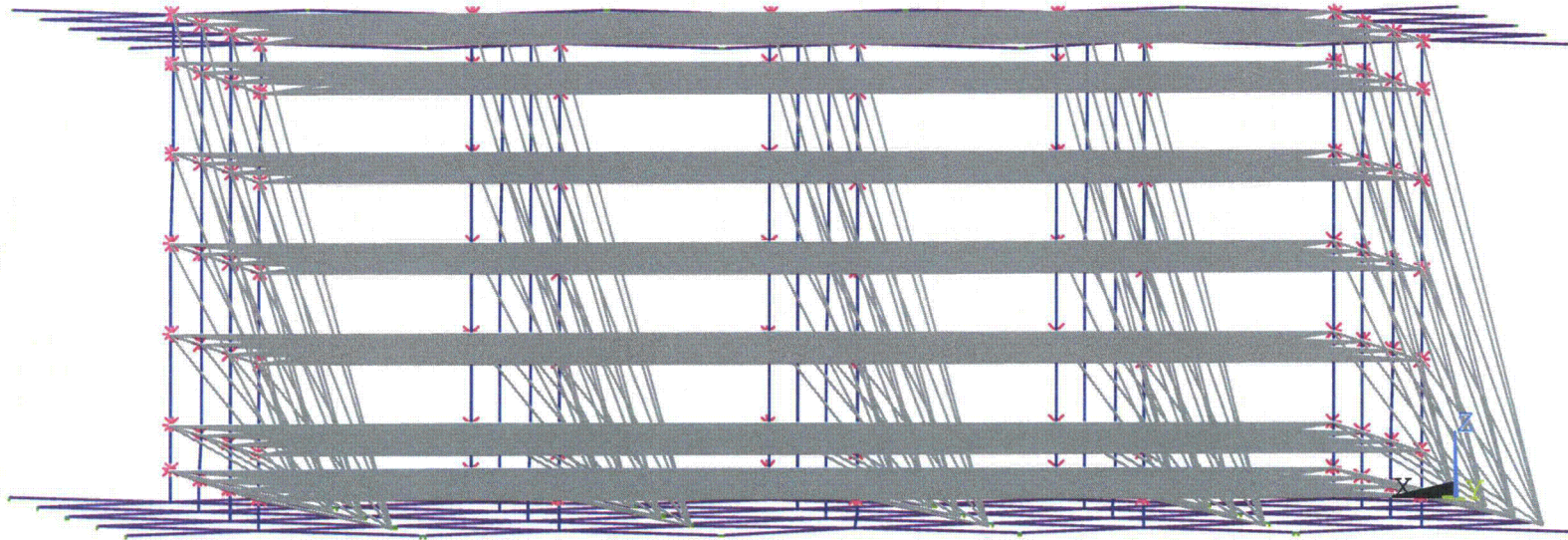


Figure A-47. ANSYS Global Model E-

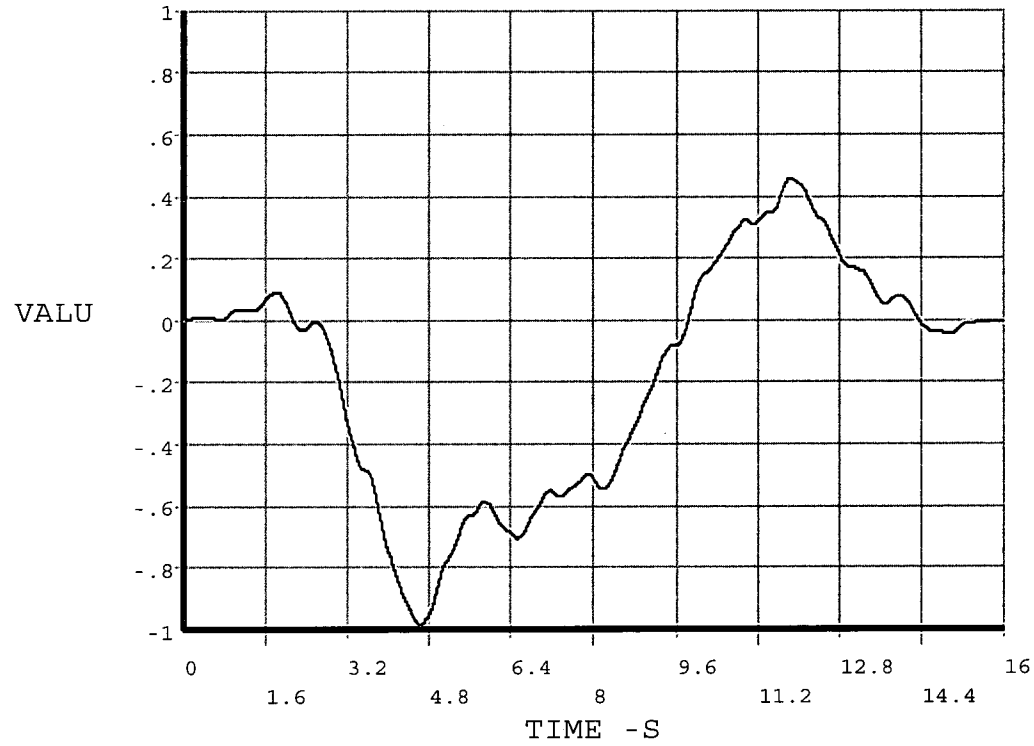


Figure A-48. Displacement (m) Time-History. X(N-S) Direction.

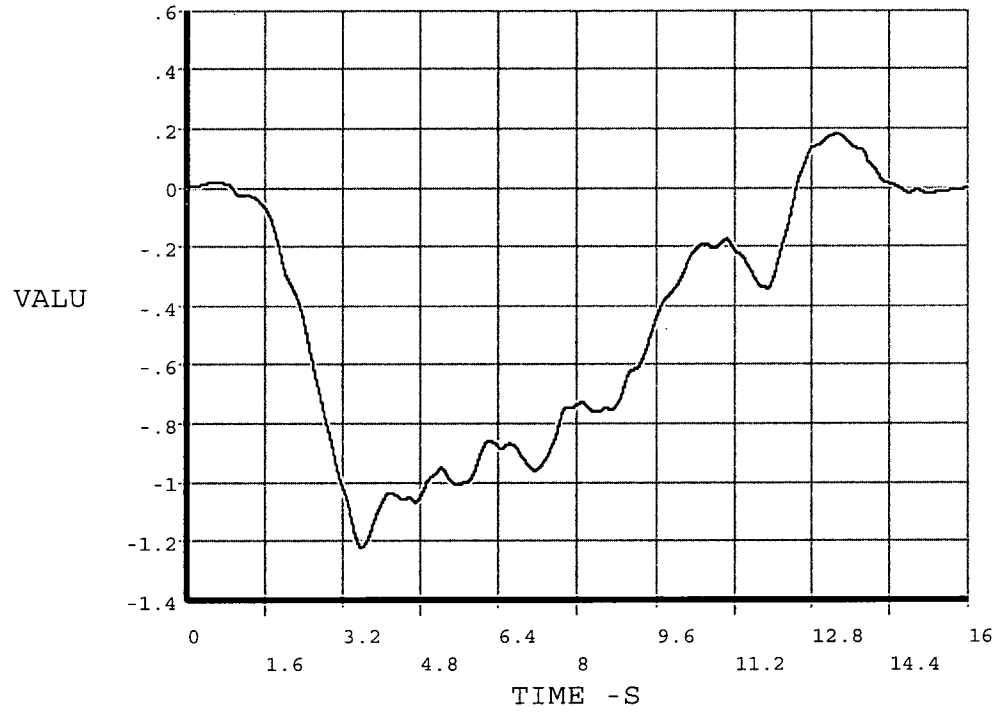


Figure A-49. Displacement (m) Time-History. Y(E-W) Direction.

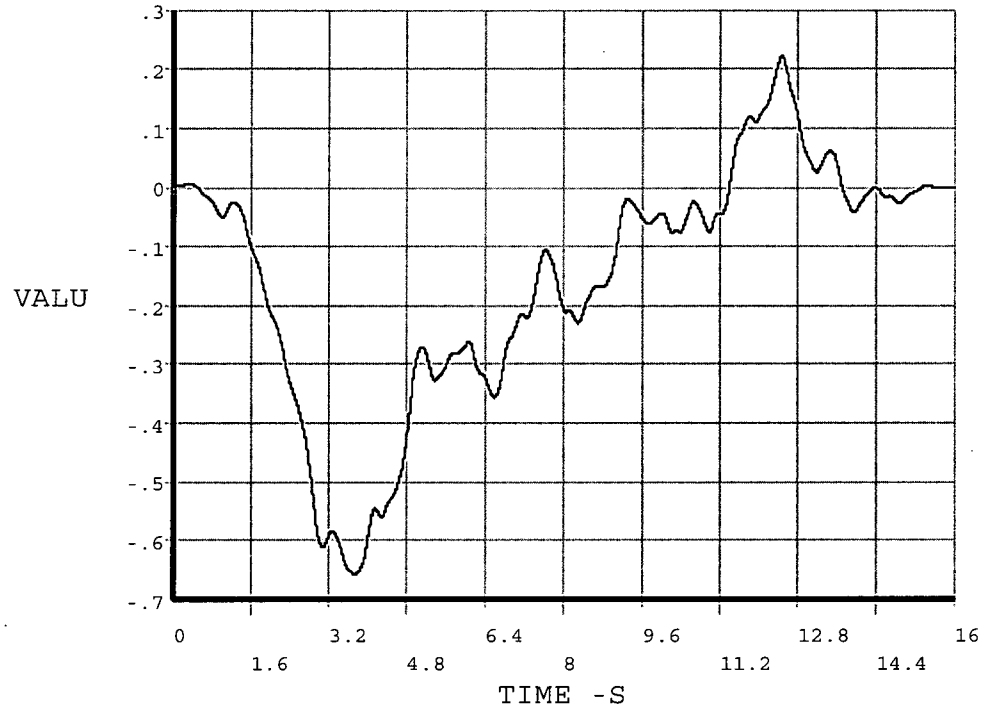


Figure A-50. Displacement (m) Time-History. Z (Vertical) Direction

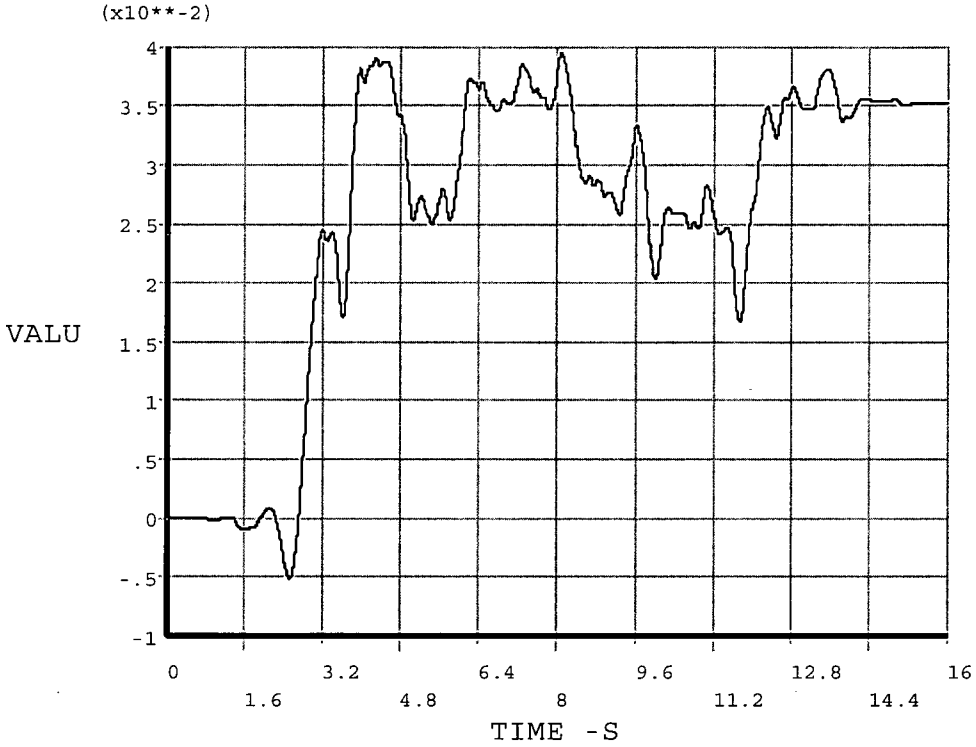


Figure A-51. Relative Horizontal Displacement (m) FSR Foot-Pool Floor. N-S Direction. Case C-3

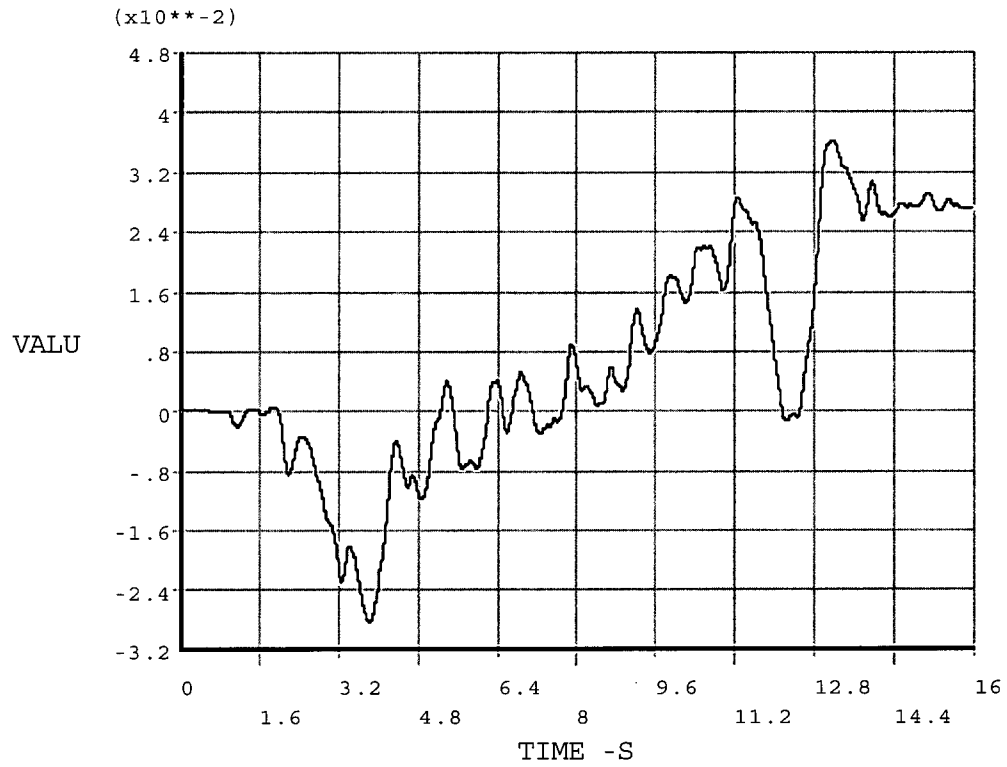


Figure A-52. Relative Horizontal E-W Displacement (m) FSR Foot-Pool Floor. Case C-6

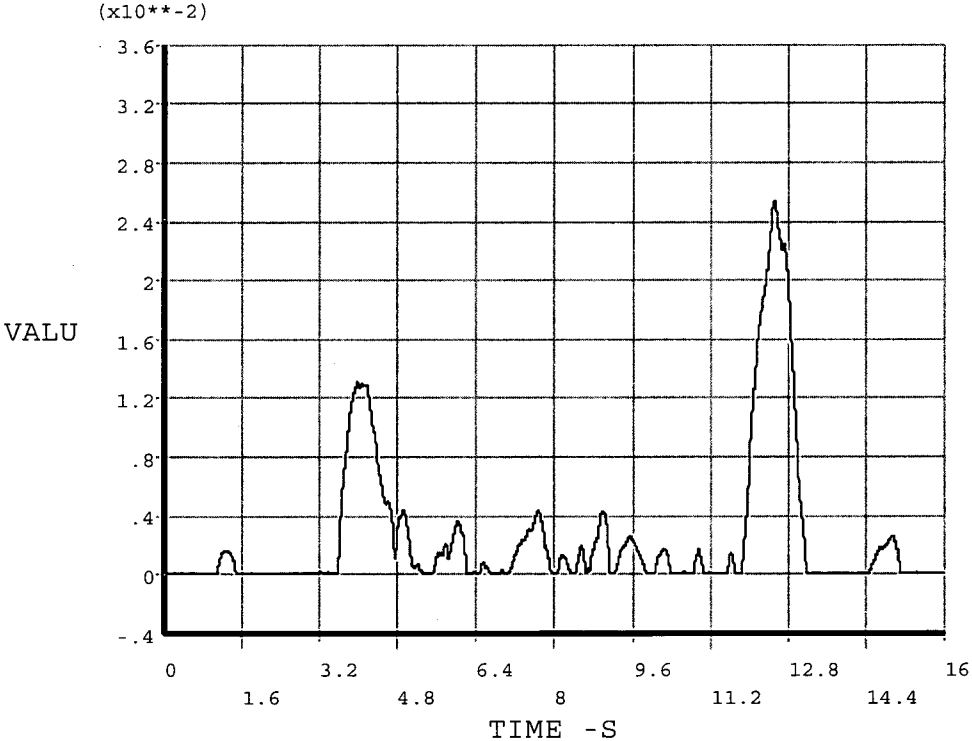


Figure A-53. Relative Vertical Displacement (m) FSR Foot-Pool Floor Case C-5

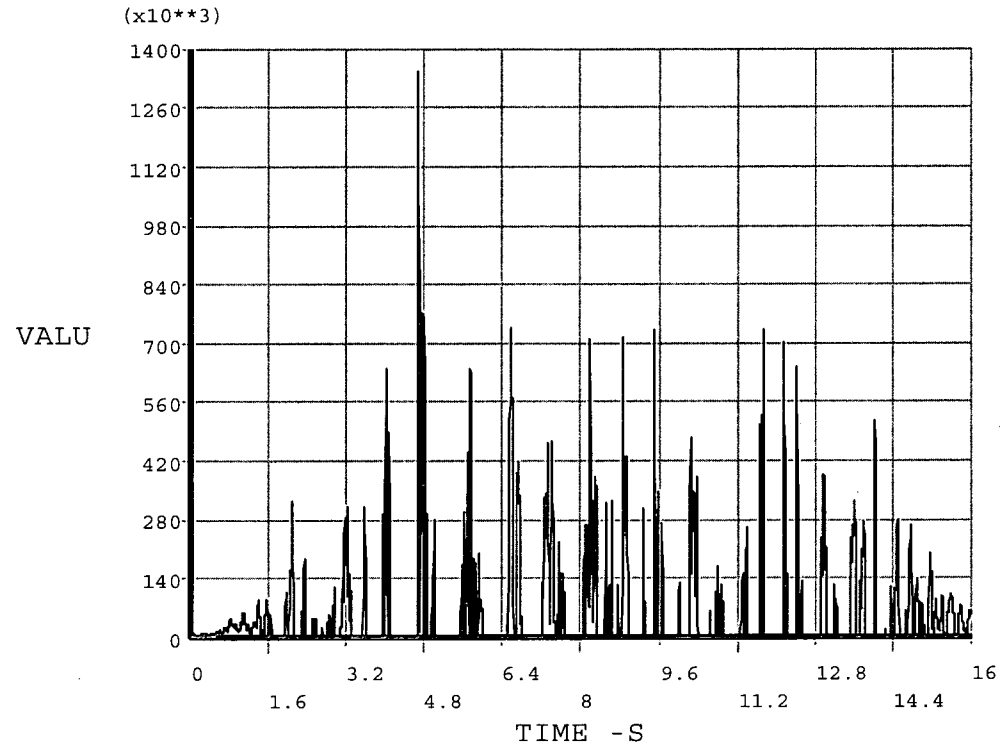


Figure A-54. Horizontal Force (N) FSR Foot-Pool Floor. Case C-4

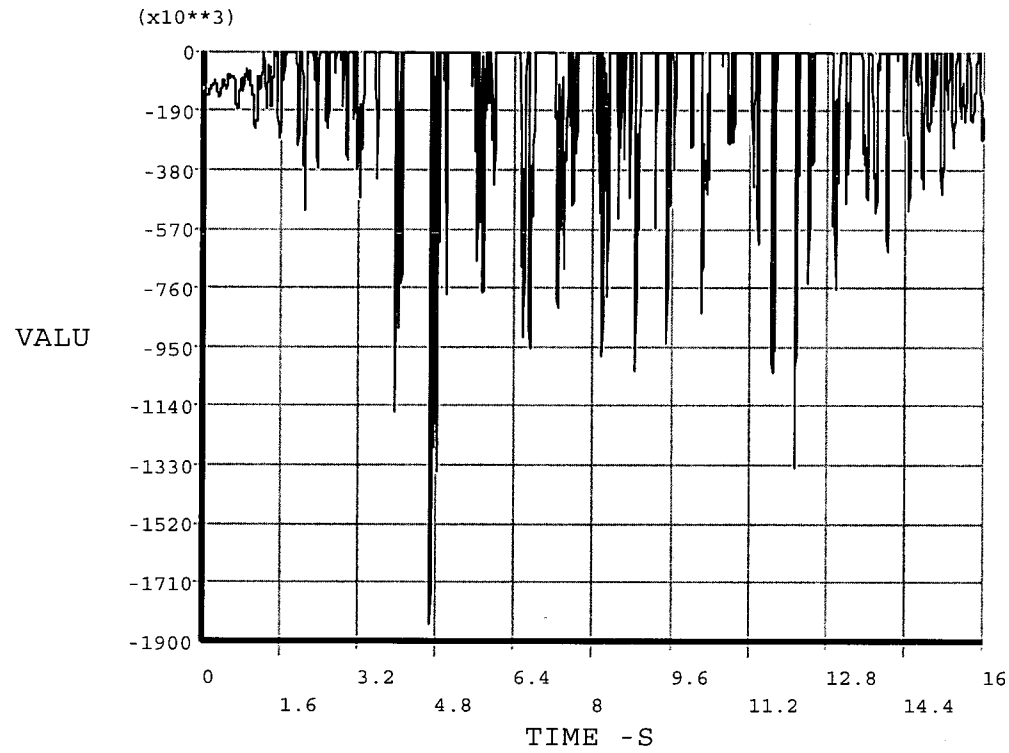


Figure A-55. Vertical Force (N) FSR Foot-Pool Floor. Case C-4

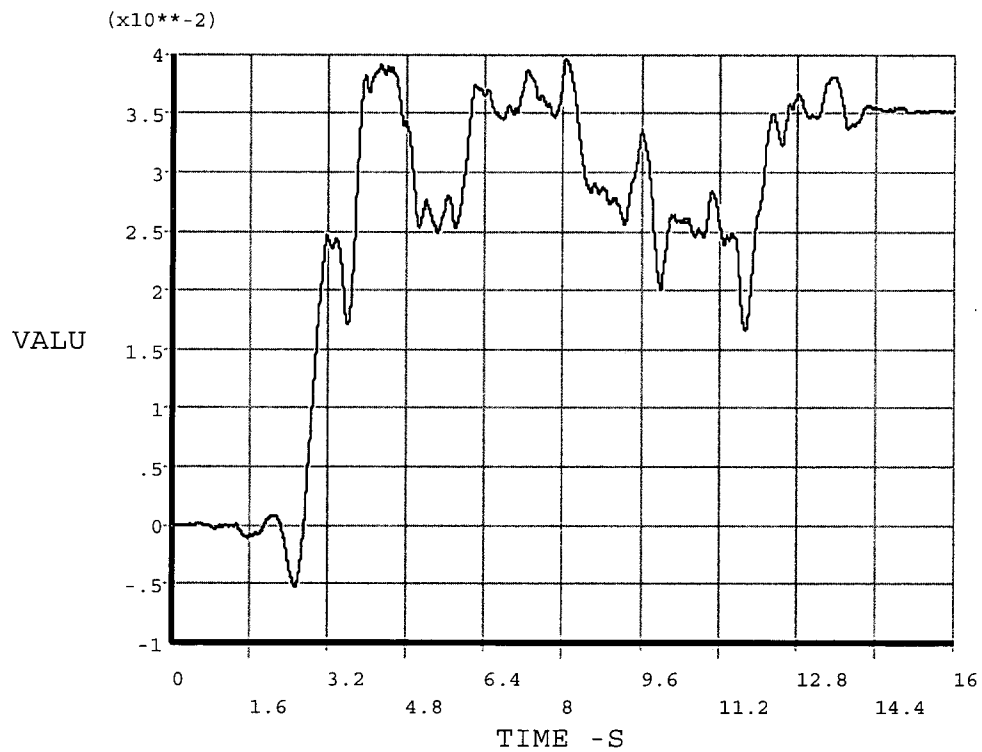


Figure A-56. Relative Horizontal N-S Displacement (m) FSR Top-Pool Wall. Case C-3

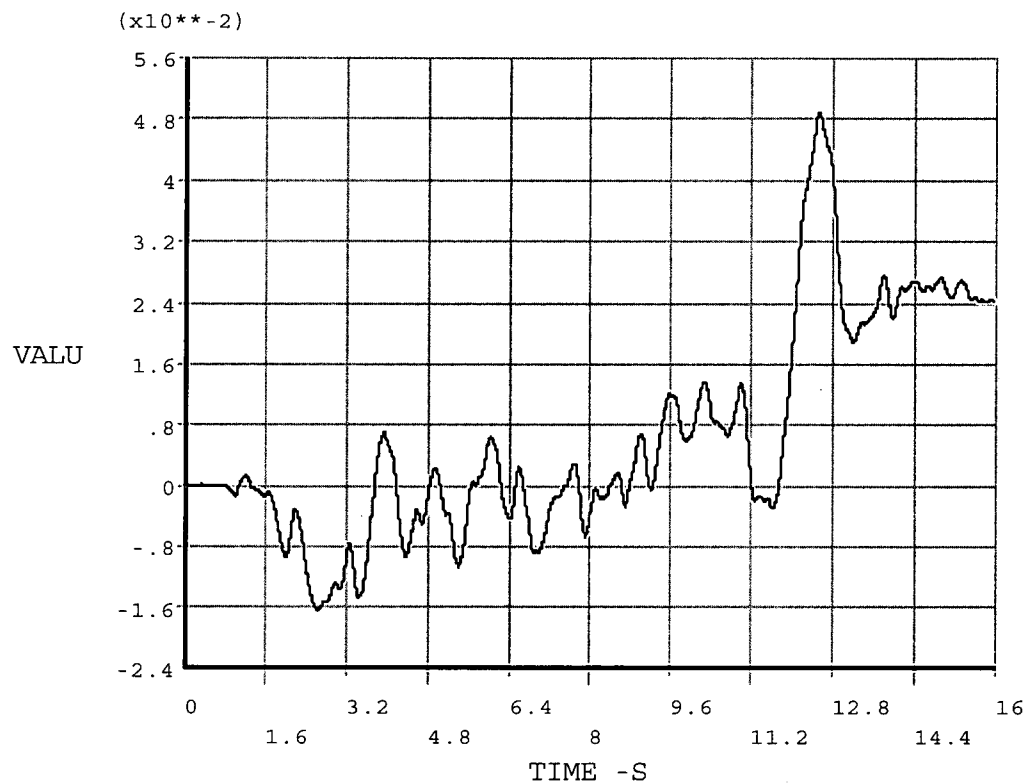


Figure A-57. Relative Horizontal E-W Displacement (m) FSR Top-Pool Wall. Case C-6

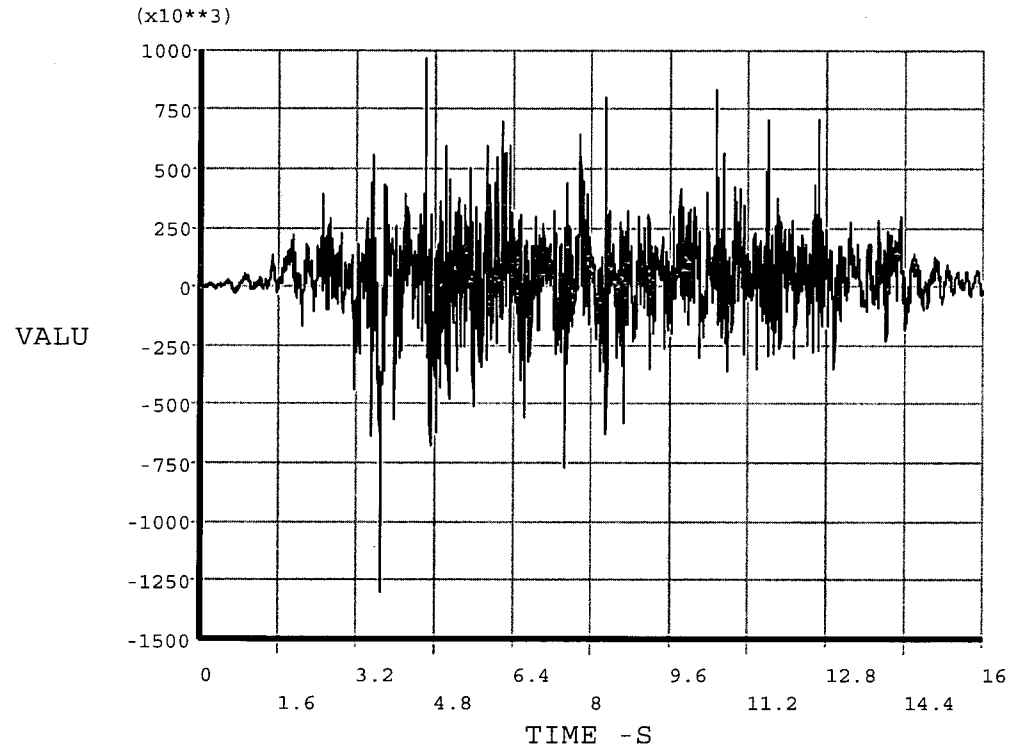


Figure A-58. Horizontal Force (N) between two FSR at the Bottom Link Device. Case C-4

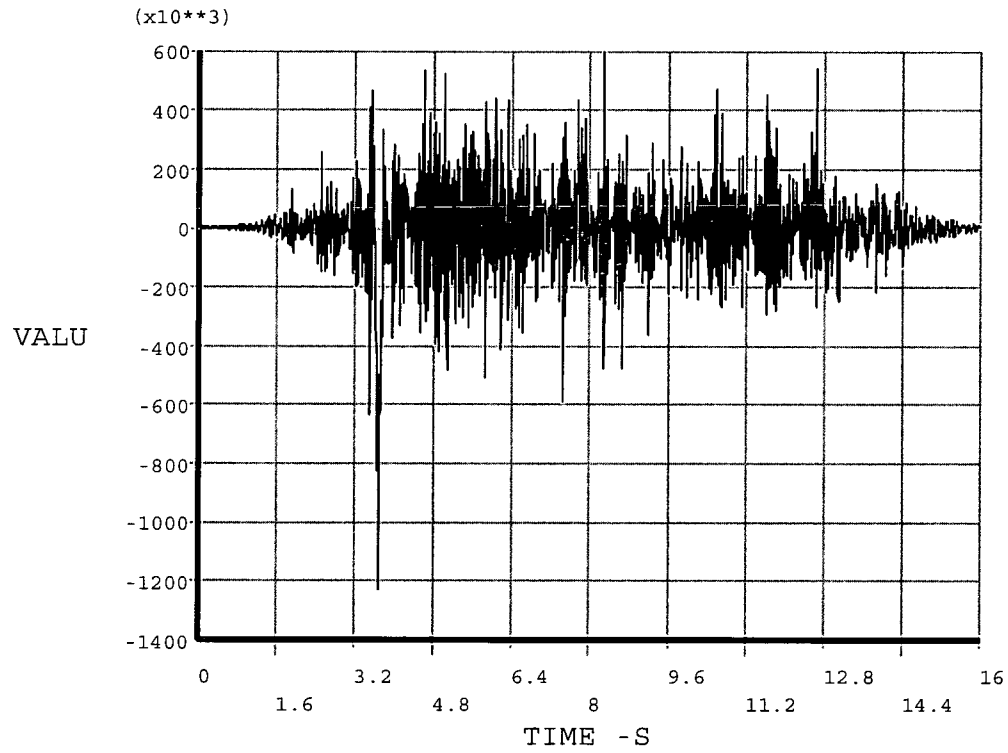


Figure A-59. Horizontal Force (N) between two FSR at the Upper Link Device. Case C-4

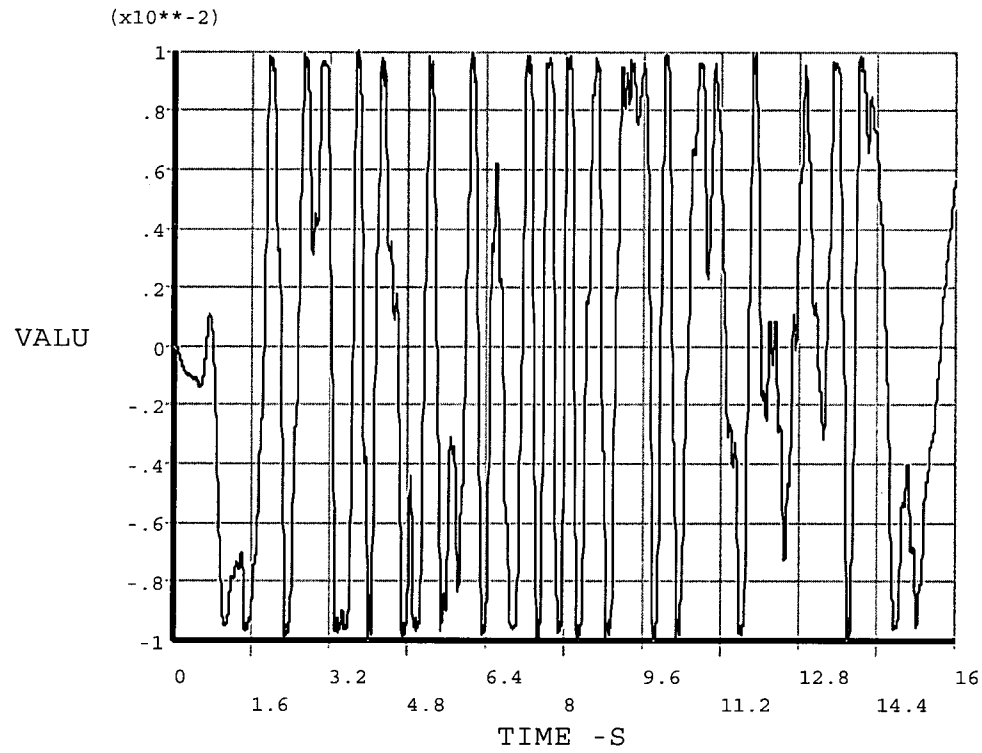


Figure A-60. Relative Horizontal Displacement (m) Top Fuel- FSR Top Cells. Case C-4

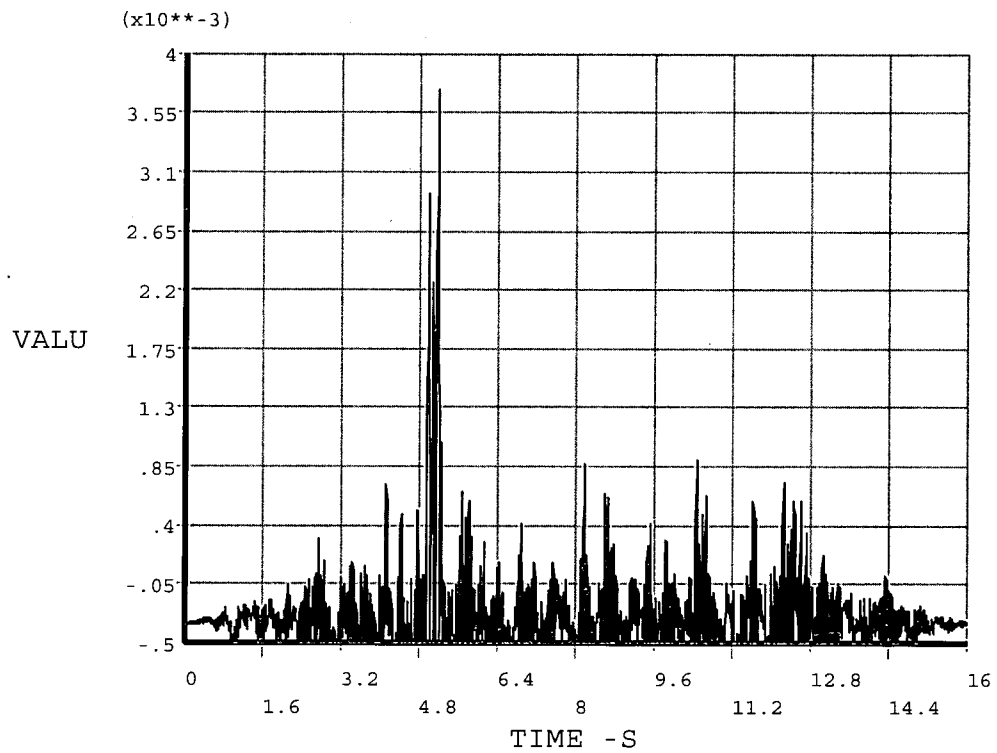


Figure A-60a. Relative Vertical Displacement (m) Bottom Fuel- FSR Base Plate. Case C-4

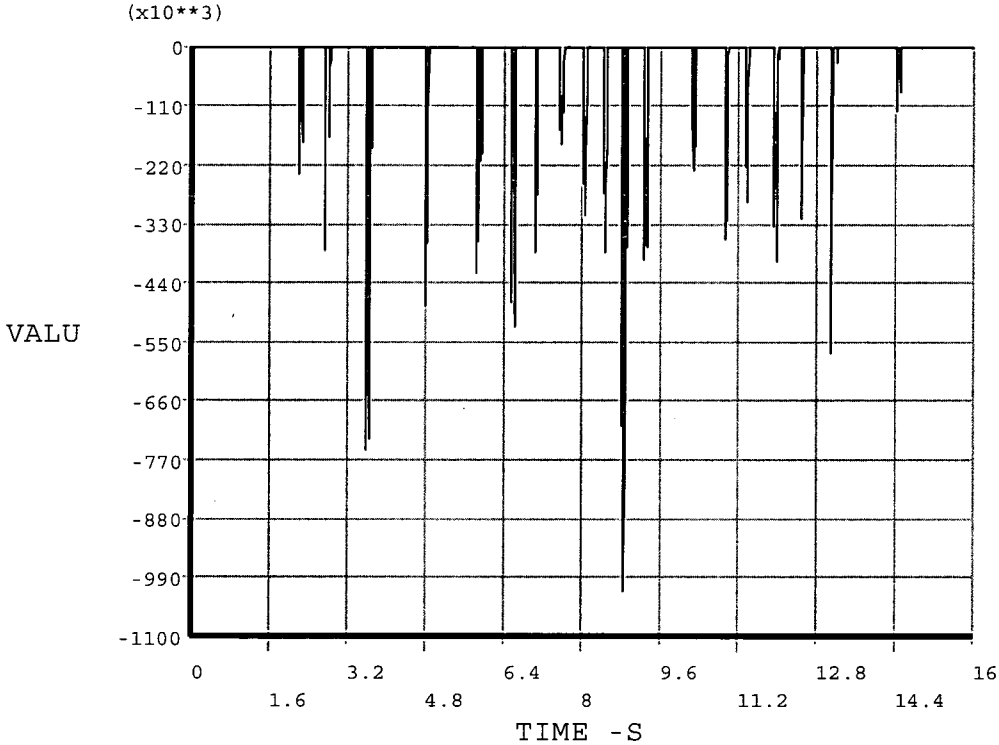


Figure A-60b. Horizontal Force (N) Top Fuel-FSR Top Cells. Case C-1

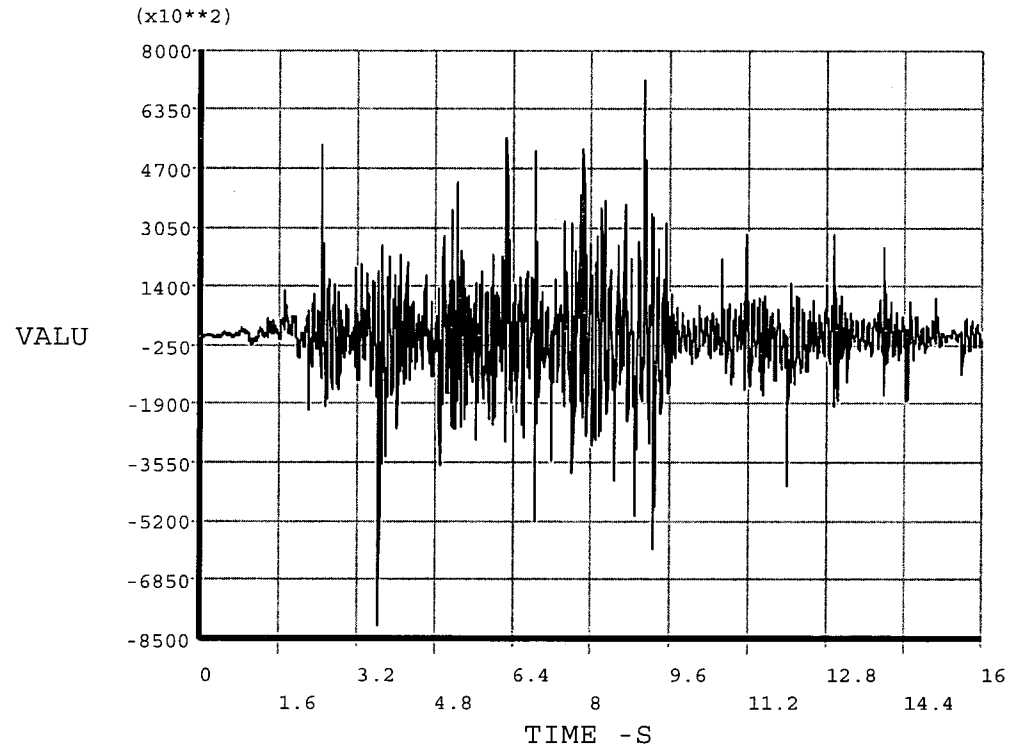


Figure A-61. Horizontal Force (N) Bottom Fuel-FSR Base Plate. Case C-4

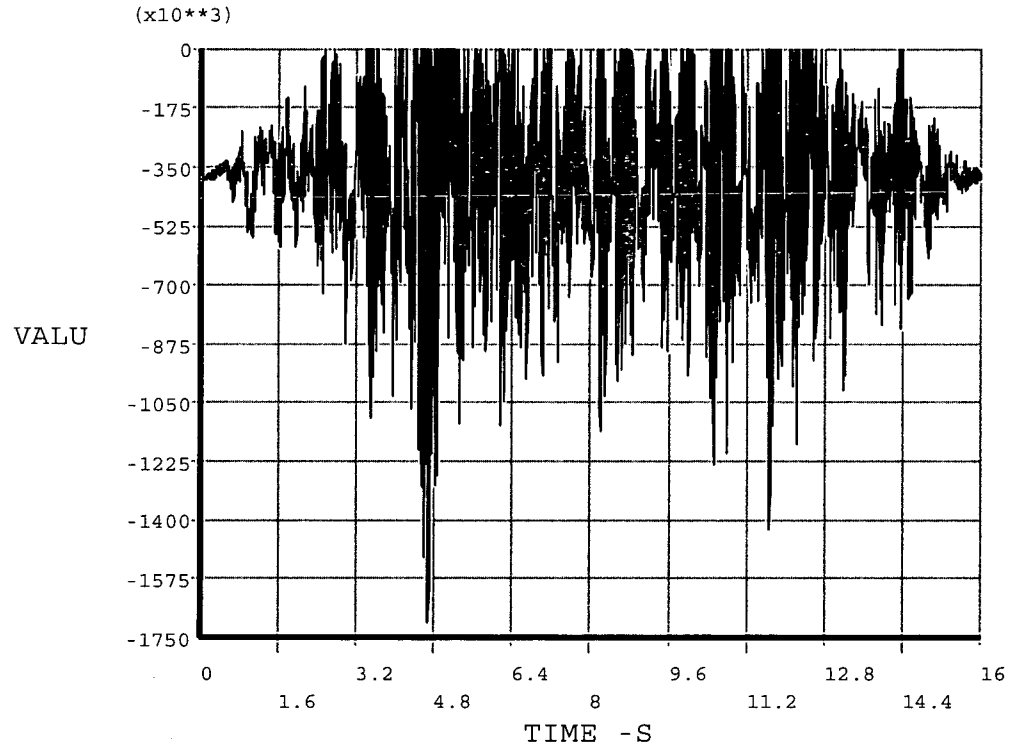


Figure A-62. Vertical Force (N) Fuel-FSR Base Plate. Case C-4

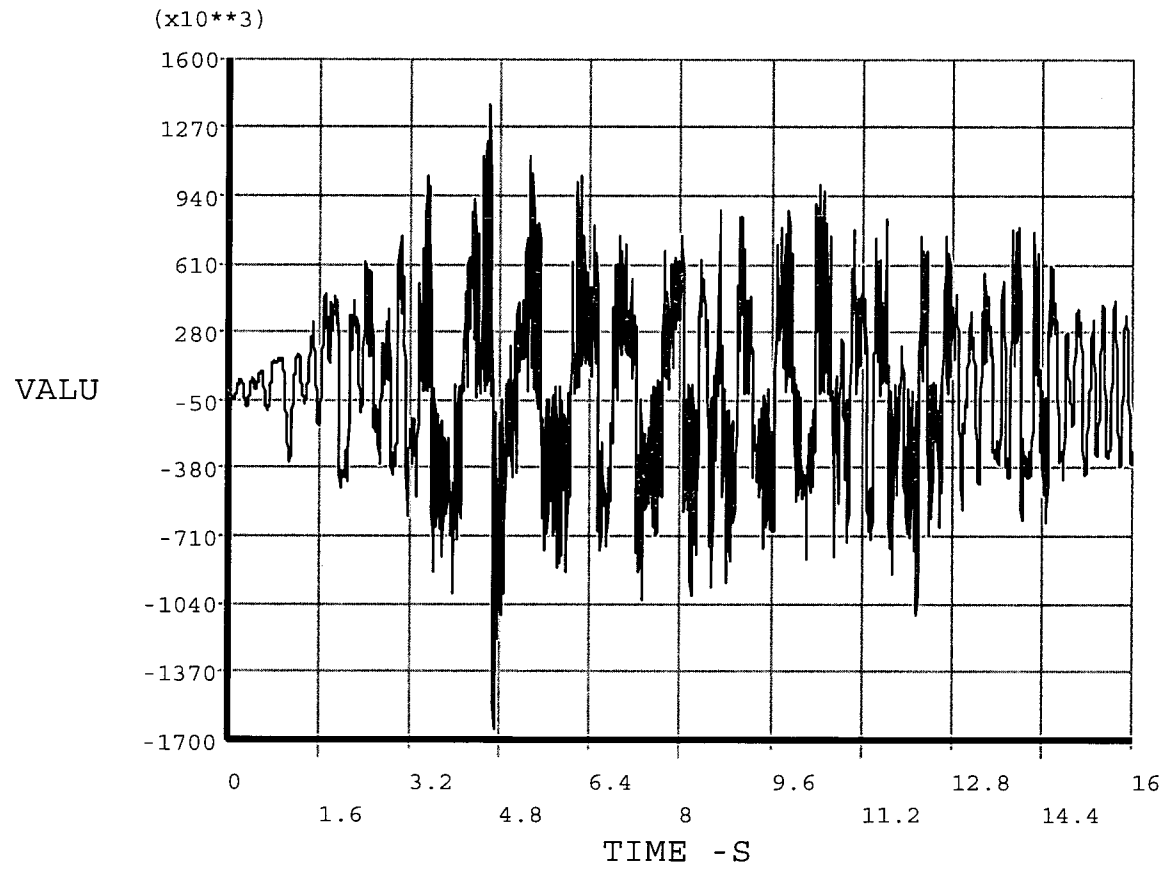


Figure A-63. N-S Bending Moment (N·m) on the FSR Base Plate. Case C-4

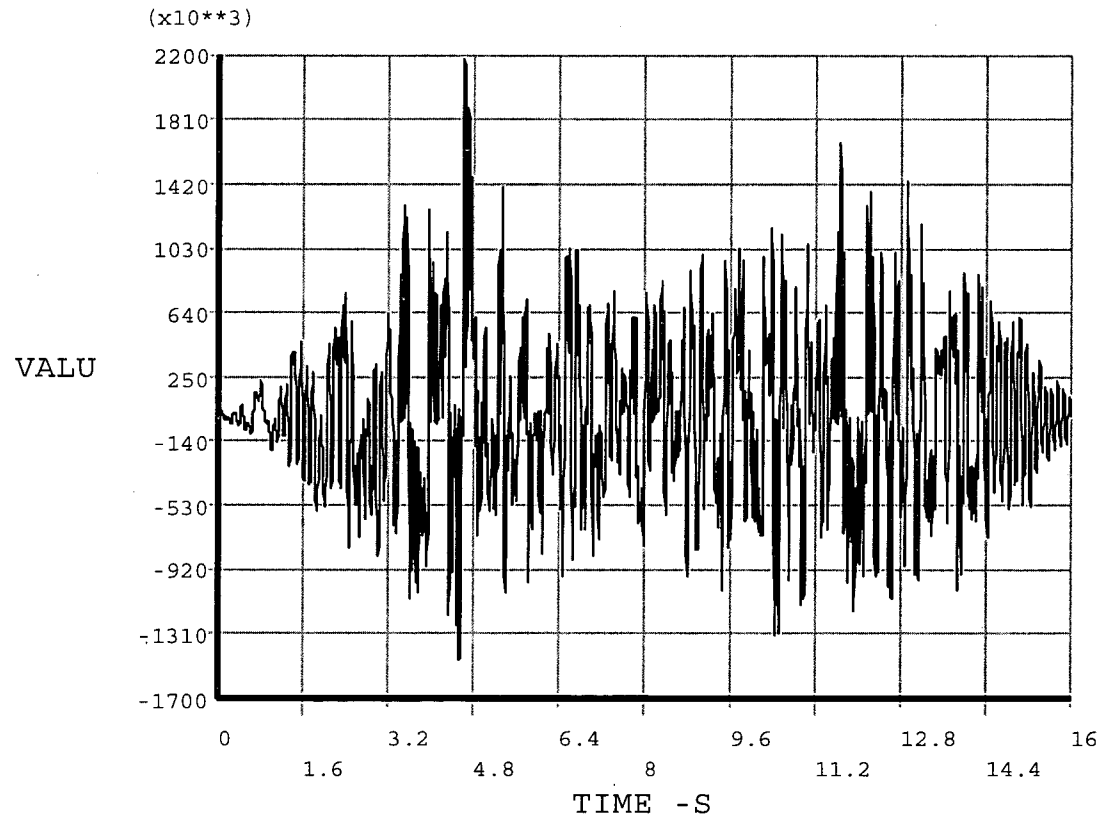


Figure A-64. E-W Bending Moment (N·m) on the FSR Base Plate. Case C-4

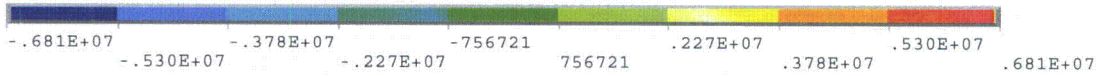
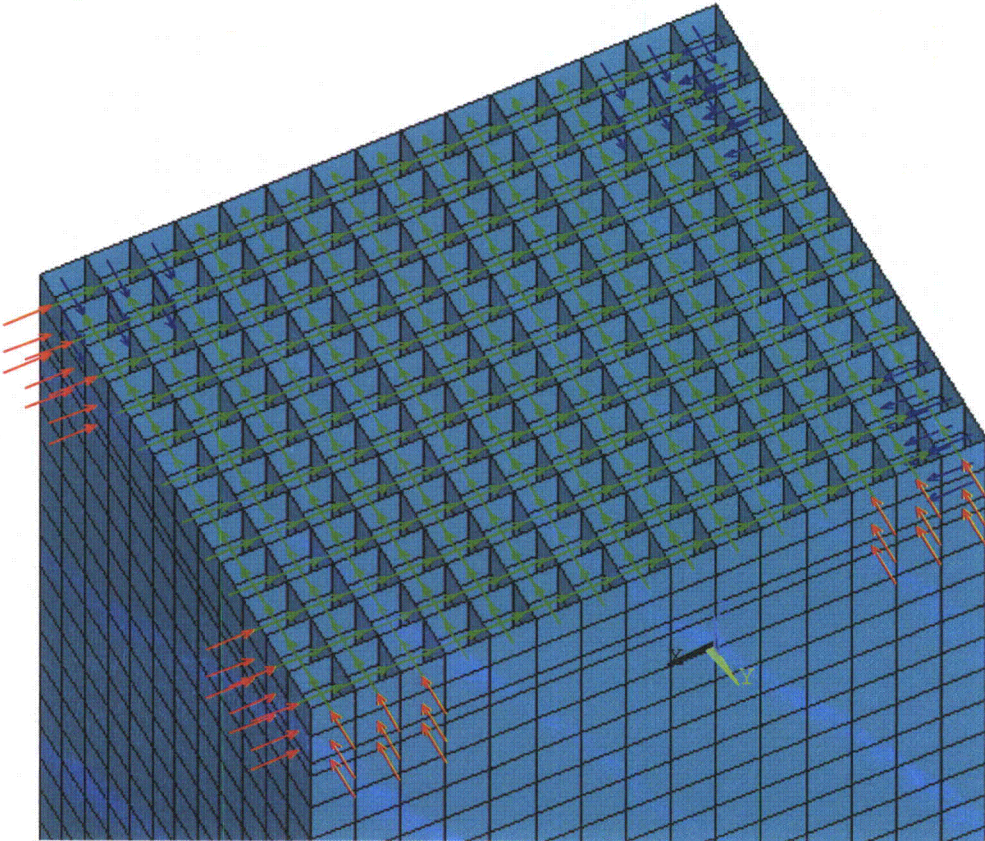


Figure A-65. Case I-1. Top Cell Plates in Compression. Impact Pressure Loads (N/m²)

F

PRES
227339

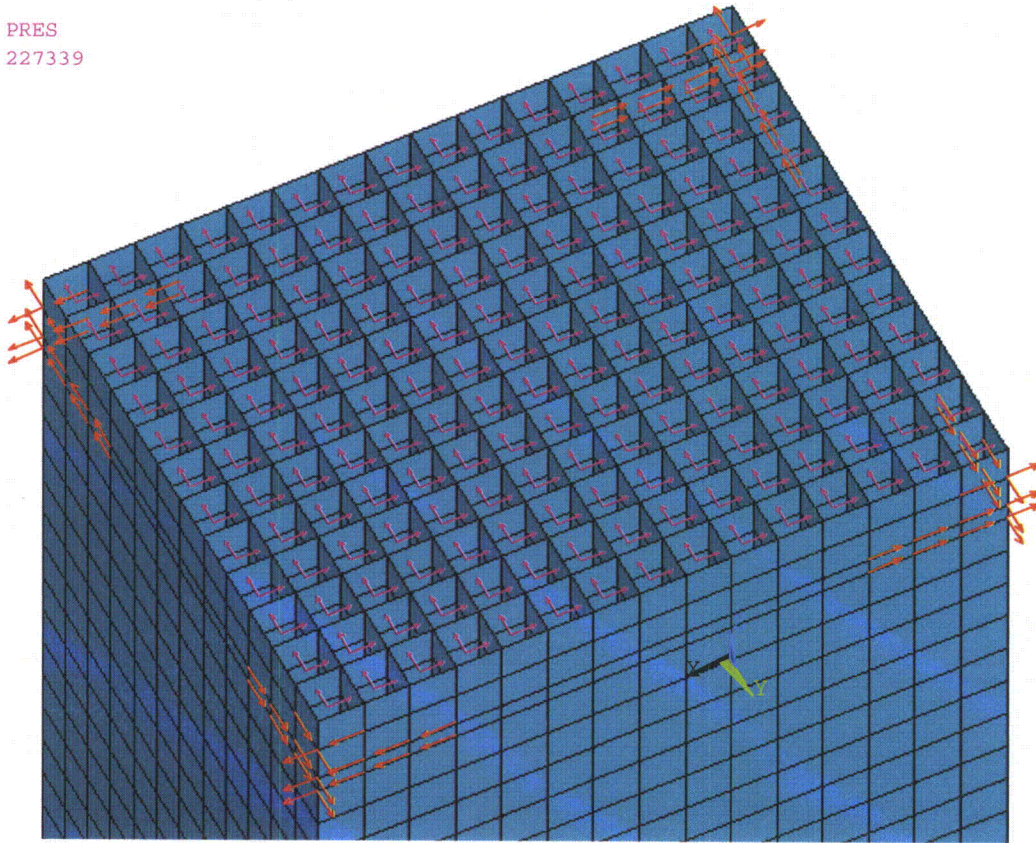


Figure A-66. Case I-2. Top Cell Plates in Tension. Impact Pressure Loads (N/m²)

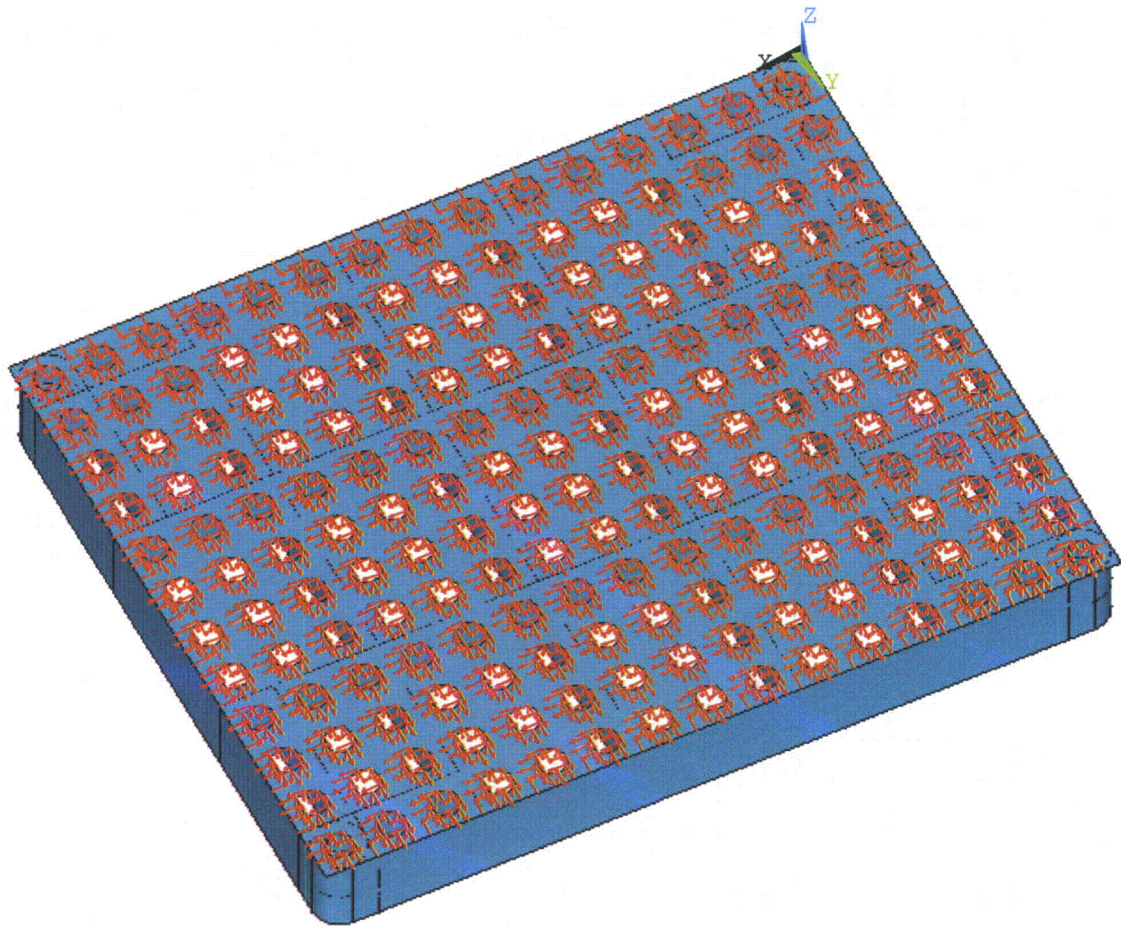


Figure A-67. Case I-3. Base Plate in Compression. Impact Pressure Loads (N/m²)

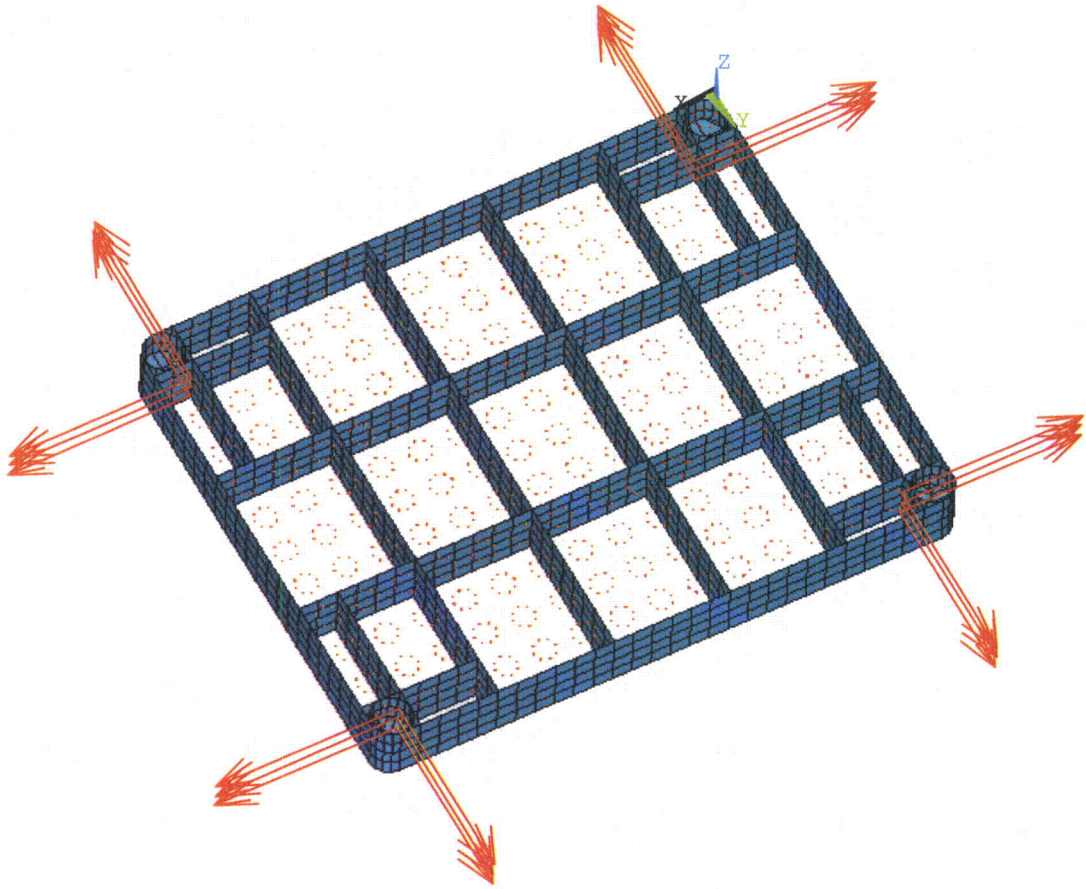


Figure A-68. Case I-4. Base Plate in Tension. Impact Pressure Loads (N/m²)

SINT (AVG)
MIDDLE
DMX = .005723
SMN = .252E+07
SMX = .803E+08

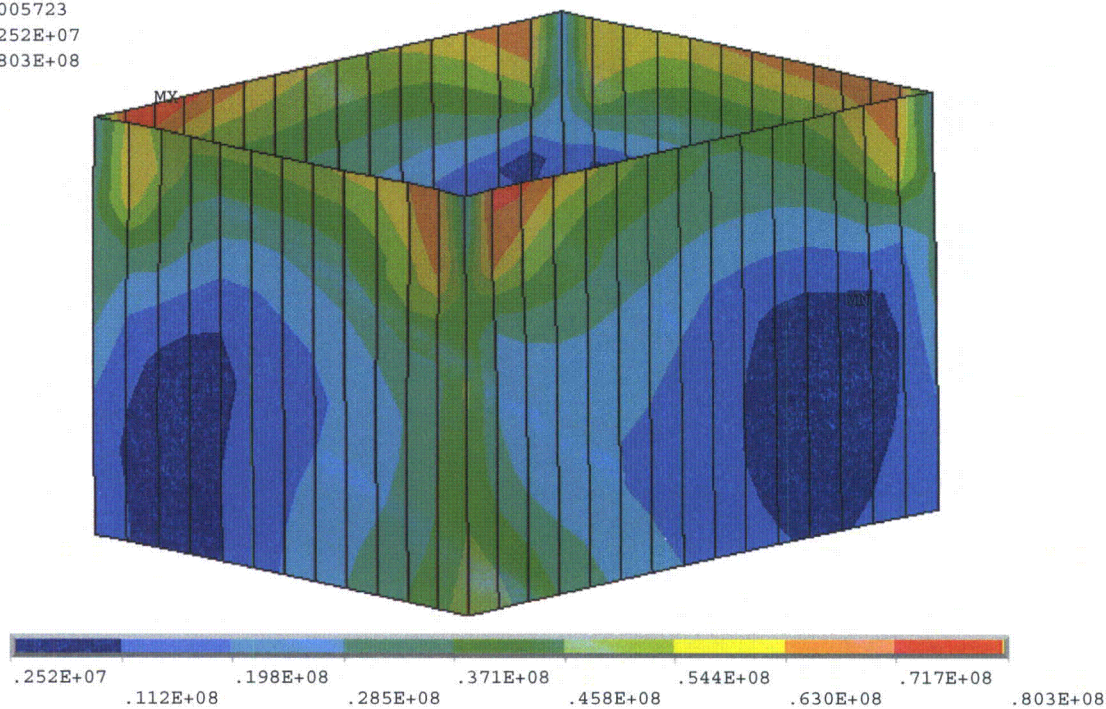


Figure A-69. Case I-1. 10 mm Thick Enveloping Plates. Impact Stresses (N/m²)

SINT (AVG)
MIDDLE
DMX = .005982
SMN = .457E+07
SMX = .188E+09

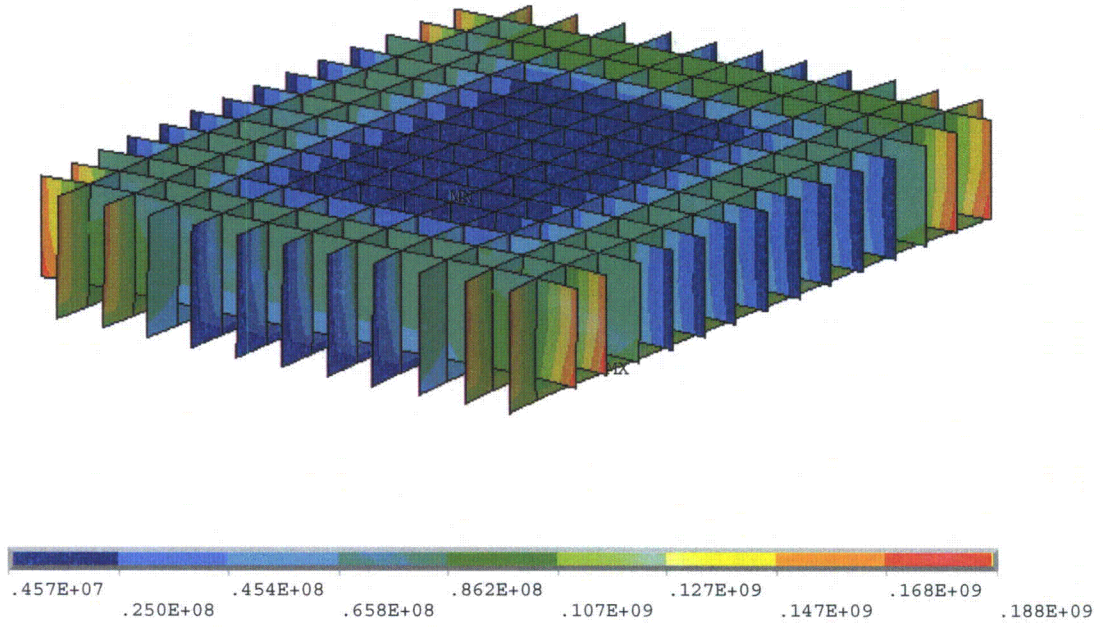


Figure A-70. Case I-1. 7 mm Thick Upper Level Plates. Impact Stresses (N/m²)

SINT (AVG)
MIDDLE
DMX = .005475
SMN = .900E+07
SMX = .226E+09

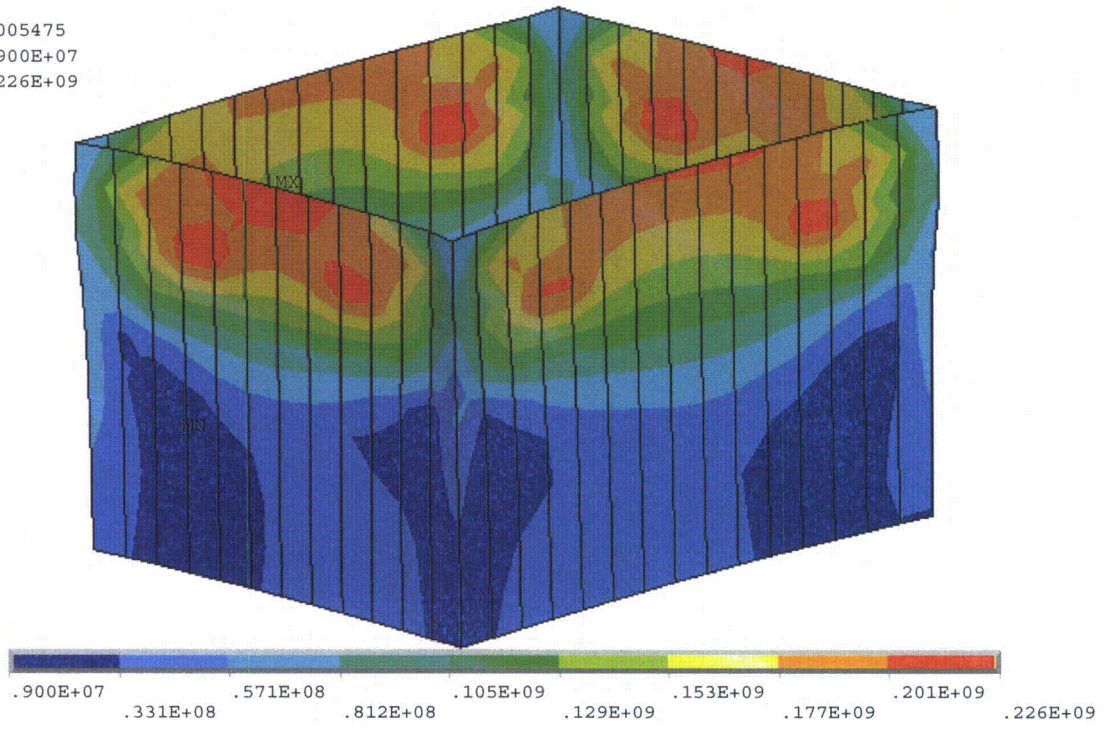


Figure A-71: Case I-2. 10 mm Thick Enveloping Plates. Impact Stresses (N/m²)

SINT (AVG)
MIDDLE
DMX = .005517
SMN = .345E+07
SMX = .864E+08

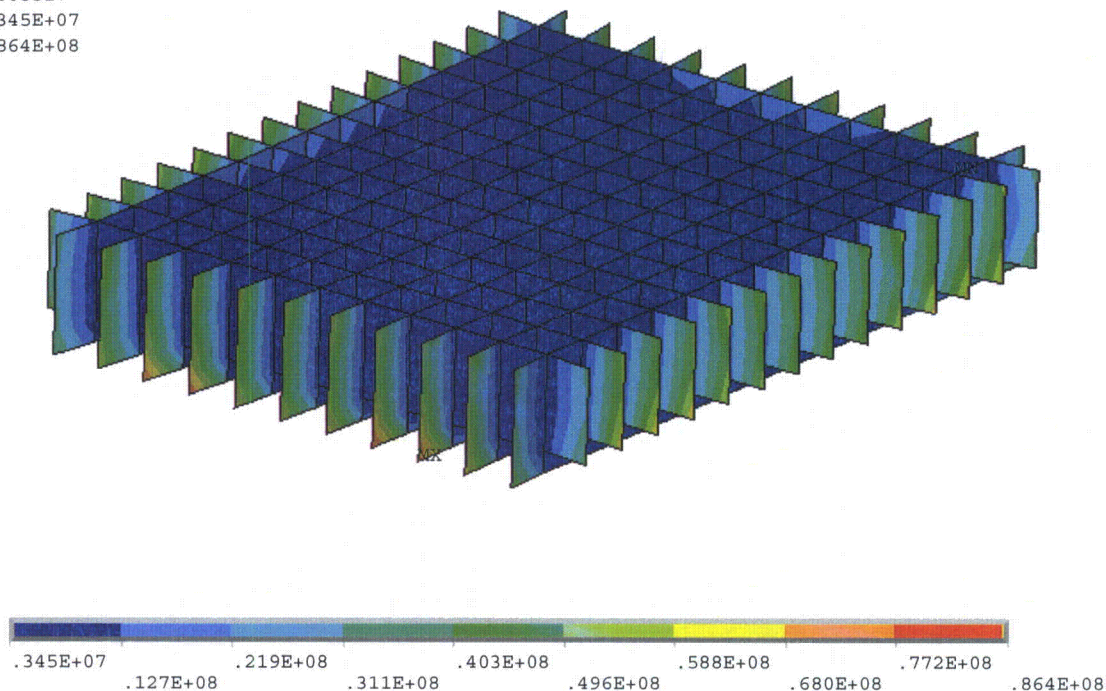


Figure A-72: Case I-2. 7 mm Thick Upper Level Plates. Impact Stresses (N/m²)

SINT (AVG)
MIDDLE
DMX = .003708
SMN = .307E+08
SMX = .184E+09

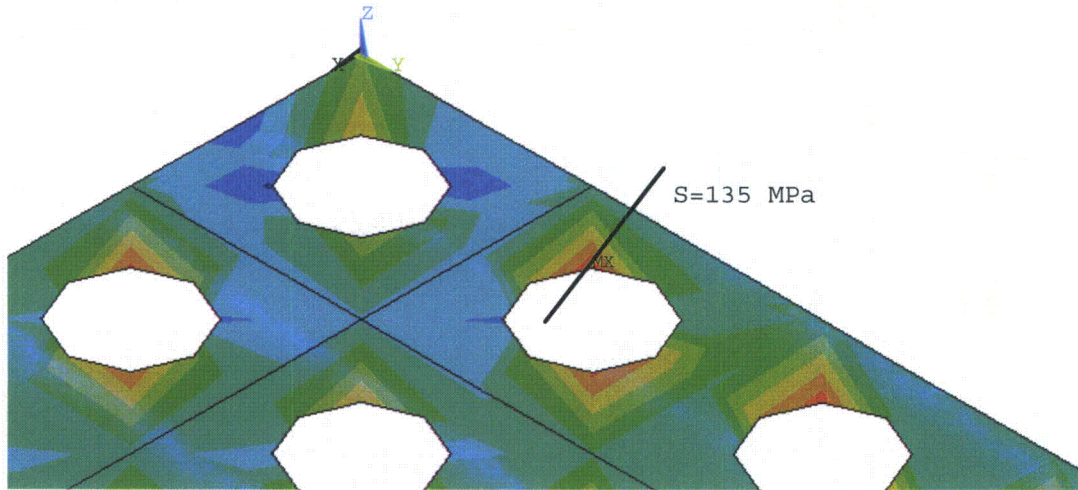
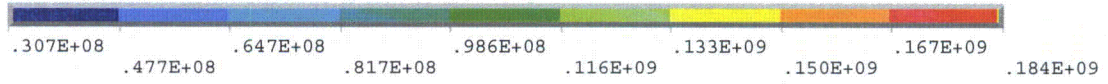
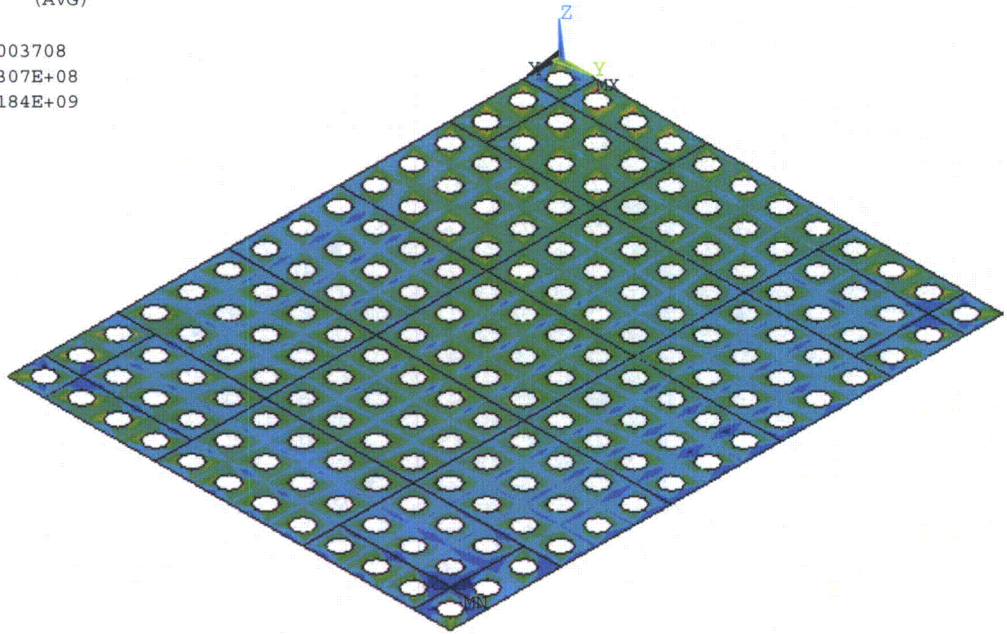


Figure A-73: Case I-3. Base Plate. Impact Stresses (N/m²)

SINT (AVG)
MIDDLE
DMX = .00318
SMN = .195E+07
SMX = .207E+09

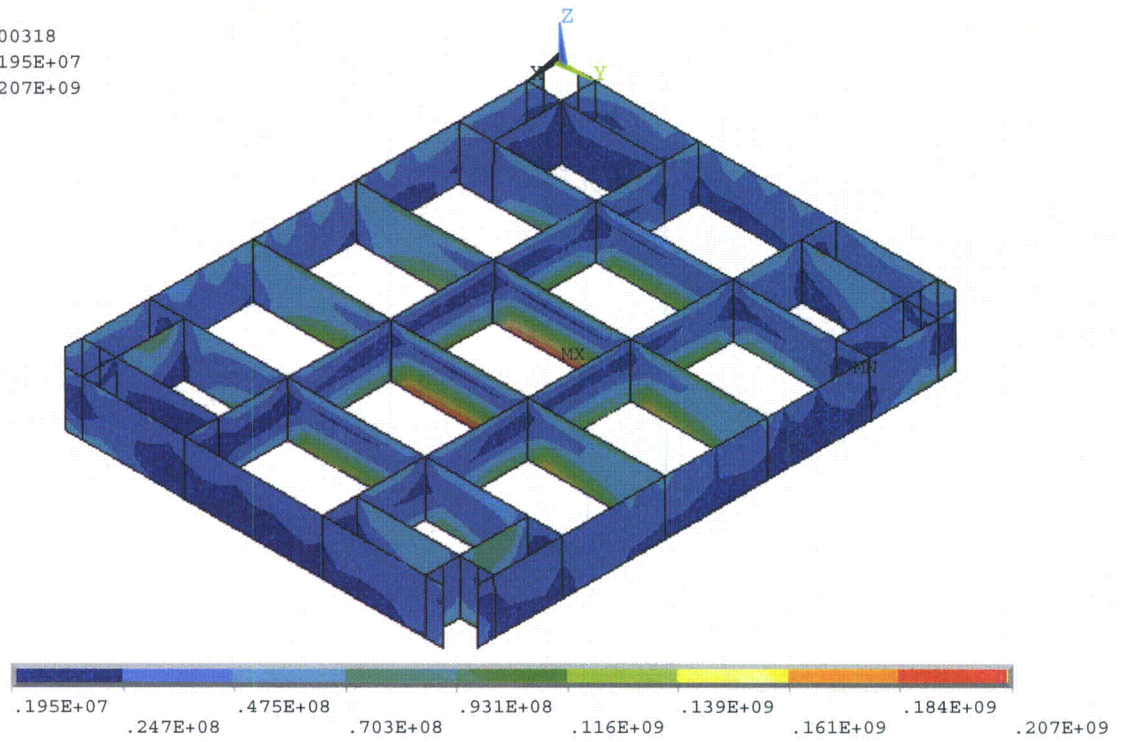


Figure A-74: Case I-3. Base Plate Stiffeners. Impact Stresses (N/m²)

SINT (AVG)
MIDDLE
DMX = .003052
SMN = .244E+07
SMX = .124E+09

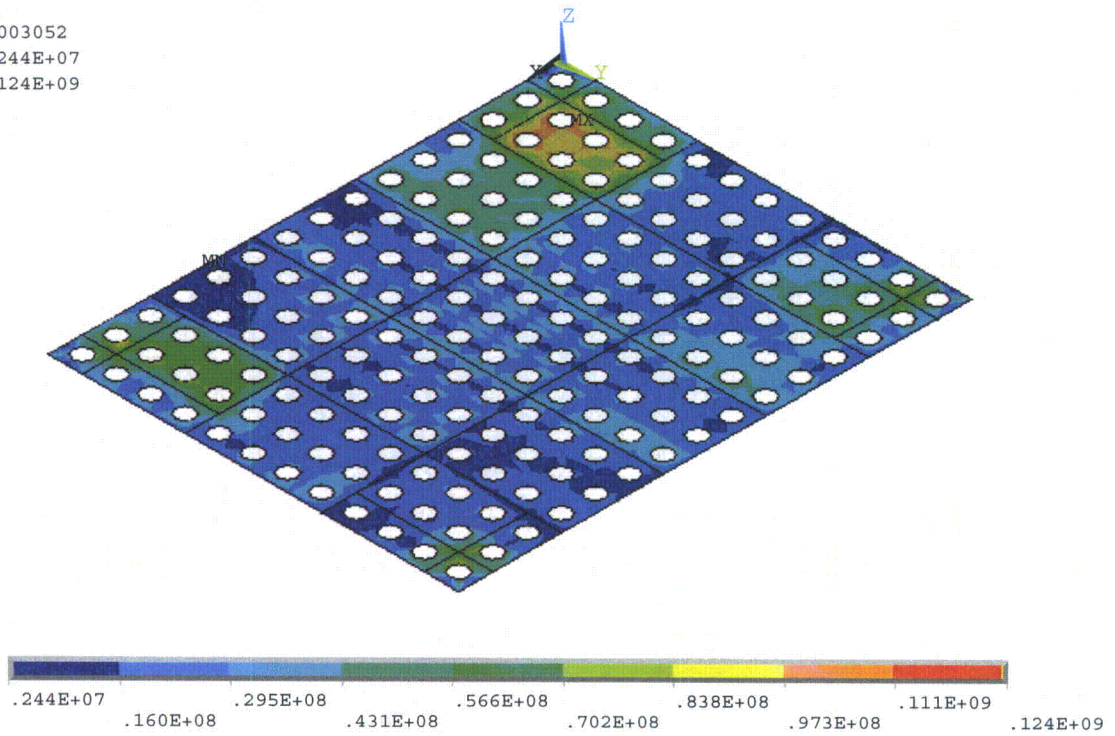


Figure A-75: Case I-4. Base Plate. Impact Stresses (N/m²)

SINT (AVG)
MIDDLE
DMX = .002547
SMN = .190E+07
SMX = .418E+09

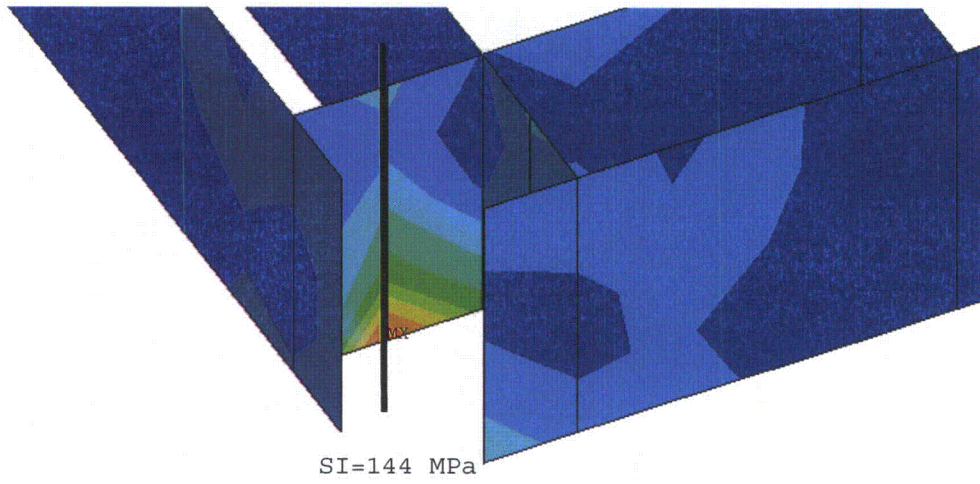
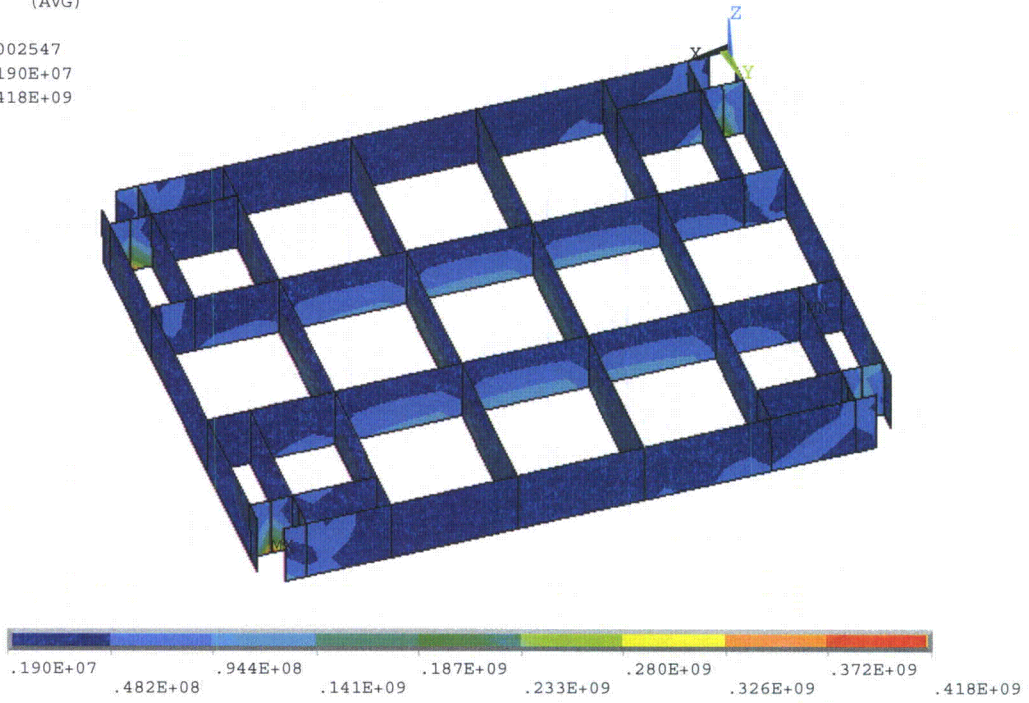


Figure A-76: Case I-4. Base Plate Stiffeners. Impact Stresses (N/m²)

APPENDIX B - OUTPUT ANALYSIS FILE

CURRENT JOBNAME REDEFINED AS fuelhandling

RESUME ANSYS DATA FROM FILE NAME=15x12.db

*** ANSYS GLOBAL STATUS ***

TITLE =

NUMBER OF ELEMENT TYPES = 3

23013 ELEMENTS CURRENTLY SELECTED. MAX ELEMENT NUMBER = 23013

15303 NODES CURRENTLY SELECTED. MAX NODE NUMBER = 87450

2021 KEYPOINTS CURRENTLY SELECTED. MAX KEYPOINT NUMBER = 15105

3035 LINES CURRENTLY SELECTED. MAX LINE NUMBER = 3076

1131 AREAS CURRENTLY SELECTED. MAX AREA NUMBER = 1139

12 VOLUMES CURRENTLY SELECTED. MAX VOL. NUMBER = 12

10 COMPONENTS CURRENTLY DEFINED

MAXIMUM LINEAR PROPERTY NUMBER = 2

MAXIMUM REAL CONSTANT SET NUMBER = 7755

ACTIVE COORDINATE SYSTEM = 0 (CARTESIAN)

MAXIMUM COUPLED D.O.F. SET NUMBER = 4775

NUMBER OF SPECIFIED CONSTRAINTS = 12

INITIAL JOBNAME = file

CURRENT JOBNAME = fuelhandling

SELECT ALL ENTITIES OF TYPE= ALL AND BELOW

ALL SELECT FOR ITEM=VOLU COMPONENT=

IN RANGE 1 TO 12 STEP 1

12 VOLUMES (OF 12 DEFINED) SELECTED BY VSEL COMMAND.

ALL SELECT FOR ITEM=AREA COMPONENT=

IN RANGE 1 TO 1139 STEP 1

1131 AREAS (OF 1131 DEFINED) SELECTED BY ASEL COMMAND.

ALL SELECT FOR ITEM=LINE COMPONENT=

IN RANGE 1 TO 3076 STEP 1

3035 LINES (OF 3035 DEFINED) SELECTED BY LSEL COMMAND.

ALL SELECT FOR ITEM=KP COMPONENT=

IN RANGE 1 TO 15105 STEP 1

2021 KEYPOINTS (OF 2021 DEFINED) SELECTED BY KSEL COMMAND.

ALL SELECT FOR ITEM=ELEM COMPONENT=

IN RANGE 1 TO 23013 STEP 1

23013 ELEMENTS (OF 23013 DEFINED) SELECTED BY ESEL COMMAND.

ALL SELECT FOR ITEM=NODE COMPONENT=

IN RANGE 1 TO 87450 STEP 1

15303 NODES (OF 15303 DEFINED) SELECTED BY NSEL COMMAND.

***** ANSYS SOLUTION ROUTINE *****

SPECIFIED NODAL LOAD FZ FOR SELECTED NODES 82314 TO 82314 BY 1

REAL= 17790.0000 IMAG= 0.00000000

SPECIFIED NODAL LOAD FY FOR SELECTED NODES 82314 TO 82314 BY 1

REAL= 4450.00000 IMAG= 0.00000000

***** ANSYS SOLVE COMMAND *****

***** ANSYS - ENGINEERING ANALYSIS SYSTEM RELEASE 10.0 *****

ANSYS Multiphysics

00265621 VERSION=INTEL NT 12:25:14 SEP 07, 2009 CP= 7.703

SOLUTION OPTIONS

PROBLEM DIMENSIONALITY.....3-D

DEGREES OF FREEDOM.....UX UY UZ ROTX ROTY ROTZ

ANALYSIS TYPE.....STATIC (STEADY-STATE)

GLOBALLY ASSEMBLED MATRIX.....SYMMETRIC

LOAD STEP OPTIONS

LOAD STEP NUMBER..... 1
TIME AT END OF THE LOAD STEP..... 1.0000
NUMBER OF SUBSTEPS..... 1
STEP CHANGE BOUNDARY CONDITIONS..... NO
PRINT OUTPUT CONTROLS.....NO PRINTOUT
DATABASE OUTPUT CONTROLS.....ALL DATA WRITTEN

FOR THE LAST SUBSTEP

SOLUTION MONITORING INFO IS WRITTEN TO FILE= fuelhandling.mntr

**** CENTER OF MASS, MASS, AND MASS MOMENTS OF INERTIA ****

CALCULATIONS ASSUME ELEMENT MASS AT ELEMENT CENTROID

TOTAL MASS = 68662.

	MOM. OF INERTIA	MOM. OF INERTIA
CENTER OF MASS	ABOUT ORIGIN	ABOUT CENTER OF MASS
XC = 1.2600	IXX = 0.3888E+06	IXX = 0.1877E+06
YC = 1.0080	IYY = 0.4415E+06	IYY = 0.2012E+06
ZC = 1.3830	IZZ = 0.2416E+06	IZZ = 0.6282E+05
	IXY = -0.8721E+05	IXY = 0.4991E-08
	IYZ = -0.9572E+05	IYZ = 0.3798E-08
	IZX = -0.1196E+06	IZX = 0.2299E-08

AN AVERAGE OF THE X-, Y-, AND Z-DIRECTION MASS TERMS ARE USED FOR MASS21 ELEMENTS.

*** MASS SUMMARY BY ELEMENT TYPE ***

TYPE MASS

1 5418.54

2 63154.0

3 89.8739

Range of element maximum matrix coefficients in global coordinates

Maximum= 9.923271517E+09 at element 22933.

Minimum= 303846387 at element 5984.

*** ELEMENT MATRIX FORMULATION TIMES

TYPE	NUMBER	ENAME	TOTAL CP	AVE CP
------	--------	-------	----------	--------

1	11071	SHELL63	1.625	0.000147
---	-------	---------	-------	----------

2	11814	MASS21	0.312	0.000026
---	-------	--------	-------	----------

3	128	SOLID45	0.031	0.000244
---	-----	---------	-------	----------

Time at end of element matrix formulation CP= 10.75.

SPARSE MATRIX DIRECT SOLVER.

Number of equations = 81934, Maximum wavefront = 102

Memory available for solver = 233.24 MB

Memory required for in-core = 195.09 MB

Optimal memory required for out-of-core = 38.89 MB

Minimum memory required for out-of-core = 21.22 MB

Element Output Element= 1000 Cum. Iter.= 1 CP= 23.938

Time= 1.0000 Load Step= 1 Substep= 1 Equilibrium Iteration= 1.

*** ELEMENT RESULT CALCULATION TIMES

TYPE	NUMBER	ENAME	TOTAL CP	AVE CP
------	--------	-------	----------	--------

1	11071	SHELL63	1.859	0.000168
---	-------	---------	-------	----------

2	11814	MASS21	0.109	0.000009
---	-------	--------	-------	----------

3	128	SOLID45	0.016	0.000122
---	-----	---------	-------	----------

*** NODAL LOAD CALCULATION TIMES

TYPE	NUMBER	ENAME	TOTAL CP	AVE CP
------	--------	-------	----------	--------

1	11071	SHELL63	0.141	0.000013
---	-------	---------	-------	----------

2	11814	MASS21	0.078	0.000007
---	-------	--------	-------	----------

3 128 SOLID45 0.016 0.000122

*** LOAD STEP 1 SUBSTEP 1 COMPLETED. CUM ITER = 1

*** TIME = 1.00000 TIME INC = 1.00000 NEW TRIANG MATRIX

*** NOTE *** CP = 26.188 TIME= 12:25:39

Solution is done!

*** ANSYS BINARY FILE STATISTICS

BUFFER SIZE USED= 16384

7.688 MB WRITTEN ON ELEMENT MATRIX FILE: fuelhandling.emat

22.812 MB WRITTEN ON ELEMENT SAVED DATA FILE: fuelhandling.esav

15.125 MB WRITTEN ON ASSEMBLED MATRIX FILE: fuelhandling.full

30.312 MB WRITTEN ON RESULTS FILE: fuelhandling.rst

FINISH SOLUTION PROCESSING

***** ROUTINE COMPLETED ***** CP = 26.500

***** ANSYS RESULTS INTERPRETATION (POST1) *****

ENTER /SHOW,DEVICE-NAME TO ENABLE GRAPHIC DISPLAY

ENTER FINISH TO LEAVE POST1

USE LOAD STEP 1 SUBSTEP 0 FOR LOAD CASE 0

SET COMMAND GOT LOAD STEP= 1 SUBSTEP= 1 CUMULATIVE ITERATION= 1

TIME/FREQUENCY= 1.0000

TITLE=

WRITE LOAD CASE 1 TO FILE fuelhandling.101

EXIT THE ANSYS POST1 DATABASE PROCESSOR

***** ROUTINE COMPLETED ***** CP = 27.031

CLEAR DATABASE AND RERUN START.ANS

RUN SETUP PROCEDURE FROM FILE= C:\ansys100\v100\ANSYS\apdl\start100.ans

ANSYS Multiphysics

/INPUT FILE= C:\ansys100\v100\ANSYS\apdl\start100.ans LINE= 0

CURRENT JOBNAME REDEFINED AS D+B

RESUME ANSYS DATA FROM FILE NAME=15x12.db

*** ANSYS GLOBAL STATUS ***

TITLE =

NUMBER OF ELEMENT TYPES = 3

23013 ELEMENTS CURRENTLY SELECTED. MAX ELEMENT NUMBER = 23013

15303 NODES CURRENTLY SELECTED. MAX NODE NUMBER = 87450

2021 KEYPOINTS CURRENTLY SELECTED. MAX KEYPOINT NUMBER = 15105

3035 LINES CURRENTLY SELECTED. MAX LINE NUMBER = 3076

1131 AREAS CURRENTLY SELECTED. MAX AREA NUMBER = 1139

12 VOLUMES CURRENTLY SELECTED. MAX VOL. NUMBER = 12

10 COMPONENTS CURRENTLY DEFINED

MAXIMUM LINEAR PROPERTY NUMBER = 2

MAXIMUM REAL CONSTANT SET NUMBER = 7755

ACTIVE COORDINATE SYSTEM = 0 (CARTESIAN)

MAXIMUM COUPLED D.O.F. SET NUMBER = 4775

NUMBER OF SPECIFIED CONSTRAINTS = 12

INITIAL JOBNAME = file

CURRENT JOBNAME = D+B

SELECT ALL ENTITIES OF TYPE= ALL AND BELOW

ALL SELECT FOR ITEM=VOLU COMPONENT=

IN RANGE 1 TO 12 STEP 1

12 VOLUMES (OF 12 DEFINED) SELECTED BY VSEL COMMAND.

ALL SELECT FOR ITEM=AREA COMPONENT=

IN RANGE 1 TO 1139 STEP 1

1131 AREAS (OF 1131 DEFINED) SELECTED BY ASEL COMMAND.

ALL SELECT FOR ITEM=LINE COMPONENT=

IN RANGE 1 TO 3076 STEP 1

3035 LINES (OF 3035 DEFINED) SELECTED BY LSEL COMMAND.

ALL SELECT FOR ITEM=KP COMPONENT=

IN RANGE 1 TO 15105 STEP 1

2021 KEYPOINTS (OF 2021 DEFINED) SELECTED BY KSEL COMMAND.

ALL SELECT FOR ITEM=ELEM COMPONENT=

IN RANGE 1 TO 23013 STEP 1

23013 ELEMENTS (OF 23013 DEFINED) SELECTED BY ESEL COMMAND.

ALL SELECT FOR ITEM=NODE COMPONENT=

IN RANGE 1 TO 87450 STEP 1

15303 NODES (OF 15303 DEFINED) SELECTED BY NSEL COMMAND.

***** ANSYS SOLUTION ROUTINE *****

ACEL= 0.0000 0.0000 8.5936

***** ANSYS SOLVE COMMAND *****

SOLUTION OPTIONS

PROBLEM DIMENSIONALITY.....3-D

DEGREES OF FREEDOM..... UX UY UZ ROTX ROTY ROTZ

ANALYSIS TYPE.....STATIC (STEADY-STATE)

GLOBALLY ASSEMBLED MATRIX.....SYMMETRIC

LOAD STEP OPTIONS

LOAD STEP NUMBER..... 1

TIME AT END OF THE LOAD STEP..... 1.0000
NUMBER OF SUBSTEPS..... 1
STEP CHANGE BOUNDARY CONDITIONS..... NO
INERTIA LOADS X Y Z
ACEL 0.0000 0.0000 8.5936
PRINT OUTPUT CONTROLSNO PRINTOUT
DATABASE OUTPUT CONTROLS.....ALL DATA WRITTEN
FOR THE LAST SUBSTEP
SOLUTION MONITORING INFO IS WRITTEN TO FILE= D+B.mntr

**** CENTER OF MASS, MASS, AND MASS MOMENTS OF INERTIA ****

CALCULATIONS ASSUME ELEMENT MASS AT ELEMENT CENTROID

TOTAL MASS = 68662.

	MOM. OF INERTIA	MOM. OF INERTIA
CENTER OF MASS	ABOUT ORIGIN	ABOUT CENTER OF MASS
XC = 1.2600	IXX = 0.3888E+06	IXX = 0.1877E+06
YC = 1.0080	IYY = 0.4415E+06	IYY = 0.2012E+06
ZC = 1.3830	IZZ = 0.2416E+06	IZZ = 0.6282E+05
	IXY = -0.8721E+05	IXY = 0.4991E-08
	IYZ = -0.9572E+05	IYZ = 0.3798E-08
	IZX = -0.1196E+06	IZX = 0.2299E-08

AN AVERAGE OF THE X-, Y-, AND Z-DIRECTION MASS TERMS ARE USED FOR MASS21 ELEMENTS.

*** MASS SUMMARY BY ELEMENT TYPE ***

TYPE MASS

1 5418.54

2 63154.0

3 89.8739

Range of element maximum matrix coefficients in global coordinates

Maximum= 9.923271517E+09 at element 22933.

Minimum= 303846387 at element 5984.

*** ELEMENT MATRIX FORMULATION TIMES

TYPE	NUMBER	ENAME	TOTAL CP	AVE CP
------	--------	-------	----------	--------

1	11071	SHELL63	1.609	0.000145
---	-------	---------	-------	----------

2	11814	MASS21	0.406	0.000034
---	-------	--------	-------	----------

3	128	SOLID45	0.031	0.000244
---	-----	---------	-------	----------

Time at end of element matrix formulation CP= 30.421875.

SPARSE MATRIX DIRECT SOLVER.

Number of equations = 81934, Maximum wavefront = 102

Memory available for solver = 233.24 MB

Memory required for in-core = 195.09 MB

Optimal memory required for out-of-core = 38.89 MB

Minimum memory required for out-of-core = 21.22 MB

Element Output Element= 1000 Cum. Iter.= 1 CP= 43.766

Time= 1.0000 Load Step= 1 Substep= 1 Equilibrium Iteration= 1.

*** ELEMENT RESULT CALCULATION TIMES

TYPE	NUMBER	ENAME	TOTAL CP	AVE CP
------	--------	-------	----------	--------

1	11071	SHELL63	2.047	0.000185
---	-------	---------	-------	----------

2	11814	MASS21	0.203	0.000017
---	-------	--------	-------	----------

3	128	SOLID45	0.016	0.000122
---	-----	---------	-------	----------

*** NODAL LOAD CALCULATION TIMES

TYPE	NUMBER	ENAME	TOTAL CP	AVE CP
------	--------	-------	----------	--------

1	11071	SHELL63	0.078	0.000007
---	-------	---------	-------	----------

2	11814	MASS21	0.156	0.000013
---	-------	--------	-------	----------

3 128 SOLID45 0.000 0.000000

*** LOAD STEP 1 SUBSTEP 1 COMPLETED. CUM ITER = 1

*** TIME = 1.00000 TIME INC = 1.00000 NEW TRIANG MATRIX

*** NOTE *** CP = 46.297 TIME= 12:26:04

Solution is done!

*** ANSYS BINARY FILE STATISTICS

BUFFER SIZE USED= 16384

7.688 MB WRITTEN ON ELEMENT MATRIX FILE: D+B.emat

22.812 MB WRITTEN ON ELEMENT SAVED DATA FILE: D+B.esav

15.125 MB WRITTEN ON ASSEMBLED MATRIX FILE: D+B.full

31.000 MB WRITTEN ON RESULTS FILE: D+B.rst

FINISH SOLUTION PROCESSING

***** ROUTINE COMPLETED ***** CP = 46.484

***** ANSYS RESULTS INTERPRETATION (POST1) *****

ENTER /SHOW,DEVICE-NAME TO ENABLE GRAPHIC DISPLAY

ENTER FINISH TO LEAVE POST1

USE LOAD STEP 1 SUBSTEP 0 FOR LOAD CASE 0

SET COMMAND GOT LOAD STEP= 1 SUBSTEP= 1 CUMULATIVE ITERATION= 1

TIME/FREQUENCY= 1.0000

TITLE=

WRITE LOAD CASE 1 TO FILE D+B.I01

C***

C*** MODAL ANALYSIS

C***

EXIT THE ANSYS POST1 DATABASE PROCESSOR

***** ROUTINE COMPLETED ***** CP = 47.078

CLEAR DATABASE AND RERUN START.ANS

RUN SETUP PROCEDURE FROM FILE= C:\ansys100\v100\ANSYS\vapdl\start100.ans

ANSYS Multiphysics

/INPUT FILE= C:\ansys100\v100\ANSYS\vapdl\start100.ans LINE= 0

CURRENT JOBNAME REDEFINED AS SSE-LOCA-SRVD

RESUME ANSYS DATA FROM FILE NAME=15x12.db

*** ANSYS GLOBAL STATUS ***

TITLE =

NUMBER OF ELEMENT TYPES = 3

23013 ELEMENTS CURRENTLY SELECTED. MAX ELEMENT NUMBER = 23013

15303 NODES CURRENTLY SELECTED. MAX NODE NUMBER = 87450

2021 KEYPOINTS CURRENTLY SELECTED. MAX KEYPOINT NUMBER = 15105

3035 LINES CURRENTLY SELECTED. MAX LINE NUMBER = 3076

1131 AREAS CURRENTLY SELECTED. MAX AREA NUMBER = 1139

12 VOLUMES CURRENTLY SELECTED. MAX VOL. NUMBER = 12

10 COMPONENTS CURRENTLY DEFINED

MAXIMUM LINEAR PROPERTY NUMBER = 2

MAXIMUM REAL CONSTANT SET NUMBER = 7755

ACTIVE COORDINATE SYSTEM = 0 (CARTESIAN)

MAXIMUM COUPLED D.O.F. SET NUMBER = 4775

NUMBER OF SPECIFIED CONSTRAINTS = 12

INITIAL JOBNAME = file

CURRENT JOBNAME = SSE-LOCA-SRVD

SELECT ALL ENTITIES OF TYPE= ALL AND BELOW

ALL SELECT FOR ITEM=VOLU COMPONENT=

IN RANGE 1 TO 12 STEP 1

12 VOLUMES (OF 12 DEFINED) SELECTED BY VSEL COMMAND.

ALL SELECT FOR ITEM=AREA COMPONENT=

IN RANGE 1 TO 1139 STEP 1

1131 AREAS (OF 1131 DEFINED) SELECTED BY ASEL COMMAND.

ALL SELECT FOR ITEM=LINE COMPONENT=

IN RANGE 1 TO 3076 STEP 1

3035 LINES (OF 3035 DEFINED) SELECTED BY LSEL COMMAND.

ALL SELECT FOR ITEM=KP COMPONENT=

IN RANGE 1 TO 15105 STEP 1

2021 KEYPOINTS (OF 2021 DEFINED) SELECTED BY KSEL COMMAND.

ALL SELECT FOR ITEM=ELEM COMPONENT=

IN RANGE 1 TO 23013 STEP 1

23013 ELEMENTS (OF 23013 DEFINED) SELECTED BY ESEL COMMAND.

ALL SELECT FOR ITEM=NODE COMPONENT=

IN RANGE 1 TO 87450 STEP 1

15303 NODES (OF 15303 DEFINED) SELECTED BY NSEL COMMAND.

***** ANSYS SOLUTION ROUTINE *****

PERFORM A MODAL ANALYSIS

THIS WILL BE A NEW ANALYSIS

USE SUBSPACE ITERATION METHOD

EXTRACT 100 MODES

NORMALIZE THE MODE SHAPES TO THE MASS MATRIX

NUMBER OF MODES TO EXPAND= 100

CALCULATE ELEMENT RESULTS AND NODAL DOF SOLUTION

PRINT ALL ITEMS WITH A FREQUENCY OF NONE

FOR ALL APPLICABLE ENTITIES

***** ANSYS SOLVE COMMAND *****

SOLUTION OPTIONS

PROBLEM DIMENSIONALITY.....3-D

DEGREES OF FREEDOM..... UX UY UZ ROTX ROTY ROTZ

ANALYSIS TYPE.....MODAL

EXTRACTION METHOD.....SUBSPACE

NUMBER OF MODES TO EXTRACT..... 100

GLOBALLY ASSEMBLED MATRIX.....SYMMETRIC

NUMBER OF MODES TO EXPAND..... 100

ELEMENT RESULTS CALCULATION.....ON

** Reordering still in progress **

** Reordering still in progress **

** Reordering still in progress **

LOAD STEP OPTIONS

LOAD STEP NUMBER..... 1

PRINT OUTPUT CONTROLS

ITEM FREQUENCY COMPONENT

ALL NONE

DATABASE OUTPUT CONTROLS.....ALL DATA WRITTEN

Estimated number of active DOF= 81934.

Maximum wavefront= 2616.

Element Formation Element= 7000 Cum. Iter.= 1 CP= 51.906

Load Step= 1 Mode= 1.

**** CENTER OF MASS, MASS, AND MASS MOMENTS OF INERTIA ****

CALCULATIONS ASSUME ELEMENT MASS AT ELEMENT CENTROID

TOTAL MASS = 68662.

MOM. OF INERTIA		MOM. OF INERTIA	
CENTER OF MASS	ABOUT ORIGIN	ABOUT CENTER OF MASS	
XC = 1.2600	IXX = 0.3888E+06	IXX = 0.1877E+06	
YC = 1.0080	IYY = 0.4415E+06	IYY = 0.2012E+06	
ZC = 1.3830	IZZ = 0.2416E+06	IZZ = 0.6282E+05	
	IXY = -0.8721E+05	IXY = 0.4991E-08	
	IYZ = -0.9572E+05	IYZ = 0.3798E-08	
	IZX = -0.1196E+06	IZX = 0.2299E-08	

AN AVERAGE OF THE X-, Y-, AND Z-DIRECTION MASS TERMS ARE USED FOR MASS21 ELEMENTS.

*** MASS SUMMARY BY ELEMENT TYPE ***

TYPE MASS

1 5418.54
2 63154.0
3 89.8739

Range of element maximum matrix coefficients in global coordinates

Maximum= 9.923271517E+09 at element 22933.

Minimum= 303846387 at element 5984.

*** ELEMENT MATRIX FORMULATION TIMES

TYPE NUMBER ENAME TOTAL CP AVE CP

1 11071 SHELL63 11.531 0.001042
2 11814 MASS21 2.609 0.000221
3 128 SOLID45 0.078 0.000610

Time at end of element matrix formulation CP= 62.5.

NEDO-33373-A, Revision 5

Time at end of matrix triangularization CP= 62.5.

SUBSPACE SIZE OF 104 VECTORS USED FOR CALCULATION OF FIRST 100 EIGENVECTORS.

MAXIMUM ITERATIONS = 100

NUMBER OF EQUATIONS = 81934

MAXIMUM WAVEFRONT = 2616

ITERATIONS PER SHIFT = 5

MAXIMUM MODES STORED = 104

MAXIMUM EIGENVALUE = 0.10000E+09

WORK SPACE = 38732813 147.00 (MB)

***** ANSYS - ENGINEERING ANALYSIS SYSTEM RELEASE 10.0 *****

ANSYS Multiphysics

00265621 VERSION=INTEL NT 13:15:37 SEP 07, 2009 CP= 2831.109

***** FREQUENCIES FROM SUBSPACE ITERATION *****

MODE FREQUENCY (HERTZ)

1	13.78674026600
2	16.69408335857
3	17.52702748515
4	30.16637983099
5	31.98585271830
6	34.31391557936
7	35.74189990891
8	38.56964037910
9	39.42365935414
10	43.44238260045
11	43.46168173949
12	44.08336352391
13	48.22046348898

14 49.09335409840
15 53.20021022675
16 53.88057082797
17 54.14665087043
18 56.50418249382
19 60.15456220515
20 62.62232230812
21 66.52133692414
22 70.00999223422
23 72.36308026538
24 76.33922981158
25 77.97583335532
26 78.46909868702
27 80.07645005772
28 82.33608553180
29 83.23221713113
30 84.74851980178
31 87.19247769628
32 87.57504735318
33 89.81965413880
34 90.25872018642
35 96.61503318312
36 97.40970990514
37 98.20980691920
38 108.8671654166
39 117.1494252504
40 119.5609806539
41 120.1911444816

42 122.5905701804
43 123.8572832225
44 125.3137770945
45 126.5327763536
46 128.1720584390
47 131.0978936592
48 131.8181943796
49 134.7559411657
50 135.1087120138
51 135.3388094301
52 136.2836661709
53 138.7156272508
54 139.4659501338
55 142.5132063109
56 143.3388393615
57 144.6605999576
58 146.8827767748
59 149.1556595013
60 149.6778965068
61 149.6833609143
62 150.1623408911
63 150.8876574059
64 151.7150582084
65 152.4758303069
66 154.2559578382
67 155.1611662179
68 156.2219185375
69 156.5537373182

70 156.8593071809
71 157.9325376914
72 159.0770188889
73 161.0289374147
74 161.4101528399
75 161.8007543235
76 163.8421462970
77 164.1138767121
78 165.6819093045
79 165.7000935141
80 166.1464657299
81 168.8087432541
82 170.2889469124
83 170.5067940700
84 171.2745934893
85 171.4844538844
86 172.1274639819
87 172.4992341762
88 173.7821352870
89 175.5753155390
90 176.1046709789
91 176.9117723374
92 177.5139539219
93 178.0348681392
94 179.4879214595
95 181.3352291696
96 182.8030716041
97 182.8955130485

98 183.0505718677

99 183.9349909681

100 185.4234114697

Element Output Element= 1000 Cum. Iter.= 1 CP= 2832.531

Load Step= 1 Mode= 1.

*** ELEMENT RESULT CALCULATION TIMES

TYPE	NUMBER	ENAME	TOTAL CP	AVE CP
------	--------	-------	----------	--------

1	11071	SHELL63	2.219	0.000200
---	-------	---------	-------	----------

2	11814	MASS21	0.203	0.000017
---	-------	--------	-------	----------

3	128	SOLID45	0.016	0.000122
---	-----	---------	-------	----------

*** NODAL LOAD CALCULATION TIMES

TYPE	NUMBER	ENAME	TOTAL CP	AVE CP
------	--------	-------	----------	--------

1	11071	SHELL63	0.063	0.000006
---	-------	---------	-------	----------

2	11814	MASS21	0.109	0.000009
---	-------	--------	-------	----------

3	128	SOLID45	0.016	0.000122
---	-----	---------	-------	----------

Element Output Element= 12000 Cum. Iter.= 3 CP= 2838.938

Load Step= 1 Mode= 3.

Element Output Element= 16000 Cum. Iter.= 7 CP= 2849.328

Load Step= 1 Mode= 7.

Element Output Element= 22000 Cum. Iter.= 11 CP= 2859.891

Load Step= 1 Mode= 11.

Element Output Element= 18000 Cum. Iter.= 15 CP= 2869.375

Load Step= 1 Mode= 15.

Element Output Element= 2000 Cum. Iter.= 20 CP= 2880.062

Load Step= 1 Mode= 20.

Element Output Element= 11000 Cum. Iter.= 24 CP= 2890.797

Load Step= 1 Mode= 24.

Element Output Element= 18000 Cum. Iter.= 28 CP= 2901.312

Load Step= 1 Mode= 28.

Element Output Element= 1000 Cum. Iter.= 33 CP= 2911.953

Load Step= 1 Mode= 33.

Element Output Element= 9000 Cum. Iter.= 37 CP= 2922.703

Load Step= 1 Mode= 37.

Element Output Element= 18000 Cum. Iter.= 41 CP= 2933.359

Load Step= 1 Mode= 41.

Element Output Element= 1000 Cum. Iter.= 46 CP= 2944.016

Load Step= 1 Mode= 46.

Element Output Element= 2000 Cum. Iter.= 50 CP= 2954.094

Load Step= 1 Mode= 50.

Element Output Element= 3000 Cum. Iter.= 54 CP= 2964.125

Load Step= 1 Mode= 54.

Element Output Element= 7000 Cum. Iter.= 58 CP= 2974.391

Load Step= 1 Mode= 58.

Element Output Element= 10000 Cum. Iter.= 62 CP= 2984.641

Load Step= 1 Mode= 62.

Element Output Element= 10000 Cum. Iter.= 66 CP= 2994.469

Load Step= 1 Mode= 66.

Element Output Element= 13000 Cum. Iter.= 70 CP= 3004.594

Load Step= 1 Mode= 70.

Element Output Element= 15000 Cum. Iter.= 74 CP= 3014.734

Load Step= 1 Mode= 74.

Element Output Element= 14000 Cum. Iter.= 78 CP= 3024.484

Load Step= 1 Mode= 78.

Element Output Element= 14000 Cum. Iter.= 82 CP= 3034.375

Load Step= 1 Mode= 82.

Element Output Element= 13000 Cum. Iter.= 86 CP= 3044.266

Load Step= 1 Mode= 86.

Element Output Element= 12000 Cum. Iter.= 90 CP= 3054.203

Load Step= 1 Mode= 90.

Element Output Element= 21000 Cum. Iter.= 92 CP= 3060.188

Load Step= 1 Mode= 92.

Element Output Element= 21000 Cum. Iter.= 96 CP= 3070.156

Load Step= 1 Mode= 96.

1

***** PARTICIPATION FACTOR CALCULATION ***** X DIRECTION

CUMULATIVE

MODE	FREQUENCY	PERIOD	PARTIC.FACTOR	RATIO	EFFECTIVE MASS	MASS FRACTION
1	13.7867	0.72533E-01	0.17254E-05	0.000000	0.297690E-11	0.397373E-16
2	16.6941	0.59901E-01	219.42	1.000000	48143.7	0.642650
3	17.5270	0.57055E-01	-0.91069E-06	0.000000	0.829354E-12	0.642650
4	30.1664	0.33149E-01	-0.58422E-06	0.000000	0.341317E-12	0.642650
5	31.9859	0.31264E-01	-0.39783E-06	0.000000	0.158270E-12	0.642650
6	34.3139	0.29143E-01	7.9266	0.036126	62.8308	0.643489
7	35.7419	0.27978E-01	0.90654E-05	0.000000	0.821820E-10	0.643489
8	38.5696	0.25927E-01	-0.50119E-05	0.000000	0.251193E-10	0.643489
9	39.4237	0.25365E-01	-0.49611E-05	0.000000	0.246122E-10	0.643489
10	43.4424	0.23019E-01	0.50457E-04	0.000000	0.254589E-08	0.643489
11	43.4617	0.23009E-01	-0.70740	0.003224	0.500411	0.643495
12	44.0834	0.22684E-01	-0.15554E-04	0.000000	0.241919E-09	0.643495
13	48.2205	0.20738E-01	-0.37129E-04	0.000000	0.137853E-08	0.643495
14	49.0934	0.20369E-01	0.33843E-04	0.000000	0.114534E-08	0.643495
15	53.2002	0.18797E-01	0.27253E-04	0.000000	0.742710E-09	0.643495
16	53.8806	0.18560E-01	0.61095E-05	0.000000	0.373263E-10	0.643495

NEDO-33373-A, Revision 5

17	54.1467	0.18468E-01	136.46	0.621912	18620.8	0.892056
18	56.5042	0.17698E-01	80.752	0.368028	6520.80	0.979100
19	60.1546	0.16624E-01	0.18136E-04	0.000000	0.328926E-09	0.979100
20	62.6223	0.15969E-01	0.47276E-04	0.000000	0.223505E-08	0.979100
21	66.5213	0.15033E-01	-0.21014E-04	0.000000	0.441607E-09	0.979100
22	70.0100	0.14284E-01	21.687	0.098839	470.323	0.985378
23	72.3631	0.13819E-01	0.10251E-03	0.000000	0.105084E-07	0.985378
24	76.3392	0.13099E-01	0.15872E-03	0.000001	0.251917E-07	0.985378
25	77.9758	0.12824E-01	-21.553	0.098227	464.515	0.991578
26	78.4691	0.12744E-01	-0.17205E-03	0.000001	0.296005E-07	0.991578
27	80.0765	0.12488E-01	-0.45391E-03	0.000002	0.206033E-06	0.991578
28	82.3361	0.12145E-01	-3.5540	0.016197	12.6309	0.991747
29	83.2322	0.12015E-01	0.83222E-03	0.000004	0.692583E-06	0.991747
30	84.7485	0.11800E-01	0.87628E-05	0.000000	0.767864E-10	0.991747
31	87.1925	0.11469E-01	-0.19133E-06	0.000000	0.366061E-13	0.991747
32	87.5750	0.11419E-01	-12.603	0.057438	158.834	0.993867
33	89.8197	0.11133E-01	-0.43993E-04	0.000000	0.193537E-08	0.993867
34	90.2587	0.11079E-01	-0.57492E-04	0.000000	0.330534E-08	0.993867
35	96.6150	0.10350E-01	0.75492E-04	0.000000	0.569897E-08	0.993867
36	97.4097	0.10266E-01	0.19517E-04	0.000000	0.380909E-09	0.993867
37	98.2098	0.10182E-01	-0.39081E-04	0.000000	0.152729E-08	0.993867
38	108.867	0.91855E-02	-0.22439E-03	0.000001	0.503506E-07	0.993867
39	117.149	0.85361E-02	-0.38892E-03	0.000002	0.151257E-06	0.993867
40	119.561	0.83639E-02	-19.897	0.090683	395.909	0.999152
41	120.191	0.83201E-02	-0.71251E-03	0.000003	0.507672E-06	0.999152
42	122.591	0.81572E-02	0.35964	0.001639	0.129343	0.999154
43	123.857	0.80738E-02	-0.39778E-03	0.000002	0.158230E-06	0.999154
44	125.314	0.79800E-02	-0.70975E-03	0.000003	0.503750E-06	0.999154

NEDO-33373-A, Revision 5

45	126.533	0.79031E-02	-0.48414E-03	0.000002	0.234391E-06	0.999154
46	128.172	0.78020E-02	-0.83335E-03	0.000004	0.694472E-06	0.999154
47	131.098	0.76279E-02	-0.23524E-02	0.000011	0.553390E-05	0.999154
48	131.818	0.75862E-02	-2.3075	0.010516	5.32450	0.999225
49	134.756	0.74208E-02	0.21992E-02	0.000010	0.483627E-05	0.999225
50	135.109	0.74014E-02	0.30351E-03	0.000001	0.921184E-07	0.999225
51	135.339	0.73889E-02	0.76002	0.003464	0.577631	0.999233
52	136.284	0.73376E-02	-0.44669E-03	0.000002	0.199531E-06	0.999233
53	138.716	0.72090E-02	-0.14802E-03	0.000001	0.219087E-07	0.999233
54	139.466	0.71702E-02	4.8974	0.022320	23.9847	0.999553
55	142.513	0.70169E-02	-2.0822	0.009490	4.33545	0.999611
56	143.339	0.69765E-02	-0.28007E-03	0.000001	0.784399E-07	0.999611
57	144.661	0.69127E-02	-0.17462E-03	0.000001	0.304935E-07	0.999611
58	146.883	0.68082E-02	-0.10701E-02	0.000005	0.114512E-05	0.999611
59	149.156	0.67044E-02	0.90678E-04	0.000000	0.822253E-08	0.999611
60	149.678	0.66810E-02	-0.16200E-03	0.000001	0.262449E-07	0.999611
61	149.683	0.66808E-02	-0.86964E-03	0.000004	0.756279E-06	0.999611
62	150.162	0.66595E-02	0.16656E-03	0.000001	0.277421E-07	0.999611
63	150.888	0.66274E-02	0.23495E-04	0.000000	0.552019E-09	0.999611
64	151.715	0.65913E-02	-0.94570E-03	0.000004	0.894351E-06	0.999611
65	152.476	0.65584E-02	-0.50505E-03	0.000002	0.255079E-06	0.999611
66	154.256	0.64827E-02	-0.64712E-03	0.000003	0.418760E-06	0.999611
67	155.161	0.64449E-02	-0.92593E-03	0.000004	0.857345E-06	0.999611
68	156.222	0.64012E-02	0.44084E-03	0.000002	0.194340E-06	0.999611
69	156.554	0.63876E-02	-0.93953E-04	0.000000	0.882724E-08	0.999611
70	156.859	0.63751E-02	0.64252E-03	0.000003	0.412826E-06	0.999611
71	157.933	0.63318E-02	-1.6913	0.007708	2.86034	0.999649
72	159.077	0.62863E-02	-0.40401E-03	0.000002	0.163225E-06	0.999649

NEDO-33373-A, Revision 5

73	161.029	0.62101E-02	0.86828E-03	0.000004	0.753904E-06	0.999649
74	161.410	0.61954E-02	4.9679	0.022642	24.6805	0.999978
75	161.801	0.61804E-02	-0.97356E-03	0.000004	0.947827E-06	0.999978
76	163.842	0.61034E-02	-0.32013E-02	0.000015	0.102482E-04	0.999978
77	164.114	0.60933E-02	-0.27289E-02	0.000012	0.744695E-05	0.999978
78	165.682	0.60357E-02	0.13484E-02	0.000006	0.181828E-05	0.999978
79	165.700	0.60350E-02	-0.21881E-02	0.000010	0.478766E-05	0.999978
80	166.146	0.60188E-02	-0.60713	0.002767	0.368601	0.999983
81	168.809	0.59239E-02	0.14067E-02	0.000006	0.197874E-05	0.999983
82	170.289	0.58724E-02	0.35134E-03	0.000002	0.123441E-06	0.999983
83	170.507	0.58649E-02	-0.20195E-01	0.000092	0.407840E-03	0.999983
84	171.275	0.58386E-02	-1.1175	0.005093	1.24880	1.00000
85	171.484	0.58314E-02	-0.31635E-03	0.000001	0.100080E-06	1.00000
86	172.127	0.58096E-02	0.30843E-03	0.000001	0.951294E-07	1.00000
87	172.499	0.57971E-02	0.61067E-04	0.000000	0.372914E-08	1.00000
88	173.782	0.57543E-02	0.72553E-01	0.000331	0.526391E-02	1.00000
89	175.575	0.56956E-02	-0.16561E-04	0.000000	0.274283E-09	1.00000
90	176.105	0.56784E-02	0.69360E-03	0.000003	0.481084E-06	1.00000
91	176.912	0.56525E-02	-0.37908E-03	0.000002	0.143702E-06	1.00000
92	177.514	0.56334E-02	0.20933E-01	0.000095	0.438182E-03	1.00000
93	178.035	0.56169E-02	-0.67051E-03	0.000003	0.449583E-06	1.00000
94	179.488	0.55714E-02	0.60126E-04	0.000000	0.361511E-08	1.00000
95	181.335	0.55146E-02	0.65888E-01	0.000300	0.434129E-02	1.00000
96	182.803	0.54704E-02	0.24776E-02	0.000011	0.613851E-05	1.00000
97	182.896	0.54676E-02	-0.57351E-03	0.000003	0.328912E-06	1.00000
98	183.051	0.54630E-02	0.33533E-01	0.000153	0.112444E-02	1.00000
99	183.935	0.54367E-02	0.40718E-01	0.000186	0.165794E-02	1.00000
100	185.423	0.53931E-02	-0.74184E-03	0.000003	0.550325E-06	1.00000

NEDO-33373-A, Revision 5

SUM OF EFFECTIVE MASSES= 74914.4

***** PARTICIPATION FACTOR CALCULATION ***** Y DIRECTION

CUMULATIVE

MODE	FREQUENCY	PERIOD	PARTIC.FACTOR	RATIO	EFFECTIVE MASS	MASS FRACTION
1	13.7867	0.72533E-01	216.07	1.000000	46688.0	0.626446
2	16.6941	0.59901E-01	0.20747E-06	0.000000	0.430422E-13	0.626446
3	17.5270	0.57055E-01	-0.52879E-06	0.000000	0.279620E-12	0.626446
4	30.1664	0.33149E-01	0.10428E-05	0.000000	0.108733E-11	0.626446
5	31.9859	0.31264E-01	-2.9888	0.013832	8.93272	0.626565
6	34.3139	0.29143E-01	0.20882E-06	0.000000	0.436061E-13	0.626565
7	35.7419	0.27978E-01	0.17761E-06	0.000000	0.315452E-13	0.626565
8	38.5696	0.25927E-01	-0.28907E-04	0.000000	0.835606E-09	0.626565
9	39.4237	0.25365E-01	5.4392	0.025173	29.5846	0.626962
10	43.4424	0.23019E-01	0.37304E-04	0.000000	0.139156E-08	0.626962
11	43.4617	0.23009E-01	0.21951E-05	0.000000	0.481826E-11	0.626962
12	44.0834	0.22684E-01	0.76291E-05	0.000000	0.582038E-10	0.626962
13	48.2205	0.20738E-01	-32.351	0.149723	1046.61	0.641005
14	49.0934	0.20369E-01	0.16834E-03	0.000001	0.283377E-07	0.641005
15	53.2002	0.18797E-01	154.97	0.717199	24015.1	0.963233
16	53.8806	0.18560E-01	0.50502E-05	0.000000	0.255048E-10	0.963233
17	54.1467	0.18468E-01	-0.94254E-05	0.000000	0.888384E-10	0.963233
18	56.5042	0.17698E-01	-0.60466E-05	0.000000	0.365613E-10	0.963233
19	60.1546	0.16624E-01	36.015	0.166677	1297.05	0.980637
20	62.6223	0.15969E-01	-0.25555E-04	0.000000	0.653081E-09	0.980637
21	66.5213	0.15033E-01	-0.10504E-03	0.000000	0.110329E-07	0.980637

NEDO-33373-A, Revision 5

22	70.0100	0.14284E-01	0.13901E-03	0.000001	0.193248E-07	0.980637
23	72.3631	0.13819E-01	-16.455	0.076154	270.761	0.984270
24	76.3392	0.13099E-01	-0.29221E-03	0.000001	0.853894E-07	0.984270
25	77.9758	0.12824E-01	0.76484E-03	0.000004	0.584977E-06	0.984270
26	78.4691	0.12744E-01	-0.35360E-03	0.000002	0.125031E-06	0.984270
27	80.0765	0.12488E-01	0.10961E-02	0.000005	0.120136E-05	0.984270
28	82.3361	0.12145E-01	0.11331E-02	0.000005	0.128397E-05	0.984270
29	83.2322	0.12015E-01	-11.119	0.051461	123.641	0.985929
30	84.7485	0.11800E-01	-0.17508E-04	0.000000	0.306546E-09	0.985929
31	87.1925	0.11469E-01	0.75187E-05	0.000000	0.565308E-10	0.985929
32	87.5750	0.11419E-01	0.78583E-05	0.000000	0.617535E-10	0.985929
33	89.8197	0.11133E-01	10.153	0.046988	103.083	0.987312
34	90.2587	0.11079E-01	0.16972E-04	0.000000	0.288060E-09	0.987312
35	96.6150	0.10350E-01	-17.464	0.080822	304.977	0.991404
36	97.4097	0.10266E-01	0.17522E-04	0.000000	0.307020E-09	0.991404
37	98.2098	0.10182E-01	0.76318E-04	0.000000	0.582449E-08	0.991404
38	108.867	0.91855E-02	0.59560E-03	0.000003	0.354744E-06	0.991404
39	117.149	0.85361E-02	-19.731	0.091315	389.301	0.996627
40	119.561	0.83639E-02	0.13080E-02	0.000006	0.171090E-05	0.996627
41	120.191	0.83201E-02	0.33411E-03	0.000002	0.111631E-06	0.996627
42	122.591	0.81572E-02	0.49680E-02	0.000023	0.246813E-04	0.996627
43	123.857	0.80738E-02	0.13714E-03	0.000001	0.188084E-07	0.996627
44	125.314	0.79800E-02	11.160	0.051649	124.546	0.998299
45	126.533	0.79031E-02	0.28608E-02	0.000013	0.818435E-05	0.998299
46	128.172	0.78020E-02	-0.47670E-03	0.000002	0.227247E-06	0.998299
47	131.098	0.76279E-02	-3.2942	0.015246	10.8519	0.998444
48	131.818	0.75862E-02	-0.73631E-02	0.000034	0.542152E-04	0.998444
49	134.756	0.74208E-02	0.12744E-01	0.000059	0.162416E-03	0.998444

NEDO-33373-A, Revision 5

50	135.109	0.74014E-02	4.5179	0.020909	20.4118	0.998718
51	135.339	0.73889E-02	-0.22795E-02	0.000011	0.519624E-05	0.998718
52	136.284	0.73376E-02	-0.86881E-02	0.000040	0.754829E-04	0.998718
53	138.716	0.72090E-02	-3.9749	0.018396	15.7999	0.998930
54	139.466	0.71702E-02	0.15044E-03	0.000001	0.226333E-07	0.998930
55	142.513	0.70169E-02	-0.44915E-03	0.000002	0.201738E-06	0.998930
56	143.339	0.69765E-02	0.75898E-03	0.000004	0.576050E-06	0.998930
57	144.661	0.69127E-02	-0.88506E-04	0.000000	0.783340E-08	0.998930
58	146.883	0.68082E-02	0.16508E-02	0.000008	0.272509E-05	0.998930
59	149.156	0.67044E-02	2.6523	0.012275	7.03492	0.999024
60	149.678	0.66810E-02	0.93547E-04	0.000000	0.875113E-08	0.999024
61	149.683	0.66808E-02	0.19444E-02	0.000009	0.378065E-05	0.999024
62	150.162	0.66595E-02	-3.0309	0.014027	9.18635	0.999148
63	150.888	0.66274E-02	3.0317	0.014031	9.19141	0.999271
64	151.715	0.65913E-02	0.11396E-02	0.000005	0.129872E-05	0.999271
65	152.476	0.65584E-02	-0.17946E-03	0.000001	0.322075E-07	0.999271
66	154.256	0.64827E-02	-0.38021	0.001760	0.144563	0.999273
67	155.161	0.64449E-02	-0.22883E-03	0.000001	0.523632E-07	0.999273
68	156.222	0.64012E-02	-0.23907E-02	0.000011	0.571540E-05	0.999273
69	156.554	0.63876E-02	0.20238E-03	0.000001	0.409557E-07	0.999273
70	156.859	0.63751E-02	-0.19855E-02	0.000009	0.394223E-05	0.999273
71	157.933	0.63318E-02	-0.27277E-02	0.000013	0.744016E-05	0.999273
72	159.077	0.62863E-02	-0.92486E-02	0.000043	0.855365E-04	0.999273
73	161.029	0.62101E-02	-0.38976E-02	0.000018	0.151910E-04	0.999273
74	161.410	0.61954E-02	0.60814E-04	0.000000	0.369828E-08	0.999273
75	161.801	0.61804E-02	0.15602E-02	0.000007	0.243418E-05	0.999273
76	163.842	0.61034E-02	-3.6592	0.016935	13.3894	0.999453
77	164.114	0.60933E-02	-2.5936	0.012003	6.72662	0.999543

NEDO-33373-A, Revision 5

78	165.682	0.60357E-02	-0.47937E-02	0.000022	0.229791E-04	0.999543
79	165.700	0.60350E-02	0.55933E-02	0.000026	0.312851E-04	0.999543
80	166.146	0.60188E-02	-0.16004E-01	0.000074	0.256134E-03	0.999543
81	168.809	0.59239E-02	-0.11983E-01	0.000055	0.143587E-03	0.999543
82	170.289	0.58724E-02	-0.44118E-02	0.000020	0.194641E-04	0.999543
83	170.507	0.58649E-02	0.24831E-03	0.000001	0.616576E-07	0.999543
84	171.275	0.58386E-02	0.61953E-03	0.000003	0.383812E-06	0.999543
85	171.484	0.58314E-02	-0.22887E-03	0.000001	0.523807E-07	0.999543
86	172.127	0.58096E-02	0.85772E-04	0.000000	0.735678E-08	0.999543
87	172.499	0.57971E-02	-0.71362	0.003303	0.509254	0.999550
88	173.782	0.57543E-02	0.44574E-03	0.000002	0.198684E-06	0.999550
89	175.575	0.56956E-02	0.10677E-02	0.000005	0.113995E-05	0.999550
90	176.105	0.56784E-02	-0.22484E-02	0.000010	0.505533E-05	0.999550
91	176.912	0.56525E-02	0.29990E-02	0.000014	0.899407E-05	0.999550
92	177.514	0.56334E-02	-0.51278E-02	0.000024	0.262941E-04	0.999550
93	178.035	0.56169E-02	-5.7898	0.026796	33.5223	0.999999
94	179.488	0.55714E-02	-0.97840E-02	0.000045	0.957260E-04	0.999999
95	181.335	0.55146E-02	0.64896E-02	0.000030	0.421152E-04	0.999999
96	182.803	0.54704E-02	0.11036E-01	0.000051	0.121796E-03	0.999999
97	182.896	0.54676E-02	0.50594E-01	0.000234	0.255971E-02	0.999999
98	183.051	0.54630E-02	0.22301E-01	0.000103	0.497341E-03	1.00000
99	183.935	0.54367E-02	0.34641E-01	0.000160	0.120000E-02	1.00000
100	185.423	0.53931E-02	0.18889	0.000874	0.356798E-01	1.00000

SUM OF EFFECTIVE MASSES= 74528.4

***** PARTICIPATION FACTOR CALCULATION ***** Z DIRECTION

NEDO-33373-A, Revision 5

CUMULATIVE

MODE	FREQUENCY	PERIOD	PARTIC.FACTOR	RATIO	EFFECTIVE MASS	MASS FRACTION
1	13.7867	0.72533E-01	0.28364E-06	0.000000	0.804497E-13	0.150537E-17
2	16.6941	0.59901E-01	-0.15462E-05	0.000000	0.239075E-11	0.462408E-16
3	17.5270	0.57055E-01	-0.22159E-05	0.000000	0.491026E-11	0.138121E-15
4	30.1664	0.33149E-01	-0.81846E-06	0.000000	0.669873E-12	0.150656E-15
5	31.9859	0.31264E-01	-0.29857E-05	0.000000	0.891419E-11	0.317457E-15
6	34.3139	0.29143E-01	0.37634E-05	0.000000	0.141633E-10	0.582478E-15
7	35.7419	0.27978E-01	0.72250E-05	0.000000	0.522013E-10	0.155926E-14
8	38.5696	0.25927E-01	-0.11717E-04	0.000000	0.137283E-09	0.412808E-14
9	39.4237	0.25365E-01	-0.21428E-05	0.000000	0.459138E-11	0.421400E-14
10	43.4424	0.23019E-01	0.30383E-04	0.000000	0.923098E-09	0.214869E-13
11	43.4617	0.23009E-01	0.19015E-07	0.000000	0.361581E-15	0.214869E-13
12	44.0834	0.22684E-01	-213.74	1.000000	45683.6	0.854826
13	48.2205	0.20738E-01	-0.85734E-04	0.000000	0.735039E-08	0.854826
14	49.0934	0.20369E-01	0.10665E-03	0.000000	0.113746E-07	0.854826
15	53.2002	0.18797E-01	-0.23518E-04	0.000000	0.553088E-09	0.854826
16	53.8806	0.18560E-01	-0.23553E-04	0.000000	0.554727E-09	0.854826
17	54.1467	0.18468E-01	0.74213E-06	0.000000	0.550758E-12	0.854826
18	56.5042	0.17698E-01	-0.20338E-04	0.000000	0.413632E-09	0.854826
19	60.1546	0.16624E-01	-0.51554E-04	0.000000	0.265777E-08	0.854826
20	62.6223	0.15969E-01	-0.51819E-04	0.000000	0.268518E-08	0.854826
21	66.5213	0.15033E-01	-0.73257E-04	0.000000	0.536661E-08	0.854826
22	70.0100	0.14284E-01	-0.62398E-04	0.000000	0.389347E-08	0.854826
23	72.3631	0.13819E-01	-0.91030E-04	0.000000	0.828641E-08	0.854826
24	76.3392	0.13099E-01	0.24185E-03	0.000001	0.584894E-07	0.854826
25	77.9758	0.12824E-01	0.26352E-03	0.000001	0.694436E-07	0.854826
26	78.4691	0.12744E-01	-0.30349E-03	0.000001	0.921045E-07	0.854826

NEDO-33373-A, Revision 5

27	80.0765	0.12488E-01	-15.415	0.072120	237.614	0.859272
28	82.3361	0.12145E-01	-0.59160E-03	0.000003	0.349993E-06	0.859272
29	83.2322	0.12015E-01	-0.42273E-03	0.000002	0.178702E-06	0.859272
30	84.7485	0.11800E-01	0.90590E-06	0.000000	0.820657E-12	0.859272
31	87.1925	0.11469E-01	0.49985E-05	0.000000	0.249852E-10	0.859272
32	87.5750	0.11419E-01	0.64045E-06	0.000000	0.410170E-12	0.859272
33	89.8197	0.11133E-01	0.35909E-04	0.000000	0.128949E-08	0.859272
34	90.2587	0.11079E-01	0.43269E-04	0.000000	0.187225E-08	0.859272
35	96.6150	0.10350E-01	-0.36090E-04	0.000000	0.130247E-08	0.859272
36	97.4097	0.10266E-01	-78.239	0.366053	6121.37	0.973815
37	98.2098	0.10182E-01	0.21597E-04	0.000000	0.466418E-09	0.973815
38	108.867	0.91855E-02	-0.81849E-03	0.000004	0.669925E-06	0.973815
39	117.149	0.85361E-02	0.73771E-03	0.000003	0.544222E-06	0.973815
40	119.561	0.83639E-02	-0.32117E-03	0.000002	0.103153E-06	0.973815
41	120.191	0.83201E-02	29.467	0.137868	868.331	0.990063
42	122.591	0.81572E-02	0.10332E-02	0.000005	0.106743E-05	0.990063
43	123.857	0.80738E-02	-0.36899E-03	0.000002	0.136155E-06	0.990063
44	125.314	0.79800E-02	0.67612E-03	0.000003	0.457139E-06	0.990063
45	126.533	0.79031E-02	-0.67240E-04	0.000000	0.452126E-08	0.990063
46	128.172	0.78020E-02	-0.25159E-04	0.000000	0.632973E-09	0.990063
47	131.098	0.76279E-02	0.28632E-03	0.000001	0.819768E-07	0.990063
48	131.818	0.75862E-02	-0.25078E-02	0.000012	0.628908E-05	0.990063
49	134.756	0.74208E-02	0.12383E-04	0.000000	0.153328E-09	0.990063
50	135.109	0.74014E-02	0.10703E-02	0.000005	0.114548E-05	0.990063
51	135.339	0.73889E-02	0.25045E-02	0.000012	0.627236E-05	0.990063
52	136.284	0.73376E-02	0.62825E-03	0.000003	0.394696E-06	0.990063
53	138.716	0.72090E-02	-0.12392E-03	0.000001	0.153557E-07	0.990063
54	139.466	0.71702E-02	-0.66365E-04	0.000000	0.440429E-08	0.990063

NEDO-33373-A, Revision 5

55	142.513	0.70169E-02	0.87087E-03	0.000004	0.758415E-06	0.990063
56	143.339	0.69765E-02	-0.77565E-03	0.000004	0.601636E-06	0.990063
57	144.661	0.69127E-02	2.6635	0.012462	7.09427	0.990196
58	146.883	0.68082E-02	-0.18791E-02	0.000009	0.353094E-05	0.990196
59	149.156	0.67044E-02	-0.30435E-03	0.000001	0.926304E-07	0.990196
60	149.678	0.66810E-02	8.2558	0.038626	68.1574	0.991471
61	149.683	0.66808E-02	0.47873E-03	0.000002	0.229183E-06	0.991471
62	150.162	0.66595E-02	0.24627E-03	0.000001	0.606483E-07	0.991471
63	150.888	0.66274E-02	-0.19246E-03	0.000001	0.370396E-07	0.991471
64	151.715	0.65913E-02	-4.2018	0.019659	17.6547	0.991801
65	152.476	0.65584E-02	2.1288	0.009960	4.53183	0.991886
66	154.256	0.64827E-02	-0.12212E-02	0.000006	0.149137E-05	0.991886
67	155.161	0.64449E-02	15.634	0.073147	244.432	0.996460
68	156.222	0.64012E-02	0.15799E-03	0.000001	0.249610E-07	0.996460
69	156.554	0.63876E-02	2.5532	0.011946	6.51883	0.996582
70	156.859	0.63751E-02	0.82421E-03	0.000004	0.679318E-06	0.996582
71	157.933	0.63318E-02	0.21341E-02	0.000010	0.455457E-05	0.996582
72	159.077	0.62863E-02	0.64777E-03	0.000003	0.419606E-06	0.996582
73	161.029	0.62101E-02	0.58999	0.002760	0.348091	0.996588
74	161.410	0.61954E-02	-0.89276E-03	0.000004	0.797012E-06	0.996588
75	161.801	0.61804E-02	-0.53928E-01	0.000252	0.290822E-02	0.996588
76	163.842	0.61034E-02	0.41960E-02	0.000020	0.176062E-04	0.996588
77	164.114	0.60933E-02	0.32189E-02	0.000015	0.103613E-04	0.996588
78	165.682	0.60357E-02	0.44960E-02	0.000021	0.202141E-04	0.996588
79	165.700	0.60350E-02	-0.15365E-02	0.000007	0.236080E-05	0.996588
80	166.146	0.60188E-02	0.36602E-02	0.000017	0.133971E-04	0.996588
81	168.809	0.59239E-02	0.65937E-01	0.000308	0.434764E-02	0.996588
82	170.289	0.58724E-02	0.10615E-02	0.000005	0.112676E-05	0.996588

NEDO-33373-A, Revision 5

83	170.507	0.58649E-02	-0.54998E-03	0.000003	0.302477E-06	0.996588
84	171.275	0.58386E-02	-0.18911E-03	0.000001	0.357626E-07	0.996588
85	171.484	0.58314E-02	0.19375E-03	0.000001	0.375394E-07	0.996588
86	172.127	0.58096E-02	-0.21978	0.001028	0.483034E-01	0.996589
87	172.499	0.57971E-02	0.32719E-03	0.000002	0.107056E-06	0.996589
88	173.782	0.57543E-02	0.27999E-03	0.000001	0.783932E-07	0.996589
89	175.575	0.56956E-02	-1.1094	0.005191	1.23079	0.996612
90	176.105	0.56784E-02	-0.43583E-04	0.000000	0.189950E-08	0.996612
91	176.912	0.56525E-02	12.829	0.060023	164.589	0.999692
92	177.514	0.56334E-02	0.34111E-03	0.000002	0.116356E-06	0.999692
93	178.035	0.56169E-02	0.53464E-03	0.000003	0.285836E-06	0.999692
94	179.488	0.55714E-02	-0.63472	0.002970	0.402867	0.999700
95	181.335	0.55146E-02	-0.66090E-03	0.000003	0.436784E-06	0.999700
96	182.803	0.54704E-02	-0.25941E-02	0.000012	0.672949E-05	0.999700
97	182.896	0.54676E-02	0.20021	0.000937	0.400833E-01	0.999700
98	183.051	0.54630E-02	-0.58050E-02	0.000027	0.336979E-04	0.999700
99	183.935	0.54367E-02	-0.77323E-02	0.000036	0.597878E-04	0.999700
100	185.423	0.53931E-02	4.0013	0.018721	16.0105	1.00000

SUM OF EFFECTIVE MASSES= 53442.0

***** PARTICIPATION FACTOR CALCULATION *****ROTX DIRECTION

CUMULATIVE

MODE	FREQUENCY	PERIOD	PARTIC.FACTOR	RATIO	EFFECTIVE MASS	MASS FRACTION
1	13.7867	0.72533E-01	-654.31	1.000000	428119.	0.869465
2	16.6941	0.59901E-01	-0.13903E-05	0.000000	0.193303E-11	0.869465
3	17.5270	0.57055E-01	-0.40725E-05	0.000000	0.165856E-10	0.869465

NEDO-33373-A, Revision 5

4	30.1664	0.33149E-01	0.89528E-06	0.000000	0.801525E-12	0.869465
5	31.9859	0.31264E-01	58.291	0.089088	3397.85	0.876366
6	34.3139	0.29143E-01	0.30392E-05	0.000000	0.923673E-11	0.876366
7	35.7419	0.27978E-01	0.10439E-04	0.000000	0.108965E-09	0.876366
8	38.5696	0.25927E-01	-0.16400E-04	0.000000	0.268960E-09	0.876366
9	39.4237	0.25365E-01	30.600	0.046767	936.348	0.878267
10	43.4424	0.23019E-01	0.47884E-04	0.000000	0.229289E-08	0.878267
11	43.4617	0.23009E-01	0.99229E-06	0.000000	0.984649E-12	0.878267
12	44.0834	0.22684E-01	-215.45	0.329275	46417.4	0.972536
13	48.2205	0.20738E-01	-34.849	0.053261	1214.46	0.975003
14	49.0934	0.20369E-01	0.18079E-03	0.000000	0.326868E-07	0.975003
15	53.2002	0.18797E-01	43.219	0.066053	1867.86	0.978796
16	53.8806	0.18560E-01	-0.33613E-04	0.000000	0.112982E-08	0.978796
17	54.1467	0.18468E-01	-0.25387E-04	0.000000	0.644490E-09	0.978796
18	56.5042	0.17698E-01	0.77161E-05	0.000000	0.595382E-10	0.978796
19	60.1546	0.16624E-01	-12.525	0.019143	156.880	0.979115
20	62.6223	0.15969E-01	-0.16984E-03	0.000000	0.288460E-07	0.979115
21	66.5213	0.15033E-01	-0.80656E-04	0.000000	0.650544E-08	0.979115
22	70.0100	0.14284E-01	-0.47821E-04	0.000000	0.228688E-08	0.979115
23	72.3631	0.13819E-01	15.789	0.024131	249.297	0.979621
24	76.3392	0.13099E-01	-0.15710E-03	0.000000	0.246818E-07	0.979621
25	77.9758	0.12824E-01	0.11595E-02	0.000002	0.134435E-05	0.979621
26	78.4691	0.12744E-01	-0.39928E-03	0.000001	0.159421E-06	0.979621
27	80.0765	0.12488E-01	-15.538	0.023747	241.415	0.980111
28	82.3361	0.12145E-01	0.14724E-03	0.000000	0.216810E-07	0.980111
29	83.2322	0.12015E-01	16.314	0.024933	266.137	0.980652
30	84.7485	0.11800E-01	0.12778E-04	0.000000	0.163286E-09	0.980652
31	87.1925	0.11469E-01	0.86722E-05	0.000000	0.752064E-10	0.980652

NEDO-33373-A, Revision 5

32	87.5750	0.11419E-01	0.13387E-05	0.000000	0.179201E-11	0.980652
33	89.8197	0.11133E-01	-24.664	0.037694	608.300	0.981887
34	90.2587	0.11079E-01	0.60286E-04	0.000000	0.363436E-08	0.981887
35	96.6150	0.10350E-01	-27.521	0.042061	757.413	0.983426
36	97.4097	0.10266E-01	-78.865	0.120532	6219.70	0.996057
37	98.2098	0.10182E-01	-0.20128E-05	0.000000	0.405131E-11	0.996057
38	108.867	0.91855E-02	-0.77987E-03	0.000001	0.608199E-06	0.996057
39	117.149	0.85361E-02	9.3714	0.014323	87.8227	0.996235
40	119.561	0.83639E-02	-0.20479E-02	0.000003	0.419385E-05	0.996235
41	120.191	0.83201E-02	29.703	0.045396	882.251	0.998027
42	122.591	0.81572E-02	0.18022E-02	0.000003	0.324801E-05	0.998027
43	123.857	0.80738E-02	-0.55124E-03	0.000001	0.303861E-06	0.998027
44	125.314	0.79800E-02	4.3559	0.006657	18.9741	0.998066
45	126.533	0.79031E-02	-0.13479E-02	0.000002	0.181678E-05	0.998066
46	128.172	0.78020E-02	-0.72002E-03	0.000001	0.518422E-06	0.998066
47	131.098	0.76279E-02	2.0980	0.003207	4.40181	0.998075
48	131.818	0.75862E-02	-0.38247E-02	0.000006	0.146282E-04	0.998075
49	134.756	0.74208E-02	0.13037E-02	0.000002	0.169956E-05	0.998075
50	135.109	0.74014E-02	2.3353	0.003569	5.45386	0.998086
51	135.339	0.73889E-02	0.28418E-02	0.000004	0.807587E-05	0.998086
52	136.284	0.73376E-02	-0.89768E-03	0.000001	0.805832E-06	0.998086
53	138.716	0.72090E-02	0.81886	0.001251	0.670529	0.998087
54	139.466	0.71702E-02	-0.32448E-03	0.000000	0.105284E-06	0.998087
55	142.513	0.70169E-02	0.11103E-02	0.000002	0.123279E-05	0.998087
56	143.339	0.69765E-02	-0.51087E-03	0.000001	0.260990E-06	0.998087
57	144.661	0.69127E-02	2.6842	0.004102	7.20510	0.998102
58	146.883	0.68082E-02	-0.20414E-02	0.000003	0.416736E-05	0.998102
59	149.156	0.67044E-02	-2.3892	0.003652	5.70840	0.998113

NEDO-33373-A, Revision 5

60	149.678	0.66810E-02	8.3220	0.012719	69.2563	0.998254
61	149.683	0.66808E-02	-0.77350E-03	0.000001	0.598309E-06	0.998254
62	150.162	0.66595E-02	-2.4859	0.003799	6.17961	0.998267
63	150.888	0.66274E-02	18.218	0.027843	331.901	0.998941
64	151.715	0.65913E-02	-4.2364	0.006475	17.9475	0.998977
65	152.476	0.65584E-02	2.1456	0.003279	4.60376	0.998986
66	154.256	0.64827E-02	-0.57348E-01	0.000088	0.328880E-02	0.998986
67	155.161	0.64449E-02	15.760	0.024086	248.368	0.999491
68	156.222	0.64012E-02	0.11966E-02	0.000002	0.143195E-05	0.999491
69	156.554	0.63876E-02	2.5737	0.003933	6.62375	0.999504
70	156.859	0.63751E-02	0.39702E-03	0.000001	0.157627E-06	0.999504
71	157.933	0.63318E-02	0.44577E-03	0.000001	0.198710E-06	0.999504
72	159.077	0.62863E-02	0.30871	0.000472	0.953016E-01	0.999505
73	161.029	0.62101E-02	0.59696	0.000912	0.356361	0.999505
74	161.410	0.61954E-02	0.12057E-02	0.000002	0.145362E-05	0.999505
75	161.801	0.61804E-02	-0.55160E-01	0.000084	0.304260E-02	0.999505
76	163.842	0.61034E-02	0.16607	0.000254	0.275804E-01	0.999505
77	164.114	0.60933E-02	-0.21672	0.000331	0.469665E-01	0.999505
78	165.682	0.60357E-02	0.62318E-02	0.000010	0.388356E-04	0.999505
79	165.700	0.60350E-02	-0.21275E-02	0.000003	0.452605E-05	0.999505
80	166.146	0.60188E-02	0.10331E-01	0.000016	0.106723E-03	0.999505
81	168.809	0.59239E-02	0.63120E-01	0.000096	0.398408E-02	0.999505
82	170.289	0.58724E-02	0.19357E-02	0.000003	0.374707E-05	0.999505
83	170.507	0.58649E-02	-0.60479E-03	0.000001	0.365769E-06	0.999505
84	171.275	0.58386E-02	-0.10300E-02	0.000002	0.106090E-05	0.999505
85	171.484	0.58314E-02	0.10256E-02	0.000002	0.105190E-05	0.999505
86	172.127	0.58096E-02	-0.22128	0.000338	0.489656E-01	0.999505
87	172.499	0.57971E-02	7.5951	0.011608	57.6856	0.999623

NEDO-33373-A, Revision 5

88	173.782	0.57543E-02	0.47231E-03	0.000001	0.223074E-06	0.999623
89	175.575	0.56956E-02	-1.1181	0.001709	1.25009	0.999625
90	176.105	0.56784E-02	0.32515E-03	0.000000	0.105722E-06	0.999625
91	176.912	0.56525E-02	12.932	0.019764	167.234	0.999965
92	177.514	0.56334E-02	0.57363E-03	0.000001	0.329053E-06	0.999965
93	178.035	0.56169E-02	-0.59320	0.000907	0.351883	0.999966
94	179.488	0.55714E-02	-0.63863	0.000976	0.407851	0.999966
95	181.335	0.55146E-02	-0.63965E-02	0.000010	0.409152E-04	0.999966
96	182.803	0.54704E-02	-0.61471E-02	0.000009	0.377863E-04	0.999966
97	182.896	0.54676E-02	0.20362	0.000311	0.414596E-01	0.999966
98	183.051	0.54630E-02	0.70434E-03	0.000001	0.496099E-06	0.999966
99	183.935	0.54367E-02	-0.14943E-01	0.000023	0.223297E-03	0.999966
100	185.423	0.53931E-02	4.0645	0.006212	16.5206	1.00000

SUM OF EFFECTIVE MASSES= 492394.

***** PARTICIPATION FACTOR CALCULATION ***** ROTY DIRECTION

CUMULATIVE

MODE	FREQUENCY	PERIOD	PARTIC.FACTOR	RATIO	EFFECTIVE MASS	MASS FRACTION
1	13.7867	0.72533E-01	-0.18993E-05	0.000000	0.360743E-11	0.676597E-17
2	16.6941	0.59901E-01	655.96	1.000000	430283.	0.807023
3	17.5270	0.57055E-01	0.76003E-05	0.000000	0.577652E-10	0.807023
4	30.1664	0.33149E-01	0.18021E-05	0.000000	0.324752E-11	0.807023
5	31.9859	0.31264E-01	0.67017E-05	0.000000	0.449131E-10	0.807023
6	34.3139	0.29143E-01	53.951	0.082248	2910.76	0.812483
7	35.7419	0.27978E-01	-0.18809E-04	0.000000	0.353763E-09	0.812483
8	38.5696	0.25927E-01	0.79915E-05	0.000000	0.638648E-10	0.812483

NEDO-33373-A, Revision 5

9	39.4237	0.25365E-01	0.23484E-04	0.000000	0.551496E-09	0.812483
10	43.4424	0.23019E-01	0.12769E-04	0.000000	0.163047E-09	0.812483
11	43.4617	0.23009E-01	43.506	0.066324	1892.77	0.816033
12	44.0834	0.22684E-01	269.31	0.410557	72527.2	0.952062
13	48.2205	0.20738E-01	0.13672E-03	0.000000	0.186917E-07	0.952062
14	49.0934	0.20369E-01	-0.18281E-03	0.000000	0.334186E-07	0.952062
15	53.2002	0.18797E-01	0.78099E-05	0.000000	0.609947E-10	0.952062
16	53.8806	0.18560E-01	0.30991E-04	0.000000	0.960447E-09	0.952062
17	54.1467	0.18468E-01	-85.127	0.129775	7246.67	0.965654
18	56.5042	0.17698E-01	-4.2941	0.006546	18.4392	0.965689
19	60.1546	0.16624E-01	0.67081E-04	0.000000	0.449992E-08	0.965689
20	62.6223	0.15969E-01	0.17025E-03	0.000000	0.289864E-07	0.965689
21	66.5213	0.15033E-01	0.10750E-03	0.000000	0.115554E-07	0.965689
22	70.0100	0.14284E-01	30.906	0.047116	955.177	0.967480
23	72.3631	0.13819E-01	0.48863E-04	0.000000	0.238762E-08	0.967480
24	76.3392	0.13099E-01	0.11888E-03	0.000000	0.141318E-07	0.967480
25	77.9758	0.12824E-01	-55.379	0.084424	3066.78	0.973232
26	78.4691	0.12744E-01	0.52637E-03	0.000001	0.277069E-06	0.973232
27	80.0765	0.12488E-01	19.422	0.029609	377.232	0.973940
28	82.3361	0.12145E-01	1.6677	0.002542	2.78109	0.973945
29	83.2322	0.12015E-01	0.10711E-02	0.000002	0.114721E-05	0.973945
30	84.7485	0.11800E-01	0.27162E-04	0.000000	0.737761E-09	0.973945
31	87.1925	0.11469E-01	-0.24067E-04	0.000000	0.579202E-09	0.973945
32	87.5750	0.11419E-01	-13.971	0.021298	195.177	0.974311
33	89.8197	0.11133E-01	-0.19091E-03	0.000000	0.364450E-07	0.974311
34	90.2587	0.11079E-01	-0.85740E-04	0.000000	0.735127E-08	0.974311
35	96.6150	0.10350E-01	0.10896E-03	0.000000	0.118721E-07	0.974311
36	97.4097	0.10266E-01	98.581	0.150286	9718.29	0.992538

NEDO-33373-A, Revision 5

37	98.2098	0.10182E-01	-0.30794E-04	0.000000	0.948246E-09	0.992538
38	108.867	0.91855E-02	0.10288E-02	0.000002	0.105853E-05	0.992538
39	117.149	0.85361E-02	-0.58936E-03	0.000001	0.347342E-06	0.992538
40	119.561	0.83639E-02	23.886	0.036414	570.533	0.993608
41	120.191	0.83201E-02	-37.129	0.056603	1378.57	0.996194
42	122.591	0.81572E-02	-17.992	0.027429	323.727	0.996801
43	123.857	0.80738E-02	0.21424E-03	0.000000	0.458987E-07	0.996801
44	125.314	0.79800E-02	-0.13370E-02	0.000002	0.178745E-05	0.996801
45	126.533	0.79031E-02	0.24926E-03	0.000000	0.621323E-07	0.996801
46	128.172	0.78020E-02	0.12040E-03	0.000000	0.144972E-07	0.996801
47	131.098	0.76279E-02	0.43541E-02	0.000007	0.189580E-04	0.996801
48	131.818	0.75862E-02	-3.1358	0.004780	9.83325	0.996819
49	134.756	0.74208E-02	-0.87865E-02	0.000013	0.772030E-04	0.996819
50	135.109	0.74014E-02	-0.51953E-03	0.000001	0.269907E-06	0.996819
51	135.339	0.73889E-02	-9.3263	0.014218	86.9796	0.996983
52	136.284	0.73376E-02	0.68318E-02	0.000010	0.466739E-04	0.996983
53	138.716	0.72090E-02	-0.54028E-03	0.000001	0.291903E-06	0.996983
54	139.466	0.71702E-02	14.782	0.022535	218.515	0.997392
55	142.513	0.70169E-02	-0.56650	0.000864	0.320918	0.997393
56	143.339	0.69765E-02	-0.35422E-03	0.000001	0.125472E-06	0.997393
57	144.661	0.69127E-02	-3.3554	0.005115	11.2590	0.997414
58	146.883	0.68082E-02	0.19443E-02	0.000003	0.378024E-05	0.997414
59	149.156	0.67044E-02	0.14553E-02	0.000002	0.211785E-05	0.997414
60	149.678	0.66810E-02	-10.402	0.015858	108.203	0.997617
61	149.683	0.66808E-02	0.99516E-04	0.000000	0.990345E-08	0.997617
62	150.162	0.66595E-02	-0.60877E-03	0.000001	0.370602E-06	0.997617
63	150.888	0.66274E-02	0.27719E-03	0.000000	0.768320E-07	0.997617
64	151.715	0.65913E-02	5.2929	0.008069	28.0144	0.997670

NEDO-33373-A, Revision 5

65	152.476	0.65584E-02	-2.6839	0.004092	7.20326	0.997683
66	154.256	0.64827E-02	0.13818E-03	0.000000	0.190948E-07	0.997683
67	155.161	0.64449E-02	-19.701	0.030033	388.110	0.998411
68	156.222	0.64012E-02	-0.15670E-02	0.000002	0.245547E-05	0.998411
69	156.554	0.63876E-02	-3.2155	0.004902	10.3397	0.998430
70	156.859	0.63751E-02	-0.41317E-02	0.000006	0.170712E-04	0.998430
71	157.933	0.63318E-02	0.72744	0.001109	0.529174	0.998431
72	159.077	0.62863E-02	-0.96607E-03	0.000001	0.933300E-06	0.998431
73	161.029	0.62101E-02	-0.74116	0.001130	0.549312	0.998432
74	161.410	0.61954E-02	19.108	0.029129	365.106	0.999117
75	161.801	0.61804E-02	0.64713E-01	0.000099	0.418773E-02	0.999117
76	163.842	0.61034E-02	-0.38513E-02	0.000006	0.148321E-04	0.999117
77	164.114	0.60933E-02	0.11090E-02	0.000002	0.122996E-05	0.999117
78	165.682	0.60357E-02	-0.34242E-02	0.000005	0.117250E-04	0.999117
79	165.700	0.60350E-02	0.62160E-02	0.000009	0.386386E-04	0.999117
80	166.146	0.60188E-02	0.11654	0.000178	0.135814E-01	0.999117
81	168.809	0.59239E-02	-0.87205E-01	0.000133	0.760466E-02	0.999117
82	170.289	0.58724E-02	-0.17557E-02	0.000003	0.308251E-05	0.999117
83	170.507	0.58649E-02	0.47955	0.000731	0.229969	0.999118
84	171.275	0.58386E-02	-0.34710	0.000529	0.120476	0.999118
85	171.484	0.58314E-02	0.47251E-02	0.000007	0.223264E-04	0.999118
86	172.127	0.58096E-02	0.27517	0.000419	0.757196E-01	0.999118
87	172.499	0.57971E-02	0.16005E-02	0.000002	0.256146E-05	0.999118
88	173.782	0.57543E-02	-0.45233	0.000690	0.204601	0.999118
89	175.575	0.56956E-02	1.3966	0.002129	1.95045	0.999122
90	176.105	0.56784E-02	-0.34641E-02	0.000005	0.119999E-04	0.999122
91	176.912	0.56525E-02	-16.162	0.024638	261.194	0.999612
92	177.514	0.56334E-02	0.56235	0.000857	0.316241	0.999613

NEDO-33373-A, Revision 5

93	178.035	0.56169E-02	-0.53635E-02	0.000008	0.287674E-04	0.999613
94	179.488	0.55714E-02	0.79611	0.001214	0.633791	0.999614
95	181.335	0.55146E-02	0.98037	0.001495	0.961117	0.999616
96	182.803	0.54704E-02	-0.68651E-02	0.000010	0.471291E-04	0.999616
97	182.896	0.54676E-02	-0.30615	0.000467	0.937259E-01	0.999616
98	183.051	0.54630E-02	13.396	0.020421	179.441	0.999952
99	183.935	0.54367E-02	-0.48203	0.000735	0.232351	0.999953
100	185.423	0.53931E-02	-5.0183	0.007650	25.1831	1.00000

SUM OF EFFECTIVE MASSES= 533172.

***** PARTICIPATION FACTOR CALCULATION ***** ROTZ DIRECTION

CUMULATIVE

MODE	FREQUENCY	PERIOD	PARTIC.FACTOR	RATIO	EFFECTIVE MASS	MASS FRACTION
1	13.7867	0.72533E-01	272.25	1.000000	74121.8	0.283183
2	16.6941	0.59901E-01	-221.17	0.812377	48917.1	0.470071
3	17.5270	0.57055E-01	-50.566	0.185733	2556.95	0.479840
4	30.1664	0.33149E-01	-172.93	0.635166	29903.4	0.594086
5	31.9859	0.31264E-01	-3.7658	0.013832	14.1816	0.594140
6	34.3139	0.29143E-01	-7.9900	0.029348	63.8402	0.594384
7	35.7419	0.27978E-01	-39.258	0.144197	1541.20	0.600272
8	38.5696	0.25927E-01	-61.665	0.226498	3802.54	0.614800
9	39.4237	0.25365E-01	6.8534	0.025173	46.9690	0.614979
10	43.4424	0.23019E-01	34.863	0.128055	1215.46	0.619623
11	43.4617	0.23009E-01	0.71307	0.002619	0.508467	0.619625
12	44.0834	0.22684E-01	-0.10889E-05	0.000000	0.118561E-11	0.619625
13	48.2205	0.20738E-01	-40.762	0.149722	1661.57	0.625973

NEDO-33373-A, Revision 5

14	49.0934	0.20369E-01	42.001	0.154273	1764.11	0.632713
15	53.2002	0.18797E-01	195.26	0.717199	38126.4	0.778375
16	53.8806	0.18560E-01	-36.788	0.135123	1353.33	0.783545
17	54.1467	0.18468E-01	-137.55	0.505227	18919.9	0.855829
18	56.5042	0.17698E-01	-81.398	0.298977	6625.56	0.881142
19	60.1546	0.16624E-01	45.378	0.166677	2059.18	0.889009
20	62.6223	0.15969E-01	31.481	0.115633	991.079	0.892795
21	66.5213	0.15033E-01	44.766	0.164426	2003.96	0.900451
22	70.0100	0.14284E-01	-21.860	0.080294	477.875	0.902277
23	72.3631	0.13819E-01	-20.733	0.076154	429.862	0.903919
24	76.3392	0.13099E-01	33.224	0.122035	1103.86	0.908137
25	77.9758	0.12824E-01	21.726	0.079801	472.018	0.909940
26	78.4691	0.12744E-01	-60.474	0.222123	3657.06	0.923912
27	80.0765	0.12488E-01	0.18966E-02	0.000007	0.359708E-05	0.923912
28	82.3361	0.12145E-01	3.5826	0.013159	12.8353	0.923961
29	83.2322	0.12015E-01	-14.012	0.051466	196.332	0.924711
30	84.7485	0.11800E-01	105.48	0.387421	11125.3	0.967215
31	87.1925	0.11469E-01	12.649	0.046462	160.006	0.967827
32	87.5750	0.11419E-01	12.704	0.046662	161.387	0.968443
33	89.8197	0.11133E-01	12.793	0.046989	163.657	0.969069
34	90.2587	0.11079E-01	25.131	0.092309	631.585	0.971481
35	96.6150	0.10350E-01	-22.004	0.080823	484.186	0.973331
36	97.4097	0.10266E-01	-0.60041E-05	0.000000	0.360495E-10	0.973331
37	98.2098	0.10182E-01	-14.610	0.053662	213.440	0.974147
38	108.867	0.91855E-02	-36.064	0.132463	1300.58	0.979116
39	117.149	0.85361E-02	-24.860	0.091312	618.020	0.981477
40	119.561	0.83639E-02	20.058	0.073676	402.343	0.983014
41	120.191	0.83201E-02	0.12505E-02	0.000005	0.156382E-05	0.983014

NEDO-33373-A, Revision 5

42	122.591	0.81572E-02	-0.35451	0.001302	0.125675	0.983014
43	123.857	0.80738E-02	22.862	0.083974	522.681	0.985011
44	125.314	0.79800E-02	14.062	0.051651	197.744	0.985767
45	126.533	0.79031E-02	8.2716	0.030382	68.4195	0.986028
46	128.172	0.78020E-02	-15.042	0.055250	226.264	0.986893
47	131.098	0.76279E-02	-4.1478	0.015235	17.2041	0.986958
48	131.818	0.75862E-02	2.3155	0.008505	5.36152	0.986979
49	134.756	0.74208E-02	8.6828	0.031892	75.3905	0.987267
50	135.109	0.74014E-02	5.6920	0.020907	32.3989	0.987391
51	135.339	0.73889E-02	-0.76790	0.002821	0.589673	0.987393
52	136.284	0.73376E-02	-9.3347	0.034287	87.1366	0.987726
53	138.716	0.72090E-02	-5.0105	0.018404	25.1055	0.987822
54	139.466	0.71702E-02	-4.9362	0.018131	24.3658	0.987915
55	142.513	0.70169E-02	2.1004	0.007715	4.41176	0.987932
56	143.339	0.69765E-02	-13.137	0.048254	172.589	0.988591
57	144.661	0.69127E-02	0.25590E-03	0.000001	0.654860E-07	0.988591
58	146.883	0.68082E-02	41.384	0.152005	1712.62	0.995134
59	149.156	0.67044E-02	3.3407	0.012271	11.1604	0.995177
60	149.678	0.66810E-02	0.40012E-03	0.000001	0.160093E-06	0.995177
61	149.683	0.66808E-02	-2.5996	0.009548	6.75780	0.995203
62	150.162	0.66595E-02	-3.8188	0.014027	14.5832	0.995258
63	150.888	0.66274E-02	3.8207	0.014033	14.5974	0.995314
64	151.715	0.65913E-02	0.19990E-02	0.000007	0.399595E-05	0.995314
65	152.476	0.65584E-02	0.19218E-03	0.000001	0.369345E-07	0.995314
66	154.256	0.64827E-02	-0.47745	0.001754	0.227956	0.995315
67	155.161	0.64449E-02	0.12198E-02	0.000004	0.148782E-05	0.995315
68	156.222	0.64012E-02	15.828	0.058137	250.528	0.996272
69	156.554	0.63876E-02	-0.41853E-03	0.000002	0.175170E-06	0.996272

NEDO-33373-A, Revision 5

70	156.859	0.63751E-02	-28.853	0.105979	832.495	0.999453
71	157.933	0.63318E-02	1.6996	0.006243	2.88879	0.999464
72	159.077	0.62863E-02	-0.11700E-01	0.000043	0.136898E-03	0.999464
73	161.029	0.62101E-02	-0.59115E-02	0.000022	0.349453E-04	0.999464
74	161.410	0.61954E-02	-5.0071	0.018391	25.0713	0.999559
75	161.801	0.61804E-02	0.35615E-02	0.000013	0.126840E-04	0.999559
76	163.842	0.61034E-02	-4.6095	0.016931	21.2479	0.999641
77	164.114	0.60933E-02	-3.2663	0.011997	10.6687	0.999681
78	165.682	0.60357E-02	-0.34053E-02	0.000013	0.115962E-04	0.999681
79	165.700	0.60350E-02	4.0601	0.014913	16.4844	0.999744
80	166.146	0.60188E-02	0.58970	0.002166	0.347748	0.999746
81	168.809	0.59239E-02	-0.21280E-01	0.000078	0.452852E-03	0.999746
82	170.289	0.58724E-02	2.2792	0.008372	5.19470	0.999766
83	170.507	0.58649E-02	0.19329E-01	0.000071	0.373622E-03	0.999766
84	171.275	0.58386E-02	1.1328	0.004161	1.28328	0.999770
85	171.484	0.58314E-02	-0.75575	0.002776	0.571164	0.999773
86	172.127	0.58096E-02	0.16490E-02	0.000006	0.271931E-05	0.999773
87	172.499	0.57971E-02	-0.89866	0.003301	0.807592	0.999776
88	173.782	0.57543E-02	-0.70748E-01	0.000260	0.500527E-02	0.999776
89	175.575	0.56956E-02	0.49031E-02	0.000018	0.240406E-04	0.999776
90	176.105	0.56784E-02	-2.3109	0.008488	5.34042	0.999796
91	176.912	0.56525E-02	0.77604E-02	0.000029	0.602246E-04	0.999796
92	177.514	0.56334E-02	-0.30499E-01	0.000112	0.930172E-03	0.999796
93	178.035	0.56169E-02	-7.2917	0.026783	53.1685	0.999999
94	179.488	0.55714E-02	-0.23350E-01	0.000086	0.545217E-03	0.999999
95	181.335	0.55146E-02	-0.59168E-01	0.000217	0.350083E-02	0.999999
96	182.803	0.54704E-02	0.30543	0.001122	0.932847E-01	1.00000
97	182.896	0.54676E-02	0.87945E-01	0.000323	0.773433E-02	1.00000

98	183.051	0.54630E-02	0.84646E-02	0.000031	0.716494E-04	1.00000
99	183.935	0.54367E-02	0.17268E-01	0.000063	0.298186E-03	1.00000
100	185.423	0.53931E-02	0.28327	0.001040	0.802444E-01	1.00000

SUM OF EFFECTIVE MASSES= 261746.

*** NOTE *** CP = 3080.922 TIME= 13:20:39

Solution is done!

*** PROBLEM STATISTICS

ACTUAL NO. OF ACTIVE DEGREES OF FREEDOM = 81934

R.M.S. WAVEFRONT SIZE = 2095.6

*** ANSYS BINARY FILE STATISTICS

BUFFER SIZE USED= 16384

5.625 MB WRITTEN ON ELEMENT MATRIX FILE: SSE-LOCA-SRVD.emat

22.812 MB WRITTEN ON ELEMENT SAVED DATA FILE: SSE-LOCA-SRVD.esav

23.625 MB WRITTEN ON ASSEMBLED MATRIX FILE: SSE-LOCA-SRVD.full

70.875 MB WRITTEN ON MODAL MATRIX FILE: SSE-LOCA-SRVD.mode

2713.188 MB WRITTEN ON RESULTS FILE: SSE-LOCA-SRVD.rst

FINISH SOLUTION PROCESSING

***** ROUTINE COMPLETED ***** CP = 3081.031

C***

C*** 4% DAMPING

C***

***** ANSYS SOLUTION ROUTINE *****

PERFORM A SPECTRUM ANALYSIS

THIS WILL BE A NEW ANALYSIS

USE SINGLE POINT EXCITATION RESPONSE SPECTRUM
USE THE FIRST 100 MODES FROM THE MODAL ANALYSIS
INCLUDE STRESS RESPONSES IN THE CALCULATIONS
COMBINE MODES USING THE GROUPING METHOD
WHOSE SIGNIFICANCE LEVEL EXCEEDS THE THRESHOLD OF 0.10000E-02
TYPE OF QUANTITIES TO BE COMBINED IS DISP

C***

C*** SSE

C***

SEISMIC EXCITATION DIRECTION = 1.0000 0.0000 0.0000

SPECTRUM TYPE KEY= 2 FACTOR= 9.81000

PRINT NSOL ITEMS WITH A FREQUENCY OF ALL

FOR ALL APPLICABLE ENTITIES

FREQ= 0.00 0.00 0.00 0.00 0.00 0.00 0.00 0.00 0.00

SPECTRUM TABLE INITIALIZED

FREQ= 10.0 32.2 32.4 32.6 32.9 55.2 55.6 56.0 57.9

NUMBER OF FREQUENCIES IN TABLE = 9

FREQ= 58.3 58.8 60.8 61.3 61.7 63.9 94.5 95.2 99.3

NUMBER OF FREQUENCIES IN TABLE = 18

FREQ= 100. 200. 0.00 0.00 0.00 0.00 0.00 0.00 0.00

NUMBER OF FREQUENCIES IN TABLE = 20

DAMPING= 0.0000 SV= 1.6960 1.6960 1.6876

1.6792 1.6770 1.6770

1.6671 1.6571 1.6080

DAMPING= 0.0000 SV= 1.5796 1.5510 1.4110

1.3931 1.3751 1.3100

1.3100 1.3055 1.2790

DAMPING= 0.0000 SV= 1.2619 1.2619 0.0000

0.0000 0.0000 0.0000

0.0000 0.0000 0.0000

NUMBER OF ENTRIES IN RESPONSE SPECTRUM TABLE = 20

WRITE ANSYS LOADS DATA AS FILE=SSE-LOCA-SRVD.s01

SEISMIC EXCITATION DIRECTION = 0.0000 1.0000 0.0000

SPECTRUM TYPE KEY= 2 FACTOR= 9.81000

PRINT NSOL ITEMS WITH A FREQUENCY OF ALL

FOR ALL APPLICABLE ENTITIES

FREQ= 0.00 0.00 0.00 0.00 0.00 0.00 0.00 0.00 0.00

SPECTRUM TABLE INITIALIZED

FREQ= 10.0 24.1 24.3 30.7 31.1 41.1 43.2 45.7 57.9

NUMBER OF FREQUENCIES IN TABLE = 9

FREQ= 58.3 64.8 68.1 77.7 82.8 85.7 94.5 95.2 99.3

NUMBER OF FREQUENCIES IN TABLE = 18

FREQ= 100. 200. 0.00 0.00 0.00 0.00 0.00 0.00 0.00

NUMBER OF FREQUENCIES IN TABLE = 20

DAMPING= 0.0000 SV= 1.8320 1.8320 1.8420

1.8420 1.8880 1.8880

1.7450 1.7260 1.7260

DAMPING= 0.0000 SV= 1.7025 1.3374 1.2549

1.0990 1.0861 1.0850

1.0850 1.0847 1.0830

DAMPING= 0.0000 SV= 1.0749 1.0749 0.0000

0.0000 0.0000 0.0000

0.0000 0.0000 0.0000

NUMBER OF ENTRIES IN RESPONSE SPECTRUM TABLE = 20

WRITE ANSYS LOADS DATA AS FILE=SSE-LOCA-SRVD.s02

SEISMIC EXCITATION DIRECTION = 0.0000 0.0000 1.0000

SPECTRUM TYPE KEY= 2 FACTOR= 9.81000

PRINT NSOL ITEMS WITH A FREQUENCY OF ALL

FOR ALL APPLICABLE ENTITIES

FREQ= 0.00 0.00 0.00 0.00 0.00 0.00 0.00 0.00 0.00

SPECTRUM TABLE INITIALIZED

FREQ= 10.0 37.3 37.7 50.0 50.4 51.9 55.2 58.8 61.7

NUMBER OF FREQUENCIES IN TABLE = 9

FREQ= 64.8 67.6 68.1 71.5 74.0 77.7 82.2 85.7 95.2

NUMBER OF FREQUENCIES IN TABLE = 18

FREQ= 100. 200. 0.00 0.00 0.00 0.00 0.00 0.00 0.00

NUMBER OF FREQUENCIES IN TABLE = 20

DAMPING= 0.0000 SV= 1.6320 1.6320 1.5880

1.5880 1.5711 1.5010

1.5010 1.3940 1.2617

DAMPING= 0.0000 SV= 1.1846 1.1354 1.1287

1.0821 1.0480 1.0040

0.95854 0.93800 0.89826

DAMPING= 0.0000 SV= 0.87987 0.87987 0.0000

0.0000 0.0000 0.0000

0.0000 0.0000 0.0000

NUMBER OF ENTRIES IN RESPONSE SPECTRUM TABLE = 20

WRITE ANSYS LOADS DATA AS FILE=SSE-LOCA-SRVD.s03

C***

C*** 4% DAMPING

C*** LOCA

C***

SEISMIC EXCITATION DIRECTION = 1.0000 0.0000 0.0000

SPECTRUM TYPE KEY= 2 FACTOR= 9.81000

PRINT NSOL ITEMS WITH A FREQUENCY OF ALL

FOR ALL APPLICABLE ENTITIES

FREQ= 0.00 0.00 0.00 0.00 0.00 0.00 0.00 0.00 0.00

SPECTRUM TABLE INITIALIZED

FREQ= 10.0 14.0 15.0 18.0 20.0 30.0 33.0 100. 200.

NUMBER OF FREQUENCIES IN TABLE = 9

DAMPING= 0.0000 SV= 0.90000E-01 0.90000E-01 0.80000E-01

0.80000E-01 0.11000 0.11000

0.80000E-01 0.72000E-01 0.72000E-01

WRITE ANSYS LOADS DATA AS FILE=SSE-LOCA-SRVD.s04

SEISMIC EXCITATION DIRECTION = 0.0000 1.0000 0.0000

SPECTRUM TYPE KEY= 2 FACTOR= 9.81000

PRINT NSOL ITEMS WITH A FREQUENCY OF ALL

FOR ALL APPLICABLE ENTITIES

WRITE ANSYS LOADS DATA AS FILE=SSE-LOCA-SRVD.s05

SEISMIC EXCITATION DIRECTION = 0.0000 0.0000 1.0000

SPECTRUM TYPE KEY= 2 FACTOR= 9.81000

PRINT NSOL ITEMS WITH A FREQUENCY OF ALL

FOR ALL APPLICABLE ENTITIES

FREQ= 0.00 0.00 0.00 0.00 0.00 0.00 0.00 0.00 0.00

SPECTRUM TABLE INITIALIZED

FREQ= 10.0 11.0 13.0 15.0 18.0 40.0 100. 200. 0.00

NUMBER OF FREQUENCIES IN TABLE = 8

DAMPING= 0.0000 SV= 0.34000 0.34000 0.25000

0.23000 0.17000 0.15000

0.14000 0.14000 0.0000

WRITE ANSYS LOADS DATA AS FILE=SSE-LOCA-SRVD.s06

C***

C*** 4% DAMPING

C***

C***

C*** SRVD

C***

SEISMIC EXCITATION DIRECTION = 1.0000 0.0000 0.0000

SPECTRUM TYPE KEY= 2 FACTOR= 9.81000

PRINT NSOL ITEMS WITH A FREQUENCY OF ALL

FOR ALL APPLICABLE ENTITIES

FREQ= 0.00 0.00 0.00 0.00 0.00 0.00 0.00 0.00 0.00

SPECTRUM TABLE INITIALIZED

FREQ= 10.0 16.0 20.0 28.0 40.0 100. 200. 0.00 0.00

NUMBER OF FREQUENCIES IN TABLE = 7

DAMPING= 0.0000 SV= 0.19200 0.19200 0.60000E-01

0.60000E-01 0.40000E-01 0.30000E-01

0.30000E-01 0.0000 0.0000

WRITE ANSYS LOADS DATA AS FILE=SSE-LOCA-SRVD.s07

SEISMIC EXCITATION DIRECTION = 0.0000 1.0000 0.0000

SPECTRUM TYPE KEY= 2 FACTOR= 9.81000

PRINT NSOL ITEMS WITH A FREQUENCY OF ALL

FOR ALL APPLICABLE ENTITIES

WRITE ANSYS LOADS DATA AS FILE=SSE-LOCA-SRVD.s08

SEISMIC EXCITATION DIRECTION = 0.0000 0.0000 1.0000

SPECTRUM TYPE KEY= 2 FACTOR= 9.81000

PRINT NSOL ITEMS WITH A FREQUENCY OF ALL

FOR ALL APPLICABLE ENTITIES

FREQ= 0.00 0.00 0.00 0.00 0.00 0.00 0.00 0.00 0.00

SPECTRUM TABLE INITIALIZED

FREQ= 10.0 11.0 12.0 14.0 18.0 28.0 100. 200. 0.00

NUMBER OF FREQUENCIES IN TABLE = 8

DAMPING= 0.0000 SV= 0.75000 0.55000 0.54000

0.32000 0.18000 0.14000

0.13000 0.13000 0.0000

WRITE ANSYS LOADS DATA AS FILE=SSE-LOCA-SRVD.s09

ANSYS RELEASE 10.0 UP20050718 13:20:47 09/07/2009

NUMBER OF FREQUENCIES IN TABLE = 4

NUMBER OF FREQUENCIES IN TABLE = 8

NUMBER OF FREQUENCIES IN TABLE = 12

NUMBER OF FREQUENCIES IN TABLE = 16

NUMBER OF FREQUENCIES IN TABLE = 20

NUMBER OF ENTRIES IN RESPONSE SPECTRUM TABLE = 20

PRINTOUT RESUMED BY /GOP

Load step file number 1. Begin solution ...

***** ANSYS SOLVE COMMAND *****

SOLUTION OPTIONS

PROBLEM DIMENSIONALITY.....3-D

DEGREES OF FREEDOM.....UX UY UZ ROTX ROTY ROTZ

ANALYSIS TYPE.....SPECTRUM

SPECTRUM TYPE.....SINGLE POINT

NUMBER OF MODES TO BE USED.....100

ELEMENT RESULTS CALCULATION.....ON

GLOBALLY ASSEMBLED MATRIX.....SYMMETRIC

LOAD STEP OPTIONS

LOAD STEP NUMBER..... 1
SPECTRUM LOADING TYPE.....ACCELERATION
EXCITATION DIRECTION..... 1.0000 0.0000 0.0000
MODE COMBINATION TYPE..... GRP
RESPONSE TYPE.....DISPLACEMENT
SIGNIFICANCE LEVEL FOR COMBINATIONS..... 0.10000E-02

PRINT OUTPUT CONTROLS

ITEM FREQUENCY COMPONENT
ALL NONE
NSOL ALL

DATABASE OUTPUT CONTROLS.....ALL DATA WRITTEN

1

***** ANSYS - ENGINEERING ANALYSIS SYSTEM RELEASE 10.0 *****

ANSYS Multiphysics

00265621 VERSION=INTEL NT 13:20:59 SEP 07, 2009 CP= 3084.172

***** RESPONSE SPECTRUM CALCULATION SUMMARY *****

CUMULATIVE

MODE	FREQUENCY	SV	PARTIC.FACTOR	MODE COEF.	M.C. RATIO	EFFECTIVE MASS	MASS FRACTION
1	13.79 16.638	0.1725E-05	0.3826E-08	0.000000	0.297690E-11	0.397373E-16	
2	16.69 16.638	219.4	0.3318	1.000000	48143.7	0.642650	
3	17.53 16.638	-0.9107E-06	-0.1249E-08	0.000000	0.829354E-12	0.642650	
4	30.17 16.638	-0.5842E-06	-0.2706E-09	0.000000	0.341317E-12	0.642650	
5	31.99 16.638	-0.3978E-06	-0.1639E-09	0.000000	0.158270E-12	0.642650	

NEDO-33373-A, Revision 5

6	34.31	16.451	7.927	0.2805E-02	0.008455	62.8308	0.643489
7	35.74	16.451	0.9065E-05	0.2957E-08	0.000000	0.821820E-10	0.643489
8	38.57	16.451	-0.5012E-05	-0.1404E-08	0.000000	0.251193E-10	0.643489
9	39.42	16.451	-0.4961E-05	-0.1330E-08	0.000000	0.246122E-10	0.643489
10	43.44	16.451	0.5046E-04	0.1114E-07	0.000000	0.254589E-08	0.643489
11	43.46	16.451	-0.7074	-0.1561E-03	0.000470	0.500411	0.643495
12	44.08	16.451	-0.1555E-04	-0.3335E-08	0.000000	0.241919E-09	0.643495
13	48.22	16.451	-0.3713E-04	-0.6654E-08	0.000000	0.137853E-08	0.643495
14	49.09	16.451	0.3384E-04	0.5851E-08	0.000000	0.114534E-08	0.643495
15	53.20	16.451	0.2725E-04	0.4013E-08	0.000000	0.742710E-09	0.643495
16	53.88	16.451	0.6110E-05	0.8770E-09	0.000000	0.373263E-10	0.643495
17	54.15	16.451	136.5	0.1940E-01	0.058455	18620.8	0.892056
18	56.50	16.125	80.75	0.1033E-01	0.031135	6520.80	0.979100
19	60.15	14.266	0.1814E-04	0.1811E-08	0.000000	0.328926E-09	0.979100
20	62.62	13.216	0.4728E-04	0.4036E-08	0.000000	0.223505E-08	0.979100
21	66.52	12.851	-0.2101E-04	-0.1546E-08	0.000000	0.441607E-09	0.979100
22	70.01	12.851	21.69	0.1440E-02	0.004341	470.323	0.985378
23	72.36	12.851	0.1025E-03	0.6373E-08	0.000000	0.105084E-07	0.985378
24	76.34	12.851	0.1587E-03	0.8866E-08	0.000000	0.251917E-07	0.985378
25	77.98	12.851	-21.55	-0.1154E-02	0.003478	464.515	0.991578
26	78.47	12.851	-0.1720E-03	-0.9096E-08	0.000000	0.296005E-07	0.991578
27	80.08	12.851	-0.4539E-03	-0.2304E-07	0.000000	0.206033E-06	0.991578
28	82.34	12.851	-3.554	-0.1707E-03	0.000514	12.6309	0.991747
29	83.23	12.851	0.8322E-03	0.3911E-07	0.000000	0.692583E-06	0.991747
30	84.75	12.851	0.8763E-05	0.3972E-09	0.000000	0.767864E-10	0.991747
31	87.19	12.851	-0.1913E-06	-0.8192E-11	0.000000	0.366061E-13	0.991747
32	87.58	12.851	-12.60	-0.5349E-03	0.001612	158.834	0.993867
33	89.82	12.851	-0.4399E-04	-0.1775E-08	0.000000	0.193537E-08	0.993867

NEDO-33373-A, Revision 5

34	90.26	12.851	-0.5749E-04	-0.2297E-08	0.000000	0.330534E-08	0.993867
35	96.62	12.716	0.7549E-04	0.2605E-08	0.000000	0.569897E-08	0.993867
36	97.41	12.665	0.1952E-04	0.6599E-09	0.000000	0.380909E-09	0.993867
37	98.21	12.615	-0.3908E-04	-0.1295E-08	0.000000	0.152729E-08	0.993867
38	108.9	12.380	-0.2244E-03	-0.5937E-08	0.000000	0.503506E-07	0.993867
39	117.1	12.380	-0.3889E-03	-0.8886E-08	0.000000	0.151257E-06	0.993867
40	119.6	12.380	-19.90	-0.4365E-03	0.001315	395.909	0.999152
41	120.2	12.380	-0.7125E-03	-0.1547E-07	0.000000	0.507672E-06	0.999152
42	122.6	12.380	0.3596	0.7504E-05	0.000023	0.129343	0.999154
43	123.9	12.380	-0.3978E-03	-0.8131E-08	0.000000	0.158230E-06	0.999154
44	125.3	12.380	-0.7098E-03	-0.1417E-07	0.000000	0.503750E-06	0.999154
45	126.5	12.380	-0.4841E-03	-0.9482E-08	0.000000	0.234391E-06	0.999154
46	128.2	12.380	-0.8334E-03	-0.1591E-07	0.000000	0.694472E-06	0.999154
47	131.1	12.380	-0.2352E-02	-0.4292E-07	0.000000	0.553390E-05	0.999154
48	131.8	12.380	-2.307	-0.4164E-04	0.000126	5.32450	0.999225
49	134.8	12.380	0.2199E-02	0.3798E-07	0.000000	0.483627E-05	0.999225
50	135.1	12.380	0.3035E-03	0.5214E-08	0.000000	0.921184E-07	0.999225
51	135.3	12.380	0.7600	0.1301E-04	0.000039	0.577631	0.999233
52	136.3	12.380	-0.4467E-03	-0.7542E-08	0.000000	0.199531E-06	0.999233
53	138.7	12.380	-0.1480E-03	-0.2412E-08	0.000000	0.219087E-07	0.999233
54	139.5	12.380	4.897	0.7896E-04	0.000238	23.9847	0.999553
55	142.5	12.380	-2.082	-0.3215E-04	0.000097	4.33545	0.999611
56	143.3	12.380	-0.2801E-03	-0.4275E-08	0.000000	0.784399E-07	0.999611
57	144.7	12.380	-0.1746E-03	-0.2617E-08	0.000000	0.304935E-07	0.999611
58	146.9	12.380	-0.1070E-02	-0.1555E-07	0.000000	0.114512E-05	0.999611
59	149.2	12.380	0.9068E-04	0.1278E-08	0.000000	0.822253E-08	0.999611
60	149.7	12.380	-0.1620E-03	-0.2268E-08	0.000000	0.262449E-07	0.999611
61	149.7	12.380	-0.8696E-03	-0.1217E-07	0.000000	0.756279E-06	0.999611

NEDO-33373-A, Revision 5

62	150.2	12.380	0.1666E-03	0.2316E-08	0.000000	0.277421E-07	0.999611
63	150.9	12.380	0.2350E-04	0.3236E-09	0.000000	0.552019E-09	0.999611
64	151.7	12.380	-0.9457E-03	-0.1288E-07	0.000000	0.894351E-06	0.999611
65	152.5	12.380	-0.5051E-03	-0.6812E-08	0.000000	0.255079E-06	0.999611
66	154.3	12.380	-0.6471E-03	-0.8528E-08	0.000000	0.418760E-06	0.999611
67	155.2	12.380	-0.9259E-03	-0.1206E-07	0.000000	0.857345E-06	0.999611
68	156.2	12.380	0.4408E-03	0.5664E-08	0.000000	0.194340E-06	0.999611
69	156.6	12.380	-0.9395E-04	-0.1202E-08	0.000000	0.882724E-08	0.999611
70	156.9	12.380	0.6425E-03	0.8189E-08	0.000000	0.412826E-06	0.999611
71	157.9	12.380	-1.691	-0.2126E-04	0.000064	2.86034	0.999649
72	159.1	12.380	-0.4040E-03	-0.5006E-08	0.000000	0.163225E-06	0.999649
73	161.0	12.380	0.8683E-03	0.1050E-07	0.000000	0.753904E-06	0.999649
74	161.4	12.380	4.968	0.5980E-04	0.000180	24.6805	0.999978
75	161.8	12.380	-0.9736E-03	-0.1166E-07	0.000000	0.947827E-06	0.999978
76	163.8	12.380	-0.3201E-02	-0.3740E-07	0.000000	0.102482E-04	0.999978
77	164.1	12.380	-0.2729E-02	-0.3177E-07	0.000000	0.744695E-05	0.999978
78	165.7	12.380	0.1348E-02	0.1540E-07	0.000000	0.181828E-05	0.999978
79	165.7	12.380	-0.2188E-02	-0.2499E-07	0.000000	0.478766E-05	0.999978
80	166.1	12.380	-0.6071	-0.6897E-05	0.000021	0.368601	0.999983
81	168.8	12.380	0.1407E-02	0.1548E-07	0.000000	0.197874E-05	0.999983
82	170.3	12.380	0.3513E-03	0.3799E-08	0.000000	0.123441E-06	0.999983
83	170.5	12.380	-0.2020E-01	-0.2178E-06	0.000001	0.407840E-03	0.999983
84	171.3	12.380	-1.117	-0.1195E-04	0.000036	1.24880	1.00000
85	171.5	12.380	-0.3164E-03	-0.3373E-08	0.000000	0.100080E-06	1.00000
86	172.1	12.380	0.3084E-03	0.3264E-08	0.000000	0.951294E-07	1.00000
87	172.5	12.380	0.6107E-04	0.6435E-09	0.000000	0.372914E-08	1.00000
88	173.8	12.380	0.7255E-01	0.7533E-06	0.000002	0.526391E-02	1.00000
89	175.6	12.380	-0.1656E-04	-0.1685E-09	0.000000	0.274283E-09	1.00000

NEDO-33373-A, Revision 5

90	176.1	12.380	0.6936E-03	0.7013E-08	0.000000	0.481084E-06	1.00000
91	176.9	12.380	-0.3791E-03	-0.3798E-08	0.000000	0.143702E-06	1.00000
92	177.5	12.380	0.2093E-01	0.2083E-06	0.000001	0.438182E-03	1.00000
93	178.0	12.380	-0.6705E-03	-0.6634E-08	0.000000	0.449583E-06	1.00000
94	179.5	12.380	0.6013E-04	0.5853E-09	0.000000	0.361511E-08	1.00000
95	181.3	12.380	0.6589E-01	0.6283E-06	0.000002	0.434129E-02	1.00000
96	182.8	12.380	0.2478E-02	0.2325E-07	0.000000	0.613851E-05	1.00000
97	182.9	12.380	-0.5735E-03	-0.5376E-08	0.000000	0.328912E-06	1.00000
98	183.1	12.380	0.3353E-01	0.3138E-06	0.000001	0.112444E-02	1.00000
99	183.9	12.380	0.4072E-01	0.3774E-06	0.000001	0.165794E-02	1.00000
100	185.4	12.380	-0.7418E-03	-0.6766E-08	0.000000	0.550325E-06	1.00000

SUM OF EFFECTIVE MASSES= 74914.4

1

***** ANSYS - ENGINEERING ANALYSIS SYSTEM RELEASE 10.0 *****

ANSYS Multiphysics

00265621 VERSION=INTEL NT 13:20:59 SEP 07, 2009 CP= 3084.172

SIGNIFICANCE FACTOR FOR COMBINING MODES = 0.10000E-02

SIGNIFICANT MODE COEFFICIENTS (INCLUDING DAMPING)

MODE	FREQUENCY	DAMPING	SV	MODE COEF.
2	16.69	0.0000	16.638	0.3318
6	34.31	0.0000	16.451	0.2805E-02
17	54.15	0.0000	16.451	0.1940E-01
18	56.50	0.0000	16.125	0.1033E-01
22	70.01	0.0000	12.851	0.1440E-02
25	77.98	0.0000	12.851	-0.1154E-02
32	87.58	0.0000	12.851	-0.5349E-03
40	119.6	0.0000	12.380	-0.4365E-03

MODAL COMBINATION COEFFICIENTS

MODE= 2 FREQUENCY= 16.694 COUPLING COEF.= 1.000

MODE= 6 FREQUENCY= 34.314 COUPLING COEF.= 1.000

FREQUENCY 54.147 HERTZ PART OF CLOSELY SPACED GROUP 1

FREQUENCY 56.504 HERTZ PART OF CLOSELY SPACED GROUP 1

MODE= 22 FREQUENCY= 70.010 COUPLING COEF.= 1.000

MODE= 25 FREQUENCY= 77.976 COUPLING COEF.= 1.000

MODE= 32 FREQUENCY= 87.575 COUPLING COEF.= 1.000

MODE= 40 FREQUENCY= 119.561 COUPLING COEF.= 1.000

GROUPING COMBINATION INSTRUCTIONS WRITTEN ON FILE SSE-LOCA-SRVD.mcom

*** NOTE *** CP = 3084.188 TIME= 13:20:59

Solution is done!

*** PROBLEM STATISTICS

ACTUAL NO. OF ACTIVE DEGREES OF FREEDOM = 81934

R.M.S. WAVEFRONT SIZE = 2095.6

*** ANSYS BINARY FILE STATISTICS

BUFFER SIZE USED= 16384

ANSYS RELEASE 10.0 UP20050718 13:20:49 09/07/2009

NUMBER OF FREQUENCIES IN TABLE = 4

NUMBER OF FREQUENCIES IN TABLE = 8

NUMBER OF FREQUENCIES IN TABLE = 12

NUMBER OF FREQUENCIES IN TABLE = 16

NUMBER OF FREQUENCIES IN TABLE = 20

NUMBER OF ENTRIES IN RESPONSE SPECTRUM TABLE = 20

PRINTOUT RESUMED BY /GOP

Load step file number 2. Begin solution ...

***** ANSYS SOLVE COMMAND *****

LOAD STEP OPTIONS

LOAD STEP NUMBER..... 2
SPECTRUM LOADING TYPE.....ACCELERATION
EXCITATION DIRECTION..... 0.0000 1.0000 0.0000
MODE COMBINATION TYPE.....GRP
RESPONSE TYPE.....DISPLACEMENT
SIGNIFICANCE LEVEL FOR COMBINATIONS..... 0.10000E-02

PRINT OUTPUT CONTROLS

ITEM FREQUENCY COMPONENT
ALL NONE
NSOL ALL

DATABASE OUTPUT CONTROLS.....ALL DATA WRITTEN

1

***** ANSYS - ENGINEERING ANALYSIS SYSTEM RELEASE 10.0 *****

ANSYS Multiphysics

00265621 VERSION=INTEL NT 13:21:01 SEP 07, 2009 CP= 3085.422

***** RESPONSE SPECTRUM CALCULATION SUMMARY *****

CUMULATIVE

MODE	FREQUENCY	SV	PARTIC.FACTOR	MODE COEF.	M.C. RATIO	EFFECTIVE MASS	MASS FRACTION
1	13.79 17.972	216.1	0.5175	1.000000	46688.0	0.626446	
2	16.69 17.972	0.2075E-06	0.3389E-09	0.000000	0.430422E-13	0.626446	
3	17.53 17.972	-0.5288E-06	-0.7836E-09	0.000000	0.279620E-12	0.626446	

NEDO-33373-A, Revision 5

4	30.17	18.070	0.1043E-05	0.5245E-09	0.000000	0.108733E-11	0.626446
5	31.99	18.521	-2.989	-0.1371E-02	0.002648	8.93272	0.626565
6	34.31	18.521	0.2088E-06	0.8320E-10	0.000000	0.436061E-13	0.626565
7	35.74	18.521	0.1776E-06	0.6523E-10	0.000000	0.315452E-13	0.626565
8	38.57	18.521	-0.2891E-04	-0.9116E-08	0.000000	0.835606E-09	0.626565
9	39.42	18.521	5.439	0.1642E-02	0.003173	29.5846	0.626962
10	43.44	17.100	0.3730E-04	0.8562E-08	0.000000	0.139156E-08	0.626962
11	43.46	17.098	0.2195E-05	0.5033E-09	0.000000	0.481826E-11	0.626962
12	44.08	17.051	0.7629E-05	0.1696E-08	0.000000	0.582038E-10	0.626962
13	48.22	16.932	-32.35	-0.5967E-02	0.011531	1046.61	0.641005
14	49.09	16.932	0.1683E-03	0.2996E-07	0.000000	0.283377E-07	0.641005
15	53.20	16.932	155.0	0.2348E-01	0.045379	24015.1	0.963233
16	53.88	16.932	0.5050E-05	0.7461E-09	0.000000	0.255048E-10	0.963233
17	54.15	16.932	-0.9425E-05	-0.1379E-08	0.000000	0.888384E-10	0.963233
18	56.50	16.932	-0.6047E-05	-0.8123E-09	0.000000	0.365613E-10	0.963233
19	60.15	15.549	36.01	0.3920E-02	0.007575	1297.05	0.980637
20	62.62	14.185	-0.2556E-04	-0.2341E-08	0.000000	0.653081E-09	0.980637
21	66.52	12.686	-0.1050E-03	-0.7628E-08	0.000000	0.110329E-07	0.980637
22	70.01	11.973	0.1390E-03	0.8602E-08	0.000000	0.193248E-07	0.980637
23	72.36	11.581	-16.45	-0.9218E-03	0.001781	270.761	0.984270
24	76.34	10.975	-0.2922E-03	-0.1394E-07	0.000000	0.853894E-07	0.984270
25	77.98	10.774	0.7648E-03	0.3433E-07	0.000000	0.584977E-06	0.984270
26	78.47	10.762	-0.3536E-03	-0.1565E-07	0.000000	0.125031E-06	0.984270
27	80.08	10.721	0.1096E-02	0.4642E-07	0.000000	0.120136E-05	0.984270
28	82.34	10.666	0.1133E-02	0.4516E-07	0.000000	0.128397E-05	0.984270
29	83.23	10.653	-11.12	-0.4331E-03	0.000837	123.641	0.985929
30	84.75	10.647	-0.1751E-04	-0.6575E-09	0.000000	0.306546E-09	0.985929
31	87.19	10.644	0.7519E-05	0.2666E-09	0.000000	0.565308E-10	0.985929

NEDO-33373-A, Revision 5

32	87.58	10.644	0.7858E-05	0.2763E-09	0.000000	0.617535E-10	0.985929
33	89.82	10.644	10.15	0.3393E-03	0.000656	103.083	0.987312
34	90.26	10.644	0.1697E-04	0.5617E-09	0.000000	0.288060E-09	0.987312
35	96.62	10.635	-17.46	-0.5040E-03	0.000974	304.977	0.991404
36	97.41	10.632	0.1752E-04	0.4973E-09	0.000000	0.307020E-09	0.991404
37	98.21	10.629	0.7632E-04	0.2130E-08	0.000000	0.582449E-08	0.991404
38	108.9	10.545	0.5956E-03	0.1342E-07	0.000000	0.354744E-06	0.991404
39	117.1	10.545	-19.73	-0.3840E-03	0.000742	389.301	0.996627
40	119.6	10.545	0.1308E-02	0.2444E-07	0.000000	0.171090E-05	0.996627
41	120.2	10.545	0.3341E-03	0.6178E-08	0.000000	0.111631E-06	0.996627
42	122.6	10.545	0.4968E-02	0.8830E-07	0.000000	0.246813E-04	0.996627
43	123.9	10.545	0.1371E-03	0.2388E-08	0.000000	0.188084E-07	0.996627
44	125.3	10.545	11.16	0.1898E-03	0.000367	124.546	0.998299
45	126.5	10.545	0.2861E-02	0.4773E-07	0.000000	0.818435E-05	0.998299
46	128.2	10.545	-0.4767E-03	-0.7751E-08	0.000000	0.227247E-06	0.998299
47	131.1	10.545	-3.294	-0.5120E-04	0.000099	10.8519	0.998444
48	131.8	10.545	-0.7363E-02	-0.1132E-06	0.000000	0.542152E-04	0.998444
49	134.8	10.545	0.1274E-01	0.1875E-06	0.000000	0.162416E-03	0.998444
50	135.1	10.545	4.518	0.6611E-04	0.000128	20.4118	0.998718
51	135.3	10.545	-0.2280E-02	-0.3324E-07	0.000000	0.519624E-05	0.998718
52	136.3	10.545	-0.8688E-02	-0.1249E-06	0.000000	0.754829E-04	0.998718
53	138.7	10.545	-3.975	-0.5518E-04	0.000107	15.7999	0.998930
54	139.5	10.545	0.1504E-03	0.2066E-08	0.000000	0.226333E-07	0.998930
55	142.5	10.545	-0.4492E-03	-0.5907E-08	0.000000	0.201738E-06	0.998930
56	143.3	10.545	0.7590E-03	0.9867E-08	0.000000	0.576050E-06	0.998930
57	144.7	10.545	-0.8851E-04	-0.1130E-08	0.000000	0.783340E-08	0.998930
58	146.9	10.545	0.1651E-02	0.2044E-07	0.000000	0.272509E-05	0.998930
59	149.2	10.545	2.652	0.3184E-04	0.000062	7.03492	0.999024

NEDO-33373-A, Revision 5

60	149.7	10.545	0.9355E-04	0.1115E-08	0.000000	0.875113E-08	0.999024
61	149.7	10.545	0.1944E-02	0.2318E-07	0.000000	0.378065E-05	0.999024
62	150.2	10.545	-3.031	-0.3590E-04	0.000069	9.18635	0.999148
63	150.9	10.545	3.032	0.3557E-04	0.000069	9.19141	0.999271
64	151.7	10.545	0.1140E-02	0.1322E-07	0.000000	0.129872E-05	0.999271
65	152.5	10.545	-0.1795E-03	-0.2062E-08	0.000000	0.322075E-07	0.999271
66	154.3	10.545	-0.3802	-0.4268E-05	0.000008	0.144563	0.999273
67	155.2	10.545	-0.2288E-03	-0.2539E-08	0.000000	0.523632E-07	0.999273
68	156.2	10.545	-0.2391E-02	-0.2616E-07	0.000000	0.571540E-05	0.999273
69	156.6	10.545	0.2024E-03	0.2206E-08	0.000000	0.409557E-07	0.999273
70	156.9	10.545	-0.1986E-02	-0.2155E-07	0.000000	0.394223E-05	0.999273
71	157.9	10.545	-0.2728E-02	-0.2921E-07	0.000000	0.744016E-05	0.999273
72	159.1	10.545	-0.9249E-02	-0.9762E-07	0.000000	0.855365E-04	0.999273
73	161.0	10.545	-0.3898E-02	-0.4015E-07	0.000000	0.151910E-04	0.999273
74	161.4	10.545	0.6081E-04	0.6235E-09	0.000000	0.369828E-08	0.999273
75	161.8	10.545	0.1560E-02	0.1592E-07	0.000000	0.243418E-05	0.999273
76	163.8	10.545	-3.659	-0.3641E-04	0.000070	13.3894	0.999453
77	164.1	10.545	-2.594	-0.2572E-04	0.000050	6.72662	0.999543
78	165.7	10.545	-0.4794E-02	-0.4664E-07	0.000000	0.229791E-04	0.999543
79	165.7	10.545	0.5593E-02	0.5441E-07	0.000000	0.312851E-04	0.999543
80	166.1	10.545	-0.1600E-01	-0.1549E-06	0.000000	0.256134E-03	0.999543
81	168.8	10.545	-0.1198E-01	-0.1123E-06	0.000000	0.143587E-03	0.999543
82	170.3	10.545	-0.4412E-02	-0.4064E-07	0.000000	0.194641E-04	0.999543
83	170.5	10.545	0.2483E-03	0.2281E-08	0.000000	0.616576E-07	0.999543
84	171.3	10.545	0.6195E-03	0.5641E-08	0.000000	0.383812E-06	0.999543
85	171.5	10.545	-0.2289E-03	-0.2079E-08	0.000000	0.523807E-07	0.999543
86	172.1	10.545	0.8577E-04	0.7733E-09	0.000000	0.735678E-08	0.999543
87	172.5	10.545	-0.7136	-0.6406E-05	0.000012	0.509254	0.999550

NEDO-33373-A, Revision 5

88	173.8	10.545	0.4457E-03	0.3942E-08	0.000000	0.198684E-06	0.999550
89	175.6	10.545	0.1068E-02	0.9251E-08	0.000000	0.113995E-05	0.999550
90	176.1	10.545	-0.2248E-02	-0.1936E-07	0.000000	0.505533E-05	0.999550
91	176.9	10.545	0.2999E-02	0.2559E-07	0.000000	0.899407E-05	0.999550
92	177.5	10.545	-0.5128E-02	-0.4347E-07	0.000000	0.262941E-04	0.999550
93	178.0	10.545	-5.790	-0.4879E-04	0.000094	33.5223	0.999999
94	179.5	10.545	-0.9784E-02	-0.8112E-07	0.000000	0.957260E-04	0.999999
95	181.3	10.545	0.6490E-02	0.5271E-07	0.000000	0.421152E-04	0.999999
96	182.8	10.545	0.1104E-01	0.8821E-07	0.000000	0.121796E-03	0.999999
97	182.9	10.545	0.5059E-01	0.4040E-06	0.000001	0.255971E-02	0.999999
98	183.1	10.545	0.2230E-01	0.1778E-06	0.000000	0.497341E-03	1.00000
99	183.9	10.545	0.3464E-01	0.2735E-06	0.000001	0.120000E-02	1.00000
100	185.4	10.545	0.1889	0.1467E-05	0.000003	0.356798E-01	1.00000

SUM OF EFFECTIVE MASSES= 74528.4

1

***** ANSYS - ENGINEERING ANALYSIS SYSTEM RELEASE 10.0 *****

ANSYS Multiphysics

00265621 VERSION=INTEL NT 13:21:01 SEP 07, 2009 CP= 3085.422

SIGNIFICANCE FACTOR FOR COMBINING MODES = 0.10000E-02

SIGNIFICANT MODE COEFFICIENTS (INCLUDING DAMPING)

MODE FREQUENCY DAMPING SV MODE COEF.

1	13.79	0.0000	17.972	0.5175
5	31.99	0.0000	18.521	-0.1371E-02
9	39.42	0.0000	18.521	0.1642E-02
13	48.22	0.0000	16.932	-0.5967E-02
15	53.20	0.0000	16.932	0.2348E-01
19	60.15	0.0000	15.549	0.3920E-02

23 72.36 0.0000 11.581 -0.9218E-03

MODAL COMBINATION COEFFICIENTS

MODE= 1 FREQUENCY= 13.787 COUPLING COEF.= 1.000
MODE= 5 FREQUENCY= 31.986 COUPLING COEF.= 1.000
MODE= 9 FREQUENCY= 39.424 COUPLING COEF.= 1.000
MODE= 13 FREQUENCY= 48.220 COUPLING COEF.= 1.000
MODE= 15 FREQUENCY= 53.200 COUPLING COEF.= 1.000
MODE= 19 FREQUENCY= 60.155 COUPLING COEF.= 1.000
MODE= 23 FREQUENCY= 72.363 COUPLING COEF.= 1.000

GROUPING COMBINATION INSTRUCTIONS WRITTEN ON FILE SSE-LOCA-SRVD.mcom

*** NOTE *** CP = 3085.422 TIME= 13:21:01

Solution is done!

ANSYS RELEASE 10.0 UP20050718 13:20:49 09/07/2009

NUMBER OF FREQUENCIES IN TABLE = 4

NUMBER OF FREQUENCIES IN TABLE = 8

NUMBER OF FREQUENCIES IN TABLE = 12

NUMBER OF FREQUENCIES IN TABLE = 16

NUMBER OF FREQUENCIES IN TABLE = 20

NUMBER OF ENTRIES IN RESPONSE SPECTRUM TABLE = 20

PRINTOUT RESUMED BY /GOP

Load step file number 3. Begin solution ...

***** ANSYS SOLVE COMMAND *****

LOAD STEP OPTIONS

LOAD STEP NUMBER..... 3

SPECTRUM LOADING TYPE.....ACCELERATION

EXCITATION DIRECTION..... 0.0000 0.0000 1.0000

MODE COMBINATION TYPE.....GRP

RESPONSE TYPE.....DISPLACEMENT

SIGNIFICANCE LEVEL FOR COMBINATIONS.....0.10000E-02

PRINT OUTPUT CONTROLS

ITEM FREQUENCY COMPONENT

ALL NONE

NSOL ALL

DATABASE OUTPUT CONTROLS.....ALL DATA WRITTEN

1

***** ANSYS - ENGINEERING ANALYSIS SYSTEM RELEASE 10.0 *****

ANSYS Multiphysics

00265621 VERSION=INTEL NT 13:21:02 SEP 07, 2009 CP= 3086.672

***** RESPONSE SPECTRUM CALCULATION SUMMARY *****

CUMULATIVE

MODE	FREQUENCY	SV	PARTIC.FACTOR	MODE COEF.	M.C. RATIO	EFFECTIVE MASS	MASS FRACTION
1	13.79 16.010	0.2836E-06	0.6052E-09	0.000000	0.804497E-13	0.150537E-17	
2	16.69 16.010	-0.1546E-05	-0.2250E-08	0.000000	0.239075E-11	0.462408E-16	
3	17.53 16.010	-0.2216E-05	-0.2925E-08	0.000000	0.491026E-11	0.138121E-15	
4	30.17 16.010	-0.8185E-06	-0.3647E-09	0.000000	0.669873E-12	0.150656E-15	
5	31.99 16.010	-0.2986E-05	-0.1183E-08	0.000000	0.891419E-11	0.317457E-15	
6	34.31 16.010	0.3763E-05	0.1296E-08	0.000000	0.141633E-10	0.582478E-15	
7	35.74 16.010	0.7225E-05	0.2294E-08	0.000000	0.522013E-10	0.155926E-14	
8	38.57 15.578	-0.1172E-04	-0.3108E-08	0.000000	0.137283E-09	0.412808E-14	

NEDO-33373-A, Revision 5

9	39.42	15.578	-0.2143E-05	-0.5440E-09	0.000000	0.459138E-11	0.421400E-14
10	43.44	15.578	0.3038E-04	0.6353E-08	0.000000	0.923098E-09	0.214869E-13
11	43.46	15.578	0.1902E-07	0.3972E-11	0.000000	0.361581E-15	0.214869E-13
12	44.08	15.578	-213.7	-0.4340E-01	1.000000	45683.6	0.854826
13	48.22	15.578	-0.8573E-04	-0.1455E-07	0.000000	0.735039E-08	0.854826
14	49.09	15.578	0.1067E-03	0.1746E-07	0.000000	0.113746E-07	0.854826
15	53.20	14.725	-0.2352E-04	-0.3099E-08	0.000000	0.553088E-09	0.854826
16	53.88	14.725	-0.2355E-04	-0.3026E-08	0.000000	0.554727E-09	0.854826
17	54.15	14.725	0.7421E-06	0.9441E-10	0.000000	0.550758E-12	0.854826
18	56.50	14.328	-0.2034E-04	-0.2312E-08	0.000000	0.413632E-09	0.854826
19	60.15	13.045	-0.5155E-04	-0.4708E-08	0.000000	0.265777E-08	0.854826
20	62.62	12.143	-0.5182E-04	-0.4065E-08	0.000000	0.268518E-08	0.854826
21	66.52	11.319	-0.7326E-04	-0.4747E-08	0.000000	0.536661E-08	0.854826
22	70.01	10.811	-0.6240E-04	-0.3486E-08	0.000000	0.389347E-08	0.854826
23	72.36	10.497	-0.9103E-04	-0.4622E-08	0.000000	0.828641E-08	0.854826
24	76.34	10.003	0.2418E-03	0.1052E-07	0.000000	0.584894E-07	0.854826
25	77.98	9.8206	0.2635E-03	0.1078E-07	0.000000	0.694436E-07	0.854826
26	78.47	9.7697	-0.3035E-03	-0.1220E-07	0.000000	0.921045E-07	0.854826
27	80.08	9.6080	-15.41	-0.5851E-03	0.013481	237.614	0.859272
28	82.34	9.3952	-0.5916E-03	-0.2077E-07	0.000000	0.349993E-06	0.859272
29	83.23	9.3425	-0.4227E-03	-0.1444E-07	0.000000	0.178702E-06	0.859272
30	84.75	9.2553	0.9059E-06	0.2957E-10	0.000000	0.820657E-12	0.859272
31	87.19	9.1366	0.4999E-05	0.1522E-09	0.000000	0.249852E-10	0.859272
32	87.58	9.1201	0.6404E-06	0.1929E-10	0.000000	0.410170E-12	0.859272
33	89.82	9.0256	0.3591E-04	0.1018E-08	0.000000	0.128949E-08	0.859272
34	90.26	9.0075	0.4327E-04	0.1212E-08	0.000000	0.187225E-08	0.859272
35	96.62	8.7574	-0.3609E-04	-0.8577E-09	0.000000	0.130247E-08	0.859272
36	97.41	8.7273	-78.24	-0.1823E-02	0.042000	6121.37	0.973815

NEDO-33373-A, Revision 5

37	98.21	8.6973	0.2160E-04	0.4933E-09	0.000000	0.466418E-09	0.973815
38	108.9	8.6315	-0.8185E-03	-0.1510E-07	0.000000	0.669925E-06	0.973815
39	117.1	8.6315	0.7377E-03	0.1175E-07	0.000000	0.544222E-06	0.973815
40	119.6	8.6315	-0.3212E-03	-0.4912E-08	0.000000	0.103153E-06	0.973815
41	120.2	8.6315	29.47	0.4460E-03	0.010276	868.331	0.990063
42	122.6	8.6315	0.1033E-02	0.1503E-07	0.000000	0.106743E-05	0.990063
43	123.9	8.6315	-0.3690E-03	-0.5259E-08	0.000000	0.136155E-06	0.990063
44	125.3	8.6315	0.6761E-03	0.9414E-08	0.000000	0.457139E-06	0.990063
45	126.5	8.6315	-0.6724E-04	-0.9182E-09	0.000000	0.452126E-08	0.990063
46	128.2	8.6315	-0.2516E-04	-0.3348E-09	0.000000	0.632973E-09	0.990063
47	131.1	8.6315	0.2863E-03	0.3642E-08	0.000000	0.819768E-07	0.990063
48	131.8	8.6315	-0.2508E-02	-0.3156E-07	0.000001	0.628908E-05	0.990063
49	134.8	8.6315	0.1238E-04	0.1491E-09	0.000000	0.153328E-09	0.990063
50	135.1	8.6315	0.1070E-02	0.1282E-07	0.000000	0.114548E-05	0.990063
51	135.3	8.6315	0.2504E-02	0.2990E-07	0.000001	0.627236E-05	0.990063
52	136.3	8.6315	0.6282E-03	0.7396E-08	0.000000	0.394696E-06	0.990063
53	138.7	8.6315	-0.1239E-03	-0.1408E-08	0.000000	0.153557E-07	0.990063
54	139.5	8.6315	-0.6636E-04	-0.7460E-09	0.000000	0.440429E-08	0.990063
55	142.5	8.6315	0.8709E-03	0.9375E-08	0.000000	0.758415E-06	0.990063
56	143.3	8.6315	-0.7757E-03	-0.8254E-08	0.000000	0.601636E-06	0.990063
57	144.7	8.6315	2.664	0.2783E-04	0.000641	7.09427	0.990196
58	146.9	8.6315	-0.1879E-02	-0.1904E-07	0.000000	0.353094E-05	0.990196
59	149.2	8.6315	-0.3044E-03	-0.2991E-08	0.000000	0.926304E-07	0.990196
60	149.7	8.6315	8.256	0.8057E-04	0.001856	68.1574	0.991471
61	149.7	8.6315	0.4787E-03	0.4672E-08	0.000000	0.229183E-06	0.991471
62	150.2	8.6315	0.2463E-03	0.2388E-08	0.000000	0.606483E-07	0.991471
63	150.9	8.6315	-0.1925E-03	-0.1848E-08	0.000000	0.370396E-07	0.991471
64	151.7	8.6315	-4.202	-0.3991E-04	0.000920	17.6547	0.991801

NEDO-33373-A, Revision 5

65	152.5	8.6315	2.129	0.2002E-04	0.000461	4.53183	0.991886
66	154.3	8.6315	-0.1221E-02	-0.1122E-07	0.000000	0.149137E-05	0.991886
67	155.2	8.6315	15.63	0.1420E-03	0.003272	244.432	0.996460
68	156.2	8.6315	0.1580E-03	0.1415E-08	0.000000	0.249610E-07	0.996460
69	156.6	8.6315	2.553	0.2278E-04	0.000525	6.51883	0.996582
70	156.9	8.6315	0.8242E-03	0.7324E-08	0.000000	0.679318E-06	0.996582
71	157.9	8.6315	0.2134E-02	0.1871E-07	0.000000	0.455457E-05	0.996582
72	159.1	8.6315	0.6478E-03	0.5597E-08	0.000000	0.419606E-06	0.996582
73	161.0	8.6315	0.5900	0.4975E-05	0.000115	0.348091	0.996588
74	161.4	8.6315	-0.8928E-03	-0.7492E-08	0.000000	0.797012E-06	0.996588
75	161.8	8.6315	-0.5393E-01	-0.4504E-06	0.000010	0.290822E-02	0.996588
76	163.8	8.6315	0.4196E-02	0.3418E-07	0.000001	0.176062E-04	0.996588
77	164.1	8.6315	0.3219E-02	0.2613E-07	0.000001	0.103613E-04	0.996588
78	165.7	8.6315	0.4496E-02	0.3581E-07	0.000001	0.202141E-04	0.996588
79	165.7	8.6315	-0.1536E-02	-0.1224E-07	0.000000	0.236080E-05	0.996588
80	166.1	8.6315	0.3660E-02	0.2899E-07	0.000001	0.133971E-04	0.996588
81	168.8	8.6315	0.6594E-01	0.5059E-06	0.000012	0.434764E-02	0.996588
82	170.3	8.6315	0.1061E-02	0.8003E-08	0.000000	0.112676E-05	0.996588
83	170.5	8.6315	-0.5500E-03	-0.4136E-08	0.000000	0.302477E-06	0.996588
84	171.3	8.6315	-0.1891E-03	-0.1409E-08	0.000000	0.357626E-07	0.996588
85	171.5	8.6315	0.1938E-03	0.1441E-08	0.000000	0.375394E-07	0.996588
86	172.1	8.6315	-0.2198	-0.1622E-05	0.000037	0.483034E-01	0.996589
87	172.5	8.6315	0.3272E-03	0.2404E-08	0.000000	0.107056E-06	0.996589
88	173.8	8.6315	0.2800E-03	0.2027E-08	0.000000	0.783932E-07	0.996589
89	175.6	8.6315	-1.109	-0.7869E-05	0.000181	1.23079	0.996612
90	176.1	8.6315	-0.4358E-04	-0.3073E-09	0.000000	0.189950E-08	0.996612
91	176.9	8.6315	12.83	0.8962E-04	0.002065	164.589	0.999692
92	177.5	8.6315	0.3411E-03	0.2367E-08	0.000000	0.116356E-06	0.999692

NEDO-33373-A, Revision 5

93	178.0	8.6315	0.5346E-03	0.3688E-08	0.000000	0.285836E-06	0.999692
94	179.5	8.6315	-0.6347	-0.4308E-05	0.000099	0.402867	0.999700
95	181.3	8.6315	-0.6609E-03	-0.4394E-08	0.000000	0.436784E-06	0.999700
96	182.8	8.6315	-0.2594E-02	-0.1697E-07	0.000000	0.672949E-05	0.999700
97	182.9	8.6315	0.2002	0.1309E-05	0.000030	0.400833E-01	0.999700
98	183.1	8.6315	-0.5805E-02	-0.3788E-07	0.000001	0.336979E-04	0.999700
99	183.9	8.6315	-0.7732E-02	-0.4997E-07	0.000001	0.597878E-04	0.999700
100	185.4	8.6315	4.001	0.2544E-04	0.000586	16.0105	1.00000

SUM OF EFFECTIVE MASSES= 53442.0

1

***** ANSYS - ENGINEERING ANALYSIS SYSTEM RELEASE 10.0 *****

ANSYS Multiphysics

00265621 VERSION=INTEL NT 13:21:02 SEP 07, 2009 CP= 3086.672

SIGNIFICANCE FACTOR FOR COMBINING MODES = 0.10000E-02

SIGNIFICANT MODE COEFFICIENTS (INCLUDING DAMPING)

MODE	FREQUENCY	DAMPING	SV	MODE COEF.
12	44.08	0.0000	15.578	-0.4340E-01
27	80.08	0.0000	9.6080	-0.5851E-03
36	97.41	0.0000	8.7273	-0.1823E-02
41	120.2	0.0000	8.6315	0.4460E-03
60	149.7	0.0000	8.6315	0.8057E-04
67	155.2	0.0000	8.6315	0.1420E-03
91	176.9	0.0000	8.6315	0.8962E-04

MODAL COMBINATION COEFFICIENTS

MODE= 12 FREQUENCY= 44.083 COUPLING COEF.= 1.000

MODE= 27 FREQUENCY= 80.076 COUPLING COEF.= 1.000

MODE= 36 FREQUENCY= 97.410 COUPLING COEF.= 1.000

MODE= 41 FREQUENCY= 120.191 COUPLING COEF.= 1.000
FREQUENCY 149.68 HERTZ PART OF CLOSELY SPACED GROUP 1
FREQUENCY 155.16 HERTZ PART OF CLOSELY SPACED GROUP 1
MODE= 91 FREQUENCY= 176.912 COUPLING COEF.= 1.000

GROUPING COMBINATION INSTRUCTIONS WRITTEN ON FILE SSE-LOCA-SRVD.mcom

*** NOTE *** CP = 3086.672 TIME= 13:21:02

Solution is done!

ANSYS RELEASE 10.0 UP20050718 13:20:49 09/07/2009

NUMBER OF FREQUENCIES IN TABLE = 4

NUMBER OF FREQUENCIES IN TABLE = 8

NUMBER OF FREQUENCIES IN TABLE = 9

PRINTOUT RESUMED BY /GOP

Load step file number 4. Begin solution ...

***** ANSYS SOLVE COMMAND *****

LOAD STEP OPTIONS

LOAD STEP NUMBER..... 4
SPECTRUM LOADING TYPE.....ACCELERATION
EXCITATION DIRECTION..... 1.0000 0.0000 0.0000
MODE COMBINATION TYPE.....GRP
RESPONSE TYPE.....DISPLACEMENT
SIGNIFICANCE LEVEL FOR COMBINATIONS.... 0.10000E-02

PRINT OUTPUT CONTROLS

ITEM FREQUENCY COMPONENT
ALL NONE
NSOL ALL

DATABASE OUTPUT CONTROLS.....ALL DATA WRITTEN

1

***** ANSYS - ENGINEERING ANALYSIS SYSTEM RELEASE 10.0 *****

ANSYS Multiphysics

00265621 VERSION=INTEL NT 13:21:04 SEP 07, 2009 CP= 3087.891

***** RESPONSE SPECTRUM CALCULATION SUMMARY *****

CUMULATIVE								
MODE	FREQUENCY	SV	PARTIC.FACTOR	MODE COEF.	M.C. RATIO	EFFECTIVE MASS	MASS FRACTION	
1	13.79	0.88290	0.1725E-05	0.2030E-09	0.000000	0.297690E-11	0.397373E-16	
2	16.69	0.78480	219.4	0.1565E-01	1.000000	48143.7	0.642650	
3	17.53	0.78480	-0.9107E-06	-0.5893E-10	0.000000	0.829354E-12	0.642650	
4	30.17	1.0593	-0.5842E-06	-0.1723E-10	0.000000	0.341317E-12	0.642650	
5	31.99	0.87107	-0.3978E-06	-0.8580E-11	0.000000	0.158270E-12	0.642650	
6	34.31	0.78189	7.927	0.1333E-03	0.008519	62.8308	0.643489	
7	35.74	0.77887	0.9065E-05	0.1400E-09	0.000000	0.821820E-10	0.643489	
8	38.57	0.77325	-0.5012E-05	-0.6599E-10	0.000000	0.251193E-10	0.643489	
9	39.42	0.77165	-0.4961E-05	-0.6239E-10	0.000000	0.246122E-10	0.643489	
10	43.44	0.76456	0.5046E-04	0.5178E-09	0.000000	0.254589E-08	0.643489	
11	43.46	0.76453	-0.7074	-0.7252E-05	0.000463	0.500411	0.643495	
12	44.08	0.76350	-0.1555E-04	-0.1548E-09	0.000000	0.241919E-09	0.643495	
13	48.22	0.75702	-0.3713E-04	-0.3062E-09	0.000000	0.137853E-08	0.643495	
14	49.09	0.75573	0.3384E-04	0.2688E-09	0.000000	0.114534E-08	0.643495	
15	53.20	0.74998	0.2725E-04	0.1829E-09	0.000000	0.742710E-09	0.643495	
16	53.88	0.74907	0.6110E-05	0.3993E-10	0.000000	0.373263E-10	0.643495	
17	54.15	0.74872	136.5	0.8827E-03	0.056399	18620.8	0.892056	

NEDO-33373-A, Revision 5

18	56.50	0.74570	80.75	0.4777E-03	0.030524	6520.80	0.979100
19	60.15	0.74127	0.1814E-04	0.9411E-10	0.000000	0.328926E-09	0.979100
20	62.62	0.73845	0.4728E-04	0.2255E-09	0.000000	0.223505E-08	0.979100
21	66.52	0.73422	-0.2101E-04	-0.8832E-10	0.000000	0.441607E-09	0.979100
22	70.01	0.73066	21.69	0.8189E-04	0.005232	470.323	0.985378
23	72.36	0.72837	0.1025E-03	0.3612E-09	0.000000	0.105084E-07	0.985378
24	76.34	0.72468	0.1587E-03	0.4999E-09	0.000000	0.251917E-07	0.985378
25	77.98	0.72322	-21.55	-0.6494E-04	0.004149	464.515	0.991578
26	78.47	0.72278	-0.1720E-03	-0.5116E-09	0.000000	0.296005E-07	0.991578
27	80.08	0.72139	-0.4539E-03	-0.1294E-08	0.000000	0.206033E-06	0.991578
28	82.34	0.71949	-3.554	-0.9554E-05	0.000610	12.6309	0.991747
29	83.23	0.71875	0.8322E-03	0.2187E-08	0.000000	0.692583E-06	0.991747
30	84.75	0.71752	0.8763E-05	0.2217E-10	0.000000	0.767864E-10	0.991747
31	87.19	0.71558	-0.1913E-06	-0.4562E-12	0.000000	0.366061E-13	0.991747
32	87.58	0.71528	-12.60	-0.2977E-04	0.001902	158.834	0.993867
33	89.82	0.71356	-0.4399E-04	-0.9856E-10	0.000000	0.193537E-08	0.993867
34	90.26	0.71323	-0.5749E-04	-0.1275E-09	0.000000	0.330534E-08	0.993867
35	96.62	0.70864	0.7549E-04	0.1452E-09	0.000000	0.569897E-08	0.993867
36	97.41	0.70808	0.1952E-04	0.3689E-10	0.000000	0.380909E-09	0.993867
37	98.21	0.70753	-0.3908E-04	-0.7262E-10	0.000000	0.152729E-08	0.993867
38	108.9	0.70632	-0.2244E-03	-0.3387E-09	0.000000	0.503506E-07	0.993867
39	117.1	0.70632	-0.3889E-03	-0.5070E-09	0.000000	0.151257E-06	0.993867
40	119.6	0.70632	-19.90	-0.2490E-04	0.001591	395.909	0.999152
41	120.2	0.70632	-0.7125E-03	-0.8824E-09	0.000000	0.507672E-06	0.999152
42	122.6	0.70632	0.3596	0.4282E-06	0.000027	0.129343	0.999154
43	123.9	0.70632	-0.3978E-03	-0.4639E-09	0.000000	0.158230E-06	0.999154
44	125.3	0.70632	-0.7098E-03	-0.8086E-09	0.000000	0.503750E-06	0.999154
45	126.5	0.70632	-0.4841E-03	-0.5410E-09	0.000000	0.234391E-06	0.999154

NEDO-33373-A, Revision 5

46	128.2	0.70632	-0.8334E-03	-0.9076E-09	0.000000	0.694472E-06	0.999154
47	131.1	0.70632	-0.2352E-02	-0.2449E-08	0.000000	0.553390E-05	0.999154
48	131.8	0.70632	-2.307	-0.2376E-05	0.000152	5.32450	0.999225
49	134.8	0.70632	0.2199E-02	0.2167E-08	0.000000	0.483627E-05	0.999225
50	135.1	0.70632	0.3035E-03	0.2975E-09	0.000000	0.921184E-07	0.999225
51	135.3	0.70632	0.7600	0.7424E-06	0.000047	0.577631	0.999233
52	136.3	0.70632	-0.4467E-03	-0.4303E-09	0.000000	0.199531E-06	0.999233
53	138.7	0.70632	-0.1480E-03	-0.1376E-09	0.000000	0.219087E-07	0.999233
54	139.5	0.70632	4.897	0.4505E-05	0.000288	23.9847	0.999553
55	142.5	0.70632	-2.082	-0.1834E-05	0.000117	4.33545	0.999611
56	143.3	0.70632	-0.2801E-03	-0.2439E-09	0.000000	0.784399E-07	0.999611
57	144.7	0.70632	-0.1746E-03	-0.1493E-09	0.000000	0.304935E-07	0.999611
58	146.9	0.70632	-0.1070E-02	-0.8874E-09	0.000000	0.114512E-05	0.999611
59	149.2	0.70632	0.9068E-04	0.7292E-10	0.000000	0.822253E-08	0.999611
60	149.7	0.70632	-0.1620E-03	-0.1294E-09	0.000000	0.262449E-07	0.999611
61	149.7	0.70632	-0.8696E-03	-0.6944E-09	0.000000	0.756279E-06	0.999611
62	150.2	0.70632	0.1666E-03	0.1322E-09	0.000000	0.277421E-07	0.999611
63	150.9	0.70632	0.2350E-04	0.1846E-10	0.000000	0.552019E-09	0.999611
64	151.7	0.70632	-0.9457E-03	-0.7351E-09	0.000000	0.894351E-06	0.999611
65	152.5	0.70632	-0.5051E-03	-0.3887E-09	0.000000	0.255079E-06	0.999611
66	154.3	0.70632	-0.6471E-03	-0.4866E-09	0.000000	0.418760E-06	0.999611
67	155.2	0.70632	-0.9259E-03	-0.6881E-09	0.000000	0.857345E-06	0.999611
68	156.2	0.70632	0.4408E-03	0.3232E-09	0.000000	0.194340E-06	0.999611
69	156.6	0.70632	-0.9395E-04	-0.6858E-10	0.000000	0.882724E-08	0.999611
70	156.9	0.70632	0.6425E-03	0.4672E-09	0.000000	0.412826E-06	0.999611
71	157.9	0.70632	-1.691	-0.1213E-05	0.000078	2.86034	0.999649
72	159.1	0.70632	-0.4040E-03	-0.2856E-09	0.000000	0.163225E-06	0.999649
73	161.0	0.70632	0.8683E-03	0.5991E-09	0.000000	0.753904E-06	0.999649

NEDO-33373-A, Revision 5

74	161.4	0.70632	4.968	0.3412E-05	0.000218	24.6805	0.999978
75	161.8	0.70632	-0.9736E-03	-0.6653E-09	0.000000	0.947827E-06	0.999978
76	163.8	0.70632	-0.3201E-02	-0.2134E-08	0.000000	0.102482E-04	0.999978
77	164.1	0.70632	-0.2729E-02	-0.1813E-08	0.000000	0.744695E-05	0.999978
78	165.7	0.70632	0.1348E-02	0.8789E-09	0.000000	0.181828E-05	0.999978
79	165.7	0.70632	-0.2188E-02	-0.1426E-08	0.000000	0.478766E-05	0.999978
80	166.1	0.70632	-0.6071	-0.3935E-06	0.000025	0.368601	0.999983
81	168.8	0.70632	0.1407E-02	0.8832E-09	0.000000	0.197874E-05	0.999983
82	170.3	0.70632	0.3513E-03	0.2168E-09	0.000000	0.123441E-06	0.999983
83	170.5	0.70632	-0.2020E-01	-0.1243E-07	0.000001	0.407840E-03	0.999983
84	171.3	0.70632	-1.117	-0.6816E-06	0.000044	1.24880	1.00000
85	171.5	0.70632	-0.3164E-03	-0.1925E-09	0.000000	0.100080E-06	1.00000
86	172.1	0.70632	0.3084E-03	0.1863E-09	0.000000	0.951294E-07	1.00000
87	172.5	0.70632	0.6107E-04	0.3672E-10	0.000000	0.372914E-08	1.00000
88	173.8	0.70632	0.7255E-01	0.4298E-07	0.000003	0.526391E-02	1.00000
89	175.6	0.70632	-0.1656E-04	-0.9612E-11	0.000000	0.274283E-09	1.00000
90	176.1	0.70632	0.6936E-03	0.4001E-09	0.000000	0.481084E-06	1.00000
91	176.9	0.70632	-0.3791E-03	-0.2167E-09	0.000000	0.143702E-06	1.00000
92	177.5	0.70632	0.2093E-01	0.1189E-07	0.000001	0.438182E-03	1.00000
93	178.0	0.70632	-0.6705E-03	-0.3785E-09	0.000000	0.449583E-06	1.00000
94	179.5	0.70632	0.6013E-04	0.3339E-10	0.000000	0.361511E-08	1.00000
95	181.3	0.70632	0.6589E-01	0.3585E-07	0.000002	0.434129E-02	1.00000
96	182.8	0.70632	0.2478E-02	0.1326E-08	0.000000	0.613851E-05	1.00000
97	182.9	0.70632	-0.5735E-03	-0.3067E-09	0.000000	0.328912E-06	1.00000
98	183.1	0.70632	0.3353E-01	0.1790E-07	0.000001	0.112444E-02	1.00000
99	183.9	0.70632	0.4072E-01	0.2153E-07	0.000001	0.165794E-02	1.00000
100	185.4	0.70632	-0.7418E-03	-0.3860E-09	0.000000	0.550325E-06	1.00000

SUM OF EFFECTIVE MASSES= 74914.4

1

***** ANSYS - ENGINEERING ANALYSIS SYSTEM RELEASE 10.0 *****

ANSYS Multiphysics

00265621 VERSION=INTEL NT 13:21:04 SEP 07, 2009 CP= 3087.891

SIGNIFICANCE FACTOR FOR COMBINING MODES = 0.10000E-02

SIGNIFICANT MODE COEFFICIENTS (INCLUDING DAMPING)

MODE	FREQUENCY	DAMPING	SV	MODE COEF.
2	16.69	0.0000 0.78480	0.1565E-01	
6	34.31	0.0000 0.78189	0.1333E-03	
17	54.15	0.0000 0.74872	0.8827E-03	
18	56.50	0.0000 0.74570	0.4777E-03	
22	70.01	0.0000 0.73066	0.8189E-04	
25	77.98	0.0000 0.72322	-0.6494E-04	
32	87.58	0.0000 0.71528	-0.2977E-04	
40	119.6	0.0000 0.70632	-0.2490E-04	

MODAL COMBINATION COEFFICIENTS

MODE= 2 FREQUENCY= 16.694 COUPLING COEF.= 1.000

MODE= 6 FREQUENCY= 34.314 COUPLING COEF.= 1.000

FREQUENCY 54.147 HERTZ PART OF CLOSELY SPACED GROUP 1

FREQUENCY 56.504 HERTZ PART OF CLOSELY SPACED GROUP 1

MODE= 22 FREQUENCY= 70.010 COUPLING COEF.= 1.000

MODE= 25 FREQUENCY= 77.976 COUPLING COEF.= 1.000

MODE= 32 FREQUENCY= 87.575 COUPLING COEF.= 1.000

MODE= 40 FREQUENCY= 119.561 COUPLING COEF.= 1.000

GROUPING COMBINATION INSTRUCTIONS WRITTEN ON FILE SSE-LOCA-SRVD.mcom

*** NOTE *** CP = 3087.906 TIME= 13:21:04

Solution is done!

ANSYS RELEASE 10.0 UP20050718 13:20:49 09/07/2009

NUMBER OF FREQUENCIES IN TABLE = 4

NUMBER OF FREQUENCIES IN TABLE = 8

NUMBER OF FREQUENCIES IN TABLE = 9

PRINTOUT RESUMED BY /GOP

Load step file number 5. Begin solution ...

***** ANSYS SOLVE COMMAND *****

LOAD STEP OPTIONS

LOAD STEP NUMBER..... 5

SPECTRUM LOADING TYPE.....ACCELERATION

EXCITATION DIRECTION..... 0.0000 1.0000 0.0000

MODE COMBINATION TYPE.....GRP

RESPONSE TYPE.....DISPLACEMENT

SIGNIFICANCE LEVEL FOR COMBINATIONS..... 0.10000E-02

PRINT OUTPUT CONTROLS

ITEM FREQUENCY COMPONENT

ALL NONE

NSOL ALL

DATABASE OUTPUT CONTROLS.....ALL DATA WRITTEN

!

***** ANSYS - ENGINEERING ANALYSIS SYSTEM RELEASE 10.0 *****

ANSYS Multiphysics

00265621 VERSION=INTEL NT 13:21:05 SEP 07, 2009 CP= 3089.109

***** RESPONSE SPECTRUM CALCULATION SUMMARY *****

CUMULATIVE

MODE	FREQUENCY	SV	PARTIC.FACTOR	MODE COEF.	M.C. RATIO	EFFECTIVE MASS	MASS FRACTION
1	13.79	0.88290	216.1	0.2542E-01	1.000000	46688.0	0.626446
2	16.69	0.78480	0.2075E-06	0.1480E-10	0.000000	0.430422E-13	0.626446
3	17.53	0.78480	-0.5288E-06	-0.3422E-10	0.000000	0.279620E-12	0.626446
4	30.17	1.0593	0.1043E-05	0.3075E-10	0.000000	0.108733E-11	0.626446
5	31.99	0.87107	-2.989	-0.6446E-04	0.002535	8.93272	0.626565
6	34.31	0.78189	0.2088E-06	0.3513E-11	0.000000	0.436061E-13	0.626565
7	35.74	0.77887	0.1776E-06	0.2743E-11	0.000000	0.315452E-13	0.626565
8	38.57	0.77325	-0.2891E-04	-0.3806E-09	0.000000	0.835606E-09	0.626565
9	39.42	0.77165	5.439	0.6840E-04	0.002691	29.5846	0.626962
10	43.44	0.76456	0.3730E-04	0.3828E-09	0.000000	0.139156E-08	0.626962
11	43.46	0.76453	0.2195E-05	0.2250E-10	0.000000	0.481826E-11	0.626962
12	44.08	0.76350	0.7629E-05	0.7592E-10	0.000000	0.582038E-10	0.626962
13	48.22	0.75702	-32.35	-0.2668E-03	0.010494	1046.61	0.641005
14	49.09	0.75573	0.1683E-03	0.1337E-08	0.000000	0.283377E-07	0.641005
15	53.20	0.74998	155.0	0.1040E-02	0.040914	24015.1	0.963233
16	53.88	0.74907	0.5050E-05	0.3301E-10	0.000000	0.255048E-10	0.963233
17	54.15	0.74872	-0.9425E-05	-0.6097E-10	0.000000	0.888384E-10	0.963233
18	56.50	0.74570	-0.6047E-05	-0.3577E-10	0.000000	0.365613E-10	0.963233
19	60.15	0.74127	36.01	0.1869E-03	0.007351	1297.05	0.980637
20	62.62	0.73845	-0.2556E-04	-0.1219E-09	0.000000	0.653081E-09	0.980637
21	66.52	0.73422	-0.1050E-03	-0.4415E-09	0.000000	0.110329E-07	0.980637
22	70.01	0.73066	0.1390E-03	0.5249E-09	0.000000	0.193248E-07	0.980637
23	72.36	0.72837	-16.45	-0.5798E-04	0.002280	270.761	0.984270

NEDO-33373-A, Revision 5

24	76.34	0.72468	-0.2922E-03	-0.9204E-09	0.000000	0.853894E-07	0.984270
25	77.98	0.72322	0.7648E-03	0.2304E-08	0.000000	0.584977E-06	0.984270
26	78.47	0.72278	-0.3536E-03	-0.1051E-08	0.000000	0.125031E-06	0.984270
27	80.08	0.72139	0.1096E-02	0.3123E-08	0.000000	0.120136E-05	0.984270
28	82.34	0.71949	0.1133E-02	0.3046E-08	0.000000	0.128397E-05	0.984270
29	83.23	0.71875	-11.12	-0.2922E-04	0.001149	123.641	0.985929
30	84.75	0.71752	-0.1751E-04	-0.4431E-10	0.000000	0.306546E-09	0.985929
31	87.19	0.71558	0.7519E-05	0.1793E-10	0.000000	0.565308E-10	0.985929
32	87.58	0.71528	0.7858E-05	0.1856E-10	0.000000	0.617535E-10	0.985929
33	89.82	0.71356	10.15	0.2275E-04	0.000895	103.083	0.987312
34	90.26	0.71323	0.1697E-04	0.3764E-10	0.000000	0.288060E-09	0.987312
35	96.62	0.70864	-17.46	-0.3358E-04	0.001321	304.977	0.991404
36	97.41	0.70808	0.1752E-04	0.3312E-10	0.000000	0.307020E-09	0.991404
37	98.21	0.70753	0.7632E-04	0.1418E-09	0.000000	0.582449E-08	0.991404
38	108.9	0.70632	0.5956E-03	0.8991E-09	0.000000	0.354744E-06	0.991404
39	117.1	0.70632	-19.73	-0.2572E-04	0.001012	389.301	0.996627
40	119.6	0.70632	0.1308E-02	0.1637E-08	0.000000	0.171090E-05	0.996627
41	120.2	0.70632	0.3341E-03	0.4138E-09	0.000000	0.111631E-06	0.996627
42	122.6	0.70632	0.4968E-02	0.5914E-08	0.000000	0.246813E-04	0.996627
43	123.9	0.70632	0.1371E-03	0.1599E-09	0.000000	0.188084E-07	0.996627
44	125.3	0.70632	11.16	0.1271E-04	0.000500	124.546	0.998299
45	126.5	0.70632	0.2861E-02	0.3197E-08	0.000000	0.818435E-05	0.998299
46	128.2	0.70632	-0.4767E-03	-0.5192E-09	0.000000	0.227247E-06	0.998299
47	131.1	0.70632	-3.294	-0.3429E-05	0.000135	10.8519	0.998444
48	131.8	0.70632	-0.7363E-02	-0.7581E-08	0.000000	0.542152E-04	0.998444
49	134.8	0.70632	0.1274E-01	0.1256E-07	0.000000	0.162416E-03	0.998444
50	135.1	0.70632	4.518	0.4428E-05	0.000174	20.4118	0.998718
51	135.3	0.70632	-0.2280E-02	-0.2227E-08	0.000000	0.519624E-05	0.998718

NEDO-33373-A, Revision 5

52	136.3	0.70632	-0.8688E-02	-0.8369E-08	0.000000	0.754829E-04	0.998718
53	138.7	0.70632	-3.975	-0.3696E-05	0.000145	15.7999	0.998930
54	139.5	0.70632	0.1504E-03	0.1384E-09	0.000000	0.226333E-07	0.998930
55	142.5	0.70632	-0.4492E-03	-0.3957E-09	0.000000	0.201738E-06	0.998930
56	143.3	0.70632	0.7590E-03	0.6609E-09	0.000000	0.576050E-06	0.998930
57	144.7	0.70632	-0.8851E-04	-0.7567E-10	0.000000	0.783340E-08	0.998930
58	146.9	0.70632	0.1651E-02	0.1369E-08	0.000000	0.272509E-05	0.998930
59	149.2	0.70632	2.652	0.2133E-05	0.000084	7.03492	0.999024
60	149.7	0.70632	0.9355E-04	0.7471E-10	0.000000	0.875113E-08	0.999024
61	149.7	0.70632	0.1944E-02	0.1553E-08	0.000000	0.378065E-05	0.999024
62	150.2	0.70632	-3.031	-0.2405E-05	0.000095	9.18635	0.999148
63	150.9	0.70632	3.032	0.2382E-05	0.000094	9.19141	0.999271
64	151.7	0.70632	0.1140E-02	0.8858E-09	0.000000	0.129872E-05	0.999271
65	152.5	0.70632	-0.1795E-03	-0.1381E-09	0.000000	0.322075E-07	0.999271
66	154.3	0.70632	-0.3802	-0.2859E-06	0.000011	0.144563	0.999273
67	155.2	0.70632	-0.2288E-03	-0.1701E-09	0.000000	0.523632E-07	0.999273
68	156.2	0.70632	-0.2391E-02	-0.1753E-08	0.000000	0.571540E-05	0.999273
69	156.6	0.70632	0.2024E-03	0.1477E-09	0.000000	0.409557E-07	0.999273
70	156.9	0.70632	-0.1986E-02	-0.1444E-08	0.000000	0.394223E-05	0.999273
71	157.9	0.70632	-0.2728E-02	-0.1957E-08	0.000000	0.744016E-05	0.999273
72	159.1	0.70632	-0.9249E-02	-0.6539E-08	0.000000	0.855365E-04	0.999273
73	161.0	0.70632	-0.3898E-02	-0.2689E-08	0.000000	0.151910E-04	0.999273
74	161.4	0.70632	0.6081E-04	0.4176E-10	0.000000	0.369828E-08	0.999273
75	161.8	0.70632	0.1560E-02	0.1066E-08	0.000000	0.243418E-05	0.999273
76	163.8	0.70632	-3.659	-0.2439E-05	0.000096	13.3894	0.999453
77	164.1	0.70632	-2.594	-0.1723E-05	0.000068	6.72662	0.999543
78	165.7	0.70632	-0.4794E-02	-0.3124E-08	0.000000	0.229791E-04	0.999543
79	165.7	0.70632	0.5593E-02	0.3645E-08	0.000000	0.312851E-04	0.999543

NEDO-33373-A, Revision 5

80	166.1	0.70632	-0.1600E-01	-0.1037E-07	0.000000	0.256134E-03	0.999543
81	168.8	0.70632	-0.1198E-01	-0.7523E-08	0.000000	0.143587E-03	0.999543
82	170.3	0.70632	-0.4412E-02	-0.2722E-08	0.000000	0.194641E-04	0.999543
83	170.5	0.70632	0.2483E-03	0.1528E-09	0.000000	0.616576E-07	0.999543
84	171.3	0.70632	0.6195E-03	0.3778E-09	0.000000	0.383812E-06	0.999543
85	171.5	0.70632	-0.2289E-03	-0.1392E-09	0.000000	0.523807E-07	0.999543
86	172.1	0.70632	0.8577E-04	0.5179E-10	0.000000	0.735678E-08	0.999543
87	172.5	0.70632	-0.7136	-0.4291E-06	0.000017	0.509254	0.999550
88	173.8	0.70632	0.4457E-03	0.2641E-09	0.000000	0.198684E-06	0.999550
89	175.6	0.70632	0.1068E-02	0.6197E-09	0.000000	0.113995E-05	0.999550
90	176.1	0.70632	-0.2248E-02	-0.1297E-08	0.000000	0.505533E-05	0.999550
91	176.9	0.70632	0.2999E-02	0.1714E-08	0.000000	0.899407E-05	0.999550
92	177.5	0.70632	-0.5128E-02	-0.2911E-08	0.000000	0.262941E-04	0.999550
93	178.0	0.70632	-5.790	-0.3268E-05	0.000129	33.5223	0.999999
94	179.5	0.70632	-0.9784E-02	-0.5434E-08	0.000000	0.957260E-04	0.999999
95	181.3	0.70632	0.6490E-02	0.3531E-08	0.000000	0.421152E-04	0.999999
96	182.8	0.70632	0.1104E-01	0.5909E-08	0.000000	0.121796E-03	0.999999
97	182.9	0.70632	0.5059E-01	0.2706E-07	0.000001	0.255971E-02	0.999999
98	183.1	0.70632	0.2230E-01	0.1191E-07	0.000000	0.497341E-03	1.00000
99	183.9	0.70632	0.3464E-01	0.1832E-07	0.000001	0.120000E-02	1.00000
100	185.4	0.70632	0.1889	0.9829E-07	0.000004	0.356798E-01	1.00000

SUM OF EFFECTIVE MASSES= 74528.4

1

***** ANSYS - ENGINEERING ANALYSIS SYSTEM RELEASE 10.0 *****

ANSYS Multiphysics

00265621 VERSION=INTEL NT 13:21:05 SEP 07, 2009 CP= 3089.109

SIGNIFICANCE FACTOR FOR COMBINING MODES = 0.10000E-02

SIGNIFICANT MODE COEFFICIENTS (INCLUDING DAMPING)

MODE	FREQUENCY	DAMPING	SV	MODE COEF.
1	13.79	0.0000	0.88290	0.2542E-01
5	31.99	0.0000	0.87107	-0.6446E-04
9	39.42	0.0000	0.77165	0.6840E-04
13	48.22	0.0000	0.75702	-0.2668E-03
15	53.20	0.0000	0.74998	0.1040E-02
19	60.15	0.0000	0.74127	0.1869E-03
23	72.36	0.0000	0.72837	-0.5798E-04
29	83.23	0.0000	0.71875	-0.2922E-04
35	96.62	0.0000	0.70864	-0.3358E-04
39	117.1	0.0000	0.70632	-0.2572E-04

MODAL COMBINATION COEFFICIENTS

MODE= 1 FREQUENCY= 13.787 COUPLING COEF.= 1.000
MODE= 5 FREQUENCY= 31.986 COUPLING COEF.= 1.000
MODE= 9 FREQUENCY= 39.424 COUPLING COEF.= 1.000
MODE= 13 FREQUENCY= 48.220 COUPLING COEF.= 1.000
MODE= 15 FREQUENCY= 53.200 COUPLING COEF.= 1.000
MODE= 19 FREQUENCY= 60.155 COUPLING COEF.= 1.000
MODE= 23 FREQUENCY= 72.363 COUPLING COEF.= 1.000
MODE= 29 FREQUENCY= 83.232 COUPLING COEF.= 1.000
MODE= 35 FREQUENCY= 96.615 COUPLING COEF.= 1.000
MODE= 39 FREQUENCY= 117.149 COUPLING COEF.= 1.000

GROUPING COMBINATION INSTRUCTIONS WRITTEN ON FILE SSE-LOCA-SRVD.mcom

*** NOTE *** CP = 3089.125 TIME= 13:21:05

Solution is done!

ANSYS RELEASE 10.0 UP20050718 13:20:49 09/07/2009

NUMBER OF FREQUENCIES IN TABLE = 4

NUMBER OF FREQUENCIES IN TABLE = 8

PRINTOUT RESUMED BY /GOP

Load step file number 6. Begin solution ...

***** ANSYS SOLVE COMMAND *****

LOAD STEP OPTIONS

LOAD STEP NUMBER..... 6

SPECTRUM LOADING TYPEACCELERATION

EXCITATION DIRECTION..... 0.0000 0.0000 1.0000

MODE COMBINATION TYPE GRP

RESPONSE TYPEDISPLACEMENT

SIGNIFICANCE LEVEL FOR COMBINATIONS..... 0.10000E-02

PRINT OUTPUT CONTROLS

ITEM FREQUENCY COMPONENT

ALL NONE

NSOL ALL

DATABASE OUTPUT CONTROLS.....ALL DATA WRITTEN

1

***** ANSYS - ENGINEERING ANALYSIS SYSTEM RELEASE 10.0 *****

ANSYS Multiphysics

00265621 VERSION=INTEL NT 13:21:07 SEP 07, 2009 CP= 3090.344

***** RESPONSE SPECTRUM CALCULATION SUMMARY *****

CUMULATIVE

NEDO-33373-A, Revision 5

MODE	FREQUENCY	SV	PARTIC.FACTOR	MODE COEF.	M.C. RATIO	EFFECTIVE MASS	MASS FRACTION
1	13.79	2.3700	0.2836E-06	0.8958E-10	0.000000	0.804497E-13	0.150537E-17
2	16.69	1.8895	-0.1546E-05	-0.2655E-09	0.000000	0.239075E-11	0.462408E-16
3	17.53	1.7430	-0.2216E-05	-0.3185E-09	0.000000	0.491026E-11	0.138121E-15
4	30.17	1.5380	-0.8185E-06	-0.3504E-10	0.000000	0.669873E-12	0.150656E-15
5	31.99	1.5240	-0.2986E-05	-0.1127E-09	0.000000	0.891419E-11	0.317457E-15
6	34.31	1.5073	0.3763E-05	0.1220E-09	0.000000	0.141633E-10	0.582478E-15
7	35.74	1.4977	0.7225E-05	0.2146E-09	0.000000	0.522013E-10	0.155926E-14
8	38.57	1.4799	-0.1172E-04	-0.2953E-09	0.000000	0.137283E-09	0.412808E-14
9	39.42	1.4749	-0.2143E-05	-0.5150E-10	0.000000	0.459138E-11	0.421400E-14
10	43.44	1.4624	0.3038E-04	0.5963E-09	0.000000	0.923098E-09	0.214869E-13
11	43.46	1.4623	0.1902E-07	0.3729E-12	0.000000	0.361581E-15	0.214869E-13
12	44.08	1.4608	-213.7	-0.4070E-02	1.000000	45683.6	0.854826
13	48.22	1.4509	-0.8573E-04	-0.1355E-08	0.000000	0.735039E-08	0.854826
14	49.09	1.4490	0.1067E-03	0.1624E-08	0.000000	0.113746E-07	0.854826
15	53.20	1.4402	-0.2352E-04	-0.3031E-09	0.000000	0.553088E-09	0.854826
16	53.88	1.4389	-0.2355E-04	-0.2957E-09	0.000000	0.554727E-09	0.854826
17	54.15	1.4383	0.7421E-06	0.9222E-11	0.000000	0.550758E-12	0.854826
18	56.50	1.4337	-0.2034E-04	-0.2313E-09	0.000000	0.413632E-09	0.854826
19	60.15	1.4270	-0.5155E-04	-0.5150E-09	0.000000	0.265777E-08	0.854826
20	62.62	1.4227	-0.5182E-04	-0.4762E-09	0.000000	0.268518E-08	0.854826
21	66.52	1.4162	-0.7326E-04	-0.5939E-09	0.000000	0.536661E-08	0.854826
22	70.01	1.4108	-0.6240E-04	-0.4549E-09	0.000000	0.389347E-08	0.854826
23	72.36	1.4073	-0.9103E-04	-0.6197E-09	0.000000	0.828641E-08	0.854826
24	76.34	1.4016	0.2418E-03	0.1473E-08	0.000000	0.584894E-07	0.854826
25	77.98	1.3994	0.2635E-03	0.1536E-08	0.000000	0.694436E-07	0.854826
26	78.47	1.3987	-0.3035E-03	-0.1746E-08	0.000000	0.921045E-07	0.854826
27	80.08	1.3966	-15.41	-0.8504E-04	0.020897	237.614	0.859272

NEDO-33373-A, Revision 5

28	82.34	1.3936	-0.5916E-03	-0.3081E-08	0.000001	0.349993E-06	0.859272
29	83.23	1.3925	-0.4227E-03	-0.2152E-08	0.000001	0.178702E-06	0.859272
30	84.75	1.3906	0.9059E-06	0.4443E-11	0.000000	0.820657E-12	0.859272
31	87.19	1.3876	0.4999E-05	0.2311E-10	0.000000	0.249852E-10	0.859272
32	87.58	1.3872	0.6404E-06	0.2934E-11	0.000000	0.410170E-12	0.859272
33	89.82	1.3845	0.3591E-04	0.1561E-09	0.000000	0.128949E-08	0.859272
34	90.26	1.3840	0.4327E-04	0.1862E-09	0.000000	0.187225E-08	0.859272
35	96.62	1.3770	-0.3609E-04	-0.1349E-09	0.000000	0.130247E-08	0.859272
36	97.41	1.3761	-78.24	-0.2874E-03	0.070626	6121.37	0.973815
37	98.21	1.3753	0.2160E-04	0.7800E-10	0.000000	0.466418E-09	0.973815
38	108.9	1.3734	-0.8185E-03	-0.2402E-08	0.000001	0.669925E-06	0.973815
39	117.1	1.3734	0.7377E-03	0.1870E-08	0.000000	0.544222E-06	0.973815
40	119.6	1.3734	-0.3212E-03	-0.7816E-09	0.000000	0.103153E-06	0.973815
41	120.2	1.3734	29.47	0.7096E-04	0.017437	868.331	0.990063
42	122.6	1.3734	0.1033E-02	0.2392E-08	0.000001	0.106743E-05	0.990063
43	123.9	1.3734	-0.3690E-03	-0.8368E-09	0.000000	0.136155E-06	0.990063
44	125.3	1.3734	0.6761E-03	0.1498E-08	0.000000	0.457139E-06	0.990063
45	126.5	1.3734	-0.6724E-04	-0.1461E-09	0.000000	0.452126E-08	0.990063
46	128.2	1.3734	-0.2516E-04	-0.5328E-10	0.000000	0.632973E-09	0.990063
47	131.1	1.3734	0.2863E-03	0.5796E-09	0.000000	0.819768E-07	0.990063
48	131.8	1.3734	-0.2508E-02	-0.5021E-08	0.000001	0.628908E-05	0.990063
49	134.8	1.3734	0.1238E-04	0.2372E-10	0.000000	0.153328E-09	0.990063
50	135.1	1.3734	0.1070E-02	0.2040E-08	0.000001	0.114548E-05	0.990063
51	135.3	1.3734	0.2504E-02	0.4757E-08	0.000001	0.627236E-05	0.990063
52	136.3	1.3734	0.6282E-03	0.1177E-08	0.000000	0.394696E-06	0.990063
53	138.7	1.3734	-0.1239E-03	-0.2240E-09	0.000000	0.153557E-07	0.990063
54	139.5	1.3734	-0.6636E-04	-0.1187E-09	0.000000	0.440429E-08	0.990063
55	142.5	1.3734	0.8709E-03	0.1492E-08	0.000000	0.758415E-06	0.990063

NEDO-33373-A, Revision 5

56	143.3	1.3734	-0.7757E-03	-0.1313E-08	0.000000	0.601636E-06	0.990063
57	144.7	1.3734	2.664	0.4428E-05	0.001088	7.09427	0.990196
58	146.9	1.3734	-0.1879E-02	-0.3030E-08	0.000001	0.353094E-05	0.990196
59	149.2	1.3734	-0.3044E-03	-0.4759E-09	0.000000	0.926304E-07	0.990196
60	149.7	1.3734	8.256	0.1282E-04	0.003150	68.1574	0.991471
61	149.7	1.3734	0.4787E-03	0.7433E-09	0.000000	0.229183E-06	0.991471
62	150.2	1.3734	0.2463E-03	0.3799E-09	0.000000	0.606483E-07	0.991471
63	150.9	1.3734	-0.1925E-03	-0.2941E-09	0.000000	0.370396E-07	0.991471
64	151.7	1.3734	-4.202	-0.6351E-05	0.001560	17.6547	0.991801
65	152.5	1.3734	2.129	0.3185E-05	0.000783	4.53183	0.991886
66	154.3	1.3734	-0.1221E-02	-0.1785E-08	0.000000	0.149137E-05	0.991886
67	155.2	1.3734	15.63	0.2259E-04	0.005551	244.432	0.996460
68	156.2	1.3734	0.1580E-03	0.2252E-09	0.000000	0.249610E-07	0.996460
69	156.6	1.3734	2.553	0.3624E-05	0.000891	6.51883	0.996582
70	156.9	1.3734	0.8242E-03	0.1165E-08	0.000000	0.679318E-06	0.996582
71	157.9	1.3734	0.2134E-02	0.2977E-08	0.000001	0.455457E-05	0.996582
72	159.1	1.3734	0.6478E-03	0.8905E-09	0.000000	0.419606E-06	0.996582
73	161.0	1.3734	0.5900	0.7915E-06	0.000195	0.348091	0.996588
74	161.4	1.3734	-0.8928E-03	-0.1192E-08	0.000000	0.797012E-06	0.996588
75	161.8	1.3734	-0.5393E-01	-0.7166E-07	0.000018	0.290822E-02	0.996588
76	163.8	1.3734	0.4196E-02	0.5438E-08	0.000001	0.176062E-04	0.996588
77	164.1	1.3734	0.3219E-02	0.4158E-08	0.000001	0.103613E-04	0.996588
78	165.7	1.3734	0.4496E-02	0.5698E-08	0.000001	0.202141E-04	0.996588
79	165.7	1.3734	-0.1536E-02	-0.1947E-08	0.000000	0.236080E-05	0.996588
80	166.1	1.3734	0.3660E-02	0.4613E-08	0.000001	0.133971E-04	0.996588
81	168.8	1.3734	0.6594E-01	0.8050E-07	0.000020	0.434764E-02	0.996588
82	170.3	1.3734	0.1061E-02	0.1273E-08	0.000000	0.112676E-05	0.996588
83	170.5	1.3734	-0.5500E-03	-0.6581E-09	0.000000	0.302477E-06	0.996588

NEDO-33373-A, Revision 5

84	171.3	1.3734	-0.1891E-03	-0.2243E-09	0.000000	0.357626E-07	0.996588
85	171.5	1.3734	0.1938E-03	0.2292E-09	0.000000	0.375394E-07	0.996588
86	172.1	1.3734	-0.2198	-0.2581E-06	0.000063	0.483034E-01	0.996589
87	172.5	1.3734	0.3272E-03	0.3825E-09	0.000000	0.107056E-06	0.996589
88	173.8	1.3734	0.2800E-03	0.3225E-09	0.000000	0.783932E-07	0.996589
89	175.6	1.3734	-1.109	-0.1252E-05	0.000308	1.23079	0.996612
90	176.1	1.3734	-0.4358E-04	-0.4889E-10	0.000000	0.189950E-08	0.996612
91	176.9	1.3734	12.83	0.1426E-04	0.003504	164.589	0.999692
92	177.5	1.3734	0.3411E-03	0.3766E-09	0.000000	0.116356E-06	0.999692
93	178.0	1.3734	0.5346E-03	0.5868E-09	0.000000	0.285836E-06	0.999692
94	179.5	1.3734	-0.6347	-0.6854E-06	0.000168	0.402867	0.999700
95	181.3	1.3734	-0.6609E-03	-0.6992E-09	0.000000	0.436784E-06	0.999700
96	182.8	1.3734	-0.2594E-02	-0.2701E-08	0.000001	0.672949E-05	0.999700
97	182.9	1.3734	0.2002	0.2082E-06	0.000051	0.400833E-01	0.999700
98	183.1	1.3734	-0.5805E-02	-0.6027E-08	0.000001	0.336979E-04	0.999700
99	183.9	1.3734	-0.7732E-02	-0.7951E-08	0.000002	0.597878E-04	0.999700
100	185.4	1.3734	4.001	0.4049E-05	0.000995	16.0105	1.00000

SUM OF EFFECTIVE MASSES= 53442.0

1

***** ANSYS - ENGINEERING ANALYSIS SYSTEM RELEASE 10.0 *****

ANSYS Multiphysics

00265621 VERSION=INTEL NT 13:21:07 SEP 07, 2009 CP= 3090.344

SIGNIFICANCE FACTOR FOR COMBINING MODES = 0.10000E-02

SIGNIFICANT MODE COEFFICIENTS (INCLUDING DAMPING)

MODE	FREQUENCY	DAMPING	SV	MODE COEF.
12	44.08	0.0000	1.4608	-0.4070E-02
27	80.08	0.0000	1.3966	-0.8504E-04

36	97.41	0.0000	1.3761	-0.2874E-03
41	120.2	0.0000	1.3734	0.7096E-04
57	144.7	0.0000	1.3734	0.4428E-05
60	149.7	0.0000	1.3734	0.1282E-04
64	151.7	0.0000	1.3734	-0.6351E-05
67	155.2	0.0000	1.3734	0.2259E-04
91	176.9	0.0000	1.3734	0.1426E-04

MODAL COMBINATION COEFFICIENTS

MODE= 12 FREQUENCY= 44.083 COUPLING COEF.= 1.000

MODE= 27 FREQUENCY= 80.076 COUPLING COEF.= 1.000

MODE= 36 FREQUENCY= 97.410 COUPLING COEF.= 1.000

MODE= 41 FREQUENCY= 120.191 COUPLING COEF.= 1.000

FREQUENCY 144.66 HERTZ PART OF CLOSELY SPACED GROUP 1

FREQUENCY 149.68 HERTZ PART OF CLOSELY SPACED GROUP 1

FREQUENCY 151.72 HERTZ PART OF CLOSELY SPACED GROUP 1

FREQUENCY 155.16 HERTZ PART OF CLOSELY SPACED GROUP 1

MODE= 91 FREQUENCY= 176.912 COUPLING COEF.= 1.000

GROUPING COMBINATION INSTRUCTIONS WRITTEN ON FILE SSE-LOCA-SRVD.mcom

*** NOTE *** CP = 3090.359 TIME= 13:21:07

Solution is done!

ANSYS RELEASE 10.0 UP20050718 13:20:50 09/07/2009

NUMBER OF FREQUENCIES IN TABLE = 4

NUMBER OF FREQUENCIES IN TABLE = 7

PRINTOUT RESUMED BY /GOP

Load step file number 7. Begin solution ...

***** ANSYS SOLVE COMMAND *****

LOAD STEP OPTIONS

LOAD STEP NUMBER..... 7
SPECTRUM LOADING TYPE.....ACCELERATION
EXCITATION DIRECTION..... 1.0000 0.0000 0.0000
MODE COMBINATION TYPE.....GRP
RESPONSE TYPE.....DISPLACEMENT
SIGNIFICANCE LEVEL FOR COMBINATIONS..... 0.10000E-02

PRINT OUTPUT CONTROLS

ITEM FREQUENCY COMPONENT
ALL NONE
NSOL ALL

DATABASE OUTPUT CONTROLS.....ALL DATA WRITTEN

1

***** ANSYS - ENGINEERING ANALYSIS SYSTEM RELEASE 10.0 *****

ANSYS Multiphysics

00265621 VERSION=INTEL NT 13:21:09 SEP 07, 2009 CP= 3091.562

***** RESPONSE SPECTRUM CALCULATION SUMMARY *****

CUMULATIVE

MODE	FREQUENCY	SV	PARTIC.FACTOR	MODE COEF.	M.C. RATIO	EFFECTIVE MASS	MASS FRACTION
1	13.79	1.8835	0.1725E-05	0.4331E-09	0.000000	0.297690E-11	0.397373E-16
2	16.69	1.5095	219.4	0.3010E-01	1.000000	48143.7	0.642650
3	17.53	1.1712	-0.9107E-06	-0.8794E-10	0.000000	0.829354E-12	0.642650
4	30.17	0.54079	-0.5842E-06	-0.8794E-11	0.000000	0.341317E-12	0.642650

NEDO-33373-A, Revision 5

5	31.99	0.50596	-0.3978E-06	-0.4984E-11	0.000000	0.158270E-12	0.642650
6	34.31	0.46712	7.927	0.7966E-04	0.002646	62.8308	0.643489
7	35.74	0.44596	0.9065E-05	0.8016E-10	0.000000	0.821820E-10	0.643489
8	38.57	0.40898	-0.5012E-05	-0.3490E-10	0.000000	0.251193E-10	0.643489
9	39.42	0.39893	-0.4961E-05	-0.3225E-10	0.000000	0.246122E-10	0.643489
10	43.44	0.38236	0.5046E-04	0.2589E-09	0.000000	0.254589E-08	0.643489
11	43.46	0.38231	-0.7074	-0.3627E-05	0.000120	0.500411	0.643495
12	44.08	0.38061	-0.1555E-04	-0.7716E-10	0.000000	0.241919E-09	0.643495
13	48.22	0.37004	-0.3713E-04	-0.1497E-09	0.000000	0.137853E-08	0.643495
14	49.09	0.36796	0.3384E-04	0.1309E-09	0.000000	0.114534E-08	0.643495
15	53.20	0.35879	0.2725E-04	0.8751E-10	0.000000	0.742710E-09	0.643495
16	53.88	0.35736	0.6110E-05	0.1905E-10	0.000000	0.373263E-10	0.643495
17	54.15	0.35681	136.5	0.4207E-03	0.013974	18620.8	0.892056
18	56.50	0.35207	80.75	0.2256E-03	0.007493	6520.80	0.979100
19	60.15	0.34522	0.1814E-04	0.4383E-10	0.000000	0.328926E-09	0.979100
20	62.62	0.34089	0.4728E-04	0.1041E-09	0.000000	0.223505E-08	0.979100
21	66.52	0.33448	-0.2101E-04	-0.4024E-10	0.000000	0.441607E-09	0.979100
22	70.01	0.32916	21.69	0.3689E-04	0.001225	470.323	0.985378
23	72.36	0.32576	0.1025E-03	0.1615E-09	0.000000	0.105084E-07	0.985378
24	76.34	0.32033	0.1587E-03	0.2210E-09	0.000000	0.251917E-07	0.985378
25	77.98	0.31821	-21.55	-0.2857E-04	0.000949	464.515	0.991578
26	78.47	0.31758	-0.1720E-03	-0.2248E-09	0.000000	0.296005E-07	0.991578
27	80.08	0.31556	-0.4539E-03	-0.5658E-09	0.000000	0.206033E-06	0.991578
28	82.34	0.31282	-3.554	-0.4154E-05	0.000138	12.6309	0.991747
29	83.23	0.31176	0.8322E-03	0.9487E-09	0.000000	0.692583E-06	0.991747
30	84.75	0.30999	0.8763E-05	0.9580E-11	0.000000	0.767864E-10	0.991747
31	87.19	0.30724	-0.1913E-06	-0.1959E-12	0.000000	0.366061E-13	0.991747
32	87.58	0.30682	-12.60	-0.1277E-04	0.000424	158.834	0.993867

NEDO-33373-A, Revision 5

33	89.82	0.30439	-0.4399E-04	-0.4204E-10	0.000000	0.193537E-08	0.993867
34	90.26	0.30392	-0.5749E-04	-0.5433E-10	0.000000	0.330534E-08	0.993867
35	96.62	0.29750	0.7549E-04	0.6094E-10	0.000000	0.569897E-08	0.993867
36	97.41	0.29673	0.1952E-04	0.1546E-10	0.000000	0.380909E-09	0.993867
37	98.21	0.29597	-0.3908E-04	-0.3038E-10	0.000000	0.152729E-08	0.993867
38	108.9	0.29430	-0.2244E-03	-0.1411E-09	0.000000	0.503506E-07	0.993867
39	117.1	0.29430	-0.3889E-03	-0.2113E-09	0.000000	0.151257E-06	0.993867
40	119.6	0.29430	-19.90	-0.1038E-04	0.000345	395.909	0.999152
41	120.2	0.29430	-0.7125E-03	-0.3677E-09	0.000000	0.507672E-06	0.999152
42	122.6	0.29430	0.3596	0.1784E-06	0.000006	0.129343	0.999154
43	123.9	0.29430	-0.3978E-03	-0.1933E-09	0.000000	0.158230E-06	0.999154
44	125.3	0.29430	-0.7098E-03	-0.3369E-09	0.000000	0.503750E-06	0.999154
45	126.5	0.29430	-0.4841E-03	-0.2254E-09	0.000000	0.234391E-06	0.999154
46	128.2	0.29430	-0.8334E-03	-0.3782E-09	0.000000	0.694472E-06	0.999154
47	131.1	0.29430	-0.2352E-02	-0.1020E-08	0.000000	0.553390E-05	0.999154
48	131.8	0.29430	-2.307	-0.9900E-06	0.000033	5.32450	0.999225
49	134.8	0.29430	0.2199E-02	0.9028E-09	0.000000	0.483627E-05	0.999225
50	135.1	0.29430	0.3035E-03	0.1239E-09	0.000000	0.921184E-07	0.999225
51	135.3	0.29430	0.7600	0.3093E-06	0.000010	0.577631	0.999233
52	136.3	0.29430	-0.4467E-03	-0.1793E-09	0.000000	0.199531E-06	0.999233
53	138.7	0.29430	-0.1480E-03	-0.5734E-10	0.000000	0.219087E-07	0.999233
54	139.5	0.29430	4.897	0.1877E-05	0.000062	23.9847	0.999553
55	142.5	0.29430	-2.082	-0.7643E-06	0.000025	4.33545	0.999611
56	143.3	0.29430	-0.2801E-03	-0.1016E-09	0.000000	0.784399E-07	0.999611
57	144.7	0.29430	-0.1746E-03	-0.6221E-10	0.000000	0.304935E-07	0.999611
58	146.9	0.29430	-0.1070E-02	-0.3698E-09	0.000000	0.114512E-05	0.999611
59	149.2	0.29430	0.9068E-04	0.3038E-10	0.000000	0.822253E-08	0.999611
60	149.7	0.29430	-0.1620E-03	-0.5391E-10	0.000000	0.262449E-07	0.999611

NEDO-33373-A, Revision 5

61	149.7	0.29430	-0.8696E-03	-0.2894E-09	0.000000	0.756279E-06	0.999611
62	150.2	0.29430	0.1666E-03	0.5507E-10	0.000000	0.277421E-07	0.999611
63	150.9	0.29430	0.2350E-04	0.7693E-11	0.000000	0.552019E-09	0.999611
64	151.7	0.29430	-0.9457E-03	-0.3063E-09	0.000000	0.894351E-06	0.999611
65	152.5	0.29430	-0.5051E-03	-0.1619E-09	0.000000	0.255079E-06	0.999611
66	154.3	0.29430	-0.6471E-03	-0.2027E-09	0.000000	0.418760E-06	0.999611
67	155.2	0.29430	-0.9259E-03	-0.2867E-09	0.000000	0.857345E-06	0.999611
68	156.2	0.29430	0.4408E-03	0.1347E-09	0.000000	0.194340E-06	0.999611
69	156.6	0.29430	-0.9395E-04	-0.2858E-10	0.000000	0.882724E-08	0.999611
70	156.9	0.29430	0.6425E-03	0.1947E-09	0.000000	0.412826E-06	0.999611
71	157.9	0.29430	-1.691	-0.5055E-06	0.000017	2.86034	0.999649
72	159.1	0.29430	-0.4040E-03	-0.1190E-09	0.000000	0.163225E-06	0.999649
73	161.0	0.29430	0.8683E-03	0.2496E-09	0.000000	0.753904E-06	0.999649
74	161.4	0.29430	4.968	0.1421E-05	0.000047	24.6805	0.999978
75	161.8	0.29430	-0.9736E-03	-0.2772E-09	0.000000	0.947827E-06	0.999978
76	163.8	0.29430	-0.3201E-02	-0.8890E-09	0.000000	0.102482E-04	0.999978
77	164.1	0.29430	-0.2729E-02	-0.7553E-09	0.000000	0.744695E-05	0.999978
78	165.7	0.29430	0.1348E-02	0.3662E-09	0.000000	0.181828E-05	0.999978
79	165.7	0.29430	-0.2188E-02	-0.5941E-09	0.000000	0.478766E-05	0.999978
80	166.1	0.29430	-0.6071	-0.1640E-06	0.000005	0.368601	0.999983
81	168.8	0.29430	0.1407E-02	0.3680E-09	0.000000	0.197874E-05	0.999983
82	170.3	0.29430	0.3513E-03	0.9032E-10	0.000000	0.123441E-06	0.999983
83	170.5	0.29430	-0.2020E-01	-0.5178E-08	0.000000	0.407840E-03	0.999983
84	171.3	0.29430	-1.117	-0.2840E-06	0.000009	1.24880	1.00000
85	171.5	0.29430	-0.3164E-03	-0.8020E-10	0.000000	0.100080E-06	1.00000
86	172.1	0.29430	0.3084E-03	0.7760E-10	0.000000	0.951294E-07	1.00000
87	172.5	0.29430	0.6107E-04	0.1530E-10	0.000000	0.372914E-08	1.00000
88	173.8	0.29430	0.7255E-01	0.1791E-07	0.000001	0.526391E-02	1.00000

NEDO-33373-A, Revision 5

89	175.6	0.29430	-0.1656E-04	-0.4005E-11	0.000000	0.274283E-09	1.00000
90	176.1	0.29430	0.6936E-03	0.1667E-09	0.000000	0.481084E-06	1.00000
91	176.9	0.29430	-0.3791E-03	-0.9029E-10	0.000000	0.143702E-06	1.00000
92	177.5	0.29430	0.2093E-01	0.4952E-08	0.000000	0.438182E-03	1.00000
93	178.0	0.29430	-0.6705E-03	-0.1577E-09	0.000000	0.449583E-06	1.00000
94	179.5	0.29430	0.6013E-04	0.1391E-10	0.000000	0.361511E-08	1.00000
95	181.3	0.29430	0.6589E-01	0.1494E-07	0.000000	0.434129E-02	1.00000
96	182.8	0.29430	0.2478E-02	0.5527E-09	0.000000	0.613851E-05	1.00000
97	182.9	0.29430	-0.5735E-03	-0.1278E-09	0.000000	0.328912E-06	1.00000
98	183.1	0.29430	0.3353E-01	0.7460E-08	0.000000	0.112444E-02	1.00000
99	183.9	0.29430	0.4072E-01	0.8972E-08	0.000000	0.165794E-02	1.00000
100	185.4	0.29430	-0.7418E-03	-0.1608E-09	0.000000	0.550325E-06	1.00000

SUM OF EFFECTIVE MASSES= 74914.4

1

***** ANSYS - ENGINEERING ANALYSIS SYSTEM RELEASE 10.0 *****

ANSYS Multiphysics

00265621 VERSION=INTEL NT 13:21:09 SEP 07, 2009 CP= 3091.562

SIGNIFICANCE FACTOR FOR COMBINING MODES = 0.10000E-02

SIGNIFICANT MODE COEFFICIENTS (INCLUDING DAMPING)

MODE	FREQUENCY	DAMPING	SV	MODE COEF.
2	16.69	0.0000	1.5095	0.3010E-01
6	34.31	0.0000	0.46712	0.7966E-04
17	54.15	0.0000	0.35681	0.4207E-03
18	56.50	0.0000	0.35207	0.2256E-03
22	70.01	0.0000	0.32916	0.3689E-04

MODAL COMBINATION COEFFICIENTS

MODE= 2 FREQUENCY= 16.694 COUPLING COEF.= 1.000

MODE= 6 FREQUENCY= 34.314 COUPLING COEF.= 1.000
FREQUENCY 54.147 HERTZ PART OF CLOSELY SPACED GROUP 1
FREQUENCY 56.504 HERTZ PART OF CLOSELY SPACED GROUP 1
MODE= 22 FREQUENCY= 70.010 COUPLING COEF.= 1.000

GROUPING COMBINATION INSTRUCTIONS WRITTEN ON FILE SSE-LOCA-SRVD.mcom

*** NOTE *** CP = 3091.562 TIME= 13:21:09

Solution is done!

ANSYS RELEASE 10.0 UP20050718 13:20:50 09/07/2009

NUMBER OF FREQUENCIES IN TABLE = 4

NUMBER OF FREQUENCIES IN TABLE = 7

PRINTOUT RESUMED BY /GOP

Load step file number 8. Begin solution ...

***** ANSYS SOLVE COMMAND *****

LOAD STEP OPTIONS

LOAD STEP NUMBER..... 8
SPECTRUM LOADING TYPE.....ACCELERATION
EXCITATION DIRECTION..... 0.0000 1.0000 0.0000
MODE COMBINATION TYPE..... GRP
RESPONSE TYPE.....DISPLACEMENT
SIGNIFICANCE LEVEL FOR COMBINATIONS..... 0.10000E-02

PRINT OUTPUT CONTROLS

ITEM FREQUENCY COMPONENT
ALL NONE
NSOL ALL

DATABASE OUTPUT CONTROLS.....ALL DATA WRITTEN

NEDO-33373-A, Revision 5

***** ANSYS - ENGINEERING ANALYSIS SYSTEM RELEASE 10.0 *****

ANSYS Multiphysics

00265621 VERSION=INTEL NT 13:21:10 SEP 07, 2009 CP= 3092.766

***** RESPONSE SPECTRUM CALCULATION SUMMARY *****

CUMULATIVE

MODE	FREQUENCY	SV	PARTIC.FACTOR	MODE COEF.	M.C. RATIO	EFFECTIVE MASS	MASS FRACTION
1	13.79	1.8835	216.1	0.5424E-01	1.000000	46688.0	0.626446
2	16.69	1.5095	0.2075E-06	0.2846E-10	0.000000	0.430422E-13	0.626446
3	17.53	1.1712	-0.5288E-06	-0.5106E-10	0.000000	0.279620E-12	0.626446
4	30.17	0.54079	0.1043E-05	0.1570E-10	0.000000	0.108733E-11	0.626446
5	31.99	0.50596	-2.989	-0.3744E-04	0.000690	8.93272	0.626565
6	34.31	0.46712	0.2088E-06	0.2098E-11	0.000000	0.436061E-13	0.626565
7	35.74	0.44596	0.1776E-06	0.1571E-11	0.000000	0.315452E-13	0.626565
8	38.57	0.40898	-0.2891E-04	-0.2013E-09	0.000000	0.835606E-09	0.626565
9	39.42	0.39893	5.439	0.3536E-04	0.000652	29.5846	0.626962
10	43.44	0.38236	0.3730E-04	0.1914E-09	0.000000	0.139156E-08	0.626962
11	43.46	0.38231	0.2195E-05	0.1125E-10	0.000000	0.481826E-11	0.626962
12	44.08	0.38061	0.7629E-05	0.3785E-10	0.000000	0.582038E-10	0.626962
13	48.22	0.37004	-32.35	-0.1304E-03	0.002404	1046.61	0.641005
14	49.09	0.36796	0.1683E-03	0.6510E-09	0.000000	0.283377E-07	0.641005
15	53.20	0.35879	155.0	0.4976E-03	0.009175	24015.1	0.963233
16	53.88	0.35736	0.5050E-05	0.1575E-10	0.000000	0.255048E-10	0.963233
17	54.15	0.35681	-0.9425E-05	-0.2906E-10	0.000000	0.888384E-10	0.963233

NEDO-33373-A, Revision 5

18	56.50	0.35207	-0.6047E-05	-0.1689E-10	0.000000	0.365613E-10	0.963233
19	60.15	0.34522	36.01	0.8703E-04	0.001605	1297.05	0.980637
20	62.62	0.34089	-0.2556E-04	-0.5627E-10	0.000000	0.653081E-09	0.980637
21	66.52	0.33448	-0.1050E-03	-0.2011E-09	0.000000	0.110329E-07	0.980637
22	70.01	0.32916	0.1390E-03	0.2365E-09	0.000000	0.193248E-07	0.980637
23	72.36	0.32576	-16.45	-0.2593E-04	0.000478	270.761	0.984270
24	76.34	0.32033	-0.2922E-03	-0.4069E-09	0.000000	0.853894E-07	0.984270
25	77.98	0.31821	0.7648E-03	0.1014E-08	0.000000	0.584977E-06	0.984270
26	78.47	0.31758	-0.3536E-03	-0.4620E-09	0.000000	0.125031E-06	0.984270
27	80.08	0.31556	0.1096E-02	0.1366E-08	0.000000	0.120136E-05	0.984270
28	82.34	0.31282	0.1133E-02	0.1324E-08	0.000000	0.128397E-05	0.984270
29	83.23	0.31176	-11.12	-0.1268E-04	0.000234	123.641	0.985929
30	84.75	0.30999	-0.1751E-04	-0.1914E-10	0.000000	0.306546E-09	0.985929
31	87.19	0.30724	0.7519E-05	0.7697E-11	0.000000	0.565308E-10	0.985929
32	87.58	0.30682	0.7858E-05	0.7963E-11	0.000000	0.617535E-10	0.985929
33	89.82	0.30439	10.15	0.9703E-05	0.000179	103.083	0.987312
34	90.26	0.30392	0.1697E-04	0.1604E-10	0.000000	0.288060E-09	0.987312
35	96.62	0.29750	-17.46	-0.1410E-04	0.000260	304.977	0.991404
36	97.41	0.29673	0.1752E-04	0.1388E-10	0.000000	0.307020E-09	0.991404
37	98.21	0.29597	0.7632E-04	0.5932E-10	0.000000	0.582449E-08	0.991404
38	108.9	0.29430	0.5956E-03	0.3746E-09	0.000000	0.354744E-06	0.991404
39	117.1	0.29430	-19.73	-0.1072E-04	0.000198	389.301	0.996627
40	119.6	0.29430	0.1308E-02	0.6821E-09	0.000000	0.171090E-05	0.996627
41	120.2	0.29430	0.3341E-03	0.1724E-09	0.000000	0.111631E-06	0.996627
42	122.6	0.29430	0.4968E-02	0.2464E-08	0.000000	0.246813E-04	0.996627
43	123.9	0.29430	0.1371E-03	0.6664E-10	0.000000	0.188084E-07	0.996627
44	125.3	0.29430	11.16	0.5298E-05	0.000098	124.546	0.998299
45	126.5	0.29430	0.2861E-02	0.1332E-08	0.000000	0.818435E-05	0.998299

NEDO-33373-A, Revision 5

46	128.2	0.29430	-0.4767E-03	-0.2163E-09	0.000000	0.227247E-06	0.998299
47	131.1	0.29430	-3.294	-0.1429E-05	0.000026	10.8519	0.998444
48	131.8	0.29430	-0.7363E-02	-0.3159E-08	0.000000	0.542152E-04	0.998444
49	134.8	0.29430	0.1274E-01	0.5232E-08	0.000000	0.162416E-03	0.998444
50	135.1	0.29430	4.518	0.1845E-05	0.000034	20.4118	0.998718
51	135.3	0.29430	-0.2280E-02	-0.9277E-09	0.000000	0.519624E-05	0.998718
52	136.3	0.29430	-0.8688E-02	-0.3487E-08	0.000000	0.754829E-04	0.998718
53	138.7	0.29430	-3.975	-0.1540E-05	0.000028	15.7999	0.998930
54	139.5	0.29430	0.1504E-03	0.5766E-10	0.000000	0.226333E-07	0.998930
55	142.5	0.29430	-0.4492E-03	-0.1649E-09	0.000000	0.201738E-06	0.998930
56	143.3	0.29430	0.7590E-03	0.2754E-09	0.000000	0.576050E-06	0.998930
57	144.7	0.29430	-0.8851E-04	-0.3153E-10	0.000000	0.783340E-08	0.998930
58	146.9	0.29430	0.1651E-02	0.5704E-09	0.000000	0.272509E-05	0.998930
59	149.2	0.29430	2.652	0.8888E-06	0.000016	7.03492	0.999024
60	149.7	0.29430	0.9355E-04	0.3113E-10	0.000000	0.875113E-08	0.999024
61	149.7	0.29430	0.1944E-02	0.6469E-09	0.000000	0.378065E-05	0.999024
62	150.2	0.29430	-3.031	-0.1002E-05	0.000018	9.18635	0.999148
63	150.9	0.29430	3.032	0.9927E-06	0.000018	9.19141	0.999271
64	151.7	0.29430	0.1140E-02	0.3691E-09	0.000000	0.129872E-05	0.999271
65	152.5	0.29430	-0.1795E-03	-0.5754E-10	0.000000	0.322075E-07	0.999271
66	154.3	0.29430	-0.3802	-0.1191E-06	0.000002	0.144563	0.999273
67	155.2	0.29430	-0.2288E-03	-0.7086E-10	0.000000	0.523632E-07	0.999273
68	156.2	0.29430	-0.2391E-02	-0.7302E-09	0.000000	0.571540E-05	0.999273
69	156.6	0.29430	0.2024E-03	0.6155E-10	0.000000	0.409557E-07	0.999273
70	156.9	0.29430	-0.1986E-02	-0.6016E-09	0.000000	0.394223E-05	0.999273
71	157.9	0.29430	-0.2728E-02	-0.8152E-09	0.000000	0.744016E-05	0.999273
72	159.1	0.29430	-0.9249E-02	-0.2725E-08	0.000000	0.855365E-04	0.999273
73	161.0	0.29430	-0.3898E-02	-0.1121E-08	0.000000	0.151910E-04	0.999273

NEDO-33373-A, Revision 5

74	161.4	0.29430	0.6081E-04	0.1740E-10	0.000000	0.369828E-08	0.999273
75	161.8	0.29430	0.1560E-02	0.4443E-09	0.000000	0.243418E-05	0.999273
76	163.8	0.29430	-3.659	-0.1016E-05	0.000019	13.3894	0.999453
77	164.1	0.29430	-2.594	-0.7179E-06	0.000013	6.72662	0.999543
78	165.7	0.29430	-0.4794E-02	-0.1302E-08	0.000000	0.229791E-04	0.999543
79	165.7	0.29430	0.5593E-02	0.1519E-08	0.000000	0.312851E-04	0.999543
80	166.1	0.29430	-0.1600E-01	-0.4322E-08	0.000000	0.256134E-03	0.999543
81	168.8	0.29430	-0.1198E-01	-0.3135E-08	0.000000	0.143587E-03	0.999543
82	170.3	0.29430	-0.4412E-02	-0.1134E-08	0.000000	0.194641E-04	0.999543
83	170.5	0.29430	0.2483E-03	0.6367E-10	0.000000	0.616576E-07	0.999543
84	171.3	0.29430	0.6195E-03	0.1574E-09	0.000000	0.383812E-06	0.999543
85	171.5	0.29430	-0.2289E-03	-0.5802E-10	0.000000	0.523807E-07	0.999543
86	172.1	0.29430	0.8577E-04	0.2158E-10	0.000000	0.735678E-08	0.999543
87	172.5	0.29430	-0.7136	-0.1788E-06	0.000003	0.509254	0.999550
88	173.8	0.29430	0.4457E-03	0.1100E-09	0.000000	0.198684E-06	0.999550
89	175.6	0.29430	0.1068E-02	0.2582E-09	0.000000	0.113995E-05	0.999550
90	176.1	0.29430	-0.2248E-02	-0.5405E-09	0.000000	0.505533E-05	0.999550
91	176.9	0.29430	0.2999E-02	0.7143E-09	0.000000	0.899407E-05	0.999550
92	177.5	0.29430	-0.5128E-02	-0.1213E-08	0.000000	0.262941E-04	0.999550
93	178.0	0.29430	-5.790	-0.1362E-05	0.000025	33.5223	0.999999
94	179.5	0.29430	-0.9784E-02	-0.2264E-08	0.000000	0.957260E-04	0.999999
95	181.3	0.29430	0.6490E-02	0.1471E-08	0.000000	0.421152E-04	0.999999
96	182.8	0.29430	0.1104E-01	0.2462E-08	0.000000	0.121796E-03	0.999999
97	182.9	0.29430	0.5059E-01	0.1128E-07	0.000000	0.255971E-02	0.999999
98	183.1	0.29430	0.2230E-01	0.4962E-08	0.000000	0.497341E-03	1.00000
99	183.9	0.29430	0.3464E-01	0.7633E-08	0.000000	0.120000E-02	1.00000
100	185.4	0.29430	0.1889	0.4096E-07	0.000001	0.356798E-01	1.00000

SUM OF EFFECTIVE MASSES= 74528.4

1

***** ANSYS - ENGINEERING ANALYSIS SYSTEM RELEASE 10.0 *****

ANSYS Multiphysics

00265621 VERSION=INTEL NT 13:21:10 SEP 07, 2009 CP= 3092.766

SIGNIFICANCE FACTOR FOR COMBINING MODES = 0.10000E-02

SIGNIFICANT MODE COEFFICIENTS (INCLUDING DAMPING)

MODE	FREQUENCY	DAMPING	SV	MODE COEF.
1	13.79	0.0000	1.8835	0.5424E-01
13	48.22	0.0000	0.37004	-0.1304E-03
15	53.20	0.0000	0.35879	0.4976E-03
19	60.15	0.0000	0.34522	0.8703E-04

MODAL COMBINATION COEFFICIENTS

MODE= 1 FREQUENCY= 13.787 COUPLING COEF.= 1.000

MODE= 13 FREQUENCY= 48.220 COUPLING COEF.= 1.000

MODE= 15 FREQUENCY= 53.200 COUPLING COEF.= 1.000

MODE= 19 FREQUENCY= 60.155 COUPLING COEF.= 1.000

GROUPING COMBINATION INSTRUCTIONS WRITTEN ON FILE SSE-LOCA-SRVD.mcom

*** NOTE *** CP = 3092.781 TIME= 13:21:10

Solution is done!

ANSYS RELEASE 10.0 UP20050718 13:20:50 09/07/2009

NUMBER OF FREQUENCIES IN TABLE = 4

NUMBER OF FREQUENCIES IN TABLE = 8

PRINTOUT RESUMED BY /GOP

Load step file number 9. Begin solution ...

***** ANSYS SOLVE COMMAND *****

LOAD STEP OPTIONS

LOAD STEP NUMBER 9
 SPECTRUM LOADING TYPE ACCELERATION
 EXCITATION DIRECTION 0.0000 0.0000 1.0000
 MODE COMBINATION TYPE GRP
 RESPONSE TYPE DISPLACEMENT
 SIGNIFICANCE LEVEL FOR COMBINATIONS 0.10000E-02

PRINT OUTPUT CONTROLS

ITEM FREQUENCY COMPONENT

ALL NONE

NSOL ALL

DATABASE OUTPUT CONTROLS ALL DATA WRITTEN

1

***** ANSYS - ENGINEERING ANALYSIS SYSTEM RELEASE 10.0 *****

ANSYS Multiphysics

00265621 VERSION=INTEL NT 13:21:12 SEP 07, 2009 CP= 3093.984

***** RESPONSE SPECTRUM CALCULATION SUMMARY *****

CUMULATIVE

MODE	FREQUENCY	SV	PARTIC.FACTOR	MODE COEF.	M.C. RATIO	EFFECTIVE MASS	MASS FRACTION
1	13.79	3.3071	0.2836E-06	0.1250E-09	0.000000	0.804497E-13	0.150537E-17
2	16.69	2.0981	-0.1546E-05	-0.2949E-09	0.000000	0.239075E-11	0.462408E-16
3	17.53	1.8768	-0.2216E-05	-0.3429E-09	0.000000	0.491026E-11	0.138121E-15
4	30.17	1.3675	-0.8185E-06	-0.3115E-10	0.000000	0.669873E-12	0.150656E-15

NEDO-33373-A, Revision 5

5	31.99	1.3628	-0.2986E-05	-0.1007E-09	0.000000	0.891419E-11	0.317457E-15
6	34.31	1.3572	0.3763E-05	0.1099E-09	0.000000	0.141633E-10	0.582478E-15
7	35.74	1.3540	0.7225E-05	0.1940E-09	0.000000	0.522013E-10	0.155926E-14
8	38.57	1.3480	-0.1172E-04	-0.2689E-09	0.000000	0.137283E-09	0.412808E-14
9	39.42	1.3463	-0.2143E-05	-0.4702E-10	0.000000	0.459138E-11	0.421400E-14
10	43.44	1.3387	0.3038E-04	0.5459E-09	0.000000	0.923098E-09	0.214869E-13
11	43.46	1.3387	0.1902E-07	0.3414E-12	0.000000	0.361581E-15	0.214869E-13
12	44.08	1.3376	-213.7	-0.3726E-02	1.000000	45683.6	0.854826
13	48.22	1.3306	-0.8573E-04	-0.1243E-08	0.000000	0.735039E-08	0.854826
14	49.09	1.3292	0.1067E-03	0.1490E-08	0.000000	0.113746E-07	0.854826
15	53.20	1.3230	-0.2352E-04	-0.2785E-09	0.000000	0.553088E-09	0.854826
16	53.88	1.3220	-0.2355E-04	-0.2717E-09	0.000000	0.554727E-09	0.854826
17	54.15	1.3217	0.7421E-06	0.8474E-11	0.000000	0.550758E-12	0.854826
18	56.50	1.3184	-0.2034E-04	-0.2127E-09	0.000000	0.413632E-09	0.854826
19	60.15	1.3136	-0.5155E-04	-0.4741E-09	0.000000	0.265777E-08	0.854826
20	62.62	1.3105	-0.5182E-04	-0.4386E-09	0.000000	0.268518E-08	0.854826
21	66.52	1.3059	-0.7326E-04	-0.5476E-09	0.000000	0.536661E-08	0.854826
22	70.01	1.3020	-0.6240E-04	-0.4199E-09	0.000000	0.389347E-08	0.854826
23	72.36	1.2995	-0.9103E-04	-0.5722E-09	0.000000	0.828641E-08	0.854826
24	76.34	1.2955	0.2418E-03	0.1362E-08	0.000000	0.584894E-07	0.854826
25	77.98	1.2939	0.2635E-03	0.1420E-08	0.000000	0.694436E-07	0.854826
26	78.47	1.2934	-0.3035E-03	-0.1615E-08	0.000000	0.921045E-07	0.854826
27	80.08	1.2919	-15.41	-0.7867E-04	0.021111	237.614	0.859272
28	82.34	1.2898	-0.5916E-03	-0.2851E-08	0.000001	0.349993E-06	0.859272
29	83.23	1.2890	-0.4227E-03	-0.1992E-08	0.000001	0.178702E-06	0.859272
30	84.75	1.2876	0.9059E-06	0.4114E-11	0.000000	0.820657E-12	0.859272
31	87.19	1.2855	0.4999E-05	0.2141E-10	0.000000	0.249852E-10	0.859272
32	87.58	1.2852	0.6404E-06	0.2718E-11	0.000000	0.410170E-12	0.859272

NEDO-33373-A, Revision 5

33	89.82	1.2833	0.3591E-04	0.1447E-09	0.000000	0.128949E-08	0.859272
34	90.26	1.2829	0.4327E-04	0.1726E-09	0.000000	0.187225E-08	0.859272
35	96.62	1.2779	-0.3609E-04	-0.1251E-09	0.000000	0.130247E-08	0.859272
36	97.41	1.2772	-78.24	-0.2668E-03	0.071589	6121.37	0.973815
37	98.21	1.2766	0.2160E-04	0.7241E-10	0.000000	0.466418E-09	0.973815
38	108.9	1.2753	-0.8185E-03	-0.2231E-08	0.000001	0.669925E-06	0.973815
39	117.1	1.2753	0.7377E-03	0.1736E-08	0.000000	0.544222E-06	0.973815
40	119.6	1.2753	-0.3212E-03	-0.7258E-09	0.000000	0.103153E-06	0.973815
41	120.2	1.2753	29.47	0.6589E-04	0.017683	868.331	0.990063
42	122.6	1.2753	0.1033E-02	0.2221E-08	0.000001	0.106743E-05	0.990063
43	123.9	1.2753	-0.3690E-03	-0.7770E-09	0.000000	0.136155E-06	0.990063
44	125.3	1.2753	0.6761E-03	0.1391E-08	0.000000	0.457139E-06	0.990063
45	126.5	1.2753	-0.6724E-04	-0.1357E-09	0.000000	0.452126E-08	0.990063
46	128.2	1.2753	-0.2516E-04	-0.4947E-10	0.000000	0.632973E-09	0.990063
47	131.1	1.2753	0.2863E-03	0.5382E-09	0.000000	0.819768E-07	0.990063
48	131.8	1.2753	-0.2508E-02	-0.4662E-08	0.000001	0.628908E-05	0.990063
49	134.8	1.2753	0.1238E-04	0.2203E-10	0.000000	0.153328E-09	0.990063
50	135.1	1.2753	0.1070E-02	0.1894E-08	0.000001	0.114548E-05	0.990063
51	135.3	1.2753	0.2504E-02	0.4417E-08	0.000001	0.627236E-05	0.990063
52	136.3	1.2753	0.6282E-03	0.1093E-08	0.000000	0.394696E-06	0.990063
53	138.7	1.2753	-0.1239E-03	-0.2080E-09	0.000000	0.153557E-07	0.990063
54	139.5	1.2753	-0.6636E-04	-0.1102E-09	0.000000	0.440429E-08	0.990063
55	142.5	1.2753	0.8709E-03	0.1385E-08	0.000000	0.758415E-06	0.990063
56	143.3	1.2753	-0.7757E-03	-0.1220E-08	0.000000	0.601636E-06	0.990063
57	144.7	1.2753	2.664	0.4112E-05	0.001103	7.09427	0.990196
58	146.9	1.2753	-0.1879E-02	-0.2814E-08	0.000001	0.353094E-05	0.990196
59	149.2	1.2753	-0.3044E-03	-0.4419E-09	0.000000	0.926304E-07	0.990196
60	149.7	1.2753	8.256	0.1190E-04	0.003194	68.1574	0.991471

NEDO-33373-A, Revision 5

61	149.7	1.2753	0.4787E-03	0.6902E-09	0.000000	0.229183E-06	0.991471
62	150.2	1.2753	0.2463E-03	0.3528E-09	0.000000	0.606483E-07	0.991471
63	150.9	1.2753	-0.1925E-03	-0.2731E-09	0.000000	0.370396E-07	0.991471
64	151.7	1.2753	-4.202	-0.5897E-05	0.001582	17.6547	0.991801
65	152.5	1.2753	2.129	0.2958E-05	0.000794	4.53183	0.991886
66	154.3	1.2753	-0.1221E-02	-0.1658E-08	0.000000	0.149137E-05	0.991886
67	155.2	1.2753	15.63	0.2098E-04	0.005630	244.432	0.996460
68	156.2	1.2753	0.1580E-03	0.2091E-09	0.000000	0.249610E-07	0.996460
69	156.6	1.2753	2.553	0.3365E-05	0.000903	6.51883	0.996582
70	156.9	1.2753	0.8242E-03	0.1082E-08	0.000000	0.679318E-06	0.996582
71	157.9	1.2753	0.2134E-02	0.2764E-08	0.000001	0.455457E-05	0.996582
72	159.1	1.2753	0.6478E-03	0.8269E-09	0.000000	0.419606E-06	0.996582
73	161.0	1.2753	0.5900	0.7350E-06	0.000197	0.348091	0.996588
74	161.4	1.2753	-0.8928E-03	-0.1107E-08	0.000000	0.797012E-06	0.996588
75	161.8	1.2753	-0.5393E-01	-0.6654E-07	0.000018	0.290822E-02	0.996588
76	163.8	1.2753	0.4196E-02	0.5049E-08	0.000001	0.176062E-04	0.996588
77	164.1	1.2753	0.3219E-02	0.3861E-08	0.000001	0.103613E-04	0.996588
78	165.7	1.2753	0.4496E-02	0.5291E-08	0.000001	0.202141E-04	0.996588
79	165.7	1.2753	-0.1536E-02	-0.1808E-08	0.000000	0.236080E-05	0.996588
80	166.1	1.2753	0.3660E-02	0.4283E-08	0.000001	0.133971E-04	0.996588
81	168.8	1.2753	0.6594E-01	0.7475E-07	0.000020	0.434764E-02	0.996588
82	170.3	1.2753	0.1061E-02	0.1182E-08	0.000000	0.112676E-05	0.996588
83	170.5	1.2753	-0.5500E-03	-0.6111E-09	0.000000	0.302477E-06	0.996588
84	171.3	1.2753	-0.1891E-03	-0.2082E-09	0.000000	0.357626E-07	0.996588
85	171.5	1.2753	0.1938E-03	0.2128E-09	0.000000	0.375394E-07	0.996588
86	172.1	1.2753	-0.2198	-0.2396E-06	0.000064	0.483034E-01	0.996589
87	172.5	1.2753	0.3272E-03	0.3552E-09	0.000000	0.107056E-06	0.996589
88	173.8	1.2753	0.2800E-03	0.2995E-09	0.000000	0.783932E-07	0.996589

NEDO-33373-A, Revision 5

89	175.6	1.2753	-1.109	-0.1163E-05	0.000312	1.23079	0.996612
90	176.1	1.2753	-0.4358E-04	-0.4540E-10	0.000000	0.189950E-08	0.996612
91	176.9	1.2753	12.83	0.1324E-04	0.003553	164.589	0.999692
92	177.5	1.2753	0.3411E-03	0.3497E-09	0.000000	0.116356E-06	0.999692
93	178.0	1.2753	0.5346E-03	0.5449E-09	0.000000	0.285836E-06	0.999692
94	179.5	1.2753	-0.6347	-0.6364E-06	0.000171	0.402867	0.999700
95	181.3	1.2753	-0.6609E-03	-0.6493E-09	0.000000	0.436784E-06	0.999700
96	182.8	1.2753	-0.2594E-02	-0.2508E-08	0.000001	0.672949E-05	0.999700
97	182.9	1.2753	0.2002	0.1933E-06	0.000052	0.400833E-01	0.999700
98	183.1	1.2753	-0.5805E-02	-0.5596E-08	0.000002	0.336979E-04	0.999700
99	183.9	1.2753	-0.7732E-02	-0.7383E-08	0.000002	0.597878E-04	0.999700
100	185.4	1.2753	4.001	0.3759E-05	0.001009	16.0105	1.00000

SUM OF EFFECTIVE MASSES= 53442.0

1

***** ANSYS - ENGINEERING ANALYSIS SYSTEM RELEASE 10.0 *****

ANSYS Multiphysics

00265621 VERSION=INTEL NT 13:21:12 SEP 07, 2009 CP= 3093.984

SIGNIFICANCE FACTOR FOR COMBINING MODES = 0.10000E-02

SIGNIFICANT MODE COEFFICIENTS (INCLUDING DAMPING)

MODE FREQUENCY DAMPING SV MODE COEF.

12	44.08	0.0000	1.3376	-0.3726E-02
27	80.08	0.0000	1.2919	-0.7867E-04
36	97.41	0.0000	1.2772	-0.2668E-03
41	120.2	0.0000	1.2753	0.6589E-04
57	144.7	0.0000	1.2753	0.4112E-05
60	149.7	0.0000	1.2753	0.1190E-04
64	151.7	0.0000	1.2753	-0.5897E-05

67	155.2	0.0000	1.2753	0.2098E-04
91	176.9	0.0000	1.2753	0.1324E-04
100	185.4	0.0000	1.2753	0.3759E-05

MODAL COMBINATION COEFFICIENTS

MODE= 12 FREQUENCY= 44.083 COUPLING COEF.= 1.000

MODE= 27 FREQUENCY= 80.076 COUPLING COEF.= 1.000

MODE= 36 FREQUENCY= 97.410 COUPLING COEF.= 1.000

MODE= 41 FREQUENCY= 120.191 COUPLING COEF.= 1.000

FREQUENCY 144.66 HERTZ PART OF CLOSELY SPACED GROUP 1

FREQUENCY 149.68 HERTZ PART OF CLOSELY SPACED GROUP 1

FREQUENCY 151.72 HERTZ PART OF CLOSELY SPACED GROUP 1

FREQUENCY 155.16 HERTZ PART OF CLOSELY SPACED GROUP 1

FREQUENCY 176.91 HERTZ PART OF CLOSELY SPACED GROUP 2

FREQUENCY 185.42 HERTZ PART OF CLOSELY SPACED GROUP 2

GROUPING COMBINATION INSTRUCTIONS WRITTEN ON FILE SSE-LOCA-SRVD.mcom

*** NOTE *** CP = 3093.984 TIME= 13:21:12

Solution is done!

FINISH SOLUTION PROCESSING

***** ROUTINE COMPLETED ***** CP = 3093.984

***** ANSYS RESULTS INTERPRETATION (POST1) *****

ENTER /SHOW,DEVICE-NAME TO ENABLE GRAPHIC DISPLAY

ENTER FINISH TO LEAVE POST1

***** INDEX OF DATA SETS ON RESULTS FILE *****

SET TIME/FREQ LOAD STEP SUBSTEP CUMULATIVE

1	13.787	1	1	1
2	16.694	1	2	2
3	17.527	1	3	3
4	30.166	1	4	4

NEDO-33373-A, Revision 5

5	31.986	1	5	5
6	34.314	1	6	6
7	35.742	1	7	7
8	38.570	1	8	8
9	39.424	1	9	9
10	43.442	1	10	10
11	43.462	1	11	11
12	44.083	1	12	12
13	48.220	1	13	13
14	49.093	1	14	14
15	53.200	1	15	15
16	53.881	1	16	16
17	54.147	1	17	17
18	56.504	1	18	18
19	60.155	1	19	19
20	62.622	1	20	20
21	66.521	1	21	21
22	70.010	1	22	22
23	72.363	1	23	23
24	76.339	1	24	24
25	77.976	1	25	25
26	78.469	1	26	26
27	80.076	1	27	27
28	82.336	1	28	28
29	83.232	1	29	29
30	84.749	1	30	30
31	87.192	1	31	31
32	87.575	1	32	32

NEDO-33373-A, Revision 5

33	89.820	1	33	33
34	90.259	1	34	34
35	96.615	1	35	35
36	97.410	1	36	36
37	98.210	1	37	37
38	108.87	1	38	38
39	117.15	1	39	39
40	119.56	1	40	40
41	120.19	1	41	41
42	122.59	1	42	42
43	123.86	1	43	43
44	125.31	1	44	44
45	126.53	1	45	45
46	128.17	1	46	46
47	131.10	1	47	47
48	131.82	1	48	48
49	134.76	1	49	49
50	135.11	1	50	50
51	135.34	1	51	51
52	136.28	1	52	52
53	138.72	1	53	53
54	139.47	1	54	54
55	142.51	1	55	55
56	143.34	1	56	56
57	144.66	1	57	57
58	146.88	1	58	58
59	149.16	1	59	59
60	149.68	1	60	60

NEDO-33373-A, Revision 5

61	149.68	1	61	61
62	150.16	1	62	62
63	150.89	1	63	63
64	151.72	1	64	64
65	152.48	1	65	65
66	154.26	1	66	66
67	155.16	1	67	67
68	156.22	1	68	68
69	156.55	1	69	69
70	156.86	1	70	70
71	157.93	1	71	71
72	159.08	1	72	72
73	161.03	1	73	73
74	161.41	1	74	74
75	161.80	1	75	75
76	163.84	1	76	76
77	164.11	1	77	77
78	165.68	1	78	78
79	165.70	1	79	79
80	166.15	1	80	80
81	168.81	1	81	81
82	170.29	1	82	82
83	170.51	1	83	83
84	171.27	1	84	84
85	171.48	1	85	85
86	172.13	1	86	86
87	172.50	1	87	87
88	173.78	1	88	88

89	175.58	1	89	89
90	176.10	1	90	90
91	176.91	1	91	91
92	177.51	1	92	92
93	178.03	1	93	93
94	179.49	1	94	94
95	181.34	1	95	95
96	182.80	1	96	96
97	182.90	1	97	97
98	183.05	1	98	98
99	183.93	1	99	99
100	185.42	1	100	100

/INPUT FILE= SSE-LOCA-SRVD.mcom LINE= 0

ANSYS RELEASE 10.0 UP20050718 13:20:59 09/07/2009

SSE-LOCA-SRVD.mcom

CURRENT LOAD SET IN DATABASE IS ERASED

LOAD CASE 1 IS LOAD STEP 1 SUBSTEP 2 COMPLEX= 0

FILE= SSE-LOCA-SRVD.rst

LOAD CASE 1 FACTOR SET TO 0.33180

COPY LOAD CASE 1 FROM FILE TO DATABASE

SQUARE THE CURRENT LOAD SET IN DATABASE

LOAD CASE 1 IS LOAD STEP 1 SUBSTEP 6 COMPLEX= 0

FILE= SSE-LOCA-SRVD.rst

LOAD CASE 1 FACTOR SET TO 0.28054E-02

LCOPER OPERATION ADD USING LOAD CASE= 1 FACTOR= 0.28054E-02 ABS= 0

MULTIPLIED BY LOAD CASE= 1 FACTOR= 0.28054E-02 ABS= 0

WRITE LOAD CASE 99 TO FILE SSE-LOCA-SRVD.199

LOAD CASE 1 IS LOAD STEP 1 SUBSTEP 17 COMPLEX= 0

FILE= SSE-LOCA-SRVD.rst

LOAD CASE 1 FACTOR SET TO 0.19395E-01

LOAD CASE 1 ABS KEY SET

COPY LOAD CASE 1 FROM FILE TO DATABASE

LOAD CASE 1 IS LOAD STEP 1 SUBSTEP 18 COMPLEX= 0

FILE= SSE-LOCA-SRVD.rst

LOAD CASE 1 FACTOR SET TO 0.10331E-01

LOAD CASE 1 ABS KEY SET

LCOPER OPERATION ADD USING LOAD CASE= 1 FACTOR= 0.10331E-01 ABS= 1

SQUARE THE CURRENT LOAD SET IN DATABASE

LCOPER OPERATION ADD USING LOAD CASE= 99 FACTOR= 1.0000 ABS= 0

LOAD CASE 1 IS LOAD STEP 1 SUBSTEP 22 COMPLEX= 0

FILE= SSE-LOCA-SRVD.rst

LOAD CASE 1 FACTOR SET TO 0.14403E-02

LCOPER OPERATION ADD USING LOAD CASE= 1 FACTOR= 0.14403E-02 ABS= 0

MULTIPLIED BY LOAD CASE= 1 FACTOR= 0.14403E-02 ABS= 0

LOAD CASE 1 IS LOAD STEP 1 SUBSTEP 25 COMPLEX= 0

FILE= SSE-LOCA-SRVD.rst

LOAD CASE 1 FACTOR SET TO-0.11539E-02

LCOPER OPERATION ADD USING LOAD CASE= 1 FACTOR=-0.11539E-02 ABS= 0

MULTIPLIED BY LOAD CASE= 1 FACTOR=-0.11539E-02 ABS= 0

LOAD CASE 1 IS LOAD STEP 1 SUBSTEP 32 COMPLEX= 0

FILE= SSE-LOCA-SRVD.rst

LOAD CASE 1 FACTOR SET TO-0.53492E-03

LCOPER OPERATION ADD USING LOAD CASE= 1 FACTOR=-0.53492E-03 ABS= 0

MULTIPLIED BY LOAD CASE= 1 FACTOR=-0.53492E-03 ABS= 0

LOAD CASE 1 IS LOAD STEP 1 SUBSTEP 40 COMPLEX= 0

FILE= SSE-LOCA-SRVD.rst

LOAD CASE 1 FACTOR SET TO-0.43649E-03

LCOPER OPERATION ADD USING LOAD CASE= 1 FACTOR=-0.43649E-03 ABS= 0

MULTIPLIED BY LOAD CASE= 1 FACTOR=-0.43649E-03 ABS= 0

TAKE SQRT OF CURRENT LOAD SET IN DATABASE

ANSYS RELEASE 10.0 UP20050718 13:21:01 09/07/2009

SSE-LOCA-SRVD.mcom

SQUARE THE CURRENT LOAD SET IN DATABASE

LOAD CASE 1 IS LOAD STEP 1 SUBSTEP 1 COMPLEX= 0

FILE=SSE-LOCA-SRVD.rst

LOAD CASE 1 FACTOR SET TO 0.51750

LCOPER OPERATION ADD USING LOAD CASE= 1 FACTOR= 0.51750 ABS= 0

MULTIPLIED BY LOAD CASE= 1 FACTOR= 0.51750 ABS= 0

LOAD CASE 1 IS LOAD STEP 1 SUBSTEP 5 COMPLEX= 0

FILE=SSE-LOCA-SRVD.rst

LOAD CASE 1 FACTOR SET TO-0.13705E-02

LCOPER OPERATION ADD USING LOAD CASE= 1 FACTOR=-0.13705E-02 ABS= 0

MULTIPLIED BY LOAD CASE= 1 FACTOR=-0.13705E-02 ABS= 0

LOAD CASE 1 IS LOAD STEP 1 SUBSTEP 9 COMPLEX= 0

FILE=SSE-LOCA-SRVD.rst

LOAD CASE 1 FACTOR SET TO 0.16418E-02

LCOPER OPERATION ADD USING LOAD CASE= 1 FACTOR= 0.16418E-02 ABS= 0

MULTIPLIED BY LOAD CASE= 1 FACTOR= 0.16418E-02 ABS= 0

LOAD CASE 1 IS LOAD STEP 1 SUBSTEP 13 COMPLEX= 0

FILE=SSE-LOCA-SRVD.rst

LOAD CASE 1 FACTOR SET TO-0.59673E-02

LCOPER OPERATION ADD USING LOAD CASE= 1 FACTOR=-0.59673E-02 ABS= 0

MULTIPLIED BY LOAD CASE= 1 FACTOR=-0.59673E-02 ABS= 0

LOAD CASE 1 IS LOAD STEP 1 SUBSTEP 15 COMPLEX= 0

FILE= SSE-LOCA-SRVD.rst

LOAD CASE 1 FACTOR SET TO 0.23484E-01

LCOPER OPERATION ADD USING LOAD CASE= 1 FACTOR= 0.23484E-01 ABS= 0

MULTIPLIED BY LOAD CASE= 1 FACTOR= 0.23484E-01 ABS= 0

LOAD CASE 1 IS LOAD STEP 1 SUBSTEP 19 COMPLEX= 0

FILE= SSE-LOCA-SRVD.rst

LOAD CASE 1 FACTOR SET TO 0.39199E-02

LCOPER OPERATION ADD USING LOAD CASE= 1 FACTOR= 0.39199E-02 ABS= 0

MULTIPLIED BY LOAD CASE= 1 FACTOR= 0.39199E-02 ABS= 0

LOAD CASE 1 IS LOAD STEP 1 SUBSTEP 23 COMPLEX= 0

FILE= SSE-LOCA-SRVD.rst

LOAD CASE 1 FACTOR SET TO -0.92184E-03

LCOPER OPERATION ADD USING LOAD CASE= 1 FACTOR= -0.92184E-03 ABS= 0

MULTIPLIED BY LOAD CASE= 1 FACTOR= -0.92184E-03 ABS= 0

TAKE SQRT OF CURRENT LOAD SET IN DATABASE

ANSYS RELEASE 10.0 UP20050718 13:21:02 09/07/2009

SSE-LOCA-SRVD.mcom

SQUARE THE CURRENT LOAD SET IN DATABASE

LOAD CASE 1 IS LOAD STEP 1 SUBSTEP 12 COMPLEX= 0

FILE= SSE-LOCA-SRVD.rst

LOAD CASE 1 FACTOR SET TO-0.43400E-01

LCOPER OPERATION ADD USING LOAD CASE= 1 FACTOR=-0.43400E-01 ABS= 0

MULTIPLIED BY LOAD CASE= 1 FACTOR=-0.43400E-01 ABS= 0

LOAD CASE 1 IS LOAD STEP 1 SUBSTEP 27 COMPLEX= 0

FILE= SSE-LOCA-SRVD.rst

LOAD CASE 1 FACTOR SET TO-0.58506E-03

LCOPER OPERATION ADD USING LOAD CASE= 1 FACTOR=-0.58506E-03 ABS= 0

MULTIPLIED BY LOAD CASE= 1 FACTOR=-0.58506E-03 ABS= 0

LOAD CASE 1 IS LOAD STEP 1 SUBSTEP 36 COMPLEX= 0

FILE= SSE-LOCA-SRVD.rst

LOAD CASE 1 FACTOR SET TO-0.18228E-02

LCOPER OPERATION ADD USING LOAD CASE= 1 FACTOR=-0.18228E-02 ABS= 0

MULTIPLIED BY LOAD CASE= 1 FACTOR=-0.18228E-02 ABS= 0

LOAD CASE 1 IS LOAD STEP 1 SUBSTEP 41 COMPLEX= 0

FILE= SSE-LOCA-SRVD.rst

LOAD CASE 1 FACTOR SET TO 0.44599E-03

LCOPER OPERATION ADD USING LOAD CASE= 1 FACTOR= 0.44599E-03 ABS= 0

MULTIPLIED BY LOAD CASE= 1 FACTOR= 0.44599E-03 ABS= 0

WRITE LOAD CASE 99 TO FILE SSE-LOCA-SRVD.199

LOAD CASE 1 IS LOAD STEP 1 SUBSTEP 60 COMPLEX= 0

FILE= SSE-LOCA-SRVD.rst

LOAD CASE 1 FACTOR SET TO 0.80569E-04

LOAD CASE 1 ABS KEY SET

COPY LOAD CASE 1 FROM FILE TO DATABASE

LOAD CASE 1 IS LOAD STEP 1 SUBSTEP 67 COMPLEX= 0

FILE= SSE-LOCA-SRVD.rst

LOAD CASE 1 FACTOR SET TO 0.14198E-03

LOAD CASE 1 ABS KEY SET

LCOPER OPERATION ADD USING LOAD CASE= 1 FACTOR= 0.14198E-03 ABS= 1

SQUARE THE CURRENT LOAD SET IN DATABASE

LCOPER OPERATION ADD USING LOAD CASE= 99 FACTOR= 1.0000 ABS= 0

LOAD CASE 1 IS LOAD STEP 1 SUBSTEP 91 COMPLEX= 0

FILE= SSE-LOCA-SRVD.rst

LOAD CASE 1 FACTOR SET TO 0.89622E-04

LCOPER OPERATION ADD USING LOAD CASE= 1 FACTOR= 0.89622E-04 ABS= 0

MULTIPLIED BY LOAD CASE= 1 FACTOR= 0.89622E-04 ABS= 0

TAKE SQRT OF CURRENT LOAD SET IN DATABASE

ANSYS RELEASE 10.0 UP20050718 13:21:04 09/07/2009

SSE-LOCA-SRVD.mcom

SQUARE THE CURRENT LOAD SET IN DATABASE

LOAD CASE 1 IS LOAD STEP 1 SUBSTEP 2 COMPLEX= 0

FILE= SSE-LOCA-SRVD.rst

LOAD CASE 1 FACTOR SET TO 0.15651E-01

LCOOPER OPERATION ADD USING LOAD CASE= 1 FACTOR= 0.15651E-01 ABS= 0

MULTIPLIED BY LOAD CASE= 1 FACTOR= 0.15651E-01 ABS= 0

LOAD CASE 1 IS LOAD STEP 1 SUBSTEP 6 COMPLEX= 0

FILE= SSE-LOCA-SRVD.rst

LOAD CASE 1 FACTOR SET TO 0.13333E-03

LCOOPER OPERATION ADD USING LOAD CASE= 1 FACTOR= 0.13333E-03 ABS= 0

MULTIPLIED BY LOAD CASE= 1 FACTOR= 0.13333E-03 ABS= 0

WRITE LOAD CASE 99 TO FILE SSE-LOCA-SRVD.199

LOAD CASE 1 IS LOAD STEP 1 SUBSTEP 17 COMPLEX= 0

FILE= SSE-LOCA-SRVD.rst

LOAD CASE 1 FACTOR SET TO 0.88271E-03

LOAD CASE 1 ABS KEY SET

COPY LOAD CASE 1 FROM FILE TO DATABASE

LOAD CASE 1 IS LOAD STEP 1 SUBSTEP 18 COMPLEX= 0

FILE= SSE-LOCA-SRVD.rst

LOAD CASE 1 FACTOR SET TO 0.47774E-03

LOAD CASE 1 ABS KEY SET

LCOPER OPERATION ADD USING LOAD CASE= 1 FACTOR= 0.47774E-03 ABS= 1

SQUARE THE CURRENT LOAD SET IN DATABASE

LCOPER OPERATION ADD USING LOAD CASE= 99 FACTOR= 1.0000 ABS= 0

LOAD CASE 1 IS LOAD STEP 1 SUBSTEP 22 COMPLEX= 0

FILE= SSE-LOCA-SRVD.rst

LOAD CASE 1 FACTOR SET TO 0.81891E-04

LCOPER OPERATION ADD USING LOAD CASE= 1 FACTOR= 0.81891E-04 ABS= 0

MULTIPLIED BY LOAD CASE= 1 FACTOR= 0.81891E-04 ABS= 0

LOAD CASE 1 IS LOAD STEP 1 SUBSTEP 25 COMPLEX= 0

FILE= SSE-LOCA-SRVD.rst

LOAD CASE 1 FACTOR SET TO-0.64937E-04

LCOPER OPERATION ADD USING LOAD CASE= 1 FACTOR=-0.64937E-04 ABS= 0

MULTIPLIED BY LOAD CASE= 1 FACTOR=-0.64937E-04 ABS= 0

LOAD CASE 1 IS LOAD STEP 1 SUBSTEP 32 COMPLEX= 0

FILE= SSE-LOCA-SRVD.rst

LOAD CASE 1 FACTOR SET TO-0.29773E-04

LCOPER OPERATION ADD USING LOAD CASE= 1 FACTOR=-0.29773E-04 ABS= 0

MULTIPLIED BY LOAD CASE= 1 FACTOR=-0.29773E-04 ABS= 0

LOAD CASE 1 IS LOAD STEP 1 SUBSTEP 40 COMPLEX= 0

FILE= SSE-LOCA-SRVD.rst

LOAD CASE 1 FACTOR SET TO-0.24903E-04

LCOPER OPERATION ADD USING LOAD CASE= 1 FACTOR=-0.24903E-04 ABS= 0

MULTIPLIED BY LOAD CASE= 1 FACTOR=-0.24903E-04 ABS= 0

TAKE SQRT OF CURRENT LOAD SET IN DATABASE

ANSYS RELEASE 10.0 UP20050718 13:21:05 09/07/2009

SSE-LOCA-SRVD.mcom

SQUARE THE CURRENT LOAD SET IN DATABASE

LOAD CASE 1 IS LOAD STEP 1 SUBSTEP 1 COMPLEX= 0

FILE= SSE-LOCA-SRVD.rst

LOAD CASE 1 FACTOR SET TO 0.25423E-01

LCOPER OPERATION ADD USING LOAD CASE= 1 FACTOR= 0.25423E-01 ABS= 0

MULTIPLIED BY LOAD CASE= 1 FACTOR= 0.25423E-01 ABS= 0

LOAD CASE 1 IS LOAD STEP 1 SUBSTEP 5 COMPLEX= 0

FILE= SSE-LOCA-SRVD.rst

LOAD CASE 1 FACTOR SET TO-0.64457E-04

LCOPER OPERATION ADD USING LOAD CASE= 1 FACTOR=-0.64457E-04 ABS= 0

MULTIPLIED BY LOAD CASE= 1 FACTOR=-0.64457E-04 ABS= 0

LOAD CASE 1 IS LOAD STEP 1 SUBSTEP 9 COMPLEX= 0

FILE= SSE-LOCA-SRVD.rst

LOAD CASE 1 FACTOR SET TO 0.68403E-04

LCOPER OPERATION ADD USING LOAD CASE= 1 FACTOR= 0.68403E-04 ABS= 0

MULTIPLIED BY LOAD CASE= 1 FACTOR= 0.68403E-04 ABS= 0

LOAD CASE 1 IS LOAD STEP 1 SUBSTEP 13 COMPLEX= 0

FILE= SSE-LOCA-SRVD.rst

LOAD CASE 1 FACTOR SET TO-0.26679E-03

LCOPER OPERATION ADD USING LOAD CASE= 1 FACTOR=-0.26679E-03 ABS= 0

MULTIPLIED BY LOAD CASE= 1 FACTOR=-0.26679E-03 ABS= 0

LOAD CASE 1 IS LOAD STEP 1 SUBSTEP 15 COMPLEX= 0

FILE= SSE-LOCA-SRVD.rst

LOAD CASE 1 FACTOR SET TO 0.10402E-02

LCOPER OPERATION ADD USING LOAD CASE= 1 FACTOR= 0.10402E-02 ABS= 0

MULTIPLIED BY LOAD CASE= 1 FACTOR= 0.10402E-02 ABS= 0

LOAD CASE 1 IS LOAD STEP 1 SUBSTEP 19 COMPLEX= 0

FILE= SSE-LOCA-SRVD.rst

LOAD CASE 1 FACTOR SET TO 0.18688E-03

LCOPER OPERATION ADD USING LOAD CASE= 1 FACTOR= 0.18688E-03 ABS= 0

MULTIPLIED BY LOAD CASE= 1 FACTOR= 0.18688E-03 ABS= 0

LOAD CASE 1 IS LOAD STEP 1 SUBSTEP 23 COMPLEX= 0

FILE= SSE-LOCA-SRVD.rst

LOAD CASE 1 FACTOR SET TO-0.57976E-04

LCOPER OPERATION ADD USING LOAD CASE= 1 FACTOR=-0.57976E-04 ABS= 0

MULTIPLIED BY LOAD CASE= 1 FACTOR=-0.57976E-04 ABS= 0

LOAD CASE 1 IS LOAD STEP 1 SUBSTEP 29 COMPLEX= 0

FILE= SSE-LOCA-SRVD.rst

LOAD CASE 1 FACTOR SET TO-0.29222E-04

LCOPER OPERATION ADD USING LOAD CASE= 1 FACTOR=-0.29222E-04 ABS= 0

MULTIPLIED BY LOAD CASE= 1 FACTOR=-0.29222E-04 ABS= 0

LOAD CASE 1 IS LOAD STEP 1 SUBSTEP 35 COMPLEX= 0

FILE= SSE-LOCA-SRVD.rst

LOAD CASE 1 FACTOR SET TO-0.33582E-04

LCOPER OPERATION ADD USING LOAD CASE= 1 FACTOR=-0.33582E-04 ABS= 0

MULTIPLIED BY LOAD CASE= 1 FACTOR=-0.33582E-04 ABS= 0

LOAD CASE 1 IS LOAD STEP 1 SUBSTEP 39 COMPLEX= 0

FILE= SSE-LOCA-SRVD.rst

LOAD CASE 1 FACTOR SET TO-0.25722E-04

LCOPER OPERATION ADD USING LOAD CASE= 1 FACTOR=-0.25722E-04 ABS= 0

MULTIPLIED BY LOAD CASE= 1 FACTOR=-0.25722E-04 ABS= 0

TAKE SQRT OF CURRENT LOAD SET IN DATABASE

ANSYS RELEASE 10.0 UP20050718 13:21:07 09/07/2009

SSE-LOCA-SRVD.mcom

SQUARE THE CURRENT LOAD SET IN DATABASE

LOAD CASE 1 IS LOAD STEP 1 SUBSTEP 12 COMPLEX= 0

FILE= SSE-LOCA-SRVD.rst

LOAD CASE 1 FACTOR SET TO-0.40696E-02

LCOPER OPERATION ADD USING LOAD CASE= 1 FACTOR=-0.40696E-02 ABS= 0

MULTIPLIED BY LOAD CASE= 1 FACTOR=-0.40696E-02 ABS= 0

LOAD CASE 1 IS LOAD STEP 1 SUBSTEP 27 COMPLEX= 0

FILE= SSE-LOCA-SRVD.rst

LOAD CASE 1 FACTOR SET TO-0.85041E-04

LCOPER OPERATION ADD USING LOAD CASE= 1 FACTOR=-0.85041E-04 ABS= 0

MULTIPLIED BY LOAD CASE= 1 FACTOR=-0.85041E-04 ABS= 0

LOAD CASE 1 IS LOAD STEP 1 SUBSTEP 36 COMPLEX= 0

FILE= SSE-LOCA-SRVD.rst

LOAD CASE 1 FACTOR SET TO-0.28742E-03

LCOPER OPERATION ADD USING LOAD CASE= 1 FACTOR=-0.28742E-03 ABS= 0

MULTIPLIED BY LOAD CASE= 1 FACTOR=-0.28742E-03 ABS= 0

LOAD CASE 1 IS LOAD STEP 1 SUBSTEP 41 COMPLEX= 0

FILE= SSE-LOCA-SRVD.rst

LOAD CASE 1 FACTOR SET TO 0.70963E-04

LCOPER OPERATION ADD USING LOAD CASE= 1 FACTOR= 0.70963E-04 ABS= 0

MULTIPLIED BY LOAD CASE= 1 FACTOR= 0.70963E-04 ABS= 0

WRITE LOAD CASE 99 TO FILE SSE-LOCA-SRVD.I99

LOAD CASE 1 IS LOAD STEP 1 SUBSTEP 57 COMPLEX= 0

FILE= SSE-LOCA-SRVD.rst

LOAD CASE 1 FACTOR SET TO 0.44278E-05

LOAD CASE 1 ABS KEY SET

COPY LOAD CASE 1 FROM FILE TO DATABASE

LOAD CASE 1 IS LOAD STEP 1 SUBSTEP 60 COMPLEX= 0

FILE= SSE-LOCA-SRVD.rst

LOAD CASE 1 FACTOR SET TO 0.12820E-04

LOAD CASE 1 ABS KEY SET

LCOPER OPERATION ADD USING LOAD CASE= 1 FACTOR= 0.12820E-04 ABS= 1

LOAD CASE 1 IS LOAD STEP 1 SUBSTEP 64 COMPLEX= 0

FILE= SSE-LOCA-SRVD.rst

LOAD CASE 1 FACTOR SET TO 0.63505E-05

LOAD CASE 1 ABS KEY SET

LCOPER OPERATION ADD USING LOAD CASE= 1 FACTOR= 0.63505E-05 ABS= 1

LOAD CASE 1 IS LOAD STEP 1 SUBSTEP 67 COMPLEX= 0

FILE= SSE-LOCA-SRVD.rst

LOAD CASE 1 FACTOR SET TO 0.22592E-04

LOAD CASE 1 ABS KEY SET

LCOPER OPERATION ADD USING LOAD CASE= 1 FACTOR= 0.22592E-04 ABS= 1

SQUARE THE CURRENT LOAD SET IN DATABASE

LCOPER OPERATION ADD USING LOAD CASE= 99 FACTOR= 1.0000 ABS= 0

LOAD CASE 1 IS LOAD STEP 1 SUBSTEP 91 COMPLEX= 0

FILE= SSE-LOCA-SRVD.rst

LOAD CASE 1 FACTOR SET TO 0.14260E-04

LCOPER OPERATION ADD USING LOAD CASE= 1 FACTOR= 0.14260E-04 ABS= 0

MULTIPLIED BY LOAD CASE= 1 FACTOR= 0.14260E-04 ABS= 0

TAKE SQRT OF CURRENT LOAD SET IN DATABASE

ANSYS RELEASE 10.0 UP20050718 13:21:09 09/07/2009

SSE-LOCA-SRVD.mcom

SQUARE THE CURRENT LOAD SET IN DATABASE

LOAD CASE 1 IS LOAD STEP 1 SUBSTEP 2 COMPLEX= 0

FILE= SSE-LOCA-SRVD.rst

LOAD CASE 1 FACTOR SET TO 0.30104E-01

LCOPER OPERATION ADD USING LOAD CASE= 1 FACTOR= 0.30104E-01 ABS= 0

MULTIPLIED BY LOAD CASE= 1 FACTOR= 0.30104E-01 ABS= 0

LOAD CASE 1 IS LOAD STEP 1 SUBSTEP 6 COMPLEX= 0

FILE= SSE-LOCA-SRVD.rst

LOAD CASE 1 FACTOR SET TO 0.79655E-04

LCOPER OPERATION ADD USING LOAD CASE= 1 FACTOR= 0.79655E-04 ABS= 0

MULTIPLIED BY LOAD CASE= 1 FACTOR= 0.79655E-04 ABS= 0

WRITE LOAD CASE 99 TO FILE SSE-LOCA-SRVD.199

LOAD CASE 1 IS LOAD STEP 1 SUBSTEP 17 COMPLEX= 0

FILE= SSE-LOCA-SRVD.rst

LOAD CASE 1 FACTOR SET TO 0.42066E-03

LOAD CASE 1 ABS KEY SET

COPY LOAD CASE 1 FROM FILE TO DATABASE

LOAD CASE 1 IS LOAD STEP 1 SUBSTEP 18 COMPLEX= 0

FILE= SSE-LOCA-SRVD.rst

LOAD CASE 1 FACTOR SET TO 0.22556E-03

LOAD CASE 1 ABS KEY SET

LCOPER OPERATION ADD USING LOAD CASE= 1 FACTOR= 0.22556E-03 ABS= 1

SQUARE THE CURRENT LOAD SET IN DATABASE

LCOPER OPERATION ADD USING LOAD CASE= 99 FACTOR= 1.0000 ABS= 0

LOAD CASE 1 IS LOAD STEP 1 SUBSTEP 22 COMPLEX= 0

FILE= SSE-LOCA-SRVD.rst

LOAD CASE 1 FACTOR SET TO 0.36891E-04

LCOPER OPERATION ADD USING LOAD CASE= 1 FACTOR= 0.36891E-04 ABS= 0

MULTIPLIED BY LOAD CASE= 1 FACTOR= 0.36891E-04 ABS= 0

TAKE SQRT OF CURRENT LOAD SET IN DATABASE

ANSYS RELEASE 10.0 UP20050718 13:21:10 09/07/2009

SSE-LOCA-SRVD.mcom

SQUARE THE CURRENT LOAD SET IN DATABASE

LOAD CASE 1 IS LOAD STEP 1 SUBSTEP 1 COMPLEX= 0

FILE= SSE-LOCA-SRVD.rst

LOAD CASE 1 FACTOR SET TO 0.54236E-01

LCOPER OPERATION ADD USING LOAD CASE= 1 FACTOR= 0.54236E-01 ABS= 0

MULTIPLIED BY LOAD CASE= 1 FACTOR= 0.54236E-01 ABS= 0

LOAD CASE 1 IS LOAD STEP 1 SUBSTEP 13 COMPLEX= 0

FILE= SSE-LOCA-SRVD.rst

LOAD CASE 1 FACTOR SET TO -0.13041E-03

LCOPER OPERATION ADD USING LOAD CASE= 1 FACTOR= -0.13041E-03 ABS= 0

MULTIPLIED BY LOAD CASE= 1 FACTOR= -0.13041E-03 ABS= 0

LOAD CASE 1 IS LOAD STEP 1 SUBSTEP 15 COMPLEX= 0

FILE= SSE-LOCA-SRVD.rst

LOAD CASE 1 FACTOR SET TO 0.49762E-03

LCOPER OPERATION ADD USING LOAD CASE= 1 FACTOR= 0.49762E-03 ABS= 0

MULTIPLIED BY LOAD CASE= 1 FACTOR= 0.49762E-03 ABS= 0

LOAD CASE 1 IS LOAD STEP 1 SUBSTEP 19 COMPLEX= 0

FILE= SSE-LOCA-SRVD.rst

LOAD CASE 1 FACTOR SET TO 0.87031E-04

LCOPER OPERATION ADD USING LOAD CASE= 1 FACTOR= 0.87031E-04 ABS= 0

MULTIPLIED BY LOAD CASE= 1 FACTOR= 0.87031E-04 ABS= 0

TAKE SQRT OF CURRENT LOAD SET IN DATABASE

ANSYS RELEASE 10.0 UP20050718 13:21:12 09/07/2009

SSE-LOCA-SRVD.mcom

SQUARE THE CURRENT LOAD SET IN DATABASE

LOAD CASE 1 IS LOAD STEP 1 SUBSTEP 12 COMPLEX= 0

FILE= SSE-LOCA-SRVD.rst

LOAD CASE 1 FACTOR SET TO-0.37264E-02

LCOPER OPERATION ADD USING LOAD CASE= 1 FACTOR=-0.37264E-02 ABS= 0

MULTIPLIED BY LOAD CASE= 1 FACTOR=-0.37264E-02 ABS= 0

LOAD CASE 1 IS LOAD STEP 1 SUBSTEP 27 COMPLEX= 0

FILE= SSE-LOCA-SRVD.rst

LOAD CASE 1 FACTOR SET TO-0.78668E-04

LCOPER OPERATION ADD USING LOAD CASE= 1 FACTOR=-0.78668E-04 ABS= 0

MULTIPLIED BY LOAD CASE= 1 FACTOR=-0.78668E-04 ABS= 0

LOAD CASE 1 IS LOAD STEP 1 SUBSTEP 36 COMPLEX= 0

FILE= SSE-LOCA-SRVD.rst

LOAD CASE 1 FACTOR SET TO-0.26677E-03

LCOPER OPERATION ADD USING LOAD CASE= 1 FACTOR=-0.26677E-03 ABS= 0

MULTIPLIED BY LOAD CASE= 1 FACTOR=-0.26677E-03 ABS= 0

LOAD CASE 1 IS LOAD STEP 1 SUBSTEP 41 COMPLEX= 0

FILE= SSE-LOCA-SRVD.rst

LOAD CASE 1 FACTOR SET TO 0.65895E-04

LCOPER OPERATION ADD USING LOAD CASE= 1 FACTOR= 0.65895E-04 ABS= 0

MULTIPLIED BY LOAD CASE= 1 FACTOR= 0.65895E-04 ABS= 0

WRITE LOAD CASE 99 TO FILE SSE-LOCA-SRVD.I99

LOAD CASE 1 IS LOAD STEP 1 SUBSTEP 57 COMPLEX= 0

FILE= SSE-LOCA-SRVD.rst

LOAD CASE 1 FACTOR SET TO 0.41116E-05

LOAD CASE 1 ABS KEY SET

COPY LOAD CASE 1 FROM FILE TO DATABASE

LOAD CASE 1 IS LOAD STEP 1 SUBSTEP 60 COMPLEX= 0

FILE= SSE-LOCA-SRVD.rst

LOAD CASE 1 FACTOR SET TO 0.11904E-04

LOAD CASE 1 ABS KEY SET

LCOPER OPERATION ADD USING LOAD CASE= 1 FACTOR= 0.11904E-04 ABS= 1

LOAD CASE 1 IS LOAD STEP 1 SUBSTEP 64 COMPLEX= 0

FILE= SSE-LOCA-SRVD.rst

LOAD CASE 1 FACTOR SET TO 0.58969E-05

LOAD CASE 1 ABS KEY SET

LCOPER OPERATION ADD USING LOAD CASE= 1 FACTOR= 0.58969E-05 ABS= 1

LOAD CASE 1 IS LOAD STEP 1 SUBSTEP 67 COMPLEX= 0

FILE= SSE-LOCA-SRVD.rst

LOAD CASE 1 FACTOR SET TO 0.20978E-04

LOAD CASE 1 ABS KEY SET

LCOPER OPERATION ADD USING LOAD CASE= 1 FACTOR= 0.20978E-04 ABS= 1

SQUARE THE CURRENT LOAD SET IN DATABASE

LCOPER OPERATION ADD USING LOAD CASE= 99 FACTOR= 1.0000 ABS= 0

WRITE LOAD CASE 99 TO FILE SSE-LOCA-SRVD.I99

LOAD CASE 1 IS LOAD STEP 1 SUBSTEP 91 COMPLEX= 0

FILE= SSE-LOCA-SRVD.rst

LOAD CASE 1 FACTOR SET TO 0.13242E-04

LOAD CASE 1 ABS KEY SET

COPY LOAD CASE 1 FROM FILE TO DATABASE

LOAD CASE 1 IS LOAD STEP 1 SUBSTEP 100 COMPLEX= 0

FILE= SSE-LOCA-SRVD.rst

LOAD CASE 1 FACTOR SET TO 0.37595E-05

LOAD CASE 1 ABS KEY SET

LCOPER OPERATION ADD USING LOAD CASE= 1 FACTOR= 0.37595E-05 ABS= 1

SQUARE THE CURRENT LOAD SET IN DATABASE

LCOPER OPERATION ADD USING LOAD CASE= 99 FACTOR= 1.0000 ABS= 0

TAKE SQRT OF CURRENT LOAD SET IN DATABASE

WRITE LOAD CASE 1 TO FILE SSE-LOCA-SRVD.I01

LOAD CASE 1 IS LOAD STEP 1 SUBSTEP 1 COMPLEX= 0

FILE= D+B.I01

LOAD CASE 2 IS LOAD STEP 1 SUBSTEP 1 COMPLEX= 0

FILE= fuelhandling.I01

LOAD CASE 3 IS LOAD STEP 1 SUBSTEP 1 COMPLEX= 0

FILE= SSE-LOCA-SRVD.I01

COPY LOAD CASE 1 FROM FILE TO DATABASE

LCOPER OPERATION ADD USING LOAD CASE= 2 FACTOR= 1.0000 ABS= 0

WRITE LOAD CASE 1 TO FILE level_A.I01

LOAD CASE 1 ABS KEY SET

COPY LOAD CASE 3 FROM FILE TO DATABASE

LCOPER OPERATION ADD USING LOAD CASE= 1 FACTOR= 1.0000 ABS= 1

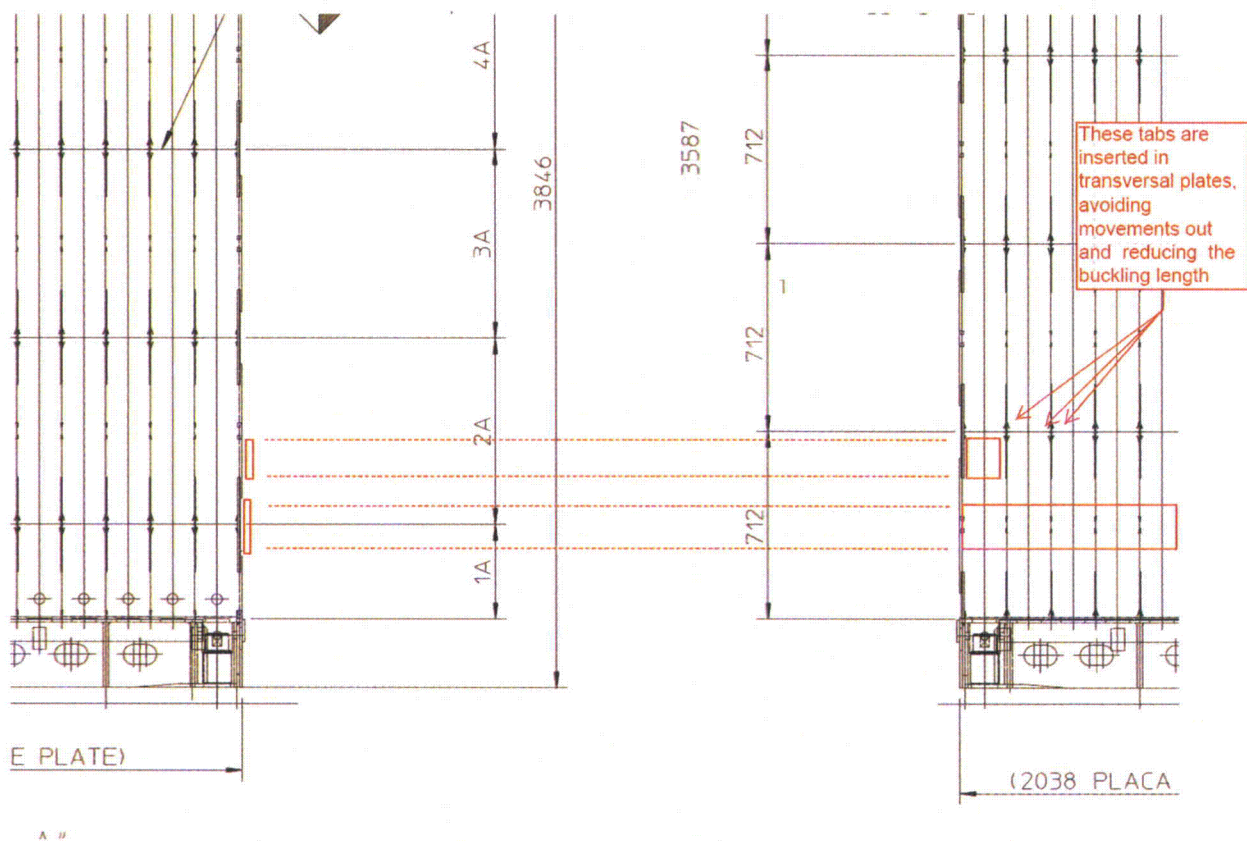
WRITE LOAD CASE 1 TO FILE level_D.101

APPENDIX B1 - Analysis Of Compressive Stresses

The conceptual design of the Interlock cell matrix racks includes multiple connections between plates. So the lateral Plain SS structural plates are braced, at several points, to transversal plates that limit the buckling length. Additionally, for this ESBWR application, we are using thick plates (10 mm and 7 mm)*. As a result, the buckling stress limits are greater than the allowable stress limit considered in this report.

Following is a calculation of the allowable buckling stress:

For lateral 10 mm plate, the typical unbraced portion of lateral plates can be seen below.



The typical unbraced length is about $712/4 = 178$ mm.

Therefore, the buckling calculation is performed for a 10 mm plate with a span of 178 mm.

* The allowable buckling stress depends on the relation between the thickness of the plate and the length of the plate.

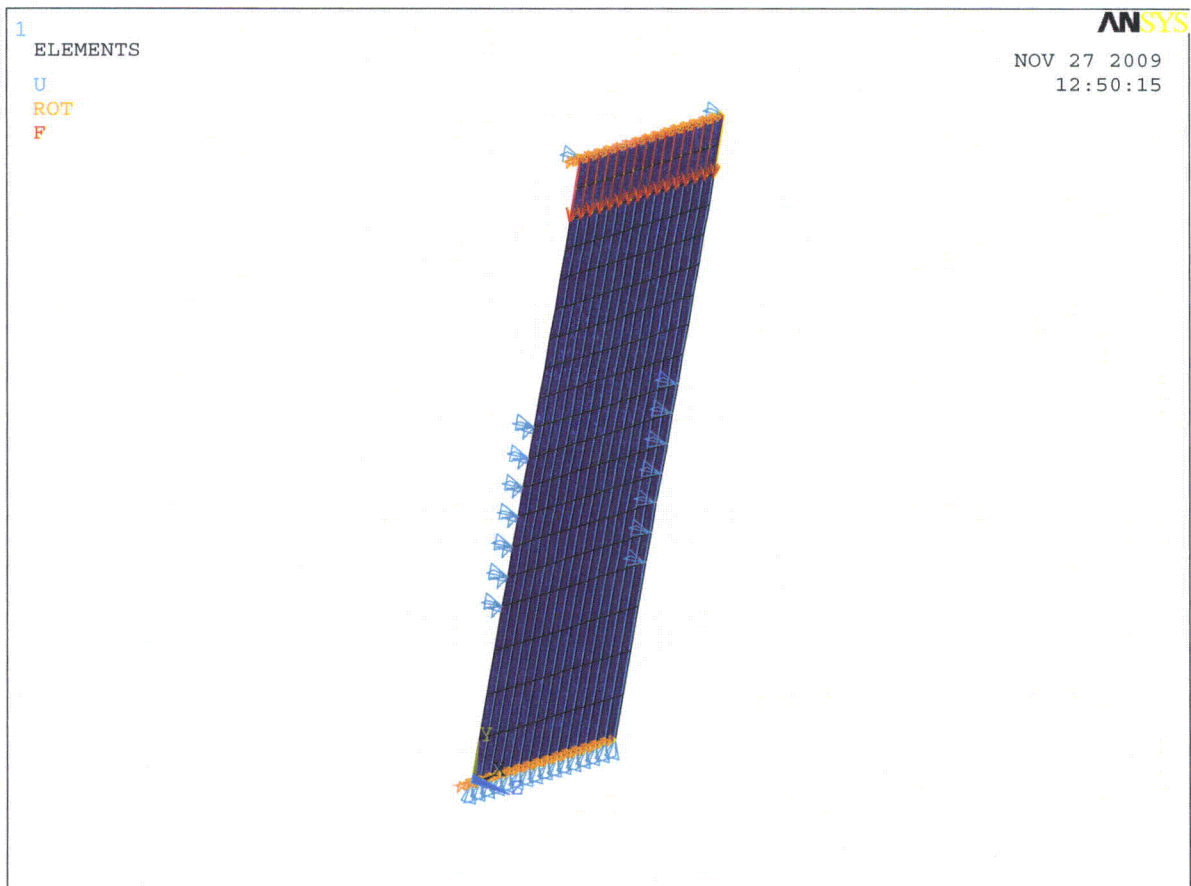
The Euler buckling formula, which is too conservative for this case, gives a buckling stress of

$$\sigma = \frac{\pi^2 \cdot E}{12 \cdot (1 - \nu^2)} \cdot \left(\frac{e}{h}\right)^2 = \frac{\pi^2 \cdot 1.95E5}{12 \cdot (1 - \nu^2)} \cdot \left(\frac{10}{178}\right)^2 = 555.68 N / mm^2$$

But additionally, since the boundary conditions for the above plates are somewhat complicated, an ANSYS FEM eigen buckling analysis was made.

The typical lateral plate portion located between two transversal plates (pitch = 168 mm) is modeled.

The mesh corresponds to a portion of 168x(712/2= 356) mm.



Mesh for Eigen Buckling and Boundary Conditions

A unitary 10 N/mm² stress was considered.

The ANSYS results are:

***** EIGENVALUES (LOAD MULTIPLIERS FOR BUCKLING) *****

*** FROM BLOCK LANCZOS ITERATION ***

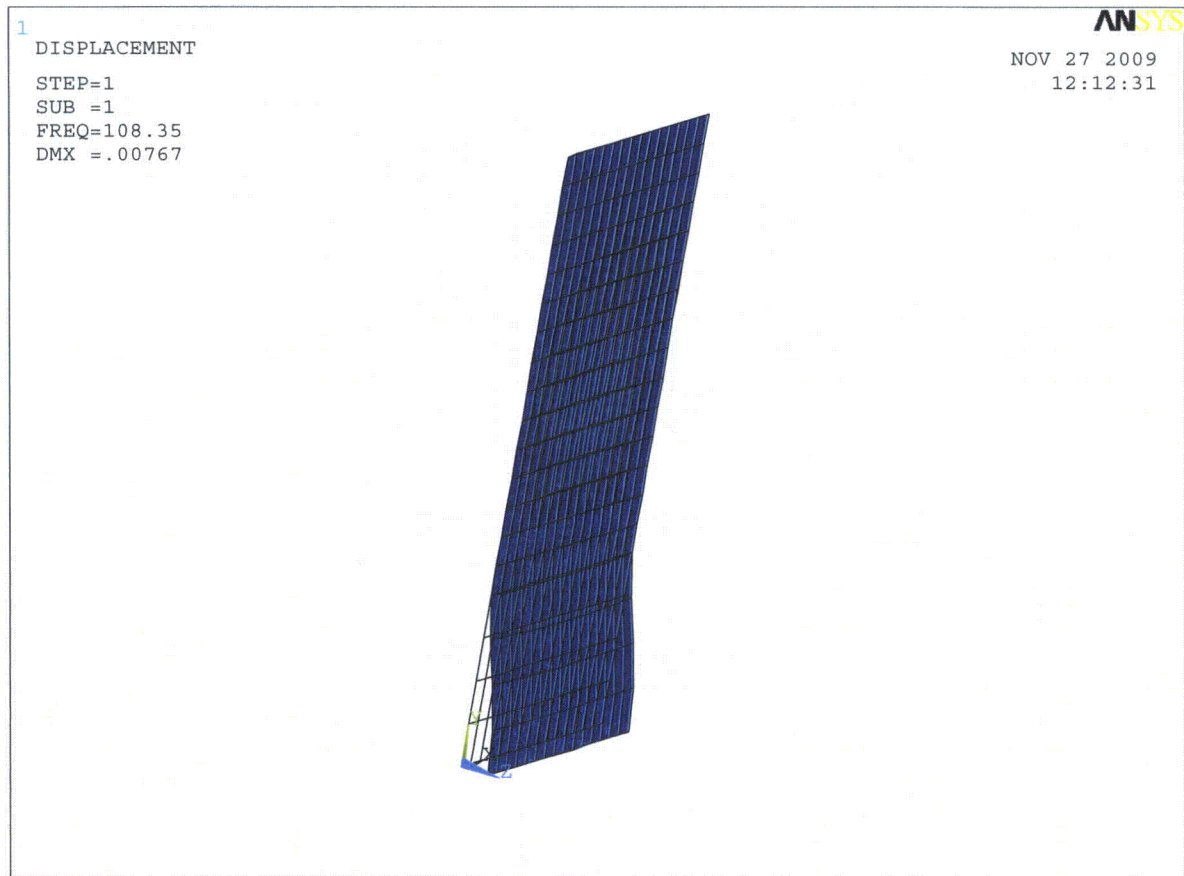
SHAPE NUMBER LOAD MULTIPLIER

1 108.35012

2 204.05621

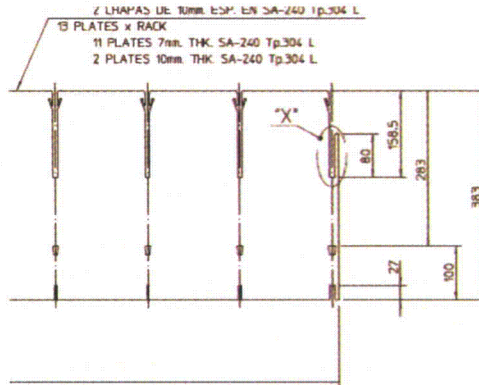
3 248.95131

First buckling mode

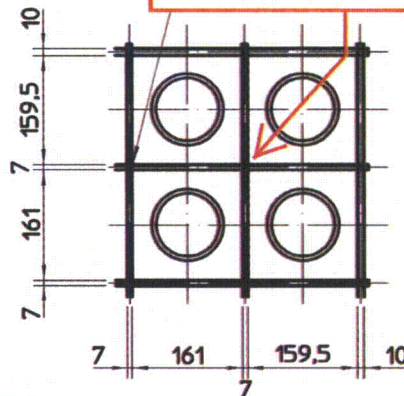


So the allowable buckling stress is $10 \cdot 108.35 \text{ N/mm}^2 = 1083.5 \text{ N/mm}^2$. If we use the safety coefficient required in F-1331.5, the allowable buckling stress = $2/3 \cdot 1083.5 = 722.3 \text{ N/mm}^2$, which is larger than the allowable limits considered in the analysis and much larger than any compressive general membrane stress in lateral plate. Therefore, allowable buckling loads are not limiting.

Upper 7 and 10 mm plates:



transversal plates are linked by the tabs



Applying the conservative euler formula, and considering a free span of a pitch = 168 mm for 10 mm plates:

$$\sigma = \frac{\pi^2 \cdot E}{12 \cdot (1 - \nu^2)} \cdot \left(\frac{e}{h}\right)^2 = \frac{\pi^2 \cdot 1.95E5}{12 \cdot (1 - \nu^2)} \cdot \left(\frac{10}{178}\right)^2 = 555.68 N / mm^2$$

And considering the internal 7 mm plates have some intermediate between clamped and simple supported boundary condition:

If we use the safety coefficient required in F-1331.5, as follows:

$$\sigma = \frac{\pi^2 \cdot E}{12 \cdot (1 - \nu^2)} \cdot \left(\frac{e}{h}\right)^2 = \frac{\pi^2 \cdot 1.95E5}{12 \cdot (1 - \nu^2)} \cdot \left(\frac{7}{0.7 \cdot 168}\right)^2 = 623.8 N / mm^2$$

The allowable buckling stress = $2/3 \cdot 555.68 = 370.5 \text{ N/mm}^2$, which is larger than the allowable limits considered in the analysis and much larger than any compressive general membrane stress in the lateral plate. Therefore, allowable buckling loads are not limiting.

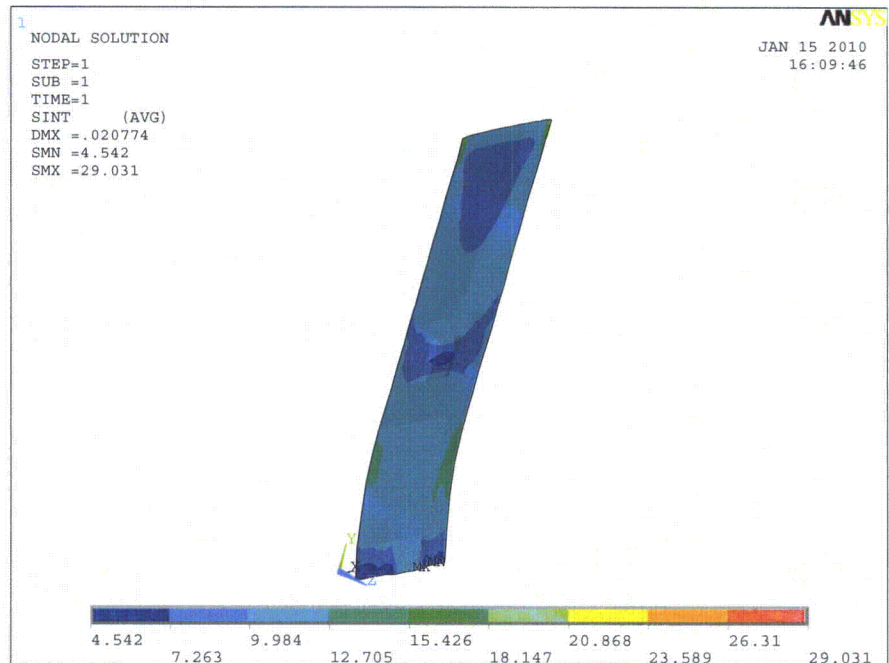
Potential Manufacturing Imperfections

The manufacturing of racks will be done according to the ASME Code, which limits the imperfections. The allowable compressible stress, if we consider potential imperfections, is very similar to the results obtained above.

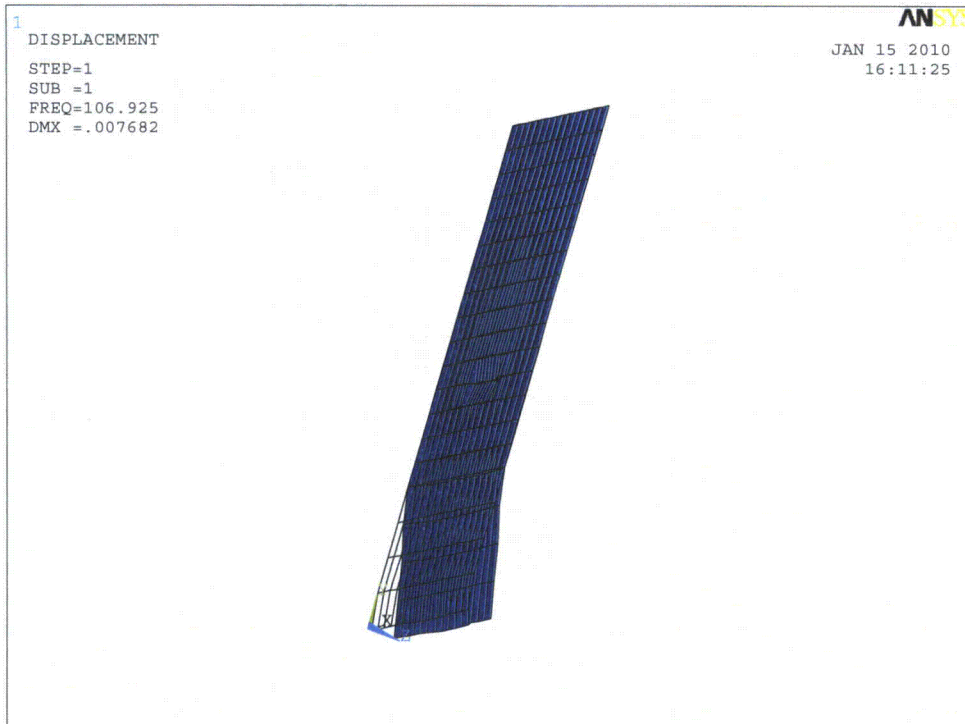
Considering a typical 5 mm imperfection, which is bigger than allowed by the ASME Code, an ANSYS buckling analysis was performed using the same mesh, boundary conditions, etc. as above.



The unitary stress field is:



And the new eigenvalue and deformed shape are:



It is seen that the new value (106.9 N/mm^2) is very similar to value determined above with no imperfections (108.35 N/mm^2).

2. DYNAMIC LOAD ANALYSIS FOR SPENT FUEL RACKS IN THE BUFFER POOL

2.1 INTRODUCTION

2.1.1 Purpose

The purpose of this section is to present the structural analysis of Spent Fuel High Density Fuel Storage Racks (FSR) for the Buffer Pool located in the Reactor Building (RB) of the ESBWR.

The FSR are structures fabricated from stainless steel and borated stainless steel plates, forming 11x7 cells to house the spent fuel assemblies. The FSR are anchored to the floor of the Buffer Pool at elevation 17500.

2.1.2 Scope

The scope of this analysis covers the design principles, load analysis and justification of the structural configuration of the FSR.

The boundaries of the analysis include all the sections of the structure, including plate and weld stress evaluations. Maximum displacements at the top of the FSR are checked. Reactions at the bottom of FSR are obtained to validate the anchor bolt section.

The maximum lateral forces between the fuel assemblies and the top of the FSR cell, along with the maximum vertical forces between fuel assemblies and the FSR base plate are determined.

The calculation of the embedment for the anchor bolts is not within the scope of this analysis. The structural evaluation of the spent fuel assemblies enclosed in the FSR is not covered in this analysis, but their masses have been taken into account in the FSR analysis. The structural evaluation of the FSR against accidental equipment drop and fatigue analysis are not within the scope of this analysis.

2.2 INPUT DATA

Table 2-1
List of Document Input Data (ID)

No.	Source Document			Requirement/Data	Status
	No.	Issue	Title		
1	5926.D400 (2 Sheets)	01	Rack Assembly Drawing (Type-11x7)	Geometry. Materials	V
2	5926.D410 (3 Sheets)	02	Rack Base Plate (Type- 11x7)	Geometry	V
3	5926.D420 (4 Sheets)	00	Rack Cutting Drawing Sheet (Type-11x7)	Geometry	V
4	26A7032	03	Fuel Storage Rack Design Specification	Design Codes. Design Requirements. Fuel assembly weight. Fuel handling loads. Applicable Response Spectra. Loading Combinations. Buffer Fuel Pool Water Temperatures	V
5	26A6558	4	General Civil Design Criteria	Stress free temperature	V
6	5926.D110	01	Rack Layout at Reactor Building	Rack layout. Distance between racks and distance to the walls	V
7	105E3908	03	General Arrangement, ESBWR Nuclear Island	Plant axes	V
8	55926ATN04	00	ESBWR Reactor Pool Bottom (elevation +27m) Synthesized SSE Acceleration Time Histories	SSE acceleration time histories	V

2.3 SUMMARY OF RESULTS

Table 2-2 summarizes the most critical results obtained from the analysis of the FSR and the comparison with the allowable values in accordance with the design code Reference 3.

**Table 2-2
SFR Main Analysis Results**

Steel Plates	Calculated Stress (MPa)	Stress Limit (MPa)	Ratio
10 mm thick enveloping plate	131	292.8	0.45
10 mm thick enveloping plate welds	185.5	198.6	0.93
7 mm thick upper level plates	55.8	292.8	0.19
20 mm thick base plate	101	292.8	0.34
20 mm thick base plate stiffener plates	142	292.8	0.48
20 mm thick base plate stiffener plate welds	155.1	198.6	0.78
60 mm thick bolted support plates	174	292.8	0.59
M48x4 anchor bolts	0.87 (*)	1 (*)	0.87

(*) This is a stress ratio, not a stress value (see Sections 2.4.9 and 2.5.3)

2.4 ANALYSIS SUMMARY

Section 2.4.1 presents a brief description of the FSR.

Section 2.4.2 presents the properties of the FSR materials.

Section 2.4.3 indicates the applicable design code for analysis of the FSR.

Section 2.4.4 presents the assumptions used in the analysis of the FSR.

Section 2.4.5 gives a detailed description of the FSR model. A detailed Finite Element Model (FEM) is developed for the FSR in order to analyze stresses, reactions and displacements.

Section 2.4.6 describes the different load cases which apply to the FSR analysis.

Section 2.4.7 presents the load combinations applied for the FSR analysis.

Section 2.4.8 presents the analysis procedure description for the FSR.

Section 2.4.9 gives the allowable stress limits used in the FSR analysis.

2.4.1 Spent Fuel Storage Rack Description

The FSR support and protect stored fuel assemblies. The FSR are structures made of stainless steel and borated stainless steel plates, forming an 11x7 array of storage cells. The FSR are located in the Buffer Pool within the Reactor Building and are anchored to the pool floor at elevation 17500.

A detailed description of FSR is shown in the assembly and detail drawings of the FSR (ID 1, 2 and 3).

The main dimensions of the FSR are 1870x1198 mm and 3876 mm in height. Different thicknesses of plates are used in the FSR: 10 mm for enveloping stainless steel (SS) plates, 3.4 mm for the internal borated stainless steel (BSS) plates, 7 mm for SS plates of the top level of cells, 20 mm for the support base SS plate and stiffeners, and 60 mm for the four bolted support SS plates.

The enveloping plates and the plates of the top level are welded together. The internal BSS plates are not welded, but are slotted to allow assembly between perpendicular plates that form the cells. The assembly is welded around the perimeter of the base plate, which is stiffened underneath with plates in both orthogonal directions. Four 60 mm thick plates welded to the stiffeners at each corner serve to anchor the FSR to the pool with M48x4 anchor bolts embedded in the pool floor.

Each FSR is able to store 77 spent fuel elements.

2.4.2 Materials

The FSR are manufactured using stainless steel SA-240 Type 304L and borated stainless steel ASTM A 887 Type 304B7. Material SA-564 Type 630 H1075 is used for anchor bolts.

The mechanical properties of type 304L stainless steel are greater than those of type 304, so the mechanical properties of the latter are used. The mechanical properties of ASTM A 887 Type 304B7 are similar to those for SA-240 Type 304, so the type 304 properties used.

Table 2-3 shows the material properties in accordance with Section II, Part D of the ASME Code Reference 2. Material properties at 250°F are assumed based on ID 4.

Table 2-3
Material Properties at 250°F (121.1°C)

Material	E	ρ	α	S_y	S_u	S
	(MPa)	(kg/m ³)	(1/°C)	(MPa)	(MPa)	(MPa)
SA-240 Type 304L (*)	1.90·10 ⁵	7850	16.4·10 ⁻⁶	162.7	472.9	134.1
ASTM A 887 Type 304B7 (*)	1.90·10 ⁵	7850	16.4·10 ⁻⁶	162.7	472.9	134.1

Table 2-3
Material Properties at 250°F (121.1°C)

	E	ρ	α	S _y	S _u	S
SA-564 Type 630 H1075	1.91·10 ⁵	7850	11.3·10 ⁻⁶	779.1	999.7	285.4

(*) Properties shown are those corresponding to type 304 stainless steel

Where.

- ρ ≡ Density (Reference 1)
- E ≡ Modulus of elasticity (Reference 2 Table TM-1)
- α ≡ Coefficient of thermal expansion (Reference 2 Table TE-1)
- S_y ≡ Yield strength (Reference 2 Table Y-1)
- S_u ≡ Ultimate strength (Reference 2 Table U)
- S ≡ Maximum –allowable Stress (Reference 2 Table 1A)

2.4.3 Design Code

Stresses in the structural components of the FSR shall not exceed the allowable stress levels given in the ASME B&PV Code, Section III, Division I, Subsection NF (Reference 3).

2.4.4 Assumptions

The calculation procedure used for the analysis has been performed based on the following assumptions of FSR behavior:

- It is assumed that the material of the structure (stainless steel) has a linear elastic behavior within the field of the small displacement/deformations.
- An assumption of FSRs with a 100% fuel load shall be considered. Since the FSRs are anchored to the pool floor and the fuel elements have a large mass but do not provide any stiffness to the assembly, it is reasonable to expect that this case will present the maximum deformations and stresses.
- For the fuel assembly the dry weight is assumed to be 540 lbs (245 kg) and the net immersed weight to be 474 lbs (215 kg) (ID 4).
- The fuel assembly shall be conservatively considered rigid enough that it is only supported on the top part of the cells, in addition to the support base plate.
- The water mass acting in the vertical direction is not considered because the water could flow inside each one of the cells in vertical direction.

- The inner BSS plates are considered non-structural components, but they are included in the analysis model so that a representative dynamic behavior can be obtained (e.g. by avoiding local modes in the 10 mm envelope plates). Section 2.4.5.1 shows how including the inner BSS plates in the model has little impact on the value of the first two global bending eigenfrequencies of the FSR.
- Prior experience in the study of the dynamic behavior of the freestanding FSR shows a significant reduction in the lateral displacements of the FSR when the hydrodynamic coupling between the FSR and the walls through the water around them are considered. It is reasonable to assume that the coupling effect shall be lower for FSRs anchored to the bottom of the pool, as in the case under study. Therefore, in order to simplify the calculations, a conservative assumption has been made to disregard the positive effect of the hydrodynamic coupling towards the FSR design. Another conservative assumption shall take into account the added mass included in the models, without considering neighboring FSR or walls.

2.4.5 FSR Analysis Model

A finite element model (FEM) for the analysis of the FSR is built with ANSYS 10.0 (Reference 7). A description of the FEM (see Figure C1) follows:

- The external boundary plates of the FSR (see figure A2) are modeled with a 10 mm thick stainless steel plate (Reference 7, SHELL 63 ANSYS elements). These boundary plates are welded in all of their plate connections and are considered a continuous plate without cuts in the model
- The upper level FSR cells (6A and 6L, see ID 3) (see Figure A-3) are modeled with 7 mm stainless steel plates (Reference 7, SHELL 63 ANSYS elements). These plate cells are welded to each other and are considered connected plates with common nodes in the model.
- The borated stainless steel plates (see Figure A-4a) are modeled with 3.4 mm plates (Reference 7, SHELL 63 ANSYS elements). These plates have slots that are used to connect two perpendicular plates. The plate slots are modeled considering the cut in the plate with different nodes overlapped. The connections between perpendicular slotted plates are represented by coupled unions in the corresponding horizontal direction between nodes of the two connected plates (see Figure A-4b).
- The base support of the FSR is modeled with stainless steel plates (Reference 7, SHELL 63 ANSYS elements). This support includes the 20 mm thick fuel support plate with 92 mm diameter holes for each one of the 77 cells (see Figure A-5), the vertical 20 mm thick stiffeners welded under the plate in the two horizontal directions (see Figure A-6) and the four 60 mm thick bolted support plates where the anchor bolts are fixed (see Figure A-7). The 60 mm diameter hole centered in the plate is also modeled. The displacement restrictions imposed by the bolt are introduced in a circular area of the support plate between an external diameter of 90 mm and the hole diameter of 60 mm. The support plate nodes located in this area are connected to a central node by high stiffness and without mass beams (see Figure A-8). The three displacements of this central point are restricted.
- 50% of the fuel mass ($245 \cdot 77 \cdot 0.5 = 9432.5$ kg) acting in each of the two horizontal directions is distributed in the nodes of the model located in the FSR upper end, and the other 50% (9432.5 kg) is distributed in the nodes of the model located in the base support plate.

100% of the mass (18865kg) shall apply vertically in the nodes of the model located in the base support plate. These fuel assembly masses are included as lumped masses (Reference 7, MASS 21 ANSYS elements) in the model.

- The internal water mass acting in the two horizontal directions is distributed in the inner nodes of the model. The node mass distribution is proportional to the volume associated with each inner node. The internal water mass is obtained from the total FSR internal volume where the fuel volume and metal volume is subtracted. Metal mass is ANSYS calculated. Each fuel assembly has a volume of 0.03 m³. The internal water masses are included as lumped masses (Reference 7, MASS 21 ANSYS elements) in the model.
- The external water added mass has been obtained from (Reference 6), where the added mass of a rigid rectangular block is obtained as $(k \cdot \phi \cdot \text{Volume})$, where (ϕ) is the water density and (k) is a factor with an approximate value of $(k=0.5)$ considering the rectangular dimensions of the FSR. The added mass of the FSR is approximately 3950 kg. This added mass corresponds to the following assumptions: (a) infinitely stiff prism, (b) moving as a stiff solid body (c) in an infinite mass of water. The FSR (a) is elastically deformable, (b) is anchored to the ground, i.e. it moves like a cantilever and (c) has a small layer of water around it, so the motion of each FSR shall be coupled through water to the motion of the neighboring FSR. Therefore, the actual added mass and the actual horizontal displacements of the top part of the FSR shall be lower than those obtained in the analysis. Introducing 3950 kg of added mass is a conservative estimate but it is verified that this added mass does not significantly impact the final results of the FSR analysis (stresses and bolt reactions). The external water added masses are included in the model multiplying the internal water masses by a factor.
- The mass of the SS plates is accounted for by means of its density. The BSS plates are modeled without mass density in order to avoid local frequencies of the borated plates produced by the vibration of their free ends between two slots. There are a high number of these local frequencies with values around 55-60 Hz. These frequencies are not significant because they do not move any significant amount of mass and could be filtered in the spectral analysis. For this same reason, the horizontal water masses are not introduced in perpendicular direction to the borated plates and are applied only in horizontal longitudinal direction. The borated stainless steel plate masses in horizontal directions are included in the model multiplying the internal water masses by a factor. The borated stainless steel plate masses in vertical directions are included as additional lumped masses (Reference 7, MASS 21 ANSYS elements) in the model.
- The coordinate system adopted in the FEM is the right hand Cartesian coordinate system. The X-direction represents the East-West direction, the Y-direction represents the North-South direction, and the Z-direction is vertical (ID 7).
- The units used in the FSR FEM are kilograms for mass, meters for length, and seconds for time.

The FSR mass considered in the analysis model is presented in Table 2-4.

Table 2-4
Mass Breakdown

Component	Horizontal mass (kg)	Vertical mass (kg)
10 mm thickness + 7 mm thickness SS Plates	2138	2138
Support Plates (Base, Stiffeners and Bolted Plates)	978	978
BSS Plates	1976	1976
Fuel Assemblies (77 elements)	18865	18865
Internal Water	5070	-
External Added Water	3950	-
Total Mass	32977	23957

2.4.5.1 Structural Considerations on the Borated Plates

To obtain most realistic eigenfrequencies, it is necessary to include the inner BSS plates in the model. The purpose is to avoid the local eigenfrequencies of the outer plates of the racks.

In order to demonstrate that the inner BSS plates do not introduce additional stiffness on the dynamic behavior of the main two horizontal bending frequencies of the racks, the results of the two main horizontal frequencies have been analyzed for the detail model anchored in the base plate and compared with the frequencies obtained by the formula for a cantilever beam.

The characteristics of the analyzed beam are:

- Total length of the beam → L= 3.587 m
- Inertia of the beam given by the 10 mm boundary plate of the FSR. The rectangular boundary plates section have a geometry of 1848x1176x10mm, with a inertia values of → IX=1.55E-2 m⁴, IY=3.06E-2 m⁴
- Horizontal water mass → Inner water mass of 5070 kg plus external added water mass of 3950 kg, uniformly distributed along the beam length
- Dead weight of the FSR → 2138+1976 = 4114 kg uniformly distributed along the beam length
- The water mass and dead weight of the FSR are applied as a single load ⇒ w= 3661 kg/m.
- Fuel mass ⇒ ½ fuel mass (W =9432.5 Kg) located at the free end of the beam.
- The two main bending frequencies of the beam, computed from (Reference 9),

$$f_{x,y} = \frac{1.732}{2\pi} \times \left(\frac{E \times I_{y,x}}{W \times L^3 + 0.236 \times w \times L^4} \right)^{1/2}$$

are calculated to be 19.6 Hz and 27.6 Hz.

Analyzing the rack with the finite element model, the following first frequencies are obtained:

- First bending mode → 18.2 Hz
- Upper rack breathing mode → 19.6 Hz
- Second bending mode → 22.7 Hz

Comparing the formula analysis results with the detail model analysis results it can be seen that the main bending frequencies of the rack are higher in the calculated analysis than in the detail analysis → (19.6 Hz > 18.2 Hz) and (27.6 Hz > 22.7 Hz). Therefore, it is reasonable to consider that the inner borated plates do not introduce any additional substantial stiffness to the main frequencies of the racks. However, the results from the detail model include some local frequencies of the racks that could have an impact on the final results and should be taken into account.

As a conclusion, the inner borated stainless steel plates must be considered as non-structural components even though they are included in the finite element model in order to obtain more accurate results.

2.4.6 Analysis Loads

The following loads are considered in the analysis of the FSR:

D	Dead Weight + Buoyancy
P _f	Upward force by postulated stuck fuel assembly
T _o	Differential temperature induced loads (normal or upset conditions)
T _a	Differential temperature induced loads (abnormal design condition)
SSE	Safe Shutdown Earthquake
SRVD	Safety Relief Valve Discharge
LOCA	Loss of Coolant Accident Dead Weight + Buoyancy (D)
L _R	Lifting FSR during installation

2.4.6.1 Dead Weight + Buoyancy (D)

In addition to the dead weight of the FSR, and fuel assemblies, it is necessary to consider the buoyancy, that is, the thrust that the water applies on the FSR and the immersed fuel. This effect is taken into account in the analysis by reducing the gravity acceleration by a reducing factor calculated as follows:

FSR steel mass:	$M_s = 2138+978+1976 = 5092 \text{ kg}$ (see Table 2-4)
Steel volume:	$V_s = M_s / \rho = 5092/7850 = 0.64 \text{ m}^3$
Fuel assemblies mass:	$M_f = 245*77 = 18865 \text{ kg}$
Fuel assemblies volume:	$V_f = 0.03*77 = 2.31 \text{ m}^3$
Total mass:	$M_T = 5092+18865 = 23957 \text{ kg}$
Total volume	$V_T = 0.64+2.31 = 2.95 \text{ m}^3$

That means 2950 kg of water mass moved. Then, the reducing factor is:

$$F = (23957-2950)/23957 = 0.876$$

And the reduced gravity acceleration is obtained from

$$g' = 0.876 \cdot g = 8.6 \text{ m/s}^2$$

2.4.6.2 Fuel Handling Loads (P_f)

The FSR shall be designed to withstand a pull-up force of 17.79 kN, which is necessary in the event of a fuel assembly or grappling device hanging up during removal and a horizontal force of 4.45 kN being applied at the top of the FSR (ID 4).

2.4.6.3 Differential Temperature Induced Loads (T_o , T_a)

The maximum Buffer Pool water temperatures are 48.9°C (120°F) in normal conditions and 60°C (140°F) in abnormal conditions (ID 4).

The stress-free temperature is assumed to be 15.5°C (ID 5).

The only restrictions on the FSR are the four anchor bolts to the pool floor.

The maximum distance between bolts is $(1680^2 + 1308^2)^{0.5} = 2129 \text{ mm}$ (ID 1).

The maximum expansion projected between these two most separated anchor points, conservatively assuming a maximum temperature of 121.1°C (250°F) (ID 4), is calculated to be:

$$\alpha \cdot L \cdot \Delta T = 16.4 \text{ E-6} * 2129 * (121.1-15.5) = 3.7 \text{ mm}$$

The M48 anchor bolts are placed in the 54 mm diameter hole located in the 60 mm thick bottom plate of the FSR. Under these conditions the tolerance between the anchor bolt diameter and the diameter of hole is enough to absorb the maximum expansion estimated. Therefore no thermal induced stresses are calculated in this analysis. The racks are submerged in water and can expand in both the vertical and horizontal directions without significant restrictions. The temperature gradient in the vertical direction is considered negligible for structural analysis.

2.4.6.4 Safe Shutdown Earthquake (SSE)

The FSR shall be designed to withstand the SSE loads specified in ID 4 Appendix A30. A structural damping value of 4% for SSE conditions is used (Reference 12). Figures A-9 and A-10 in Appendix A show the spectra applied in both horizontal and vertical directions.

2.4.6.5 Safety Relief Valve Discharge (SRVD)

The FSR shall be designed to withstand the SRVD loads specified in ID 4 Appendix A30. A structural damping value of 4% for SRVD conditions is used (Reference 12). Figures A-11 and A-12 in Appendix A show the spectra applied in both horizontal and vertical directions.

2.4.6.6 Loss of Coolant Accident (LOCA)

The FSR shall be designed to withstand the LOCA loads specified in ID 4 Appendix A30. A structural damping value of 4% for LOCA conditions is used (Reference 12). Figures A-13 and A-14 in Appendix A show the spectra applied in both horizontal and vertical directions.

2.4.6.7 Lifting FSR During Installation (L_R)

The FSR is verified to withstand the lifting load during installation. The FSR is supported in the four base plate holes indicated in ID 1 and ID 2.

2.4.7 Load Combinations

The load combinations and acceptance criteria shall be per Appendix D of SRP 3.8.4. Table 2-5 shows the envelope load combinations that will be conservatively used for the design of the FSR, based on the aforementioned load combinations.

**Table 2-5
Load Combinations**

Level A:	$D + P_f$
Level D:	$D + SSE + SRVD + LOCA + T_a$

$D + P_f$ is a Level B load combination, but it is conservatively assumed as a Level A load combination.

2.4.8 Analysis Methodology Description

Static and dynamic loads are considered in the analysis. The response spectrum analysis method is used to analyze the dynamic loads.

The static load case (D) is resolved by structural static analysis applying the reduced gravity acceleration g' (see Section 2.4.6.1).

The fuel handling load case (P_f) is analyzed by applying the forces prescribed in Section 2.4.6.2 in a central node of the 7 mm thickness upper level plates (see Figure C15).

The lifting load during installation case (L_R) is analyzed by applying the gravity acceleration, g , and supporting the FSR in the appropriate four base plate holes.

The dynamic load cases are resolved by response spectrum analysis. Before the response spectrum analysis is performed, a modal analysis is performed to determine the natural frequencies and mode shapes of the FSR. The subspace method is used for mode extraction in modal analysis. One hundred (100) eigenfrequencies are requested in the modal analysis.

Once the eigenfrequencies of the model have been determined with the modal analysis, a response spectra analysis for each dynamic event (SSE, SRVD and LOCA) is evaluated for each of the three directions, X, Y and Z.

The input response spectra are represented by no more than twenty (20) points (ANSYS limitation), beginning at a frequency lower than the lowest obtained in the FSR modal analysis.

Once the response spectrum analysis has been performed for each direction, the modal responses are combined in accordance with the grouping method established in Regulatory Guide 1.92 (Reference 5).

More than 90% of the mass is considered in each direction for the modal combination (see section 2.5). Therefore no consideration is given to computing the missing mass associated to the eigenmodes not intervening in the modal combination. See the note in Section 2.6.

Finally, as the load combination includes multiple dynamic loads, these loads are combined by the SRSS method.

2.4.9 Stress Limits

The stress limits are taken from ASME Code (3), Subsection NF an Appendix F corresponding to the Design by Analysis for Class 3 Plate and Sheet Type Supports.

Base metal SA-240 Type 304L (With Mechanical Characteristics of SA-240 Type 304)

Level A Conditions (NF-3251.1 and Table NF-3552(b)-1)

$$P_m \leq S = 134.1 \text{ MPa}$$

$$P_m + P_b \leq 1.5 \cdot S = 201.1 \text{ MPa}$$

$$\tau \leq 0.6 \cdot S = 80.4 \text{ MPa}$$

Level D Conditions (Appendix F.F-1332)

$$P_m \leq \text{Minimum of } 1.2 S_y \text{ or } 0.7 S_u = 195.2 \text{ MPa}$$

$$P_m + P_b \leq 1.5 \cdot (P_m \text{ limit}) = 292.8 \text{ MPa}$$

$$\tau \leq 0.42 \cdot S_u = 198.6 \text{ MPa}$$

For compressive stress, see Appendix D.

Bolting Material SA-564 Type 630 H1075

Level A Conditions (NF-3324.6 for austenitic steel)

$$\text{Average normal stress} = f_t \leq F_{tb} = S_u/3.33 = 300.2 \text{ MPa}$$

$$\text{Shear stress} = f_v \leq F_{vb} = 0.62S_u/5 = 123.9 \text{ MPa}$$

$$\text{Combined tensile and shear stress: } f_t^2 / F_{tb}^2 + f_v^2 / F_{vb}^2 \leq 1$$

Level D Conditions (Appendix F.F-1335)

$$\text{Average normal stress} = f_t \leq F_{tb} = \text{Minimum of } S_y \text{ or } 0.7 S_u = 699.8 \text{ MPa}$$

$$\text{Shear stress} = f_v \leq F_{vb} = \text{Minimum of } 0.42 \cdot S_u \text{ or } 0.6 S_y = 419.8 \text{ MPa}$$

$$\text{Combined tensile and shear stress: } f_t^2 / F_{tb}^2 + f_v^2 / F_{vb}^2 \leq 1$$

Welds

Level A Conditions (NF-3324.5 and Table NF-3324.5(a)-1)

Fillet welds:

$$\text{Shear Stress on effective throat} \leq 0.3 \cdot S_u^{(1)} = 165.4 \text{ MPa}$$

$$\text{Shear Stress on base metal} \leq 0.4 \cdot S_y = 65.1 \text{ MPa}$$

Tension or compression parallel to axis of weld \leq Same as base metal(1)

⁽¹⁾ Base metal tensile strength range between 472.9 MPa and 551.5 MPa (68.6 and 80 ksi), minimum weld metal tensile strength, 551.5 MPa (80 ksi).

Level D Conditions (Appendix F.F-1332)

$$\text{Shear Stress} \leq 0.42 S_u = 198.6 \text{ MPa}$$

Tension or compression parallel to axis of weld \leq Same as base metal

2.5 RESULTS OF THE ANALYSIS

The ANSYS output for static, modal and spectrum analyses, including the modal combination, is included in Appendix D.

Table 2-6 presents the main eigenfrequencies, obtained from the modal analysis, with of the associated effective mass. Additionally, two lower frequency modes (modes 2 and 4) are

included as examples of typical “breathing” mode shapes that do not contribute to the solution response.

Figures C16 through C23 in Appendix C show the deformed shapes of these eigenmodes.

Table 2-6
Main Eigenfrequencies

Mode	Frequency (Hz)	Effective Mass (kg)	Description	Figure in Appendix C
1	13.64	17941	X Bending	C16
2	17.74	-	Breathing	C17
3	17.95	19985.5	Y Bending	C18
4	35.38	-	Breathing	C19
13	72.38	11592	2nd Y Bending	C20
15	76.13	20659	Base Plate Bending	C21
16	80.64	7649	2nd X Bending	C22
36	155.1	1846	2nd Base Plate Bending	C23

Table 2-7 indicates the amount of mass considered in the modal combination and the corresponding percentage with respect to the total mass.

Table 2-7
Combined Effective Masses

Event	X direction		Y direction		Z direction	
	Mass (kg)	(%)	Mass (kg)	(%)	Mass (kg)	(%)
SSE	32215 (97.7%)		30590 (92.7%)		23081 (96.3%)	
LOCA	32617 (98.9%)		30744 (93.2%)		23081 (96.3%)	
SRVD	31707 (96.2%)		29744 (90.2%)		23081 (96.3%)	

2.5.1 Displacement Results

The maximum horizontal displacement obtained at the top of the FSR for the most unfavorable load combinations are 2.8 mm for the X-direction, and 3.8 mm for the Y-direction (see Figures C24 and C25, respectively, in Appendix C).

One half of the expansion due to thermal expansion (Section 2.4.6.3) is applied to each rack in opposing horizontal directions. If the abnormal pool temperature were to occur simultaneously with a seismic event, the resulting total displacement is calculated as:

$$3.8 \text{ mm} + 3.7 \text{ mm}/2 = 5.7 \text{ mm}$$

The minimum distance between adjacent FSR at the top level or between FSR and pool wall is 100 mm (ID 6). Therefore, no contact occurs between the FSR or between the FSR and the pool walls.

2.5.2 Plate Stress Results

The stress results obtained for the different load combinations are checked in the most critical sections of the different plates of the FSR. Figures C26 to C31 in Appendix C show the results.

2.5.2.1 10 mm Thick Enveloping Plate

The maximum stresses obtained on the 10mm thickness enveloping plate compared with the corresponding allowable stresses are given in Table 2-8, where:

- $S_Z \equiv$ Vertical direction (Z) membrane stress
- $S_H \equiv$ Horizontal direction (X or Y) membrane stress
- $S_{HZ} \equiv$ Shear membrane stresses on the plane of the plate.
- Bending stresses across the plate thickness are negligible and are classified as secondary stresses; however, other directions of the plate contain primary bending stresses that are included in the stress analysis results.

Table 2-8

10mm Thickness Enveloping Plate Stress Results

Stress Category	Calculated Stress (MPa)	Allowable Stress (MPa)
Level A Conditions Maximum Membrane Stresses	$S_Z = 7.0$	134.1
	$S_H = 2.1 \times 2 = 4.2$	134.1
	$S_{HZ} = 2.2$	80.4
Level D Conditions Maximum Membrane Stresses	$S_Z = 131$ (Figure C26)	292.8
	$S_H = 35 \times 2 = 70$	292.8

Table 2-8
10mm Thickness Enveloping Plate Stress Results

Stress Category	Calculated Stress (MPa)	Allowable Stress (MPa)
	$S_{HZ} = 31$	198.6

The horizontal stresses (general membrane) are multiplied by a factor of (2) in order to take into account that the 10mm plates are not continuous in the vertical direction because they are slotted to support the borated plates.

The maximum stresses obtained for the horizontal welds compared with the corresponding allowable stresses are given in Table 2-9.

Table 2-9
10mm Thickness Enveloping Plate Welds Stress Results

Stress Category	Calculated Stress (MPa)	Allowable Stress (MPa)
Horizontal lower 6mm fillet welds (160-168). In the corners (2 cells)	$(106) \times (10/6) \times (168/160) = 185.5$	198.6
Horizontal lower 6mm fillet welds (50-95). Out the corners	$(49) \times (10/6) \times (95/50) = 155.1$	198.6
Horizontal 6mm butt welds (150-168). In the corners (3 cells). Level Z=356mm	$(77) \times (10/6) \times (168/150) = 143.7$	195.2
Horizontal 6mm butt welds (50-95). Out the corners. Level Z=356mm	$(32) \times (10/6) \times (95/50) = 101.3$	195.2
Horizontal 6mm butt welds (150-168). In the corners (1 cells). Level Z=712mm	$(52) \times (10/6) \times (168/150) = 97.1$	195.2
Horizontal 6mm butt welds (50-95). Out the corners. Level Z=712mm	$(41) \times (10/6) \times (95/50) = 129.8$	195.2
Horizontal 6mm butt welds (50-95). Level Z=1068mm	$(42) \times (10/6) \times (95/50) = 133.$	195.2
Horizontal 6mm butt welds (50-95). Level Z=1424mm	$(33) \times (10/6) \times (95/50) = 104.5$	195.2
Horizontal 3mm butt welds (50-95). Level Z=1780mm	$(27) \times (10/3) \times (95/50) = 171.1$	195.2
Horizontal 3mm butt welds (50-95). Level Z=2136mm	$(20) \times (10/3) \times (95/50) = 126.6$	195.2

Note The stress used to check the fillet welds is the maximum shear stress for the weld localization, given by $(S_z^2 + S_{HZ}^2)^{1/2}$

The stress used to check the butt welds is the maximum stress on the vertical direction for the weld localization (S_z).

Butt welds located at levels with ($Z > 2136$) have lower stresses than those in ($Z = 2136$) level, therefore the same 3mm butt welds (50-95) will apply.

It is verified that enough stress margin is obtained for welds of the 10mm thick plates, even with the conservative assumptions in the analysis. This margin is judged to be useful to absorb any small differences between the FEM and the actual structure. It should be taken into account that the integrity of the upper part of the FSRs is provided by the welds of the 10mm plates (the plates themselves have low stresses).

2.5.2.2 47 mm Thick Upper Level Plates

The maximum stress obtained for the 7 mm thick upper level plates compared with the corresponding allowable stresses are given in Table 2-10, where:

- S_Z \equiv Vertical direction (Z) membrane stress
- S_H \equiv Horizontal direction (X or Y) membrane stress
- S_{HZ} \equiv Shear membrane stresses on the plane of the plate.
- Bending stresses across the plate thickness are negligible and are classified as secondary stresses; however, other directions of the plate contain primary bending stresses that are included in the stress analysis results.

Table 2-10
7 mm Thickness Upper Level Plates Stress Results

Stress Category	Calculated Stress (MPa)	Allowable Stress (MPa)
Level A Conditions Maximum Membrane Stresses	$S_Z = 7.8$ (Figure C27)	134.1
	$S_H = 3.2$	134.1
	$S_{HZ} = 1.1$	80.4
Level D Conditions Maximum Membrane Stresses	$S_Z = 21.0$	292.8
	$S_H = 55.8$ (Figure C28)	292.8
	$S_{HZ} = 7.3$	198.6

The 7 mm thickness plates are welded with a 3 mm fillet weld, 30 mm in length, in each corner connection between perpendicular plates.

The maximum stress on these welds due to the pull-up force of 17.79 kN (Section 2.4.6.2) is obtained assuming that this force is transmitted through the four fillet welds of one cell. That is,

$$S_{max} = 17790 / (4 \times 30 \times 3) = 49.4 \text{ MPa} < 65.1 \text{ MPa}$$

The maximum vertical force in a corner between perpendicular plates for level D conditions is 9117 N. Therefore, the maximum stress on the fillet weld is

$$S_{max} = 9117 \times 1.4142 / (30 \times 3) = 143.2 \text{ MPa} < 198.6 \text{ MPa}$$

2.5.2.3 20 mm Thick Base Plate Stiffener Plates

The maximum stress obtained for the 20 mm thickness base plate stiffener plates and welds compared with the corresponding allowable stresses are given in Table 2-11, where:

- $S_z \equiv$ Vertical direction (Z) membrane stress
- $S_H \equiv$ Horizontal direction (X or Y) membrane stress
- $S_{HZ} \equiv$ Shear membrane stresses on the plane of the plate
- Bending stresses across the plate thickness are negligible and are classified as secondary stresses; however, other directions of the plate contain primary bending stresses that are included in the stress analysis results.

Table 2-11
20mm Thickness Base Plate Stiffener Plates Stress Results

Stress Category	Calculated Stress (MPa)	Allowable Stress (MPa)
Level A Conditions Maximum Membrane Stresses	$S_z=8.4$	134.1
	$S_H=6.4$	134.1
	$S_{HZ}=5.3$	80.4
Level D Conditions Maximum Membrane Stresses	$S_z=142$ (Figure C29)	2092.8
	$S_H=116$	292.8
	$S_{HZ}=83.6$	198.6
Welds to base support plate. On corners (3 cells) 2x6mm fillet weld (100–168)	$S_{max} = 55.4 \times (20/12) \times (168/100) = 155.1$	198.6
Welds to base support plate. Out of corners, 2x6mm fillet welds (2x100–504) 'maximum'	$S_{max} = 24.3 \times (20/12) \times (504/200) = 102.1$	198.6

Note The stress used to check the fillet weld is the maximum shear stress for the weld localization, given by $(S_z^2 + S_{HZ}^2)^{1/2}$

2.5.2.4 20 mm Thick Base Plate and 60 mm Thick Bolted Support Plates

The maximum stress obtained for the 20 mm thick base plate and in 60 mm thick bolted support plates compared with the corresponding allowable stresses are indicated in Table 2-12.

Table 2-12
20 mm Thickness Base Plate and 60 mm Thickness Bolted Support Plates
Stress Results

Stress Category	Calculated Stress (MPa)	Allowable Stress (MPa)
Level A Conditions. Base plate	6.4	201.1
Level D Conditions. Base plate	101 (Figure C30)	292.8
Lifting Load. Base plate	46 (Figure C32)	292.8
Level A Conditions. Bolted support plate	11.6	201.1
Level D Conditions. Bolted support plate	174 (Figure C31)	292.8

2.5.3 Bolt Stress Results

The actual stress area available for M48x4 bolts is 1498 mm², based on the minor diameter of the bolt root of 43.670 mm (Reference 8). The maximum reaction forces obtained at the bolt location and the calculated stresses compared with the corresponding allowable stresses are presented in Table 2-13.

Table 2-13
Bolt Stress Results

Stress Category	Reaction Force (N)	Calculated Stress (MPa)	Allowable Stress (MPa)
Level A Conditions. Shear	27665	18.5	123.9
Level A Conditions. Tensile (*)	54220 (*)	0 (*)	300.2
Level D Conditions. Shear	396554	264.7	419.8
Level D Conditions. Tensile	718507	479.7	699.8

(*) Bolts are not subject to compression load.

In addition, the condition for combined shear and tensile stress $f_t^2 / F_{tb}^2 + f_v^2 / F_{vb}^2 \leq 1$ is met:

- Level A Condition: $f_t^2 / F_{tb}^2 + f_v^2 / F_{vb}^2 = 0.02 \leq 1$
- Level D Condition: $f_t^2 / F_{tb}^2 + f_v^2 / F_{vb}^2 = 0.87 \leq 1$

2.5.4 Fuel Impact Forces Analysis

In order to obtain the maximum fuel impact forces, a simplified finite element model for the FSR is built with ANSYS 10.0 (Reference 7), one model for the North-South direction and one for the East-West direction.

Each simplified model is composed of 2-D elastic beam BEAM3 elements, and concentrated mass MASS21 elements.

A vertical line of beam elements represents the enveloping plate of the FSR cells, and another vertical line of beam elements represents the fuel elements assembly.

The area properties and inertias of the cell beams have been adequately adjusted so that the model will have the same eigenfrequencies as the detail model in Section 2.4.5. The structural characteristics of the fuel assembly beams are adjusted based on their first axial frequency (ID 4), their axial area, and their moment of inertia.

The coupling between FSR cell and fuel beam immersed in water, are modeled through MATRIX27 elements applied by node pairs (see Reference 10 for details).

Mass elements reproducing the mass of borated stainless steel plates, and the mass of internal water are concentrated on the connection nodes of the beam elements simulating the FSR cells.

The fuel beam is coupled in the horizontal direction with the FSR beam at the bottom node. One vertical contact element is located at this same location to evaluate whether the fuel uplifts then impacts with a vertical load when it falls and strikes the base plate.

Between the FSR beam top node and fuel beam top node, two horizontal contact elements (one for each direction of movement) are located to evaluate any potential lateral impacts that may be produced against the FSR cells. The stiffness of these contacts has been estimated by a local analysis made with the detail analysis model, applying local loads at the top cell level.

Based on the acceleration time-histories corresponding to the SSE (ID 8), double integration is used to generate the displacement histories to be applied at the node of the model that represent the pool. Intervals of 0.005 s were used, which means 3200 load steps for a 16-s transient.

The dead weight and the buoyancy effect are considered during the process by application of a constant vertical downward acceleration value of 8.6 g (reduced gravity acceleration, see Section 2.4.6.1).

The maximum impact loads obtained from this local analysis are:

$$\text{Maximum top fuel horizontal force} \Rightarrow \text{FHT} \approx 1.7 \text{ E}+4 / 77 = 221 \text{ N}$$

Maximum bottom fuel horizontal force \Rightarrow FHB $\approx 9.6 \text{ E}+4 / 77 = 1247 \text{ N}$

Maximum bottom fuel vertical force \Rightarrow FHT $\approx 315 \text{ E}+4 / 77 = 40909 \text{ N}$

The stresses produced by these impact forces are analyzed using the detailed FSR model defined in Section 2.4.5. The analysis is only focused on the stress produced for the FSR fuel base plate, since the top fuel impact forces obtained show low values and therefore judged non-significant.

The impact forces are applied in the three directions by nodal forces on the circular holes of the fuel support base plate.

The vertical fuel impact forces have high values. For this reason a plastic material analysis is considered for the FSR fuel base plate. The plastic stress-strain material curve is obtained from (Reference 11).

The stress distribution on the base plate is show in figure C33. The maximum stress is $S_{\max} = 208 \text{ MPa}$.

This maximum stress is lower than the maximum membrane plus bending admissible stress per Appendix F, F-1341.2 (Reference 4), considering support plastic analysis, $S_{\text{adm}} = 0.9 \times S_U = 436 \text{ MPa}$.

2.6 CONCLUSIONS

The analyses performed for the FSR with the geometry of drawings ID 1, 2 and 3 demonstrate the integrity of these structures when subjected to the applicable loads and load combinations as described in the report.

Table 2-2 summarizes results obtained from the analysis of the FSR components: plate thickness, welds, and anchor bolts. Included in the table are the ratios of the actual results with their allowable values.

The analyses presented herein demonstrate that the FSR satisfy the structural requirements of ASME B&PV Code, Section III, Subsection NF (Reference 3) for all proposed loading condition specified in FSR Design Specification (ID 4).

Note on Section 2.4.8:

The response of the racks is mainly due to the first frequencies under the SSE loads. For racks in the buffer pool, the minimum mass percentage combined in the SSE modal response is 92.7%, indicating 7.3% missing mass. The most critical stress ratio is 0.93.

The global response of the rack from the response spectrum analysis developed can be expressed as:

$$R = (\sum R_{ij}^2)^{1/2} ; i = \text{SSE, LOCA, SRVD}; j = x, y, z$$

where R_{ij} is linearly dependant of $(\sum (M_k \cdot a_k)^2)^{1/2}$, where M_k and a_k are, respectively, the effective mass and acceleration for the mode k . Including the missing mass for each event and each

direction means to add the term $M_{\text{miss}} \cdot a_{\text{ZPA}}$ in that SRSS. Since the ZPA acceleration is always lower than any of the modal accelerations, it can be conservatively assumed that the global response will be increased by $100/92.7=1.078$. Therefore, the most critical stress ratio becomes $0.93 \cdot 1.078=1.00$.

These increasing factors, in fact, will be much smaller because the ZPA acceleration and the missing mass are smaller than, for instance, the spectral acceleration and effective mass of the two main eigenmodes corresponding to the two first global bending eigenfrequencies. From the ANSYS output it is shown, as an example, that the acceleration in X direction for the main frequency (17.95 Hz) is 27.445 m/s^2 (and the ZPA is 12.557 m/s^2) and the effective mass is 19985.5 kg (and the missing mass is $0.073 \cdot 32977=2407 \text{ kg}$).

Thus, it is concluded that the missing masses are small and do not affect the final results.

2.7 REFERENCES

1. ASME Boiler & Pressure Vessel Code, Section II Materials, Part A Ferrous Material Specifications, 2001 Edition with Add. 2003
2. ASME Boiler & Pressure Vessel Code, Section II Materials, Part D Properties (Customary), 2001 Edition with Add. 2003
3. ASME Boiler & Pressure Vessel Code, Section III Rules for Construction of Nuclear Facility Components, Division 1, Subsection NF, Supports, 2001 Edition with Add. 2003
4. ASME Boiler & Pressure Vessel Code, Section III Rules for Construction of Nuclear Facility Components, Division 1, Appendices, 2001 Edition with Add. 2003
5. Regulatory Guide 1.92, Rev. 1, Combining Modal Responses and Spatial Components in Seismic Response Analysis
6. Sarpkaya: Mechanics of Wave Forces on Off-Shore Structures
7. ANSYS 10.0 Documentation (User Manual, Theoretical Manual)
8. ASME B1.13M-2001 Metric Screw Threads: M Profile
9. ROARK'S Formulas for Stress & Strain, 6th Edition
10. 092-175-F-M-00001, Issue 2, Spent High Density Fuel Storage Racks Design Report
11. NUREG/CR-0841, "An Assessment of Stress-Strain Data Suitable for Finite-Element Elastic-Plastic Analysis of Shipping Containers", H. J. Rack and G. A. Knorovsky, Syia Laboratories, SY77-1872, September 1978
12. Regulatory Guide 1.61, Rev.1. Damping Values for Seismic Design of Nuclear Power Plants

APPENDIX C - FIGURES

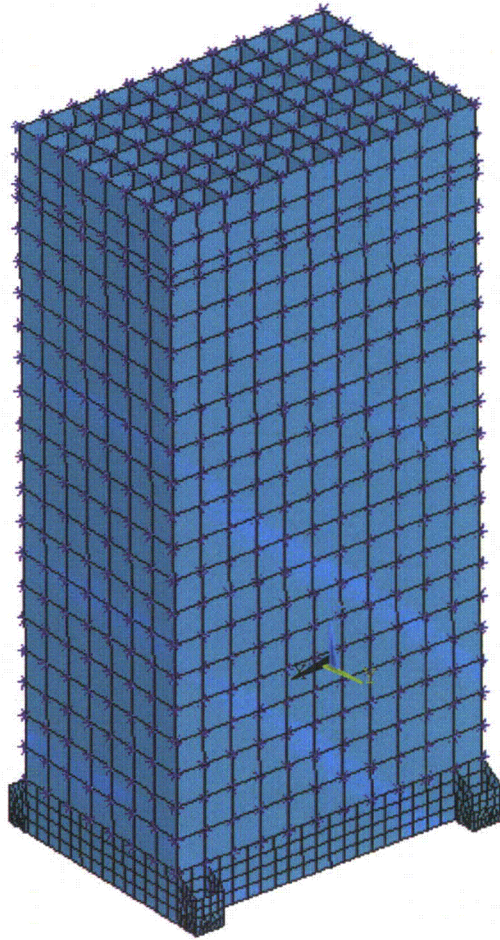


Figure C-1. FSR FEM

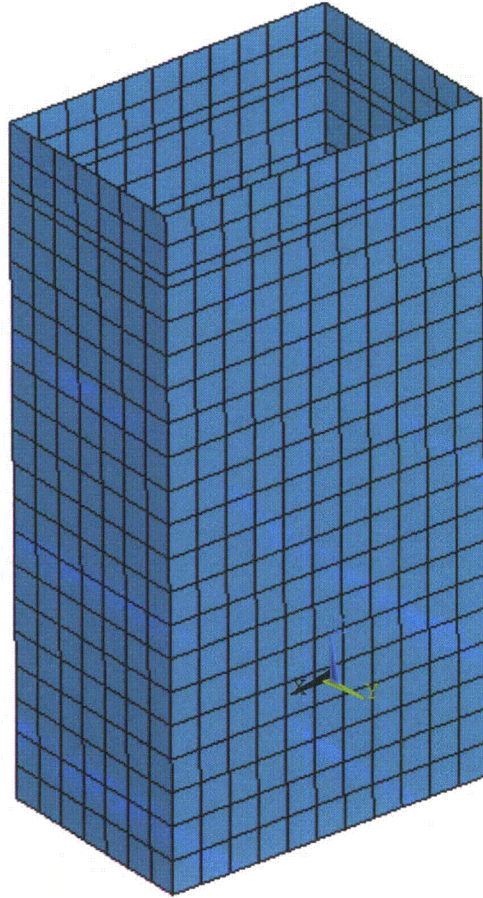


Figure C-2. FSR FEM 10 mm Thickness SS Plates

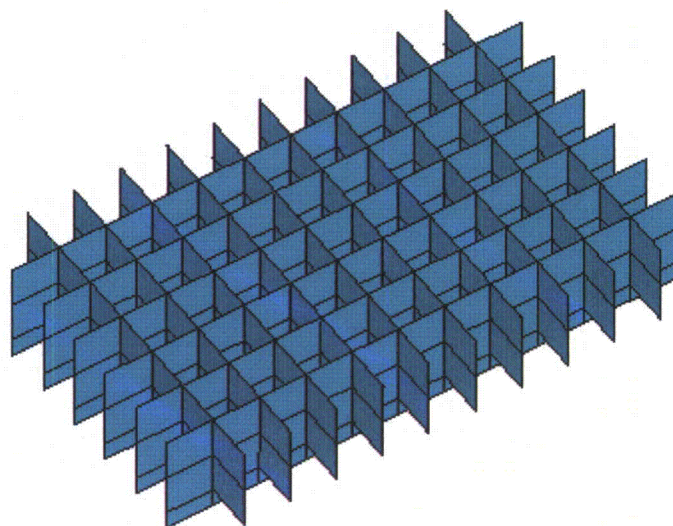


Figure C-3. FSR FEM 7 mm Thickness SS Plates

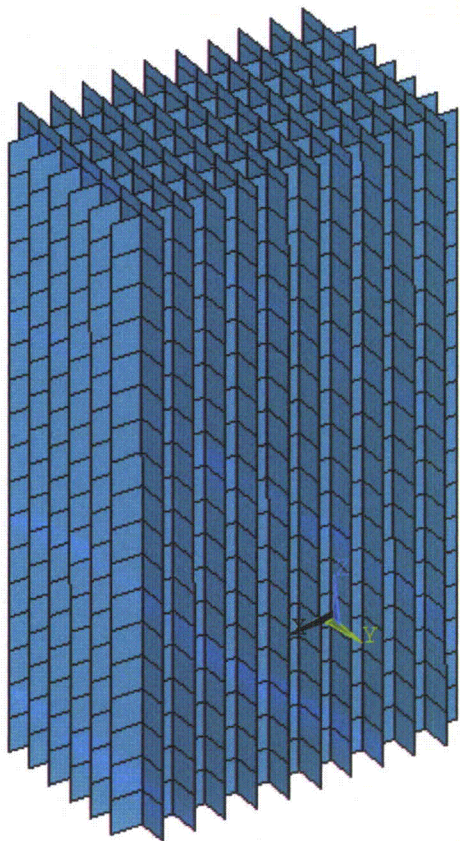
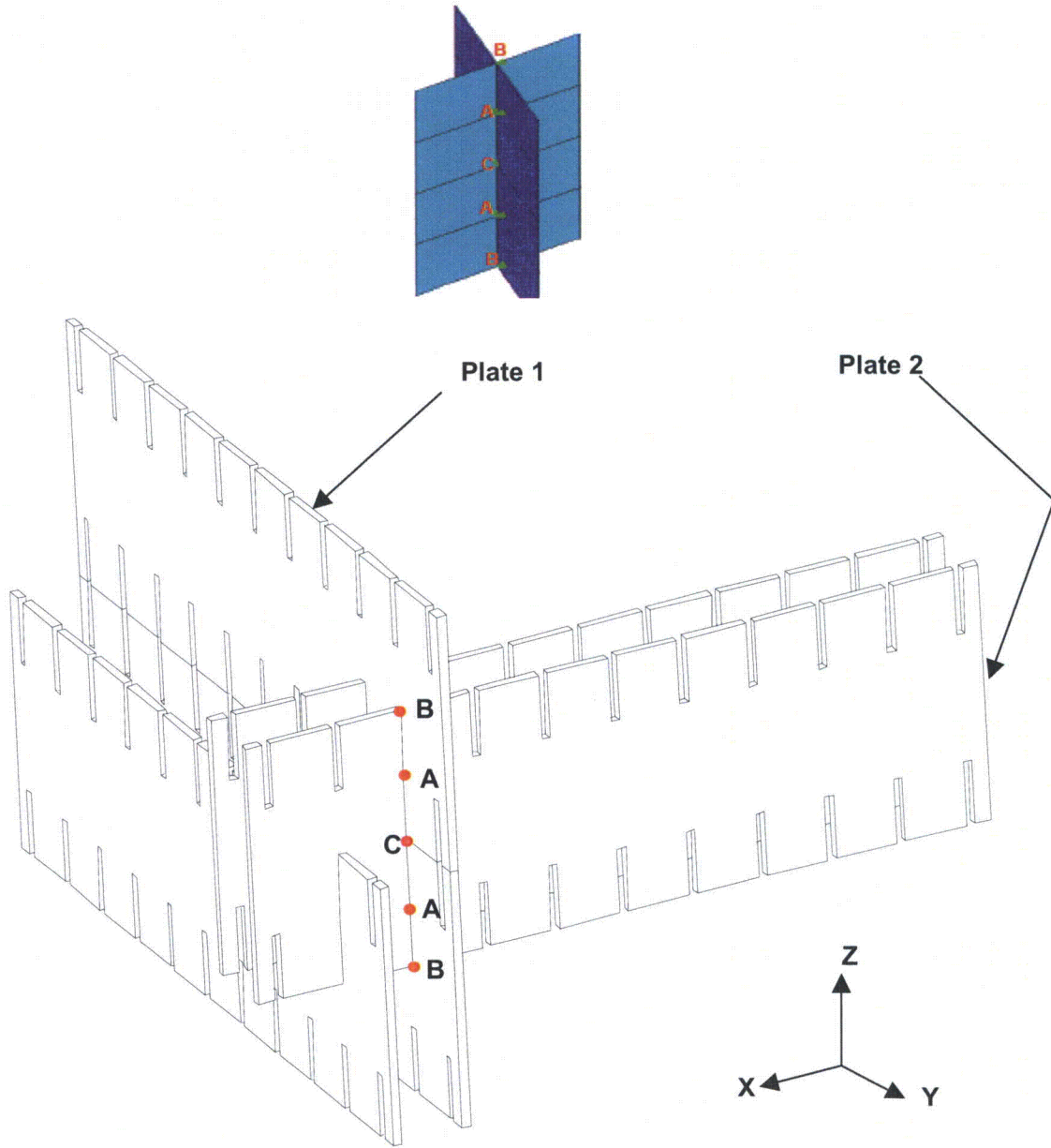


Figure C-4a. FSR FEM 3.4 mm Thickness BSS Plates



There are two (2) nodes on each intersection point: one node for Plate 1 and one node for

In Points A : $U_{1x} = U_{2x}$; $U_{1y} = U_{2y}$; $U_{1z} \neq U_{2z}$

In Points B : $U_{1x} = U_{2x}$; $U_{1y} \neq U_{2y}$; $U_{1z} \neq U_{2z}$

In Points C: $U_{1x} \neq U_{2x}$; $U_{1y} = U_{2y}$; $U_{1z} \neq U_{2z}$

Figure C-4b. Couples in Slotted Areas

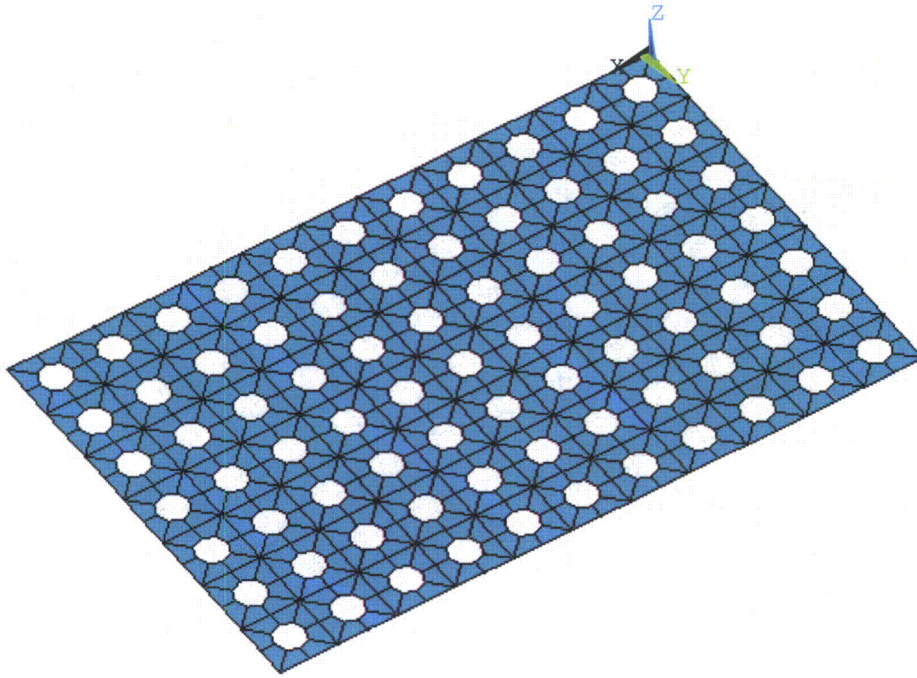


Figure C-5. FSR FEM 20 mm Thickness SS Base Plate

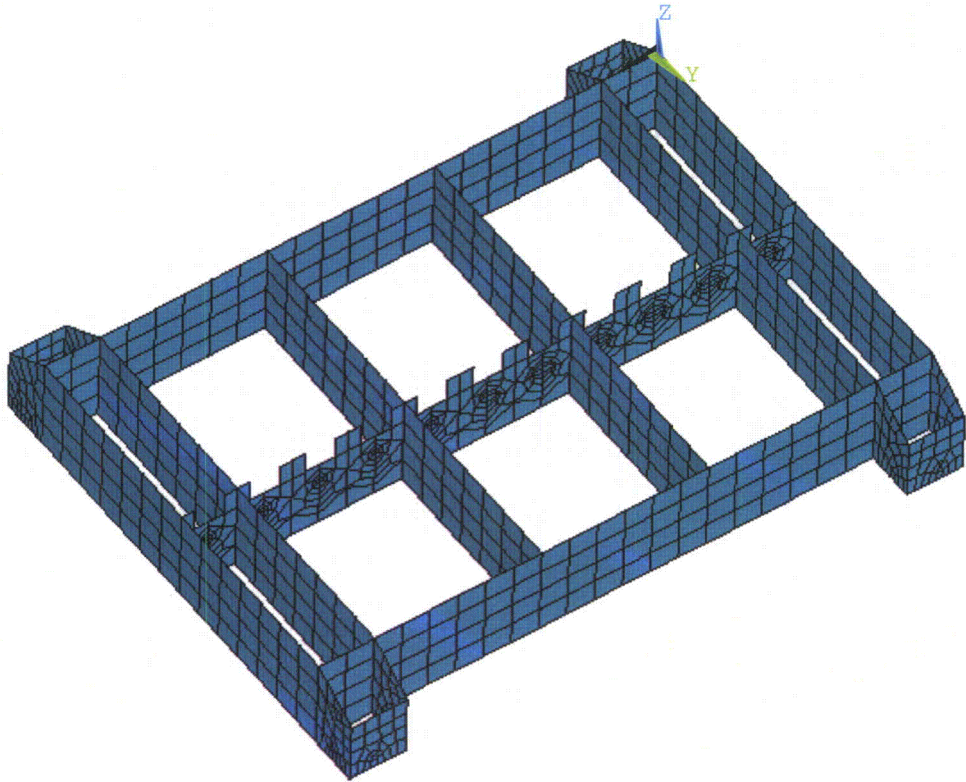


Figure C-6. FSR FEM 20 mm Thickness SS Base Plate Stiffeners

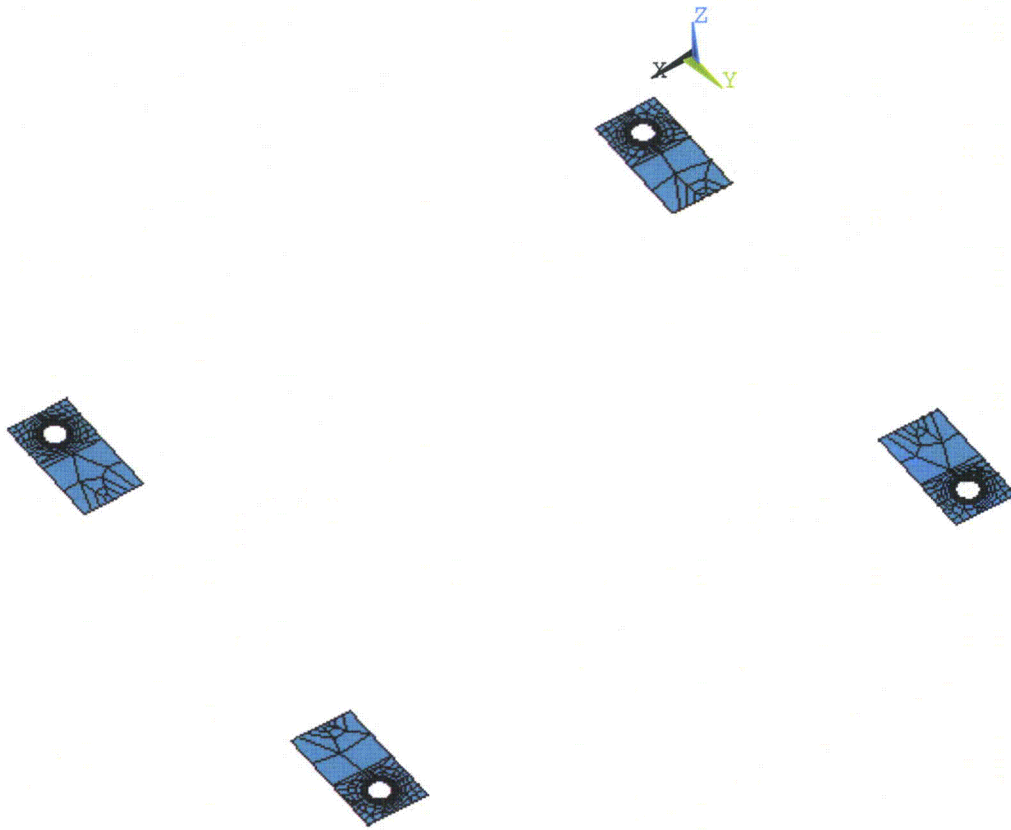


Figure C-7. FSR FEM 60 mm Thickness SS Bolted Support Plates

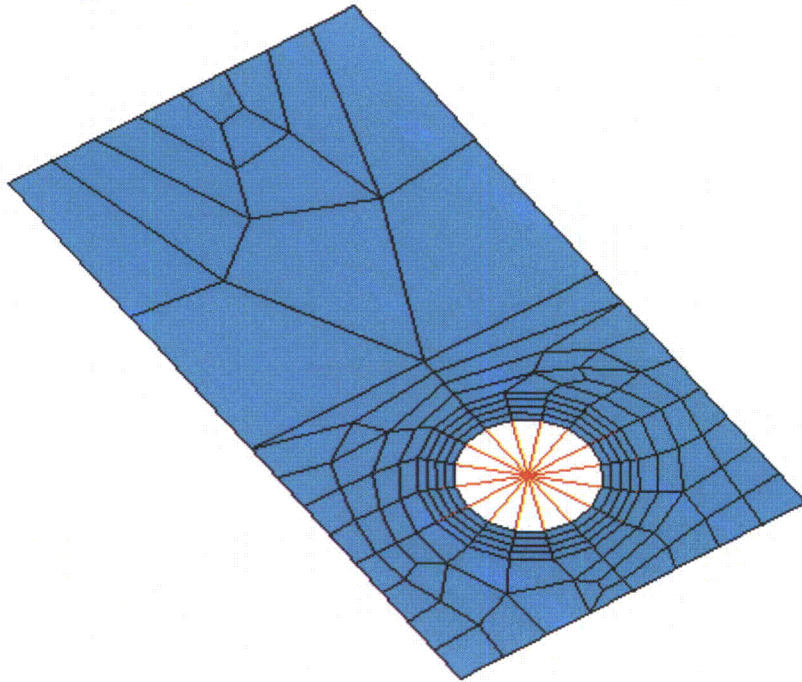


Figure C-8. FSR FEM Bolted Support Plate Detail (With High Stiffness Bars)

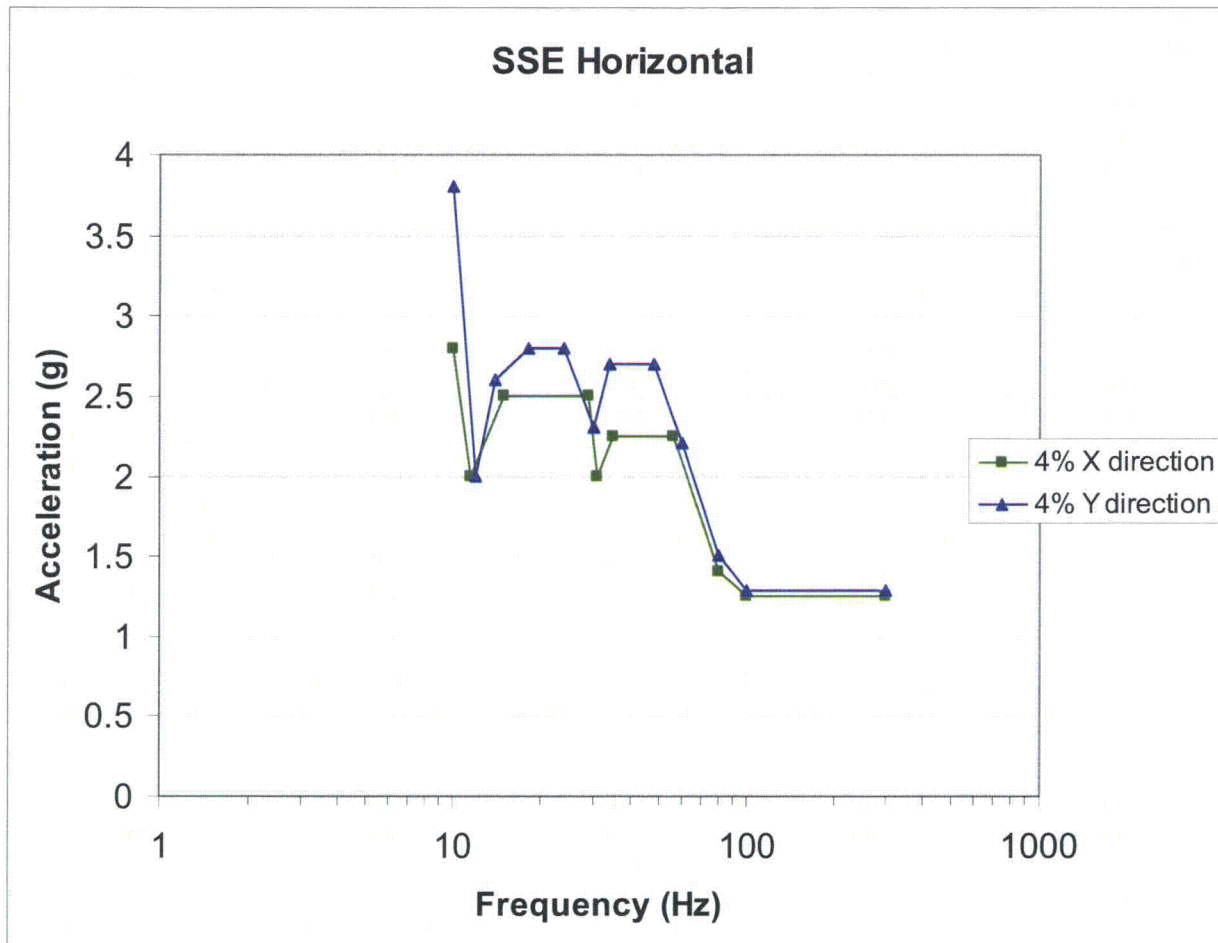


Figure C-9. SSE Horizontal Floor Response Spectra

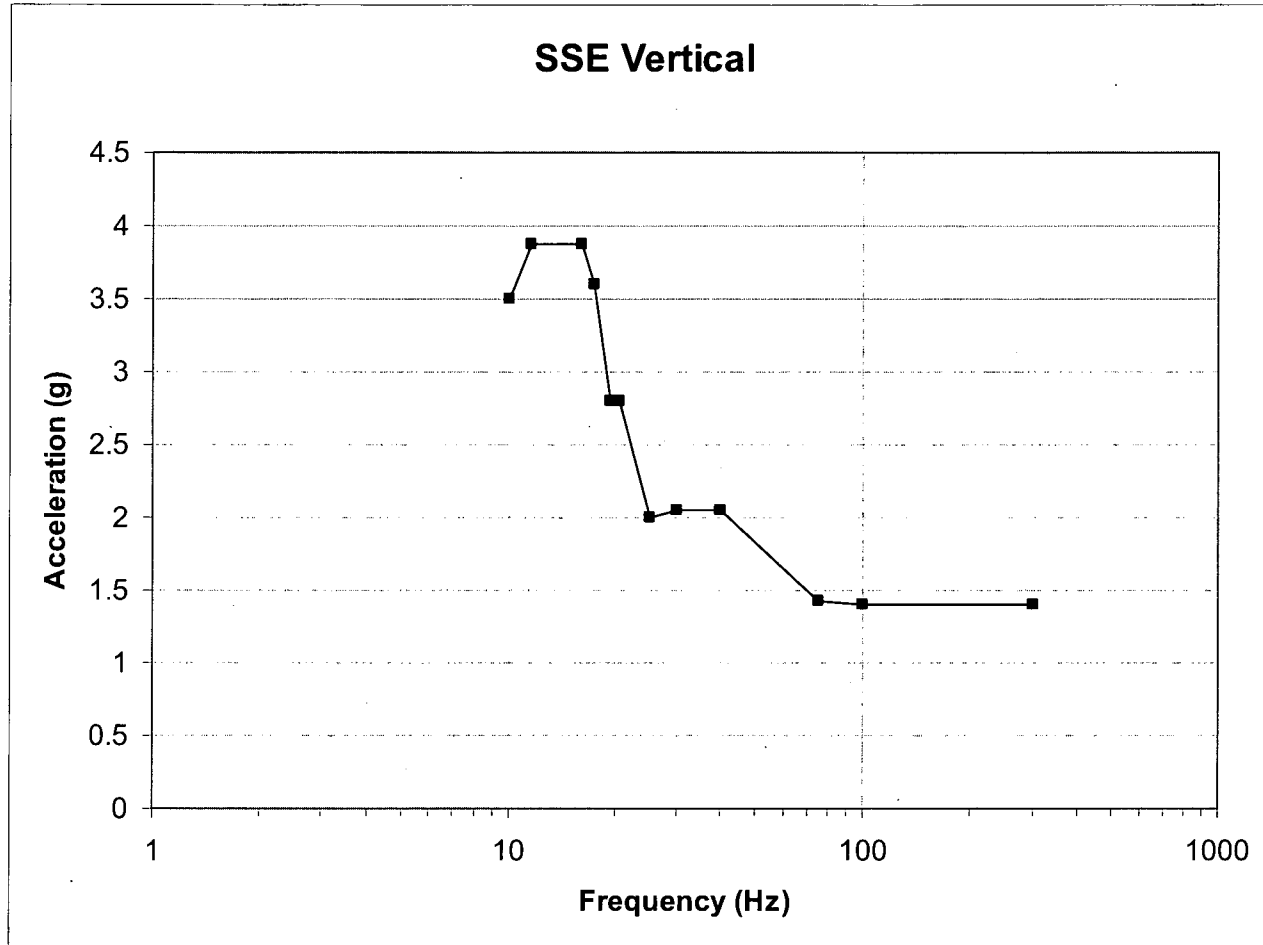


Figure C-10. SSE Vertical Floor Response Spectra

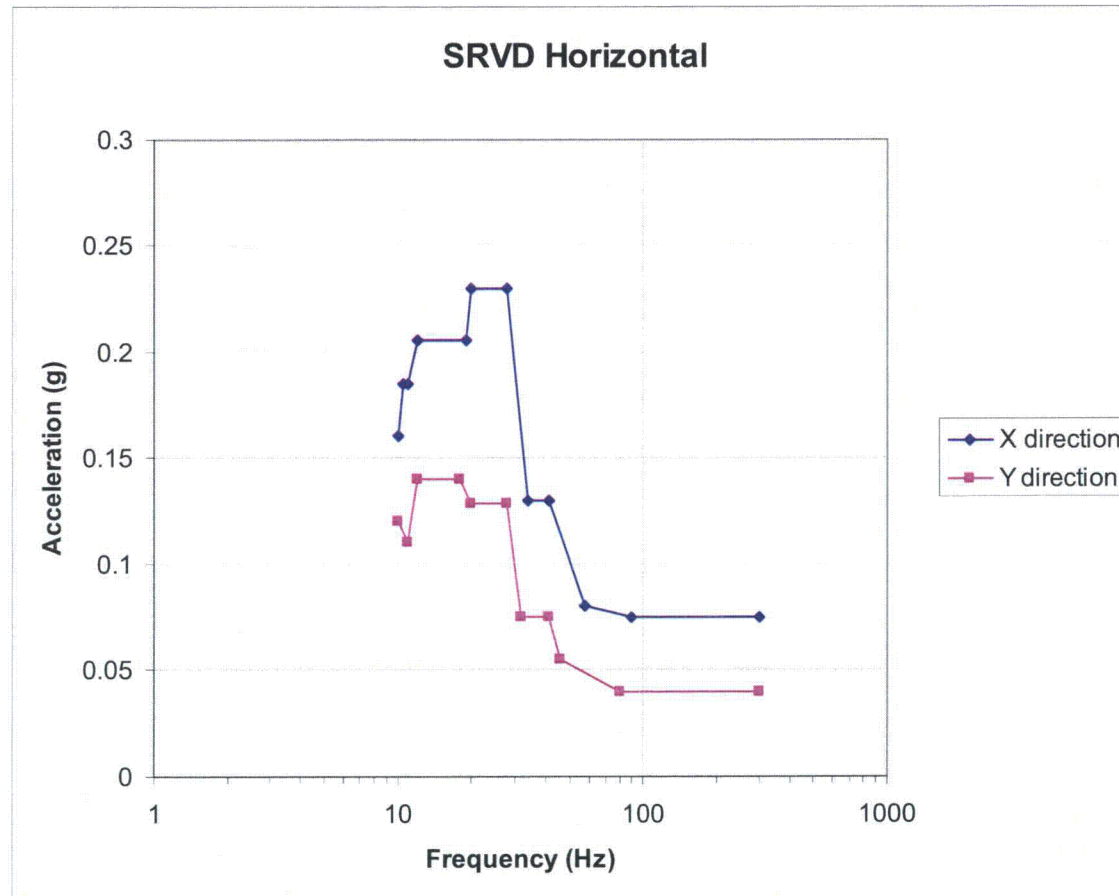


Figure C-11. SRVD Horizontal Floor Response Spectra

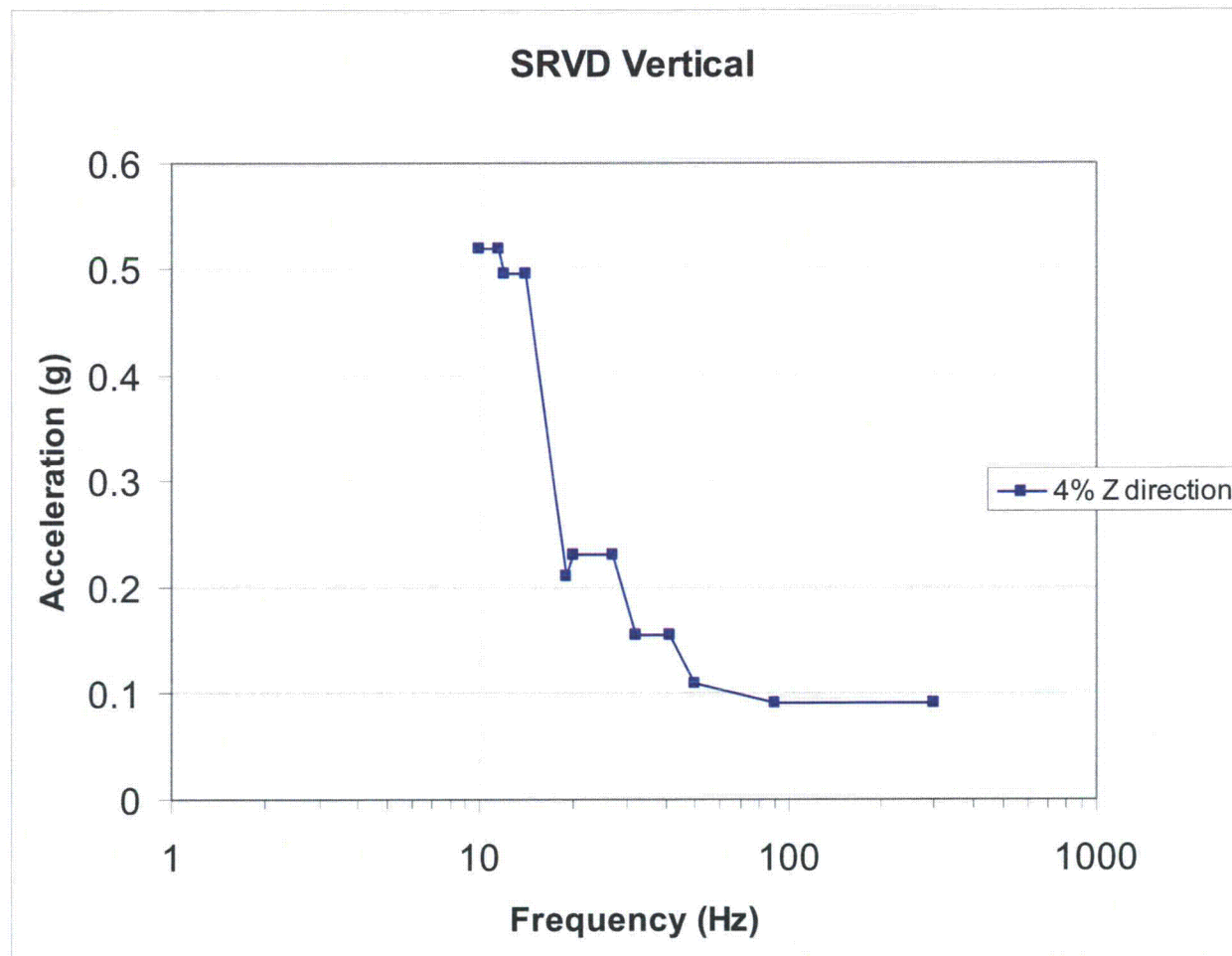


Figure C-12. SRVD Vertical Floor Response Spectra

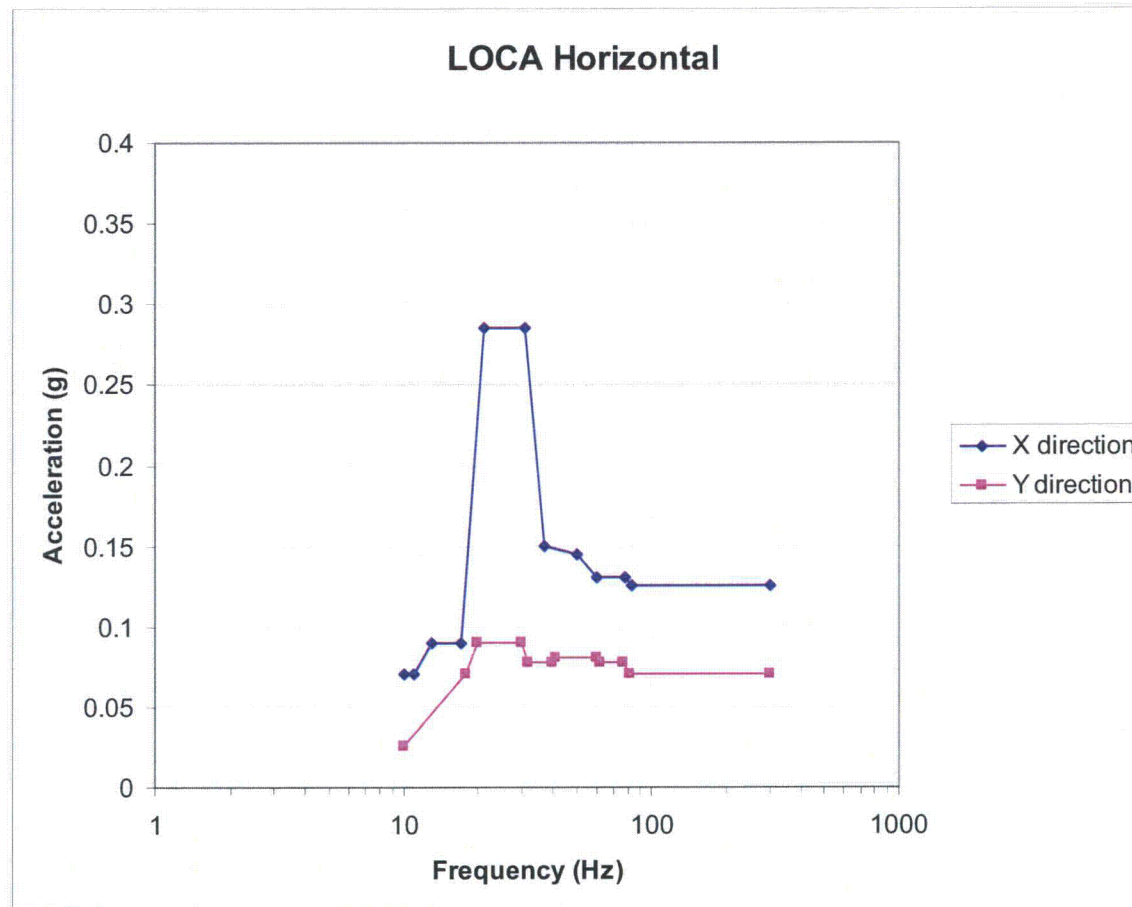


Figure C-13. LOCA Horizontal Floor Response Spectra

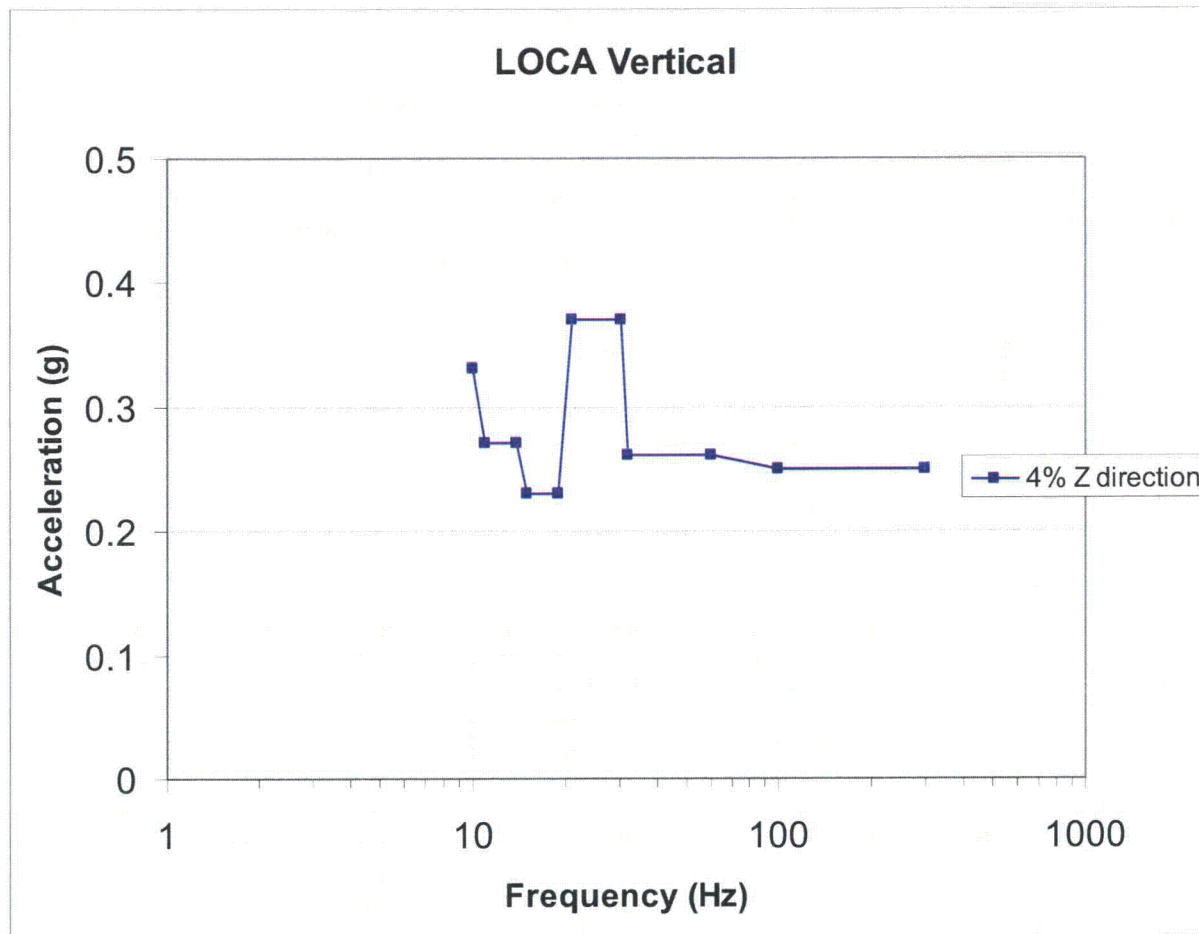


Figure C-14. LOCA Vertical Floor Response Spectra

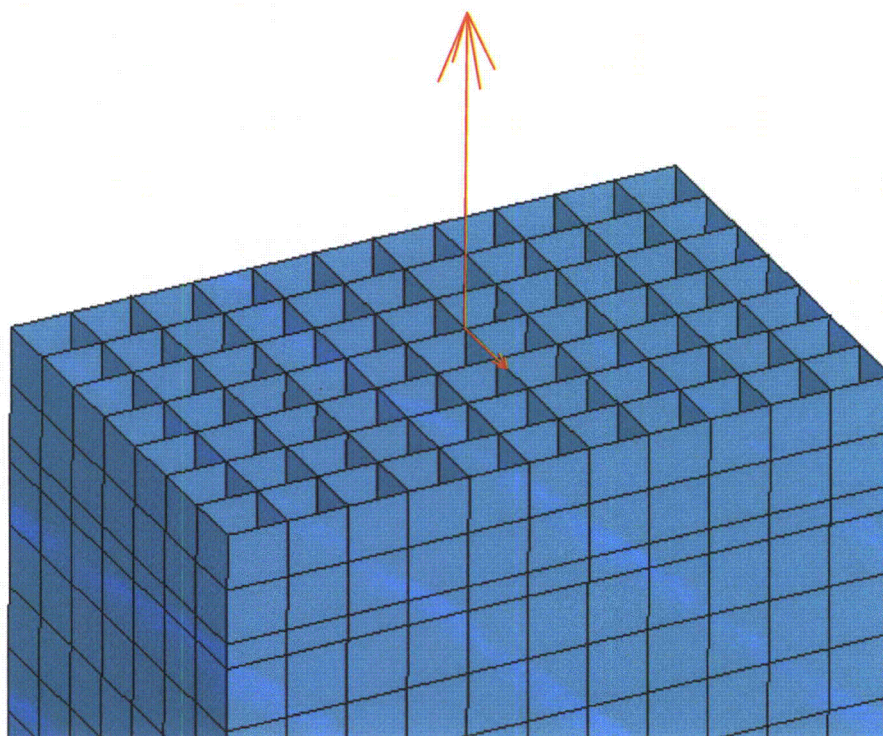


Figure C-15. FSR Fuel Handling Loads

DISPLACEMENT

STEP=1

SUB =1

FREQ=13.644

DMX = .009284

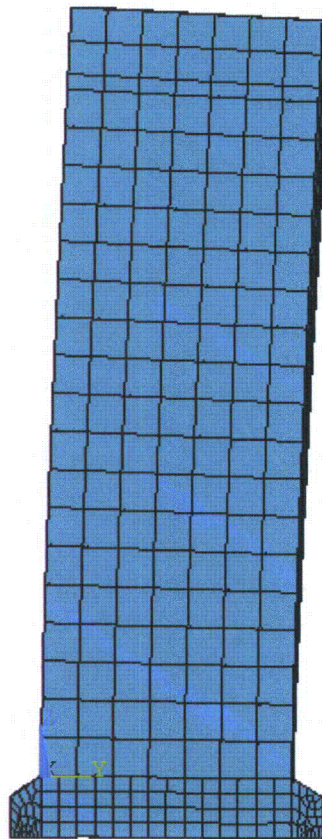


Figure C-16. FSR Deformed Shape Eigenmode 1

DISPLACEMENT
STEP=1
SUB =2
FREQ=17.742
DMX =.01247

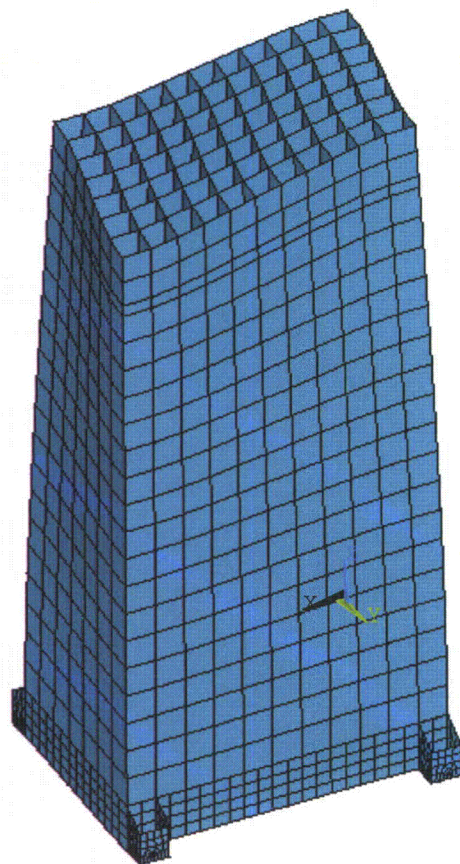


Figure C-17. FSR Deformed Shape Eigenmode 2

DISPLACEMENT

STEP=1

SUB =3

FREQ=17.95

DMX =.009421

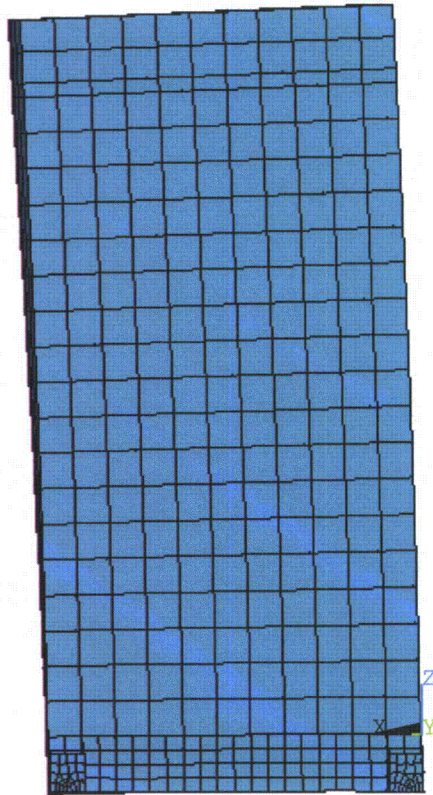


Figure C-18. FSR Deformed Shape Eigenmode 3

DISPLACEMENT
STEP=1
SUB =4
FREQ=35.375
DMX =.011349

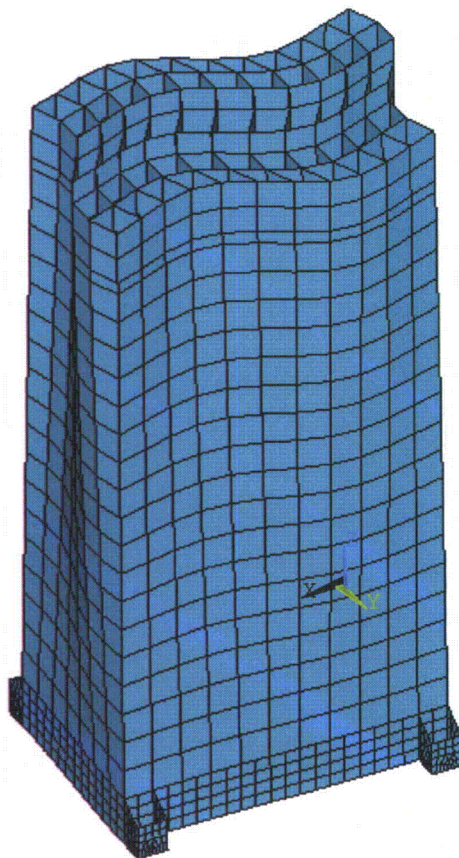


Figure C-19. FSR Deformed Shape Eigenmode 4

DISPLACEMENT

STEP=1

SUB =13

FREQ=72.378

DMX = .009568

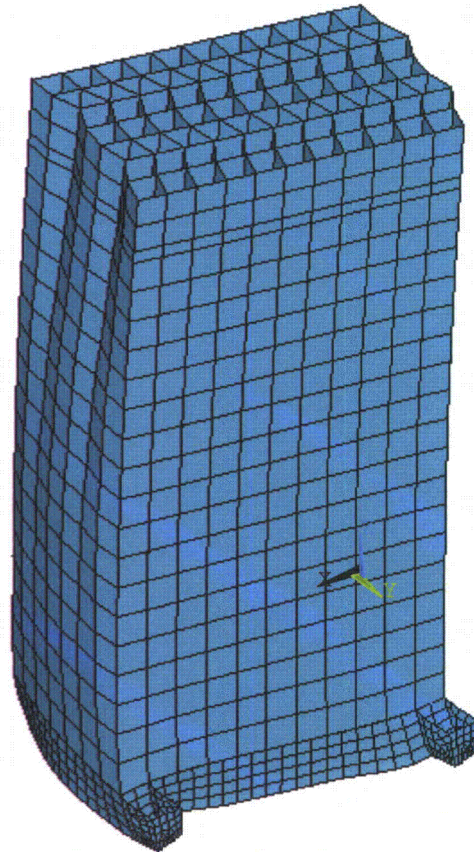


Figure C-20. FSR Deformed Shape Eigenmode 13

DISPLACEMENT

STEP=1

SUB =15

FREQ=76.128

DMX =.01021

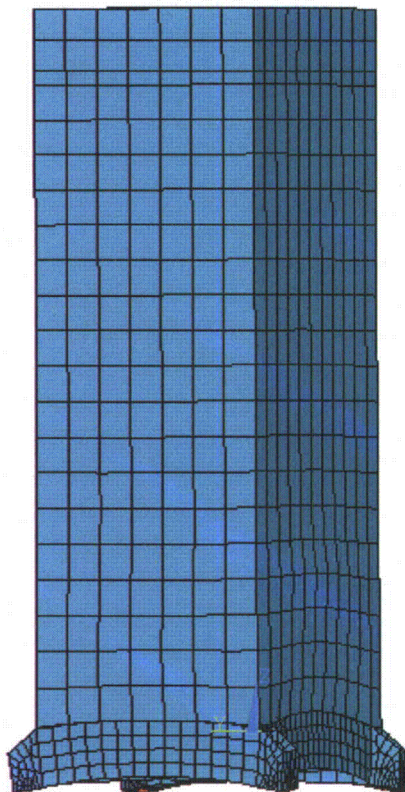


Figure C-21. FSR Deformed Shape Eigenmode 15

DISPLACEMENT
STEP=1
SUB =16
FREQ=80.637
DMX =.012391

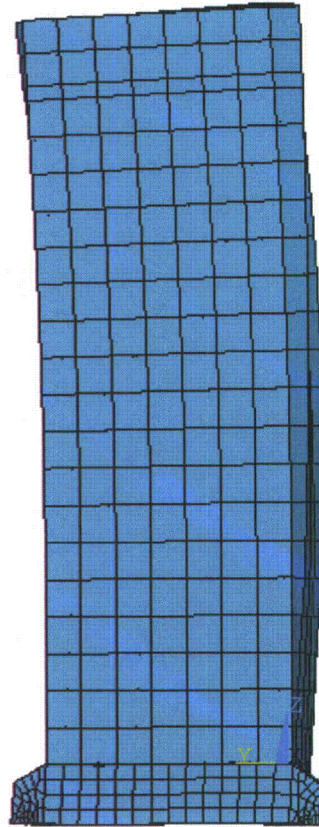


Figure C-22. FSR Deformed Shape Eigenmode 16

DISPLACEMENT
STEP=1
SUB =36
FREQ=155.148
DMX =.014241

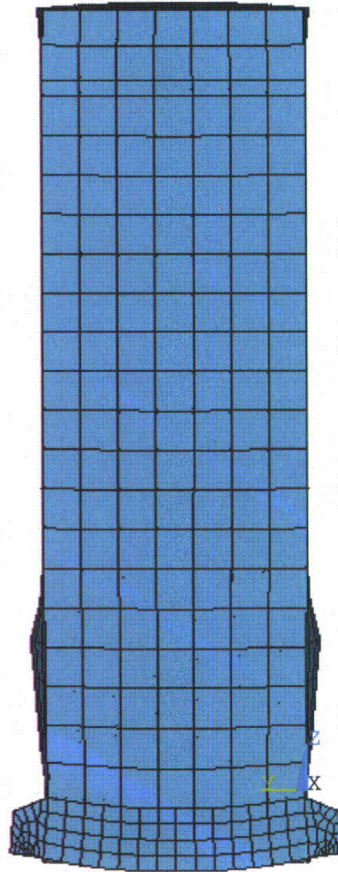


Figure C-23. FSR Deformed Shape Eigenmode 36

UX
TOP
RSYS=0
DMX = .004744
SMX = .002824

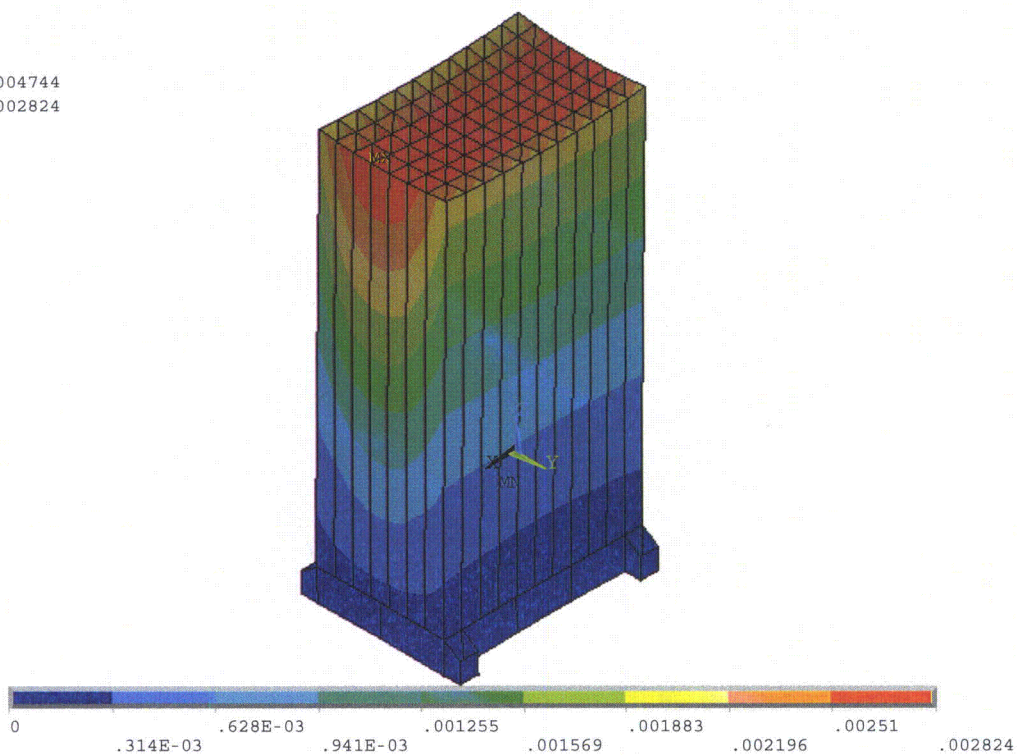


Figure C-24. FSR Horizontal Displacement X (m)

UY
TOP
RSYS=0
DMX = .004744
SMX = .003813

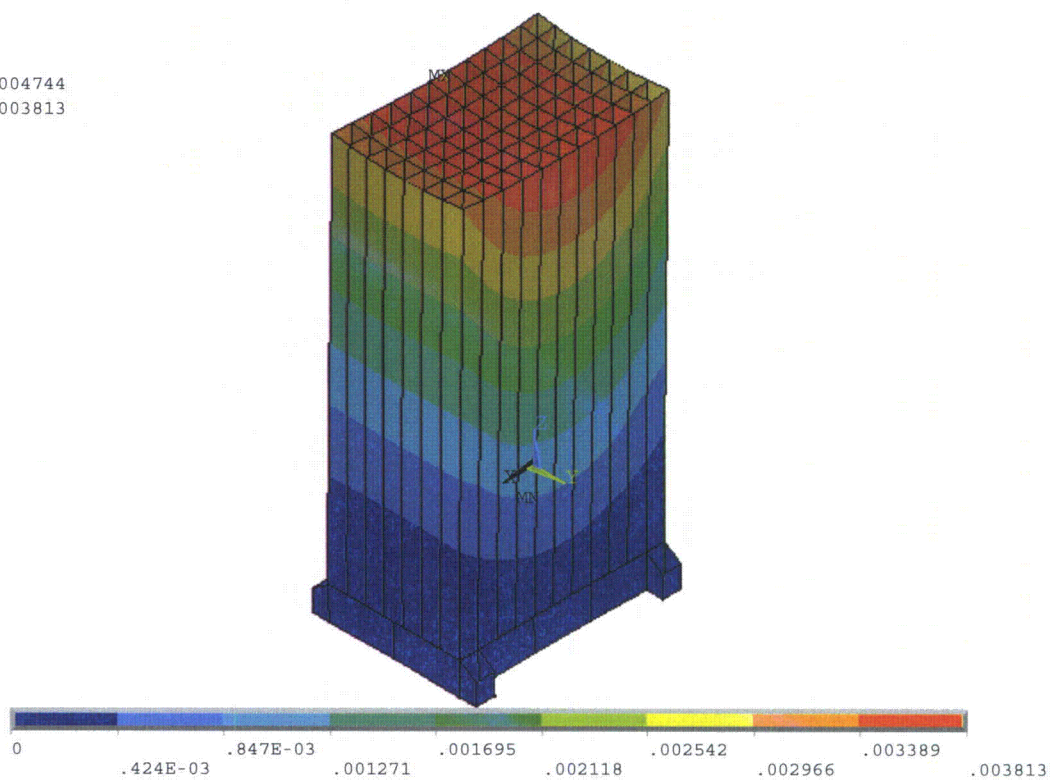


Figure C-25. FSR Horizontal Displacement Y (m)

SZ (AVG)
MIDDLE
RSYS=0
DMX = .004375
SMN = .256E+07
SMX = .131E+09

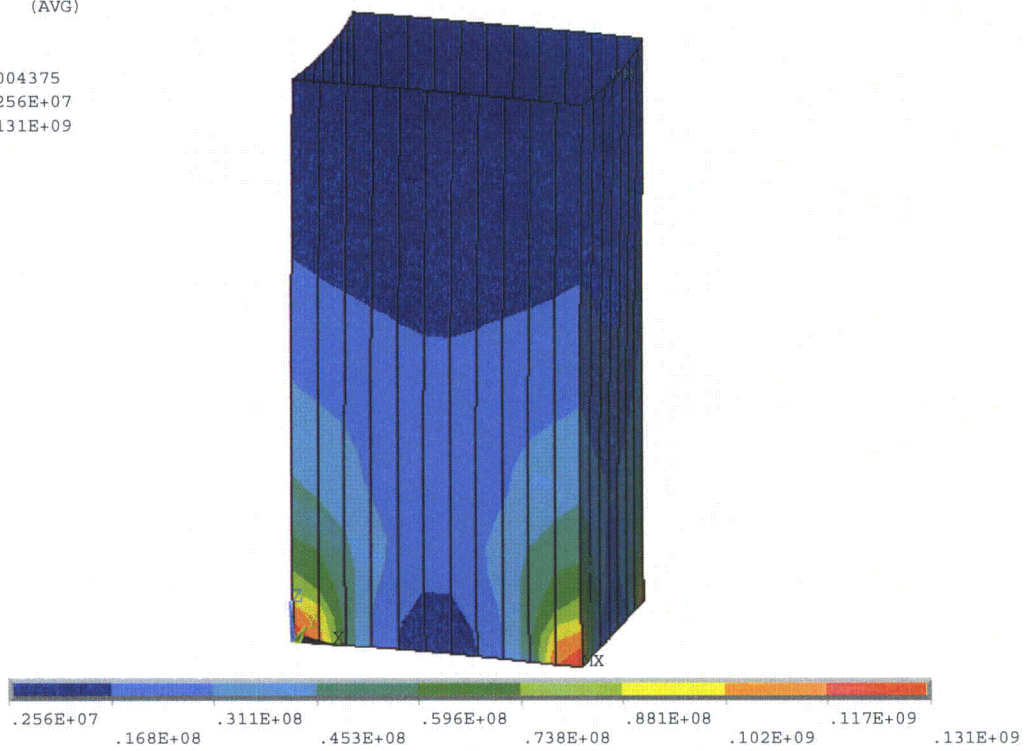


Figure C-26. FSR 10 mm Enveloping Plates. Level D Vertical Stress (N/m²)

SZ (AVG)
MIDDLE
RSYS=0
DMX = .950E-04
SMN = -845722
SMX = .787E+07

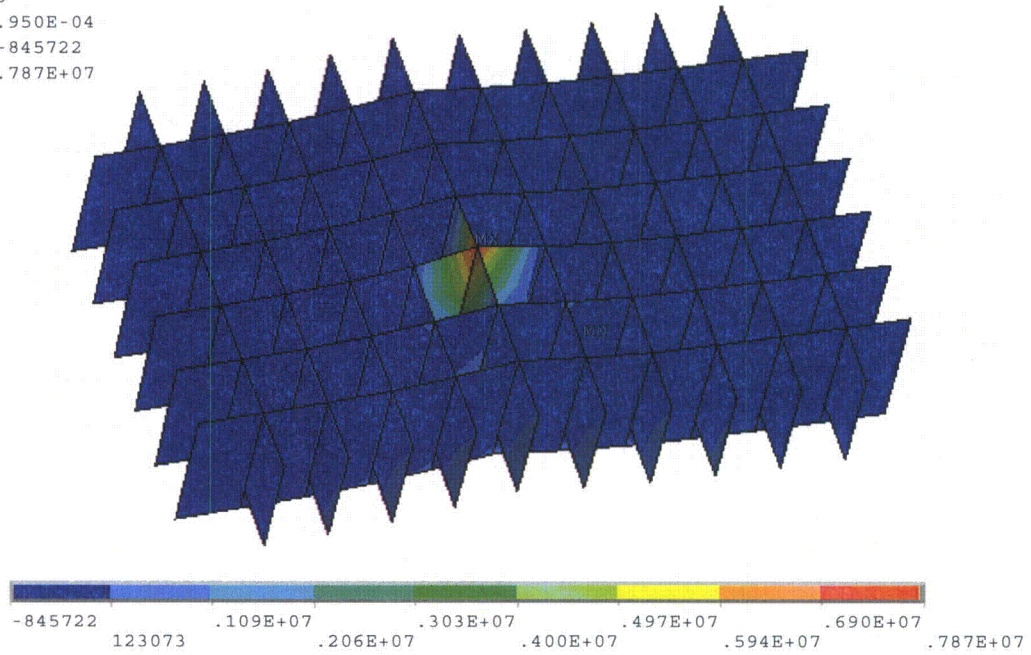


Figure C-27. FSR 7 mm Upper Level Plates. Level A Vertical Stress (N/m²)

SY (AVG)
MIDDLE
RSYS=0
DMX = .004744
SMN = 0
SMX = .558E+08

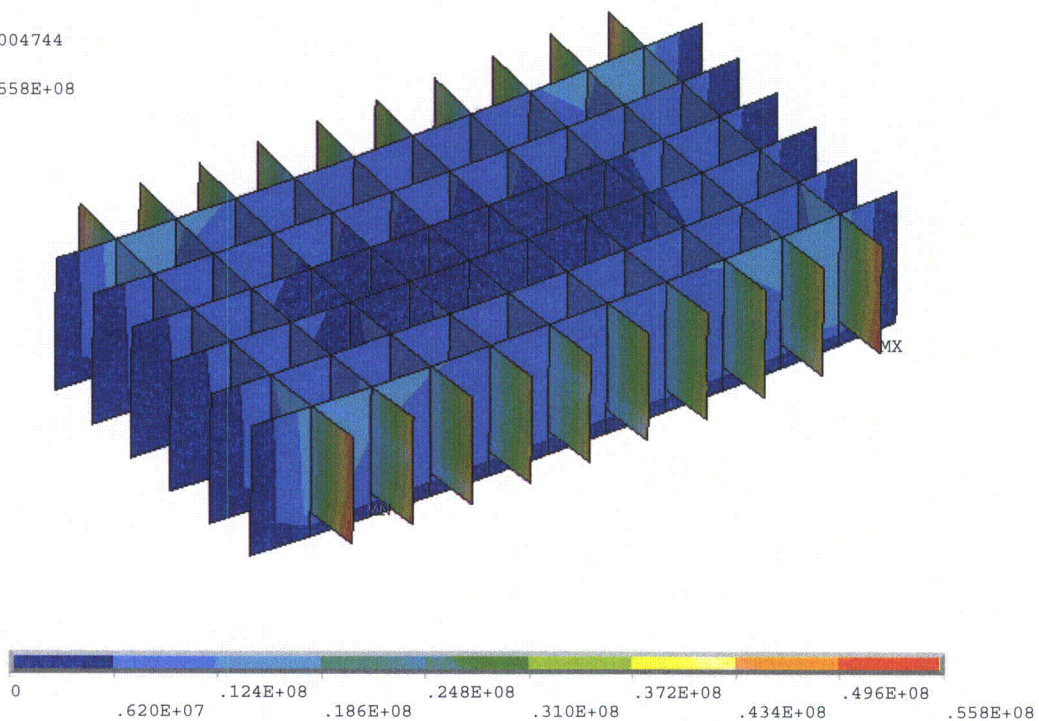


Figure C-28. FSR 7 mm Upper Level Plates. Level D Horizontal Stress (N/m²)

SZ (AVG)
MIDDLE
RSYS=0
DMX = .457E-03
SMN = -.580E+07
SMX = .142E+09

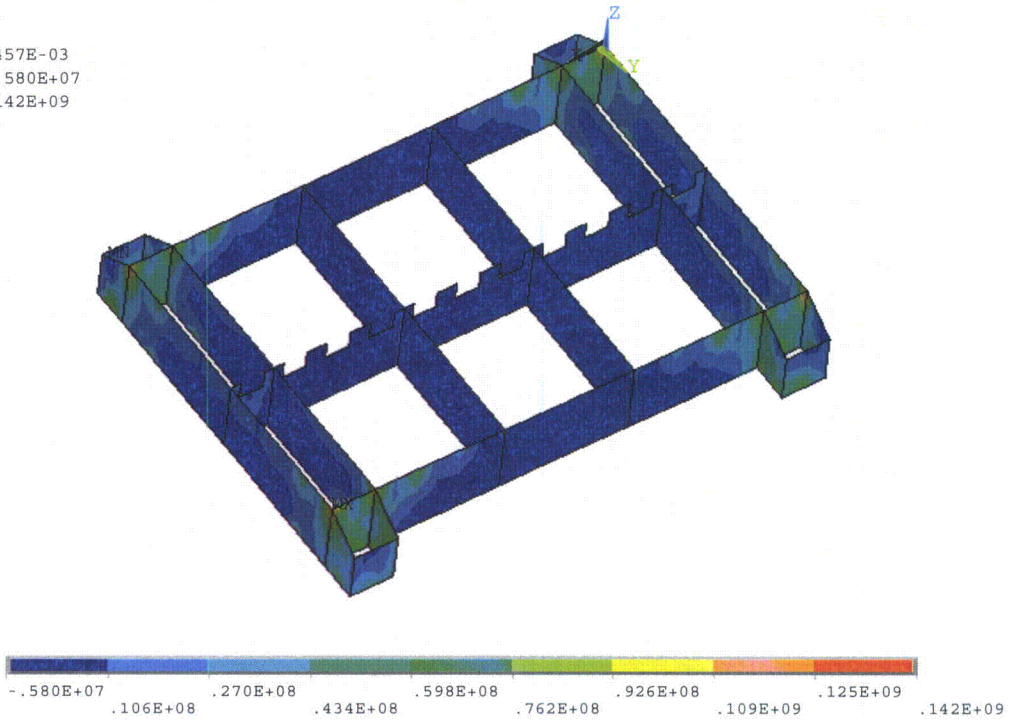


Figure C-29. FSR Base Plate Stiffener Plates. Level D Vertical Stress (N/m²)

SINT (AVG)
TOP
DMX = .457E-03
SMN = .356E+07
SMX = .101E+09

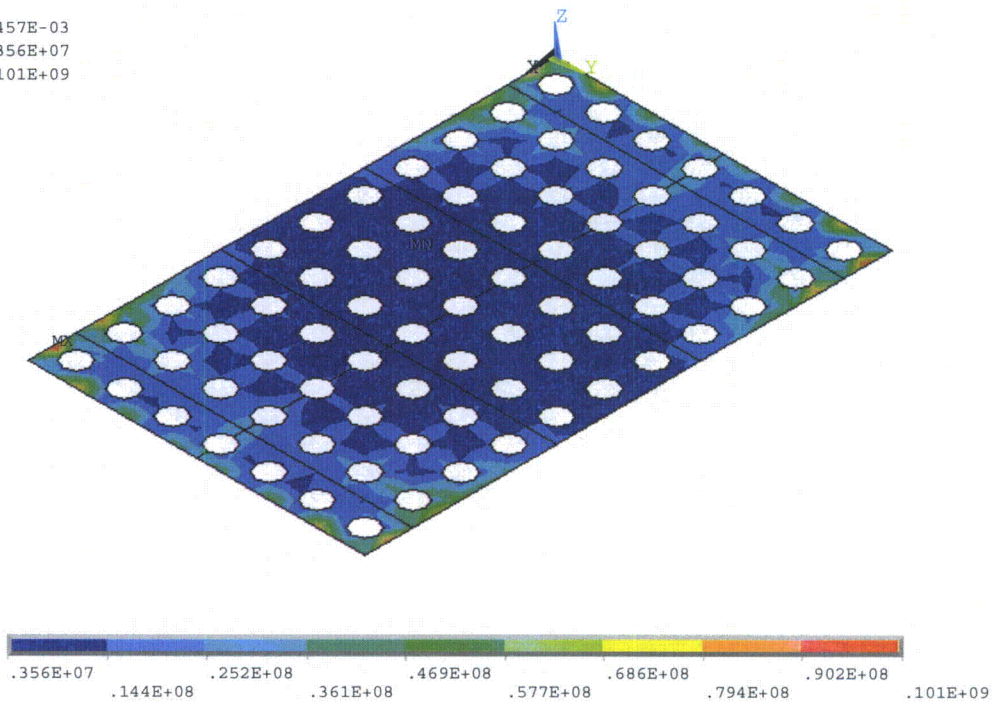


Figure C-30. FSR Base Plate. Level D Stress (N/m²)

SINT (AVG)
TOP
DMX = .318E-03
SMN = 44.15
SMX = .174E+09

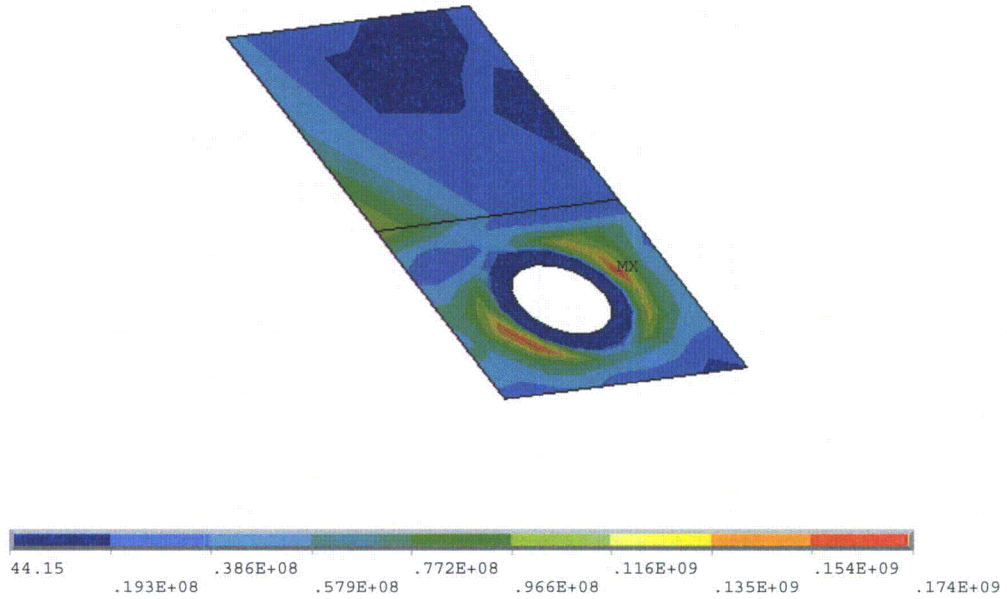


Figure C-31. FSR Bolted Support Plate. Level D Stress (N/m²)

SINT (AVG)
TOP
DMX = .416E-04
SMN = 64950
SMX = .460E+08

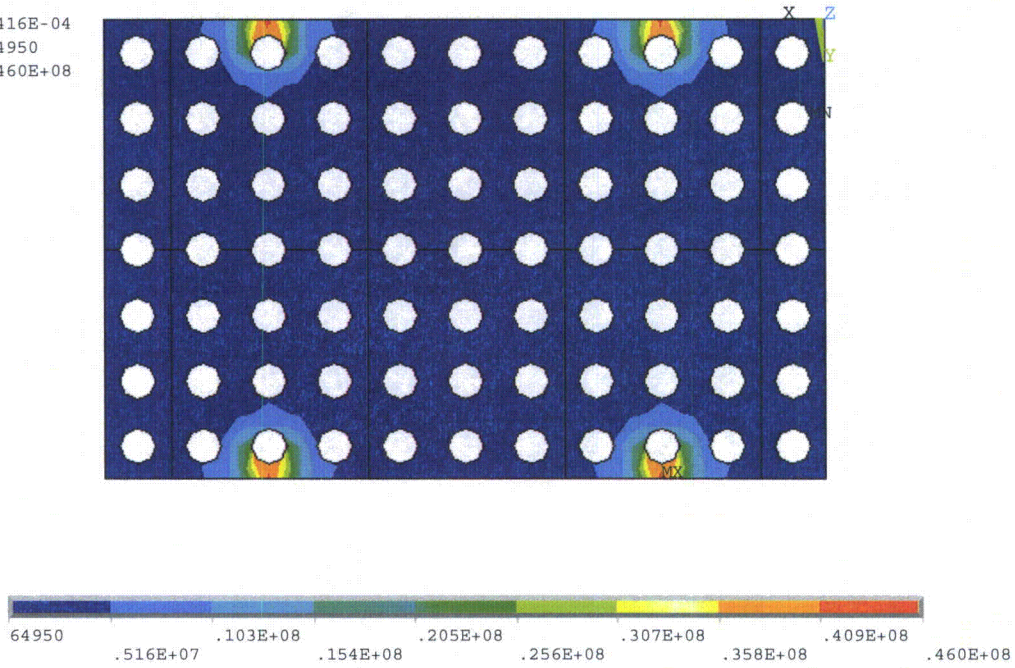


Figure C-32. Base Plate. Lifting Load Stresses (N/m²)

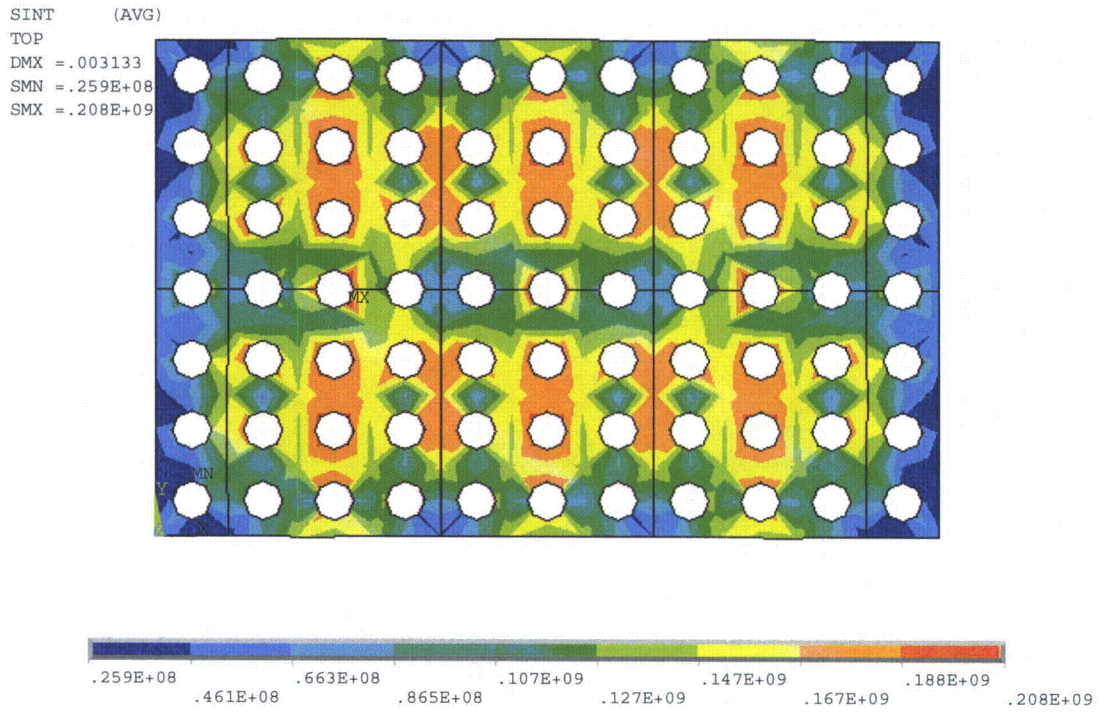


Figure C-33. Fuel Impact Forces. Base Plate Stresses (N/m²)

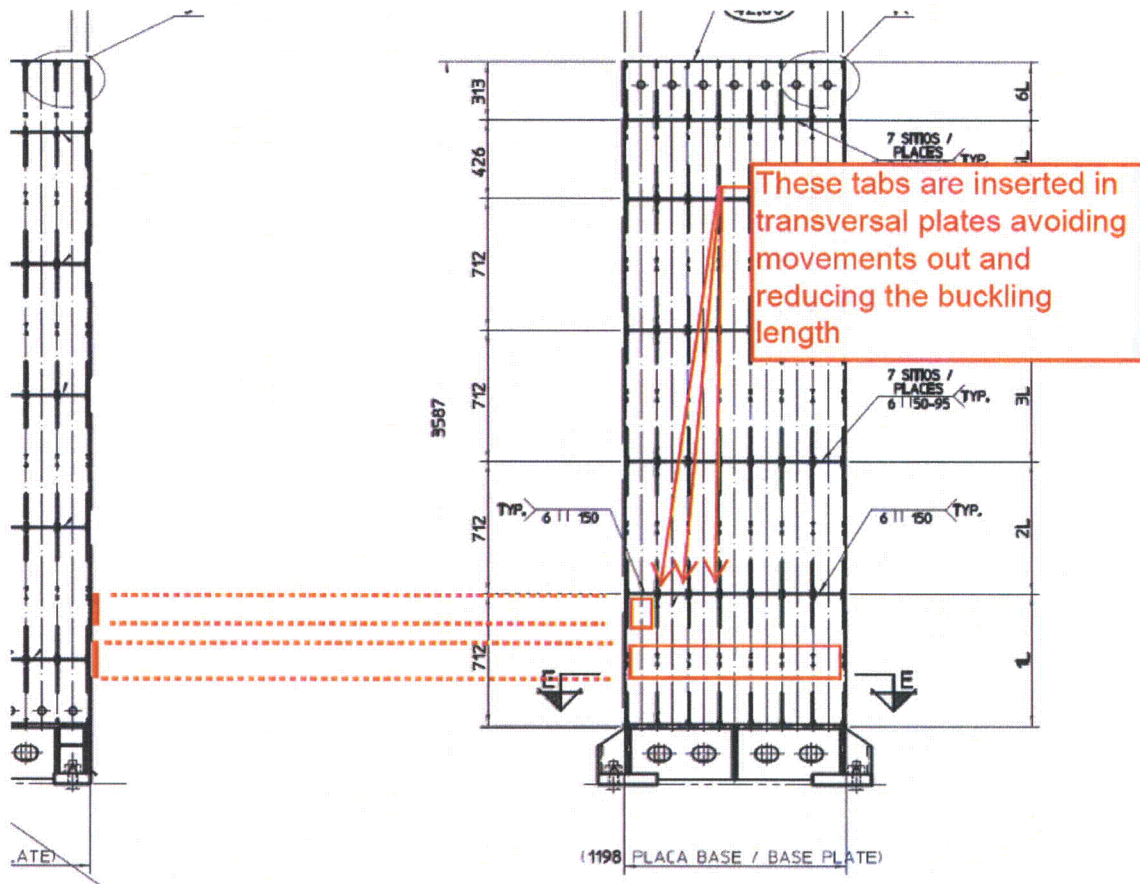
APPENDIX D - Analysis Of Compressive Stresses

The conceptual design of the Interlock cell matrix racks includes multiple connections between plates. So the lateral Plain SS structural plates are braced, at several points, to transversal plates that limit the buckling length. Additionally, for this ESBWR application, we are using thick plates (10 mm and 7 mm)*. As a result the buckling stress limits are greater than the allowable stress limit considered in report.

Allowable buckling stress is calculated below:

For lateral 10 mm plate:

The typical unbraced portion of lateral plates can be seen below.



The typical unbraced length is about $712/4 = 178$ mm.

* The allowable buckling stress depends on the relation between the thickness of the plate and the length of the plate.

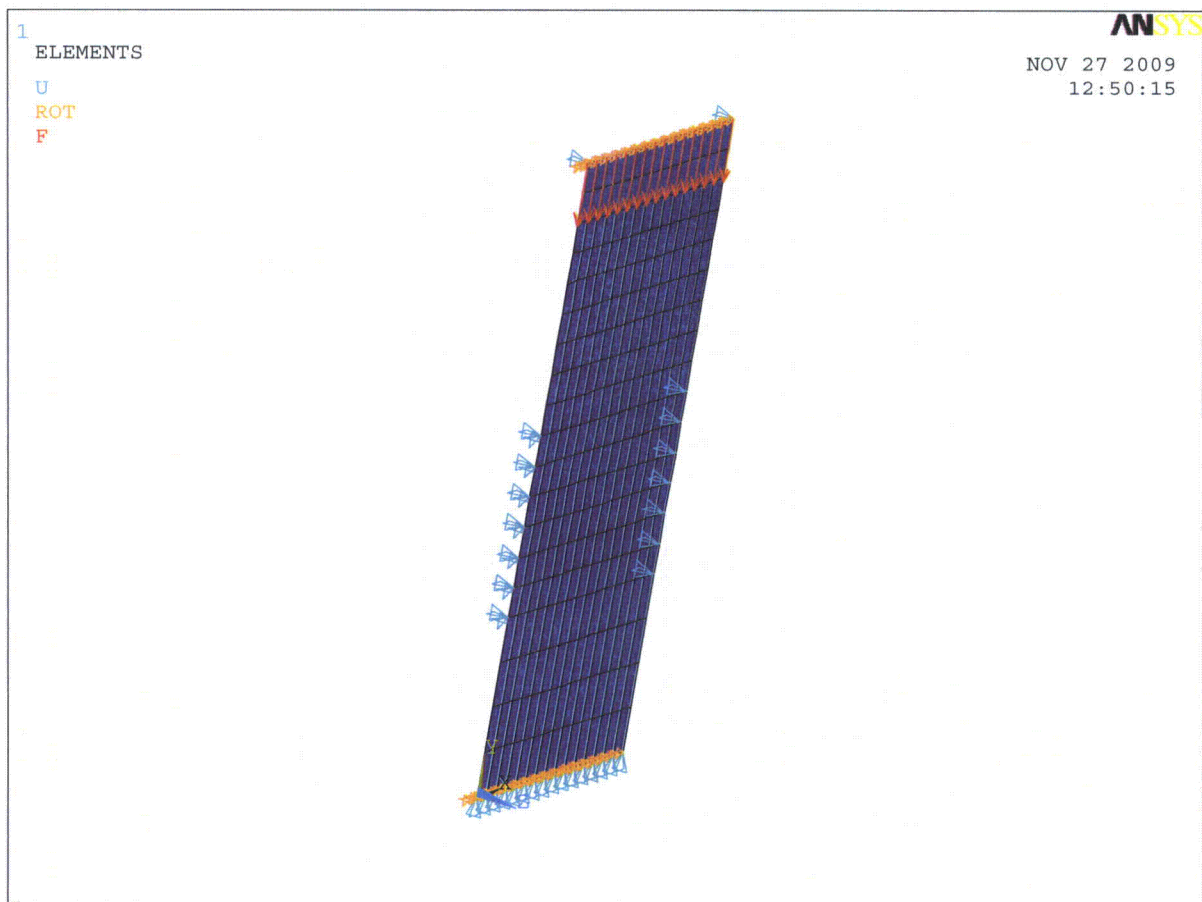
Therefore, the buckling calculation is performed for a 10 mm plate with a span of 178 mm.

The Euler buckling formula, that is too much conservative for this case, gives a buckling stress of

$$\sigma = \frac{\pi^2 \cdot E}{12 \cdot (1 - \nu^2)} \cdot \left(\frac{e}{h}\right)^2 = \frac{\pi^2 \cdot 1.95E5}{12 \cdot (1 - \nu^2)} \cdot \left(\frac{10}{178}\right)^2 = 555.68 \text{ N/mm}^2$$

But additionally, since the boundary conditions for the above plates are complicated, an ANSYS FEM eigen buckling analysis was performed.

The typical lateral plate portion located between two transversal plates (pitch = 168 mm) is modeled. The mesh corresponds to a portion of 168x(712/2= 356) mm.



Mesh for Eigen Buckling and Boundary Conditions

A unitary 10 N/mm² stress was considered.

The ANSYS results are:

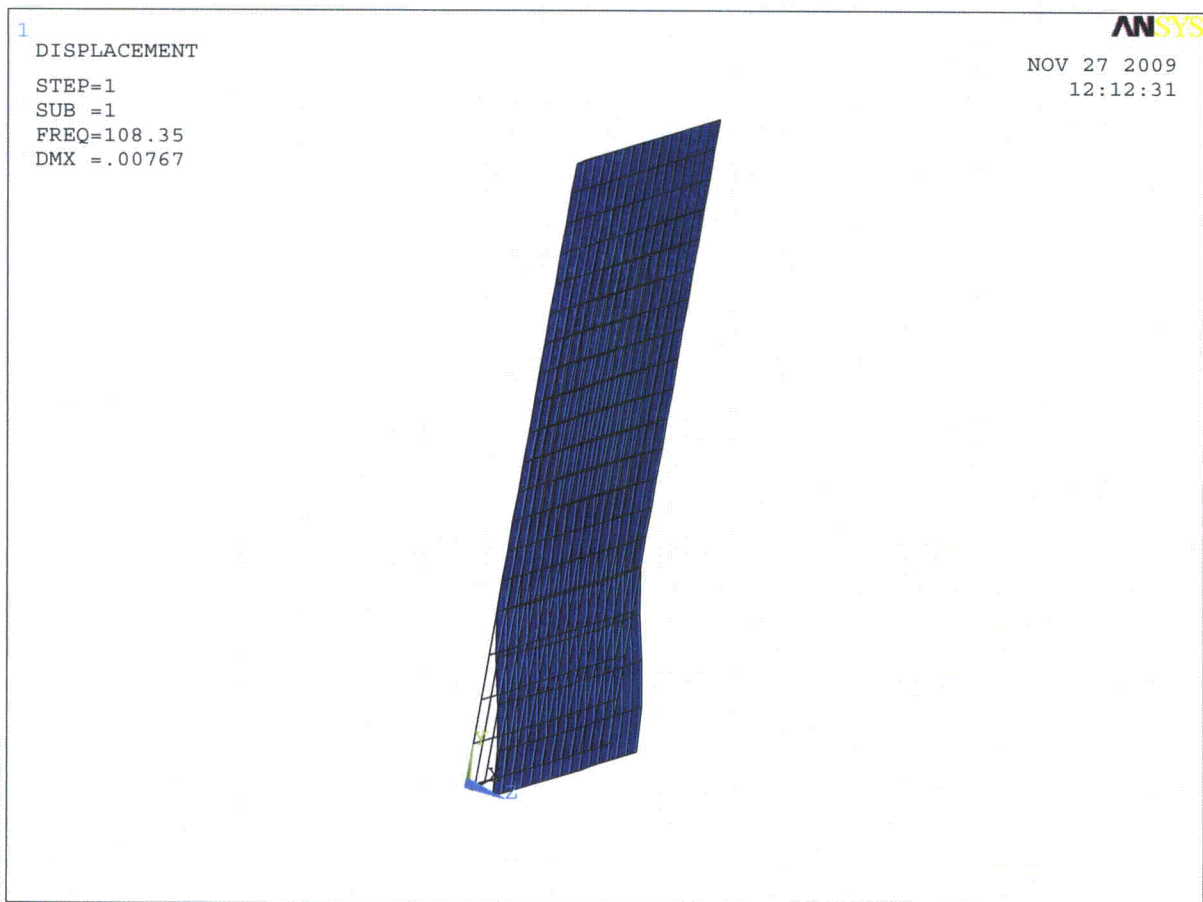
***** EIGENVALUES (LOAD MULTIPLIERS FOR BUCKLING) *****

*** FROM BLOCK LANZOS ITERATION ***

SHAPE NUMBER LOAD MULTIPLIER

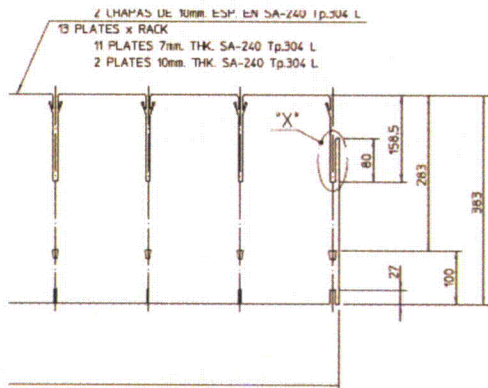
1	108.35012
2	204.05621
3	248.95131

First buckling mode

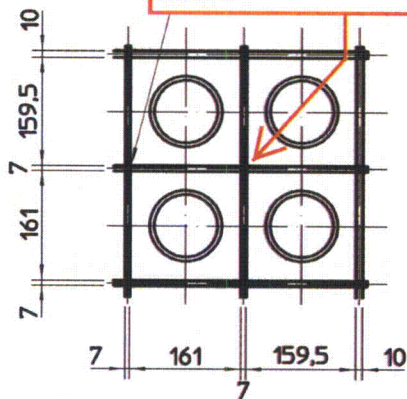


So the allowable buckling stress is $10 \cdot 108.35 \text{ N/mm}^2 = 1083.5 \text{ N/mm}^2$. If we use the safety coefficient required in F-1331.5, the allowable buckling stress = $2/3 \cdot 1083.5 = 722.3 \text{ N/mm}^2$, which is larger than the allowable limits considered in the analysis and much larger than any compressive general membrane stress in lateral plate. Therefore, allowable buckling loads are not limiting.

Upper 7 and 10 mm plates:



transversal plates
are linked by the
tabs



Applying the conservative euler formula, and considering a free span of a pitch = 168 mm for 10 mm plates

$$\sigma = \frac{\pi^2 \cdot E}{12 \cdot (1 - \nu^2)} \cdot \left(\frac{e}{h}\right)^2 = \frac{\pi^2 \cdot 1.95E5}{12 \cdot (1 - \nu^2)} \cdot \left(\frac{10}{178}\right)^2 = 555.68 N / mm^2$$

and considering the internal 7 mm plates have some intermediate between clamped and simple supported boundary condition are:

If we use the safety coefficient required in F-1331.5, as follows:

$$\sigma = \frac{\pi^2 \cdot E}{12 \cdot (1 - \nu^2)} \cdot \left(\frac{e}{h}\right)^2 = \frac{\pi^2 \cdot 1.95E5}{12 \cdot (1 - \nu^2)} \cdot \left(\frac{7}{0.7 \cdot 168}\right)^2 = 623.8 N / mm^2$$

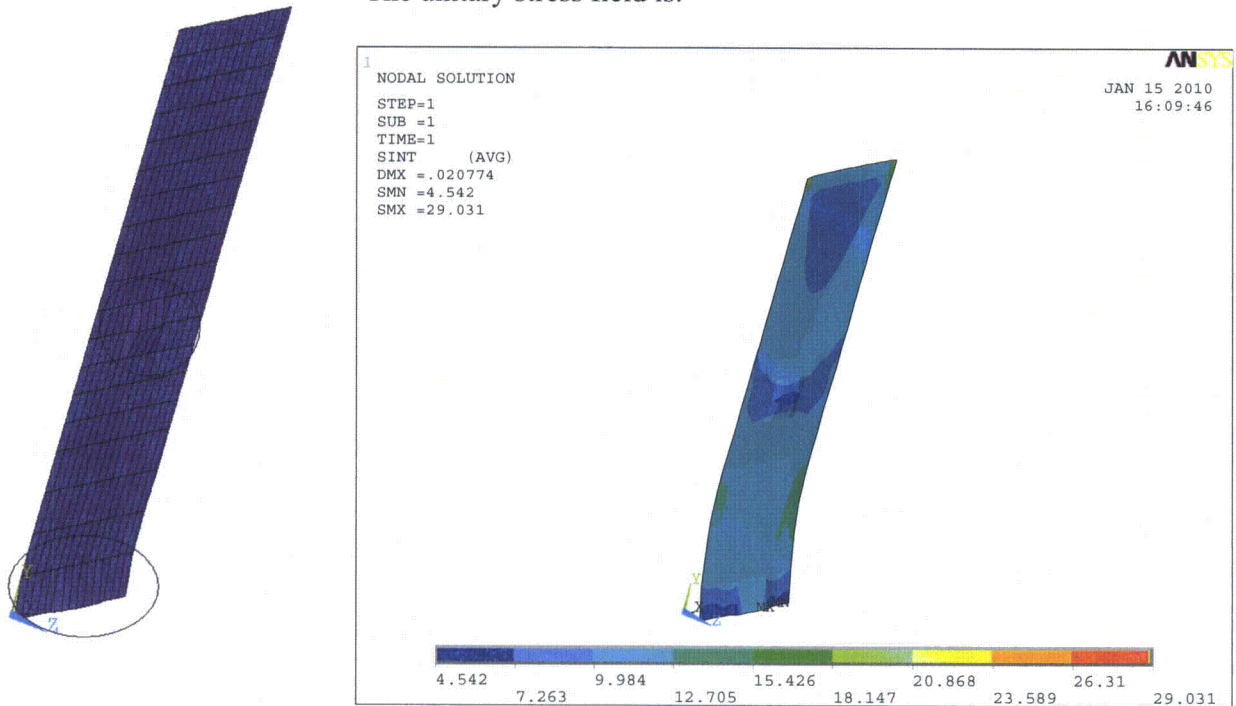
The allowable buckling stress = $2/3 \cdot 555.68 = 370.5 \text{ N/mm}^2$, which is larger than the allowable limits considered in the analysis and much larger than any compressive general membrane stress in lateral plate. Therefore, allowable buckling loads are not limiting.

Potential Manufacturing Imperfections

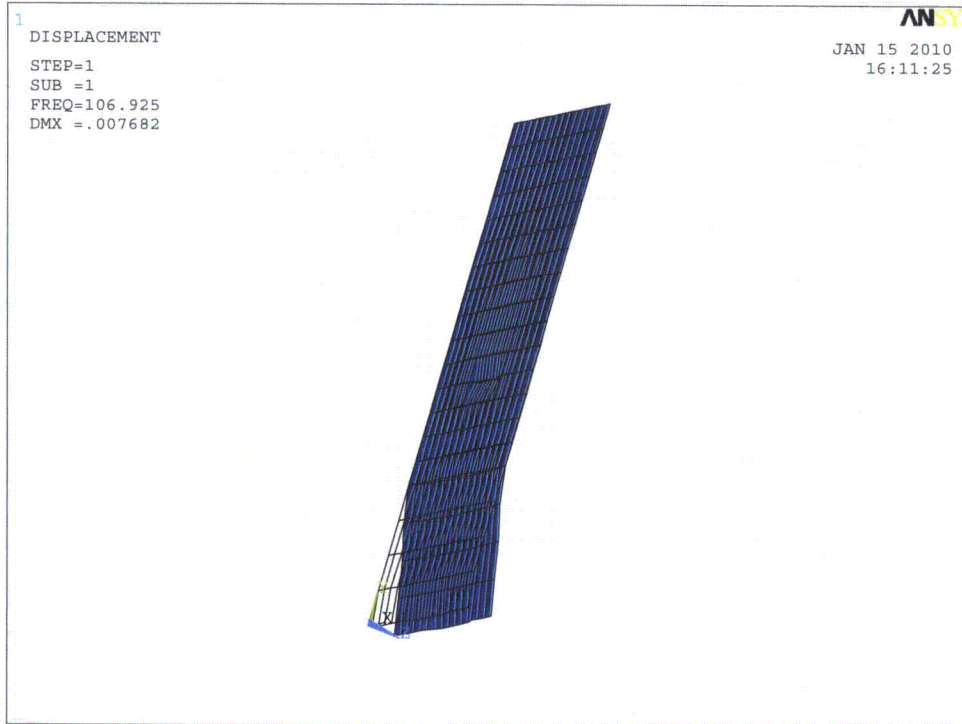
The manufacturing of racks will be done according to the ASME Code, which limits the imperfections. The allowable compressible stress, if we consider potential imperfections, is very similar to the results obtained above.

Considering a typical 5 mm imperfection, which is bigger than allowed by the ASME Code, an ANSYS buckling analysis was performed using the same mesh, boundary conditions, etc. as above.

The unitary stress field is:



And the new eigenvalue and deformed shape are:



It is seen that the new value (106.9 N/mm^2) is very similar to value determined above with no imperfections (108.35 N/mm^2).